T H E M E 10

Emerging Technologies and Special Sessions

WESC 2021
25 – 28 MAY
HANNOVER, GERMANY

Table of Contents

Theme Chairs 1
Mini-Symposium: Challenges in wind tunnel testing in wind energy research 2
Mini-Symposium: Challenges in wind tunnel testing in wind energy research (I) 3
Mini-Symposium: Challenges in wind tunnel testing in wind energy research (II) 13
Mini-Symposium: Research at Germany's First Offshore Wind Farm alpha ventus 24
Mini-Symposium: Research at Germany's First Offshore Wind Farm alpha ventus (I) 25
Mini-Symposium: Research at Germany's First Offshore Wind Farm alpha ventus (II) 30
Mini-Symposium: Machine Learning and big data applications in wind energy 35
Mini-Symposium: Machine Learning and big data applications in wind energy (I) 36
Mini-Symposium: Machine Learning and big data applications in wind energy (II) 42
Mini-Symposium: Demystifying Complex Terrain 48
Mini-Symposium: IEA Wind Task 32: Wind Lidar 59
Mini-Symposium: Advances in High-Performance Computing for Wind Energy Applications 73
Mini-Symposium: Digital Twin Technology 82
Mini-Symposium: Airborne Wind Energy System Modelling, Control and Optimisation 99
Mini-Symposium: Airborne Wind Energy System Modelling, Control and Optimisation (I) 100
Mini-Symposium: Airborne Wind Energy System Modelling, Control and Optimisation (II) 112
Mini-Symposium: Airborne Wind Energy System Modelling, Control and Optimisation (III) 123
Mini-Symposium: Airborne Wind Energy System Modelling, Control and Optimisation (IV) 131
Mini-Symposium: Performance Metrics and Technology Assessment of Airborne Wind Energy Systems 141
Regular Session: Innovative Rotor Concepts and Small Wind Turbines 154

Theme Chairs

Peter Jamieson
University of Strathclyde

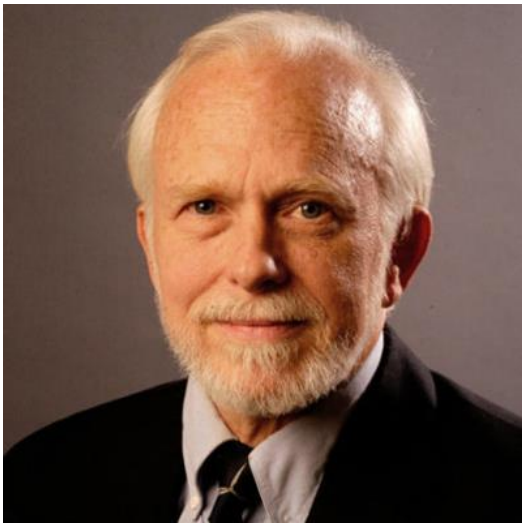

Prof. James Manwell
University of Massachusetts

Prof. Roland Schmehl
TU Delft

John Olav Tande
SINTEF

Mini-Symposium: Challenges in wind tunnel testing in wind energy research

Oguz Uzol
METU Center for Wind Energy Research (RÜZGEM)

Joachim Peinke
ForWind, University of Oldenburg

Michael Hölling
ForWind, University of Oldenburg

Wind turbines operate under complex wind conditions that are constantly changing. Turbine data is a result of the interaction of the turbine's controller with these inflow conditions and result in an averaged picture of the current situation. This becomes even more complicated due to the presence of wakes in wind farms. Trying to improve turbine performance under special wind conditions is a challenging topic since the inflow can neither be controlled nor repeated. Here wind tunnel tests under controlled conditions are used in general to gain a better understanding of the complex interactions in the free field. Nevertheless, wind tunnel experiments also face many problems, which are beyond just scaling. This mini-symposium will focus on the challenges and possible solutions as to how we can reduce the variability and increase repeatability/reliability of data obtained from different experiments/facilities. Therefore, we invite abstracts that address mainly these issues. The mini-symposium is expected to trigger the discussion on topics such as wind energy research wind tunnel infrastructure, Reynolds number effects and correction/extrapolation methods, new measurement techniques, improved and consistent calibration methods to be applied for round robin tests, round robin test ideas, standardization and improving the consistency of wind tunnel inflow.

Mini-Symposium: Challenges in wind tunnel testing in wind energy research (I)

Effects of Wind Tunnel Blockage and Turbulence Intensity on the Performance of a Small Wind Turbine: An In-House Round Robin Study

Burcu Erol*, Anas Abdulrahim, Mustafa Perçin, and Oğuz Uzol
Middle East Technical University
*Presenting author

Keywords: round robin test | small wind turbine | wind tunnel

In order to improve the reliability of wind tunnel tests and to investigate the variability of data among different wind tunnels, round robin test campaigns are generally conducted. One recent example of this is by Aubrun et al [2019], in which wake measurements of porous discs with uniform and non-uniform porosity were conducted by nine different institutions. In another previous campaign and as a part of another research project on the use of winglets in wind turbines we have tested a 0.95 m diameter horizontal axis wind turbine in an open-jet facility at the Center for Wind Energy Research (RÜZGEM) at The Middle East Technical University (METU) in Ankara, Turkey as well as in the 3m x 2m cross-section closed test section of the large-scale wind tunnel at the Norwegian University of Science and Technology (NTNU) in Trondheim, Norway. The measured power coefficient variations obtained in these two very different facilities are given in Figure 1 (Ostovan and Uzol [2016]). Although there seems to be a general agreement, some differences can be observed after about a Tip Speed Ratio (TSR) of 4, most probably due to different blockage and freestream turbulence intensity levels of the two wind tunnels.

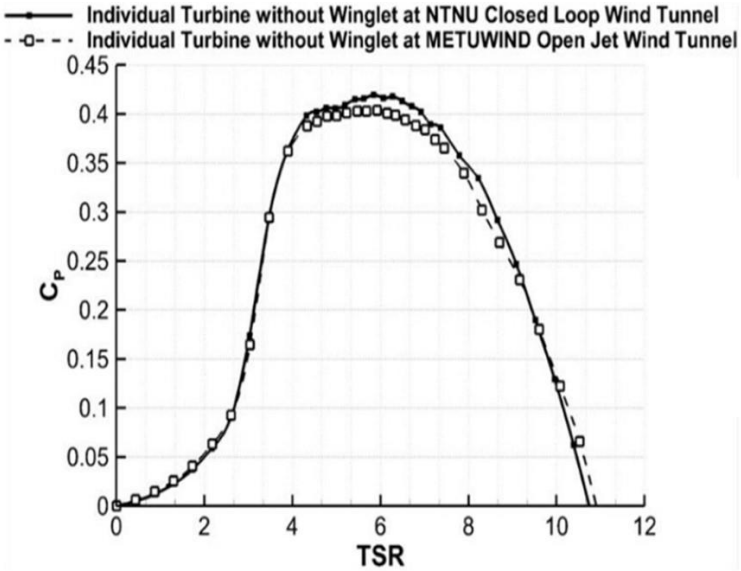

Figure 1.Variation of Power Coefficient with TSR as measured in METU Open-jet and NTNU Large Scale Wind Tunnel

To further investigate this variability, we will be testing the same wind turbine in different test facilities at RÜZGEM. This wind turbine has a 3-bladed rotor with precision machined Aluminium blades that have nonlinear twist and chord distributions with a NREL S826 profile throughout the blade span. The blade taper and twist distributions are the same as the ones used in the experiments performed at NTNU as reported in Adaramola and Krogstad [2011]. The rotor is driven by a precision speed controlled 1.5 kW servo-motor in order to obtain controlled TSR conditions during the experiments. The torque on the rotor shaft is measured using an HBM T20WN/5Nm torque transducer and the thrust is measured using an ATI Gamma type six-

component force-moment transducer on which the entire nacelle is placed. The measurements will be mainly focusing on the performance of the wind turbine in terms of power and thrust coefficient variations with TSR at a freestream windspeed of 11 m/s. A picture of the wind turbine is shown in Figure 2.

Figure 2. Different facilities that will be used in the in-house round robin test campaign

The tests will be conducted in four different facilities (Figure 2): The first one is a 1.7 m diameter open-jet wind tunnel; the second, third and the fourth ones are all different configurations of the new Large Scale Wind Tunnel of RÜZGEM, i.e. a 3 m diameter open-jet test section, a 3 m x 7 m cross-section and 20 m long boundary layer test section and a 2.5 m x 2.5 m cross-section test section. The range of blockage in these tests will be from 3.3% to 31% and the range of freestream turbulence intensity levels will be approximately from 0.2% to 2%. Comparisons will be made to quantify the effects of these on measured turbine performance.

References:

S. Aubrun, M. Bastankhah, R.B. Cal, B. Conan, R.J. Hearst, D. Hoek, M. Hölling, M. Huang, C. Hur, B. Karlsen, I. Neunaber, M. Obligado, J. Peinke, M. Percin, L. Saetran, P Schito, B. Schliffke, D. Sims-Williams, O. Uzol, M.K. Vinnes, A. Zasso, (2019), "Round-robin tests of porous disc models," Wake Conference 2019, IOP Conf. Series: Journal of Physics: Conf. Series 1256 (2019) 012004, doi:10.1088/1742-6596/1256/1/012004.

Y. Ostovan, O. Uzol, (2016), "Experimental Study on the Effects of Winglets on the Performance of Two Interacting Horizontal Axis Model Wind Turbines," The Science of Making Torque from Wind (TORQUE 2016), Journal of Physics: Conference Series 753 (2016) 022015 doi:10.1088/1742-6596/753/2/022015.

Adaramola, Krogstad, (2011), "Experimental investigation of wake effects on wind turbine performance" Renewable Energy Vol. 36 Issue 8 pp. 2078-2086.

Impact of wall blockage on wake steering by yawing

Filippo Campagnolo[1,*], Franz Mühle[1], Paul Hulsman[2], Vlaho Petrović[2], Michael Hölling[2], Lars Neuhaus[2], Abdulkarim Abdulrazek[2], Martin Kühn[2], and Carlo L. Bottasso[1]
[1]Technical University Munich
[2]ForWind - University of Oldenburg
*Presenting author

Keywords: Wind Tunnel Testing | Wind Tunnel Inflow | Wind Tunnel Blockage

The last years have seen an increased scientific production on wind tunnel testing of scaled wind turbines and wind farms. In fact, wind tunnel tests can be conducted in a repeatable and a highly controllable environment, with good knowledge of the boundary conditions. These advantages have been widely exploited to investigate some physical phenomena governing the formation and propagation of wakes behind wind turbines, and their impact on the conditions experienced by downstream machines. Additionally, various techniques for altering the behavior of wakes, such as wake-steering by yawing, power derating, or enhanced wake mixing, have been investigated with respect to their ability to increase power and reduce loading[1]. Regarding the wind tunnel testing of wake control techniques, the effects of the wind tunnel walls on wake behavior is an aspect that still needs to be fully clarified. The goal of this paper is to fill this gap, with respect to wake steering by yawing.

Figure 1a: G1 model in the POLIMI wind tunnel

To this end, two experimental campaigns were performed by using the same scaled wind turbine model in two different wind tunnels. The G1 turbine model has a rotor diameter equal to 1.1 meters, features yaw, torque, and individual pitch control capabilities, and it is equipped with main shaft and tower root load sensors[2]. One campaign was performed in the civil test section of the wind tunnel of the Politecnico di Milano (POLIMI, Fig. 1a), whose large cross section (14 x 4 meters) compared to the G1 size implies an almost negligible blockage[3]. A second campaign was performed in the wind tunnel of the ForWind research center of the University of Oldenburg (UOL, Fig. 1b). Since the cross section has a size of 3 x 3 meters, blockage cannot be considered negligible in this case. In fact, the ratio between the areas of the rotor and of the test section is approximately 0.1. A turbulent atmospheric boundary layer was simulated in each wind tunnel: spires were located at the inlet and bricks were placed on the ground for the POLIMI wind tunnel[4], while an active grid was used in the UOL wind tunnel[5]. The two wind tunnels achieved very similar vertical profiles of the mean speed and turbulence intensity, as well as similar turbulent spectra. Given the similarity of the inflows, differences in wake behavior can be directly attributed to blockage.

Figure 1b: G1 model in the UOL wind tunnel

Results indicate an effect of the wind tunnel size on power, loads, and wake behavior in wind-misaligned conditions. Particularly, a lower power loss and reduced yaw-induced deflection were observed in the UOL wind tunnel, a fact that suggests the need for specific corrections when testing at higher blockage ratios. During the oral presentation, a detailed description of the experimental setup and a complete overview of the results will be given.

References:
[1] Campagnolo, F., Petrović, V., Bottasso, C.L. and Croce, A., 2016, July. Wind tunnel testing of wake control strategies. In 2016 American Control Conference (ACC) (pp. 513-518). IEEE.
2] Bottasso, C. L. and Campagnolo, F., 2020. chap. Wind Tunnel Testing of Wind Turbines and Farms. Handbook of Wind Energy Aerodynamics, Springer, 2020.
[3] Wang, C., Campagnolo, F., Canet, H., Barreiro, D.J. and Bottasso, C.L., 2020. How realistic are the wakes of scaled wind turbine models?. Wind Energy Science Discussions, pp.1-27.
[4] Wang J, Wang C, Campagnolo F, Bottasso CL. Wake behavior and control: comparison of LES simulations and wind tunnel measurements. Wind Energy Science. 2019;4(1):71-88.
[5] Kröger, L., Frederik, J., van Wingerden, J.W., Peinke, J. and Hölling, M., 2018. Generation of user defined turbulent inflow conditions by an active grid for validation experiments. In Journal of Physics: Conference Series (Vol. 1037, No. 5).

Customization and Characterization of a perturbation system for gust generation: The chopper – 2

Ingrid Neunaber[1,*], Martin Obligado[2,3], and Caroline Braud[1]
[1]Centrale Nantes
[2]Grenoble-INP
[3]Université Grenoble Alpes
[*]Presenting author

Keywords: Wind tunnel experiment | Gust | Turbulent inflow | Dynamic inflow | The chopper

Wind energy converters operate in the naturally turbulent atmospheric boundary layer. They are therefore exposed to instationary, gusty inflow. As sudden, strong variations of the inflow cause high loads and unsteady aerodynamic effects on the rotor blades, it is important to understand the interaction between the flow and the rotor blades. To study this, wind tunnel setups that create reproducible strong, sudden flow changes are used. For example, active grids can be used to generate extreme gusts [1].
Here, we follow a new approach: A rotating bar, the chopper blade, passes through the inlet of a wind tunnel, thus creating a velocity deficit, or an inverse gust. This system is called the chopper, and it was first presented at the WESC 2019 [2]. Since then, we have customized this system, and we will present the new results.
For the experiments, we used a chopper blade of 10 cm width that is rotating with the chopper frequency fCH. The inflow velocity is u = 25 ms-1. To add background turbulence, a regular grid can be installed upstream of the chopper blade in the inlet. All experiments have been carried out with and without the grid, and therefore with background turbulence intensities of 3% (grid) and 0.3% (no grid). The flow field was scanned using a hot-wire array that was equipped with 5 probes (see fig. 1).

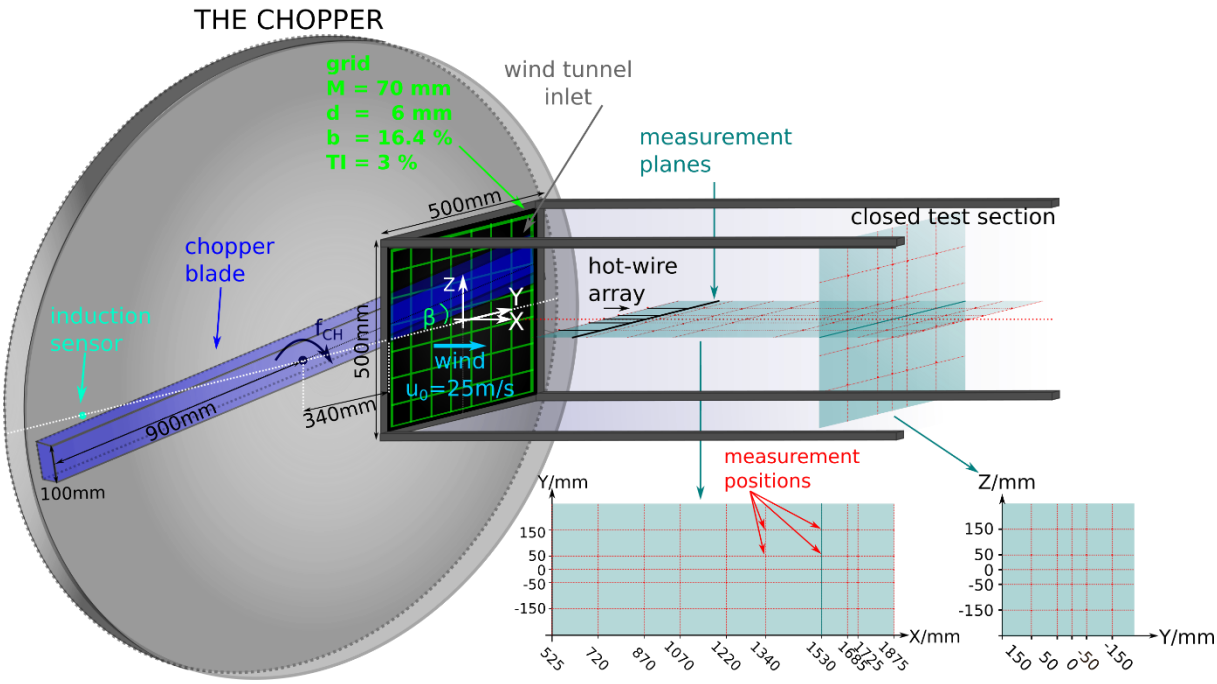

Figure 1: Setup: The chopper consists of a rotating bar, the chopper blade, that cuts through the inlet of the test section. Upstream of the chopper blade, a grid can be installed to add background turbulence to the flow. The flow is scanned with an array of five hot-wire probes. A horizontal and a vertical plane are investigated.

A horizontal plane and a vertical plane have been scanned for two chopper frequencies, 0.04 Hz and 0.4 Hz. In addition, at fixed positions, the frequency was varied between 0.01 Hz and 2 Hz, and the wind velocity was changed from 5 ms-1 to 25ms-1. Also, a characterization of the flow downstream of the static blade fixed at certain angles in the test section was performed to better understand the turbulence generation.

The flow will be analyzed both with respect to the mean flow field and with respect to the structure of the inverse gust and its dependence on the chopper frequency, which has been done in a similar manner in [3] for a chopper blade with 20 cm width. There and in [4], it has already been shown that the inverse gust generated by the chopper can be split into the mean gust shape and the superimposed turbulence structures. Also, the gust is reproducible. For the evaluation of the new data sets, a focus will be on the evolution of the turbulence with increasing distance and increasing chopper frequency. So far, we could show that the gust length is anti-proportional to the chopper frequency. Also, the influence of the background turbulence will be evaluated.

In summary, we will present results from new measurements of the the customized chopper that expand the results presented at the WESC 2019.

References:

[1] Traphan, D.; Wester, T. T. B.; Peinke, J.; Gülker G. (2018) On the aerodynamic behavior of an airfoil under tailored turbulent inflow conditions. Proceedings of the 5th International Conference on Experimental Fluid Mechanics ICEFM 2018 Munich

[2] Neunaber, I.; Braud, C.; Soulier, A.; Aubrun, S. (2019) Characterization of a new perturbation system for gust generation: The chopper. WESC 2019, presentation, doi:10.5281/zenodo.3405976

[3] Neunaber, I.; Braud, C. (2020) First characterization of a new perturbation system for gust generation: The Chopper. Wind Energy Science, 5, 759–773

[4] Neunaber, I.; Braud, C. (2020) Aerodynamic behavior of an airfoil under extreme wind conditions. J. Phys.: Conf. Ser. 1618 032035

Tailoring inflows for wind turbine testing

Lars Neuhaus*, Frederik Berger, Joachim Peinke, and Michael Hölling
ForWind, University of Oldenburg
*Presenting author

Keywords: Turbulence | Active Grid | Wind Tunnel | Gust | Experiments

New concepts for wind turbines, such as controller designs or add-ons, require appropriate investigations, including experiments. To ensure significant and transferable results, there are certain requirements for the measurement conditions, such as realistic and reproducible inflows in the wind tunnel.
Generating certain inflows by means of active grids in the wind tunnel becomes more common nowadays. At ForWind Oldenburg, investigations are carried out in the large 3 x 3 m^2 wind tunnel with a test section length of 30 m. An active grid consisting of 80 shafts with rectangular vanes is used for the flow field generation (Fig. 1, [1]). The active grid is operated in a constant blockage mode, which allows to generate comparable inflow conditions over a large cross-sectional area (corresponding to the rotor swept area of a model wind turbine, e.g. MoWiTO 1.8 Fig.1, [2]), while keeping the global blockage constant and thus reducing pumping effects of the wind tunnel. Each shaft motion is specified by a predefined motion protocol, which can be repeated arbitrarily and allows reproducible flow conditions for follow-up experiments.

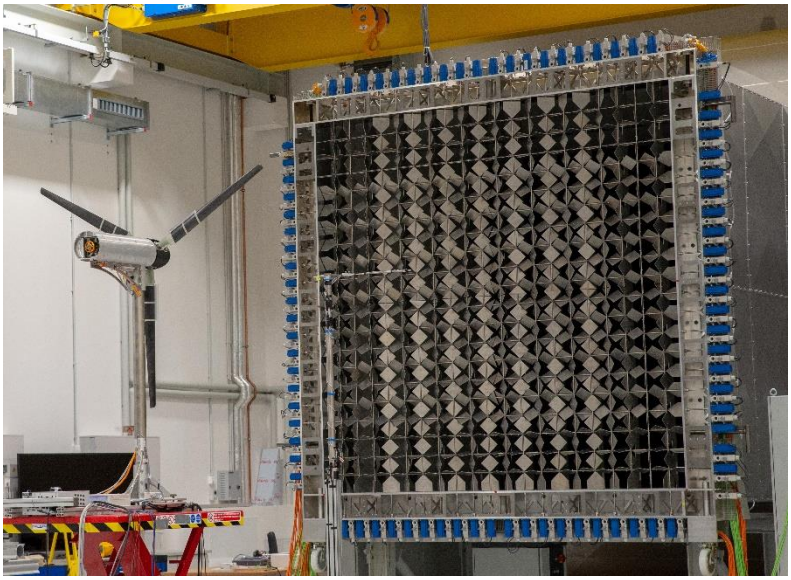

Figure 1: Active grid and MoWiTO 1.8 installed in the big wind tunnel in Oldenburg.

A transfer function of the active grid is measured (velocity as a function of the shaft angle). By means of the transfer function, it is possible to tailor the active grid motion protocol to generate specific inflow structures. In the presentation, generated flows such as sinusoidal velocity variations, steps, and Mexican hat shaped gusts will be shown (Fig. 2). These defined shapes help to understand the dynamic response of a turbine to various single events (steps and gusts). The response to periodic wind fields can be tested with sinusoidal velocity variation, e.g., to test the switching between two controller regions. Furthermore, fully developed turbulent wind fields of different turbulence intensity and various other characteristics, e.g. shear, partial gusts, or wakes, can be tailored and generated by the active grid. This allows for investigating the turbine behavior for different inflows, e.g. under IEC standard conditions.

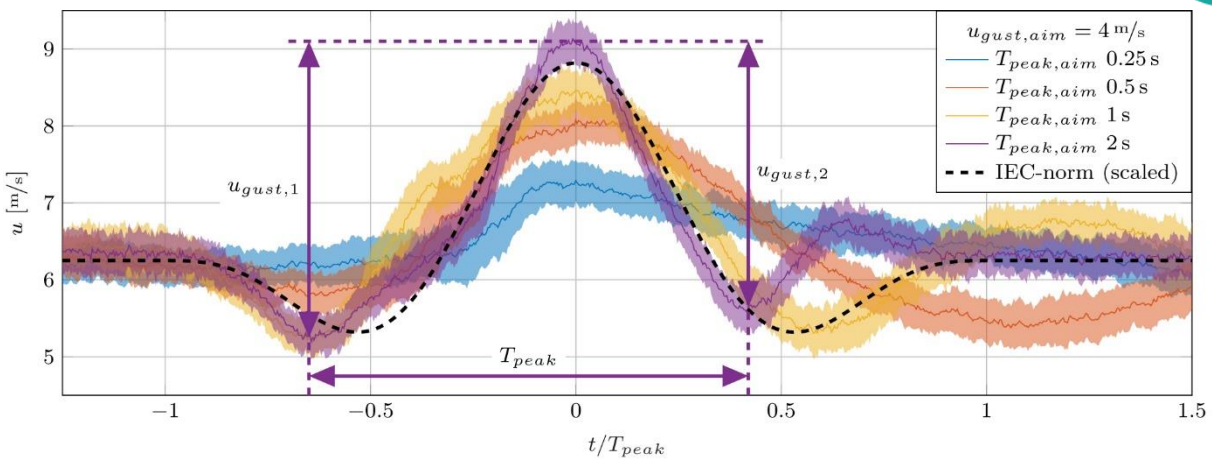

Figure 2: Active grid generated inflow with Mexican hat shape and different gust durations.

The generated flow fields are examined for their cross-sectional correlation, which is desired for pronounced shapes, such as steps and gusts, of the velocity timeseries. Furthermore, the individual limits of the generation process are investigated. Due to the temporal scaling of wind turbine models, very fast velocity fluctuations are necessary. Although some damping of the gust magnitude was observed for high frequencies (short gust durations), it is possible to generate very fast and large velocity fluctuations with the active grid.
With this active grid excitation method, tailored inflow conditions for wind turbine investigations can be generated on a wide range of scales and with large velocity increments even on small time scales.
This provides a good basis for testing wind turbine concepts in the wind tunnel under various reproducible inflow conditions.

References:
[1] Kröger, L., Frederik, J., van Wingerden, J. W., Peinke, J., & Hölling, M. (2018, June). Generation of user defined turbulent inflow conditions by an active grid for validation experiments. In Journal of Physics: Conference Series (Vol. 1037, No. 5, p. 052002). IOP Publishing.
[2] Berger, F., Kröger, L., Onnen, D., Petrović, V., & Kühn, M. (2018, October). Scaled wind turbine setup in a turbulent wind tunnel. In Journal of Physics: Conference Series (Vol. 1104, No. 1, p. 012026). IOP Publishing.

Relevant Wind Energy Research in Small Low-Speed Wind Tunnels

Marlin Holmes[1], Christopher Rumple[1], William Schutz[1], Pourya Nikoueeyan[2], and Jonathan Naughton[1,*]
[1]University of Wyoming
[2]Resono Pressure Systems INC
*Presenting author

Keywords: Turbulence | Wake | Airfoil | Active Grid | Wind Tunnel

Performing testing relevant to wind energy in small, low-speed wind tunnels is challenging. Testing at relevant Reynolds numbers and creating inflows representative of conditions wind turbines experience are examples of these challenges. If such challenges can be overcome, testing in such facilities is attractive due to the low cost of such tests when compared to testing in larger wind tunnels and in the field. As a result, significant investment in developing relevant testing conditions has been undertaken by many groups. Here, approaches employed at the University of Wyoming are discussed and some example results are presented.

Most wind tunnels fail to create free-stream conditions that mimic the inflow experienced by wind turbines. This is important because the interaction of the flow with the blade and the subsequent wake development are highly dependent on the inflow conditions. To address this issue, active grids have been used by several groups to create turbulent inflows that can be controlled to a degree (Hearst 2015, Neuhaus 2020). At the University of Wyoming, an active grid has been developed and installed in the convergent section upstream of the test section. This approach was taken to allow for a longer development length for the turbulence before interacting with the flow of interest. Initial results have shown that this approach is effective in producing turbulence at the test section entrance that is more independent of the grid geometry than traditional installations at the test section entrance.

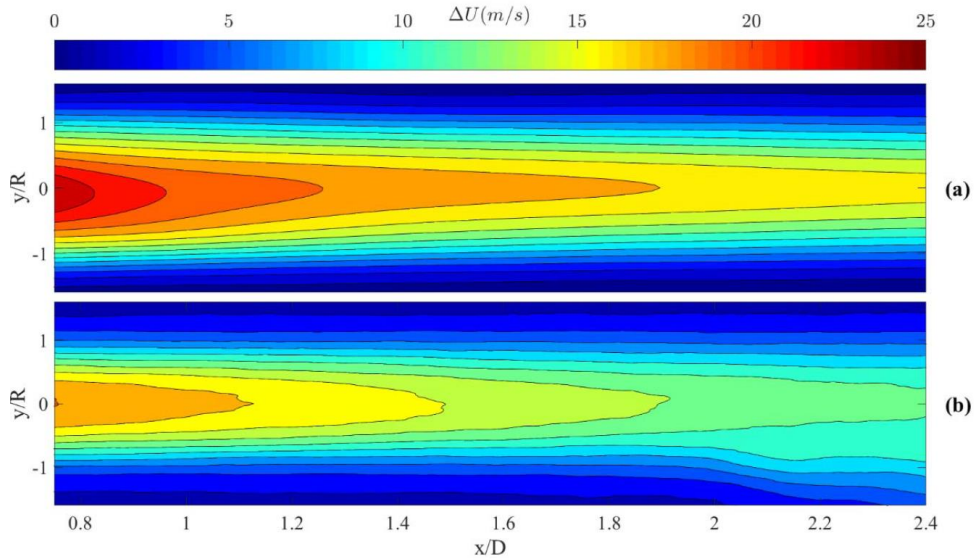

Figure 1: Mean velocity deficit of a rotating wake with and without turbulent inflow

For wind energy applications, the primary interest in the turbulence produced by the active grid is the interaction of the turbulence with a flow of interest. One flow that can be tested effectively in small wind tunnels is the axisymmetric wake as these wakes behave similarly as long as they are beyond a critical Reynolds number (Johansson 2003). At the University of Wyoming, a wake generator capable of producing wakes with rotation, another critical feature of wind turbine wakes, has been developed (Holmes 2017). Recently, the effect of turbulent inflow on the wake produced by this wake generator was investigated. The turbulent inflow clearly increases the wake decay as compared to the wake with the non-turbulent inflow.

Future testing will quantify the impact of the turbulence on wake development for a range of inflow and wake conditions.

Another area where inflow conditions are important is airfoil testing. Most airfoils are characterized in low turbulence conditions that contrast with the highly turbulent conditions in which they often operate. Therefore, testing airfoils under both low- and high-turbulence conditions is necessary to fully understand their performance. At the University of Wyoming, dynamically pitching airfoils have been investigated for the last decade (Naughton 2013). Recently, pitching airfoils have been tested in the presence of turbulent inflow, and large changes in airfoil performance have been observed when compared to that of airfoils tested in typical low-turbulence inflow.

Although challenging, wind tunnel testing relevant to wind energy can be conducted in small, lowspeed wind tunnels. Although such testing is not alone sufficient to fully understand wind turbine flows, tests such as those carried out at the University of Wyoming can be informative when coupled with tests in larger wind tunnels and field tests.

References:

Hearst, R.J. and Lavoie, P. (2015) 'The effect of active grid initial conditions on high Reynolds number turbulence,' Experiments in Fluids, 56(10), p.185. Available at: https://link.springer.com/article/10.1007/s00348-015-2052-1 [Accessed 17 Jan. 2021]

Holmes, M.J., DeMillard, E.J., and Naughton, J.W. (2017) 'Characterization of Wake Initial Condition In uence on Swirling Wake Behavior,' AIAA Paper 2017-0919. Grapevine, TX, 9-13 January. Available at: https://arc.aiaa.org/doi/abs/10.2514/6.2017-0919 [Accessed 17 Jan. 2021]

Johannson, P., George, W., and Gourlay, M. (2003). 'Equilibrium similarity, effects of initial conditions and local Reynolds number on the axisymmetric wake,' Physics of Fluids, [online] Volume 15(2), p. 610-614. Available at: https://aip.scitation.org/doi/10.1063/1.1536976 [Accessed 17 Jan. 2021]

Naughton, J., Strike, J., Hind, M., Magstadt, A., Babbitt, A., (2013) 'Measurement of dynamic stall on the DU wind turbine airfoil series,' Proceedings of the AHS International 69th Annual Forum & Technology Display. Phoenix, AZ, 20-23 May. Available at: https://vtol.org/store/product/measurement-of-dynamic-stall-on-the-du-wind-turbine-airfoil-series-8901.cfm [Accessed 17 Jan. 2021]

Neuhaus, L., Hölling, M., Bos, W.J. and Peinke, J. (2020) 'Generation of Atmospheric Turbulence with Unprecedentedly Large Reynolds Number in a Wind Tunnel,' Physical Review Letters, 125(15), p 154503. Available at: https://journals.aps.org/prl/abstract/10.1103/PhysRevLett.125.154503 [Accessed 17 Jan. 2021]

Mini-Symposium: Challenges in wind tunnel testing in wind energy research (II)

Dynamic induction control for wind farms – an experimental analysis using 3D particle tracking velocimetry

Daan van der Hoek, Carlos Simao Ferreira, and Jan-Willem van Wingerden
Delft University of Technology

Keywords: Wind farm control | Dynamic induction control | Particle tracking velocimetry | Experimental analysis

Wind farms traditionally suffer from wake losses caused by upstream turbines influencing the incoming flow of turbines further down the field. These losses can be partially mitigated by actively influencing the wakes of upstream turbines using wind farm control methods. One of these methods is called Dynamic Induction Control (DIC), which is based on the principle of a periodically varying induction factor (Munters and Meyers, 2018). This action induces additional turbulence in the wake of a turbine, which enhances mixing and subsequently results in faster wake recovery, allowing downstream turbines to extract more energy from the wake.

The potential of DIC was initially shown by means of high-fidelity simulations. More recently, wind tunnel experiments also proved that DIC is able to increase the overall performance of a two-turbine array by measuring the generated power (Frederik et al., 2019). However, a detailed examination of the wake mechanics in an experimental environment is still missing.

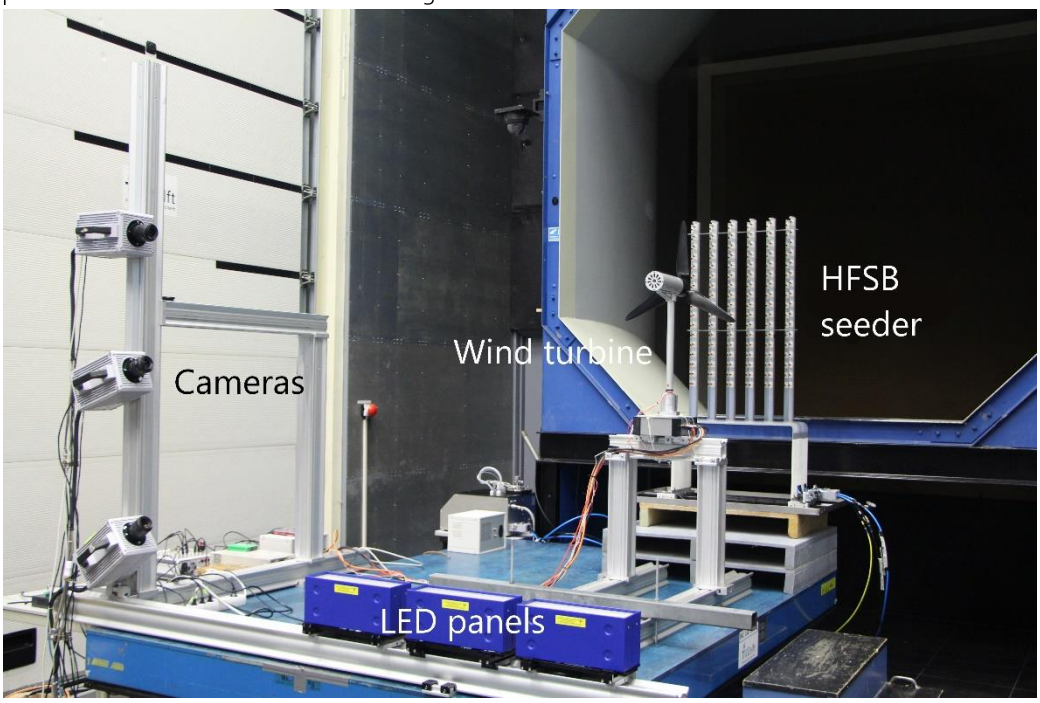

Figure 1: Experimental setup for measuring the wake of a turbine with 3D PTV.

In order to investigate the wake of turbine operating with DIC, a measurement setup for 3D Particle Tracking Velocimetry (PTV) was designed at the TU Delft Open Jet Facility (see figure). Within this setup, Helium-filled soap bubbles (HFSBs) are released in the flow in front of a MoWiTO-0.6 wind turbine (Schottler et al., 2016). After passing the wind turbine, the HFSBs are illuminated by LED panels and simultaneously recorded by a set of three high-speed cameras. This allows the tracking of the HFSBs over time, resulting in a three-dimensional

reconstruction of the wind turbine wake. For comparison, the wind turbine is operated with a baseline controller as well as DIC. The latter consists of applying a sinusoidal reference to the pitch controller. Different pitch frequencies were implemented in order to examine their effectiveness.
Based on the time-averaged measurements that were obtained, it can be seen that the wake of a turbine operating with DIC has a lower velocity deficit compared to baseline operation. This enables downstream turbines to extract more energy from the wind, possibly resulting in an overall increase in power.

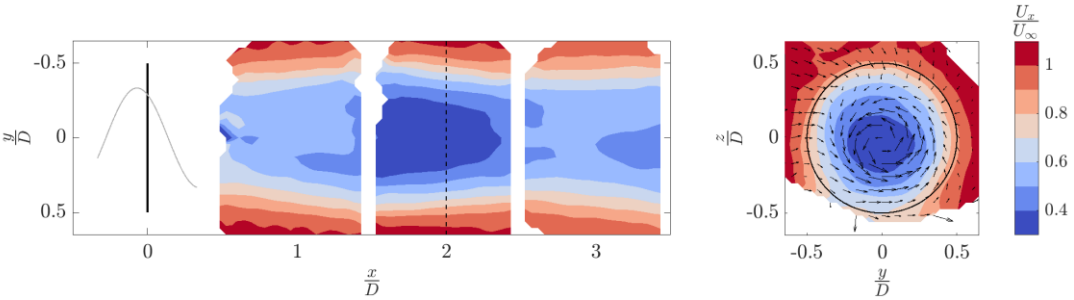

Figure 2: Snapshot of the dynamic streamwise velocity contour of a wind turbine wake obtained with 3D PTV. The turbine is operated with periodically changing pitch angles with the goal of increasing the available energy in the wake.

In order to find out how DIC is able to achieve this lower velocity deficit, the dynamic wake measurements are examined. This is generally done by averaging over the dominant phase of the measurement object (e.g. the rotor speed) in order to obtain a sufficient number of particles and increase the accuracy of the obtained flow fields. In this case, averaging is performed over the pitch frequency, which clearly shows the effect of DIC on the wake over time (see figure). However, this averaging approach can also result in a loss of information, e.g., the vortical structures of the turbine are averaged out. It is possible to solve this problem by increasing the length of the experiment and averaging over both frequencies simultaneously, but the required acquisition time and amount of data make this an infeasible solution. Additional challenges that are encountered are a lower resolution of the wake, illuminating and filming a large volume, and limitations to model wind turbine pitch actuators, among others. The goal of this abstract is to incite discussion on best practice
for measuring dynamic wake effects in large volumes.

References:
Munters, W. and Meyers, J.: Towards practical dynamic induction control of wind farms: analysis of optimally controlled wind-farm boundary layers and sinusoidal induction control of first-row turbines, Wind Energy Science, 3, 409-425, 2018.
Frederik, J. and Weber, R. and Cacciola, S. and Campagnolo, F. and Croce, A. and Botasso, C. and van Wingerden, J.W.: Periodic dynamic induction control of wind farms: proving the potential in simulations and wind tunnel experiments, Wind Energy Science, 5, 245–257, 2020
Schottler, J. and Holling, A. and Peinke, J. and Holling, M.: Design and implementation of a controllable model wind turbine for experimental studies, Journal of Physics: Conference Series, 753, 2016.

Lidar developments for remote wind sensing in an aeroacoustic wind tunnel

Mikael Sjöholm*, Shahbaz Pathan, Sigurd Ildvedsen, Jimmie Beckerlee, Andreas Fischer, Robert Mikkelsen, Jakob Mann, and Christian Bak
DTU Wind Energy
*Presenting author

Keywords: Lidar | wind tunnel | continuous-wave | new concepts and configurations | wake

Simultaneous wind and acoustic measurements in combined aerodynamic and aeroacoustic wind tunnels are challenging using traditional Pitot tube techniques placed inside the wind flow. This is because of the potential acoustic noise generation from in situ probes submerged in a high-speed flow. The potential adverse influence has to be handled with care in aeroacoustic experiments in general and especially in experiments with wind turbine blade profiles optimized to be silent.

At DTU Wind Energy, a project with the aim to accelerate and increase quality in aerodynamic and aeroacoustic design loops (AeroLoop) is currently pursued. One avenue leading towards faster wind tunnel testing procedures would be the use of wind sensing probes that are free from generating acoustic noise, which would allow for simultaneous aerodynamic and aeroacoustic measurements.

The concept explored on this route is based on remote sensing continuous-wave Doppler lidars that are widely used in full-scale wind turbine field experiments where spatially detailed measurements at measurement distances below a few hundred meters are of interest. For instance, the DTU-developed short-range WindScanners are based on continuous-wave wind lidars that also have showed promising potential for remote wind sensing in large boundary layer wind tunnels (Van Dooren et al., 2017) as well as in smaller wind tunnels of various kind (Sjöholm et al., 2017).

Here we present the latest very-short-range wind lidar developments and their application in highspeed aerodynamic and aeroacoustic wind tunnels. Since the length of the probe volume of a continuous-wave lidar varies quadratically with the measurement distance, relevant probe lengths in the centimeter regime can be obtained at measurement distances of a few meters using 3" optics. In particular, the recently established Danish National Poul la Cour wind tunnel at DTU Wind Energy with capability to generate speeds well above 100 m/s in a 3m by 2 m wide tunnel cross-section placed inside an anechoic chamber is used for the experiments reported.

Figure 1: A wind lidar telescope in an anechoic chamber outside of a wind tunnel used for aerodynamic and aeroacoustic measurements of wind turbine blade sections (Photo: Mikael Sjöholm).

The lidar design considerations are outlined with regard to sampling volumes and the beam scanning mechanism. Furthermore, the challenges of optically accessing the wake flow regions of interest in the wind tunnel without generating additional flow-induced acoustic noise are discussed, as well as the challenges of obtaining enough backscattering for the lidar laser light in clean and dry environments. Finally, some first preliminary lidar measurements of the wake from a wind turbine blade section are provided as an example of the capabilities of the concept presented.

Acknowledgments:
Funding from the EUDP grant 64018-0144, "AeroLoop - Accelerate and increase quality in aerodynamic and aeroacoustic design loops" is greatly acknowledged as well as the PhD training network LIKE (Lidar Knowledge Europe) H2020-MSCA-ITN-2019, Grant number 858358 funded by the European Union. Furthermore, the assistance from technicians and engineers at DTU Wind Energy is highly valued.

References:
1. Sjöholm, M, Vignaroli, A, Angelou, N, Nielsen, MB, Mann, J, Mikkelsen, TK, Bolstad, HC, Merz, KO, Sætran, LR, Mühle, FV, Tiihonen, M & Lehtomäki, V 2017, 'Lidars for Wind Tunnels - an IRPWind Joint Experiment Project', Energy Procedia, vol. 137, pp. 339-345. https://doi.org/10.1016/j.egypro.2017.10.358
2. van Dooren, MF, Campagnolo, F, Sjöholm, M, Angelou, N, Mikkelsen, TK & Kühn, M 2017, 'Demonstration and uncertainty analysis of synchronised scanning lidar measurements of 2-D velocity fields in a boundary-layer wind tunnel', Wind Energy Science, vol. 2, pp. 329-341. https://doi.org/10.5194/wes-2-329-2017
3. https://www.plct.dk/

High Reynolds number dynamic stall testing of a harmonic pitching NACA 63-418 aerofoil

Robert Mikkelsen*, Christian Bak, Mac Gaunaa, Andreas Fischer, Anders S. Olsen, Sigurd Ildvedsen, and Jimmie Beckerlee
DTU Wind Energy
*Presenting author

Keywords: Wind tunnel | Dynamic stall | NACA63418

Introduction

Flexing wind turbine blades experience oscillating loads and angle of attack changes when in operation. The impact from turbulence, wind shear and the blade elastic response produce the AoA changes with dynamic stall flow behaviour present at all blade section. Dynamic testing of two dimensional aerofoils have served to explain details of the periodic aerodynamic forces, but are in many cases limited experimentally to moderate Reynolds numbers as compared to Reynolds numbers at operating wind turbine blade, e.g. the Risø-1 profile tested at Re=1.6M [1]. For the NACA 23012, Leishman [2] tested at several Reynolds numbers Re=0.8-2.0M although only found a weakly Re no. dependency for the dynamic stall characteristics of this aerofoil. A different approach to high Re no. testing (Re=3M) using compressed air (~220bar) by Kiefer[3] investigated ramp up/down maneuvers of a NACA0021 foil at relatively high AoA. This setup opens for high Re measurements, but with significant added complexity in testing. Effective experimental investigations of the high Re

dynamic stall phenomenon remains an open and relevant challenge in wind tunnel testing, van Kuik et al.[4]. The present work investigates the dynamic stall characteristics of the NACA 63-418 measured in the Poul la Cour tunnel (PLCT) at Reynolds numbers Re=1.5M-3M and reduced frequencies up to k~0.1 at moderate mean AoA and amplitude variation, $\Delta\alpha$ =2-4deg.

Methodology

The NACA63-418 aerofoil is tested in the Poul la Cour tunnel (PLCT [5]) at DTU Risø campus. The test section measures 2m in height and 3m in width and 9m in length. The 2D aerofoil section is placed vertically having a nominal model chord of 1m and a span of 2m. At midspan, 100 surface pressure tabs are placed in a staggered arrangement around the pressure and suction side. Pressure scanners are placed inside the model, ensuring short tubing and fast response. Whereas the reduced frequency, $k=f\pi c/V$, is in a range comparable to wind turbine blade conditions, the Reynolds number of Re=3M is a step up compared to previous tests, although still not near actual large blade Reynolds numbers.

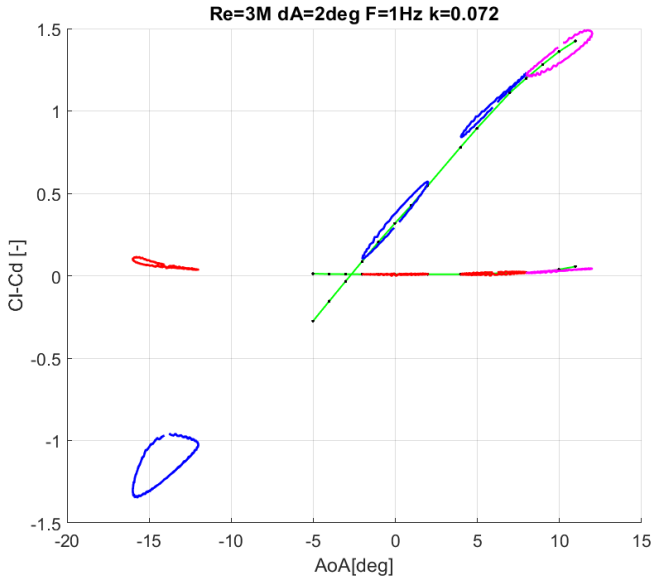

Figure 1: Harmonic pitching of the NACA63418 airfoil, lift and drag coefficients, Re=3M, k=0.072, dAoA=2deg

Results

Harmonic foil pitching is controlled directly through the servo drive i.e. no added mechanism is needed for the PLCT turntable arrangement. First results presented is based purely on gage measurement, shown in the figures with at pitching amplitude of $\Delta\alpha$ =2 deg. A reduced frequency of k=0.072 and Reynolds number 1.5-3M is compared for the 120s binned averaged measured data.

Gage zero data is subtracted, also measured for 120s at zero wind tunnel speed to acquire the resulting dynamic loops for the lift and drag coefficients.

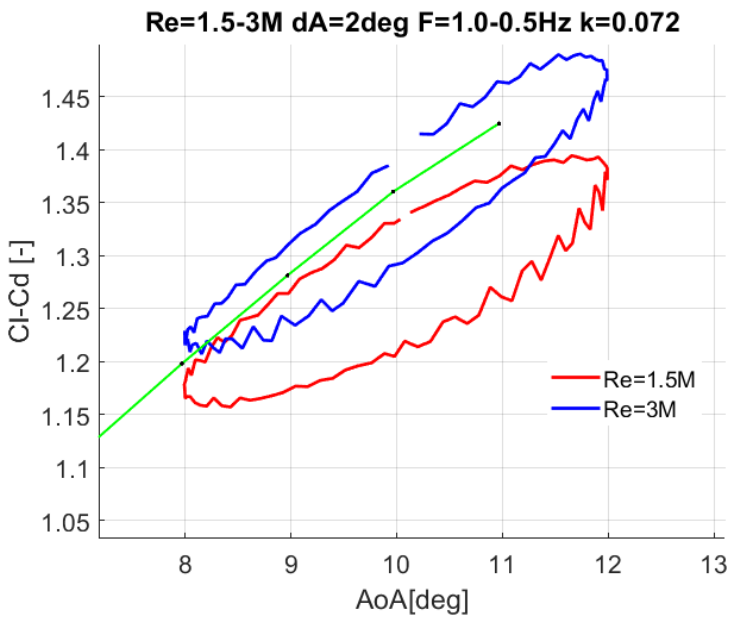

Figure 2: Lift loop at Re=1.5M and 3M, gage measurements only

A clear shift appear present in the lift when increasing Re=1.5M to 3M for mean AoA=10deg, although the mean AoA remains in attached flow. Measurement at negative stalled mean AoA could appear irrelevant for dynamic stall investigation, however, the most outboard part of pitch controlled wind turbine blades does operate in this regime in high winds. Loops at mean AoA =-14deg is shown in the figure and further result will be presented for higher mean AoA.

Conclusions

The Reynolds number dependency on dynamics stall characteristics is mapped out between Re=1.5-3M for the NACA63-418 aerofoil at moderate harmonic pitch amplitudes and in attached flow as well as stalled mean AoA. Also, the dynamic capabilities of the present PLCT turntable arrangement will be reported on.

References:

[1] Fuglsang, P., Antoniou, I., Bak, C., & Aagaard Madsen, H. (1998). Wind tunnel test of the RISØ-1 airfoil. Denmark. Forskningscenter Risoe. Risoe-R, No. 999(EN)

[2] Leishman, JG. Dynamic stall experiments on the NACA 23012 aerofoil. Experiments in Fluids 9, 49 58 (1990)

[3] Kiefer, J.; Brunner, C. E.; Hultmark, M.; Hansen, M. O. L. Dynamic stall at high Reynolds numbers due to variant types of airfoil motion. J. Physics: Conf. Series, DOI:10.1088/1742-6596/1618/5/052028. 2020

[4] van Kuik GAM et al.(chair) . Long-term research challenges in wind energy - a research agenda by the European Academy of Wind Energy. Wind Energy Science 1 pp:1-39 ISSN 2366-7451. 2016

[5] www.plct.dk

Acknowledgement: EUDP-2018-I AeroLoop (64018-0144)

Design and validation of the Poul la Cour Tunnel

Christian Bak[1], Jens Österlund[2], Peter Davidsson[3], Jimmie Beckerlee[1], Andreas Fischer[1], Oliver Lylloff[1], Robert Mikkelsen[1], Sigurd Ildvedsen[1], and Anders S. Olsen[1]
[1]DTU Wind Energy
[2]Fluid Thinking
[3]Faurecia Creo

Keywords: Wind tunnel | Aerodynamics | Aeroacoustics

Introduction

Since the 1990's there has been an increasing need for wind tunnel tests to support wind turbine design. Especially there has been a need within design and characterization of wind turbine airfoils.

In the start, aerodynamic tunnels were used, where there was only minor focus on the flow quality and no focus on the aeroacoustic characteristics. With the increasing size of the wind turbines, there has been an enhanced focus on both the flow quality and the aeroacoustic characteristics.

DTU Wind Energy observed a need for a wind energy dedicated wind tunnel. In 2011 specifications for a new wind tunnel were established in a collaboration with the Danish stakeholders within wind energy. It was decided to establish a large wind tunnel dedicated to airfoil tests where both aerodynamics and aeroacoustics could be characterized. The wind tunnel was designed from 2012 to 2015 and the wind tunnel with all its aerodynamic and aeroacoustic features was established in December 2019. The basic specifications for the wind tunnel is presented in the list below and a sketch of the wind tunnel is shown in Figure 1.

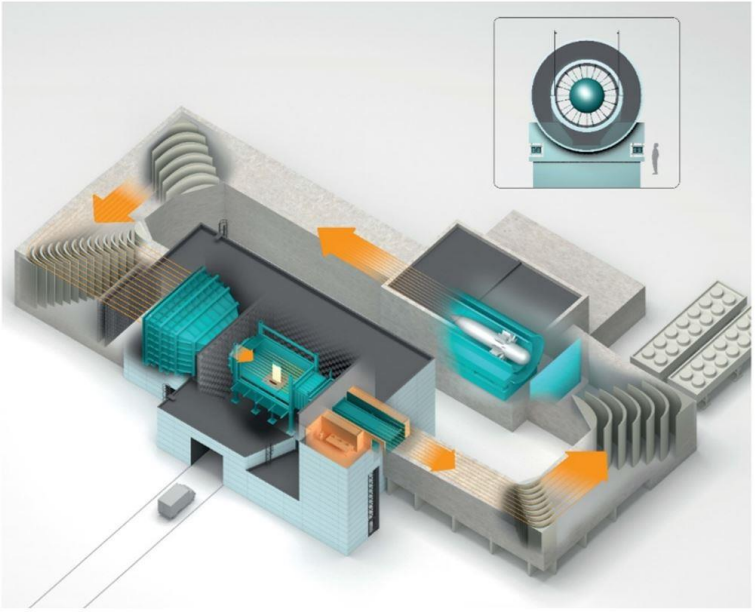

Figure 1: Sketch of the Poul la Cour Tunnel

- Maximum Reynolds number per meter [-] = 7.0x106 [-]
- Maximum flow speed = ~105m/s or 378km/h
- Test section: Width = 3.00m
- Test section: Height = 2.00m
- Test section: Length = 9.00m
- Maximum turbulence intensity = Max 0.1%
- Anechoic chamber: background noise at 60m/s with Kevlar walls 2m from airfoil < 70dB
- Design flow speed for acoustic measurements = 60m/s

The resulting design was a closed-return airline with a closed test section. The test section has two different configurations: 1) the aerodynamic test section with hard walls and 2) the aeroacoustic test section with

Kevlar walls that are porous. The resulting test section configurations can be seen in Figure 2 and a further description can be found at www.plct.dk.

Figure 2: The Poul la Cour Tunnel test section

Results

In the presentation the background and the arguments for the specifications will be presented. Details of the design will be shown such as the airline design with its choice of material, diffusor designs, the corner designs with their guide vanes, the contraction with its contraction ratio of 9, the turbulent screen design, the components contributing to the acoustic absorption, the fan design with its 4.7m diameter and 2.4MW power and the cooling system. Apart from the airline design also the design of the test section design with details on the turntable and wake rake will be presented. Apart from the design, also validation of the aerodynamic and the aeroacoustic performance will be shown, such as the predicted losses compared to the actual losses, the maximum flow speed, the turbulence level and the background noise. Finally, a benchmark of an airfoil with other wind tunnels will be shown.

In the presentation the appropriateness of the specifications will be discussed, the decisions made in the design process will be explained and the challenges in the aerodynamic and aeroacoustic airfoil measurements will be presented.

Acknowledgement

The establishment of the Poul la Cour Tunnel was supported by the Danish Agency for Research and Innovation and Region Zealand. Measurements are supported by the Danish Energy Agency in the EUDP-2018-I project AeroLoop.

How to get more out of your PIV data: A hybrid approach to increasing temporal resolution

Tom T. B. Wester*, André Fuchs, Joachim Peinke, and Gerd Gülker
ForWind, University of Oldenburg
*Presenting author

Keywords: Particle Image Velocimetry (PIV) | High Resolved Spectra | Fractal Grid | Turbulence

Compared to other measurement techniques, Particle Image Velocimetry (PIV) has become increasingly popular in the field of fluid dynamics in recent years. PIV has the advantage that a spatial measurement of flows is possible without traversing. Moreover, the systems available today allow an increasingly simple application of this spatio-temporal measurement method to all types of flows e.g. turbulent flows ([Lavoie2007, Doorne2007, Piirto2003]). This outweighs in many experiments the high temporal resolution of hot-wires. For further statistical evaluations of the turbulent structures, however, the 1-10 kHz frame rates available today are often not sufficient to adequately resolve the turbulent spectra, for example. For this reason, one-point measurements with hot wires are often used again for these measurements.
This study will present a new approach of using high speed PIV data to extract temporal high resolved time series. This new approach makes it possible to calculate spectra from the given flow fields with frequencies far above the frame rate of the measurement itself. In contrast to the previously known methods, which use either the high temporal resolution or the good spatial resolution [Foucaut2004], this approach combines both of these advantages of PIV. This allows a local analysis comparable to hot-wire measurements of the flow, covering a large spectral range.

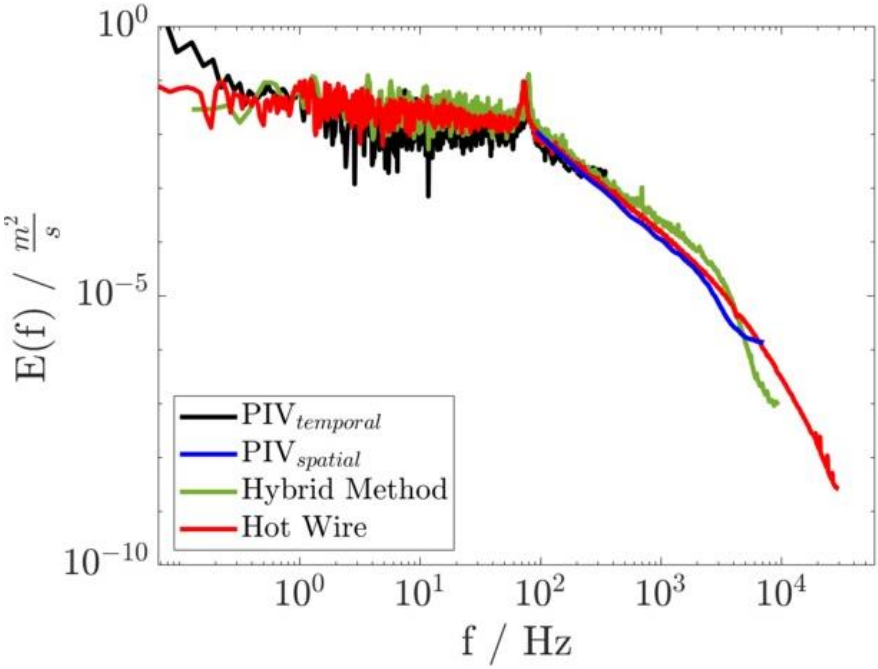

Figure 1: Spectra 25 cm behind a fractal grid calculated from PIV data using temporal resolution, spatial resolution, and a combination of the two compared to high-resolution hot-wire measurements.

In order to validate the method experiments were carried out in a Göttingen type wind tunnel with the test section size of 25cm x 25cm x 200cm (height x width x length) made from acrylic glass to enable optical access. To generate a characteristic and well-known turbulent flow, a fractal grid with three iterations was used, which fits exactly into the nozzle with the dimensions 25cm x 25cm. During the experiments the free stream velocity was set to u_\infty = 10 m/s. This given flow field was investigated by high speed PIV with a sampling rate of 693Hz at four positions covering a range from 11cm to 119cm behind the grid with a spatial resolution of around 1mm x 1mm. The field of view (FOV) of each position was about 21cm x 19cm. To verify

the spectra from the new approach, hotwire measurements were made using a 1D probe and a Dantec StreamLine system along the centerline from 5cm to 176cm at 2cm-5cm intervals and a sampling rate of 60kHz for 60s per measurement point.

Fig. 1 shows the calculated spectra using the temporal resolution of the PIV measurement (black), the spatial resolution of the measurement(blue), the hot-wire measurement(red) and the new approach (green) at a position 25cm behind the grid. In the figure, a peak can be seen at about 75Hz, which is characteristic of the fractal grid. It can also be seen that this peak is detected by all methods except spatial method. The reason for this is that the low frequency range of the spatial method is limited by the size of the FOV. Therefore, large structures are not captured sufficiently well. On the other hand, the high frequency range can be covered with this approach. The situation is different for the temporal approach. This approach captures the peak very well, but due to the temporal resolution no frequencies above 346.5Hz can be captured. The new hybrid method, on the other hand, shows very high agreement with the hot-wire measurements from very low to very high frequencies.

References:
P. Lavoie, G. Avallone, F. De Gregorio, G. Romano, R. Antonia, Experiments in Fluids 43(1), 39 (2007) C. Van Doorne, J. Westerweel, Experiments in Fluids 42(2), 259 (2007)

Mini-Symposium: Research at Germany's First Offshore Wind Farm alpha ventus

Bernhard Lange
Fraunhofer Institute for Wind Energy Systems (IWES)

Kai Herklotz
Federal Maritime and Hydrographic Agency (BSH)

Since 2010, the first German offshore wind farm alpha ventus is operating successfully in the German North Sea. The accompanying research initiative RAVE (research at alpha ventus) has been collecting more than 30TB of data from some 1200 measurement channels in alpha ventus. Funded by the German government, RAVE's goal is to promote research into offshore wind energy by making this completely unique data available for research purposes. Since 2019, these data are available through a simplified access concept and are hosted by the German Federal Maritime and Hydrographic Agency, providing longterm availability. We invite you to learn more about RAVE, the RAVE data and the research results obtained with it in this Mini Symposium. The aim of the symposium is to foster the exchange between all researchers interested in data from alpha ventus. The workshop will present current research at alpha ventus on the one hand, on the other provide room for intensive exchange between researchers from diverse fields. You are welcome to join by presenting your research and/or adding your expertise to the discussion

Mini-Symposium: Research at Germany's First Offshore Wind Farm alpha ventus (I)

Research at the German test site alpha ventus – an overview

Bernhard Lange[1,*], Kai Herklotz[2], and Marten Schmager[2]
[1]Fraunhofer IWES
[2]Federal Maritime and Hydrographic Agency (BSH)
[*]Presenting author

Keywords: offshore | test field | measurement data | RAVE

The first German offshore test site „alpha ventus" was built in 2009 to support the development of offshore wind power. Twelve 5 MW wind turbines were erected under genuine offshore conditions.
Alpha ventus' mission was to gather fundamental experience with focus on the commercial use of offshore wind power in Germany. The research initiative „Research at alpha ventus" (RAVE), with support by the Federal Ministry for Economic affairs and Energy, brings together technical and environmental research, development and demonstration (R,D&D) activities of turbine manufacturers and research institutions in a coordinated effort.
A comprehensive measurement program lays the basis for a multitude of scientific activities in more than 35 research projects. 4 of the 12 turbines of alpha ventus are equipped with extensive measurement systems. These include measurements at the two different turbine types (Adwen 5000M und Senvion 5M) and foundation types (tripod and jacket). Electrical measurements are performed at both the offshore and onshore substations. Directly next to the wind farm there is the 100m high meteorological measurement mast FINO 1, accompanied by oceanographic measurements at the mast and in the wind farm. At times, there were more than 1200 measurement channels in operation and more than 30 TB measurement data were collected up to now. The measurements are continued, and the data basis is continuously growing.
It is the main objective of RAVE to foster research in offshore wind power by providing these worldwide unique data to researchers. All measurement data are stored in the RAVE data base, which is operated by the German Federal Maritime and Hydrographic Agency (BSH).
In this contribution, the results and experiences of RAVE will be summarized and the available measurement data and access to them will be discussed.

Virtual loads predictions of wake-affected wind turbine: comparing Gaussian Process Regression with Artificial Neural Networks

Imad Abdallah[1,*], Luis David Avendaño-Valencia[2], Anish Venu[3], and Eleni Chatzi[1]
[1]ETH Zurich
[2]University of Southern Denmark
[3]DNV GL
[*]Presenting author

Keywords: virtual sensing | Gaussian Process Regression | Artificial Neural Networks

Load analysis of wind turbines may be performed either via physics-based models or via direct measurement. On the first case, loads are calculated with aero-elastic models, based on significant assumptions on the mechanical and aeroelastic properties of the structure and the acting forces (wind, wave and control). Otherwise, loads can be directly measured based on a sensor network, which entails increased costs due to installation, maintenance and calibration of sensors and IT infrastructure. These costs can be manageable for a single wind turbine but become substantial on densely instrumented wind farms. In turn, the increased costs negatively affect the levelized cost of energy. This is, in fact, the main reason why stakeholders shy away from applying monitoring technologies in wind farms. To overcome the above challenges, we need an alternative way of estimating the loads which would involve a reduced number of sensors while replicating the actual load measurement scenario. To this end, we propose data-driven models to predict the loads acting on different components of a wind turbine. These models use SCADA, wind inflow and other variables to predict loads in components of interest of a wind turbine. We have already successfully demonstrated this concept in the past on simulated wind turbine Damage Equivalent Loads (DELs) based on Gaussian Process regression [1,2], and on real wind turbine data [3].

In this work, we validate this approach on actual wind turbine data from the Alpha Ventus Wind Farm obtained within the framework of the Research Alpha Ventus (RAVE) project. Two Senvion turbines are selected for this study. One of the wind turbines is used to train and validate a regression model to predict the tower base DELs based on SCADA, wind inflow and other environmental variables.

Afterwards, the trained model is used to predict the loads in the second wind turbine. Load prediction is attained with two machine learning methods, the first one based on Gaussian Process Regression (GPR) and the second one based on Artificial Neural Networks (ANN). For the first one, a decision tree is used to separate the different operating modes of the wind turbine (idling, operating and transitioning). The decision tree is built on simple heuristics on a subset of SCADA variables (mean and standard deviation of the rotor RPM and blade pitch angle). Subsequently, a GPR is built for each one of the operating modes. In the second method, the SCADA variables are fed to the ANN after undergoing an initial transformation for data compression and collinearity reduction.

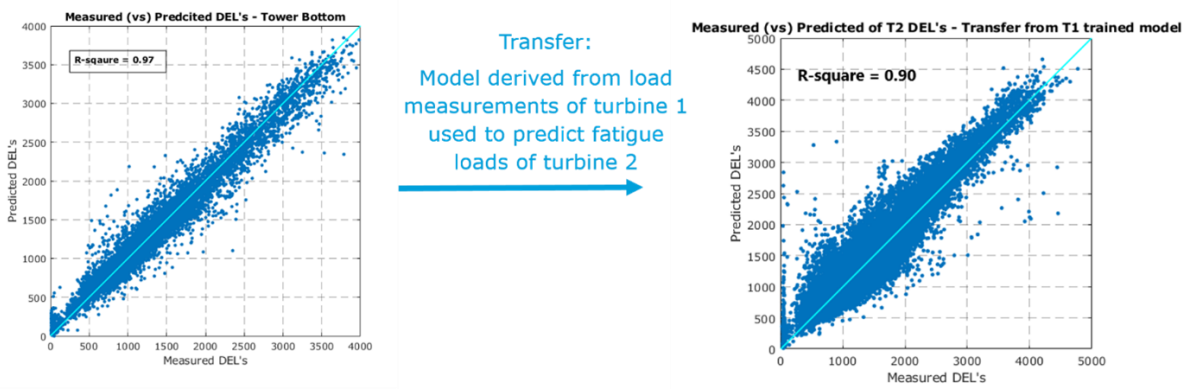

Figure 1: Method 2 ANN: results of tower bottom bending moment after model transfer from AV04 to AV05.

Figure 1 shows the loads predicted with the ANN method vs measured loads on both wind turbines (AV04 for model training/validation; AV05 only validation). The coefficient of determination (R^2) on the validation set in AV04 is about 0.97, while in AV05 reaches 0.9. The method based on GPR reaches a value of R^2>0.99 in the prediction of average tower base loads in AV04, while the implementation on DELs from AV04 and AV05 is still under construction. Both implementations would enable owners/operators to obtain realistic estimates of the loads acting on the turbines (including wake effects) in a cost-effective way. The models are not limited to any structural component. Instead, these can be used to estimate the loads acting on all prominent structural components of the turbine.

References:
1. Avendaño-Valencia, L.D., Abdallah, I., and Chatzi, E., 2020. Virtual fatigue diagnostics of wake-affected wind turbine via Gaussian Process Regression. URL engrxiv.org/ygrkf
2. Avendaño-Valencia, L.D., Abdallah, I., and Chatzi, E., 2018. "On the differences in the dynamic response of up-wind and waked wind turbines: Analysis via surrogate Gaussian Process time-series models", in Proceedings of the joint ICVRAM, ISUMA, UNCERTAINTIES conference, Florianopolis, Brazil, April 2018.
3. Venu, A., Lüdde, M., and Omole, J., Prediction and Validation of Fatigue loads using Artificial Intelligence on Real World Measurement Data, Journal of Physics: Conference Series, 1618, 022006, 2020.

The use of sensor data for the monitoring of corrosion processes on offshore wind power structures

Andreas Momber[1,*], and Daniel Brün[2]
[1]Muehlhan AG
[2]saltation GmbH
[*]Presenting author

Keywords: Sensor | Corrosion | Monitoring | Maintenance

Corrosion is one of the most demanding challenges with respect to a high reliability of wind power structures during their operation time. This applies particularly to load-carrying structural parts, such as foundations and towers.
In recent times, permanent sensor-based monitoring of critical parts of offshore wind power structures became an interesting tool in terms of maintenance and lifetime assessment. This new approach is basically related to atmospheric data, vibration data and power output data. The use of sensor data for the assessment of corrosion processes, however, has not been thoroughly investigated yet.

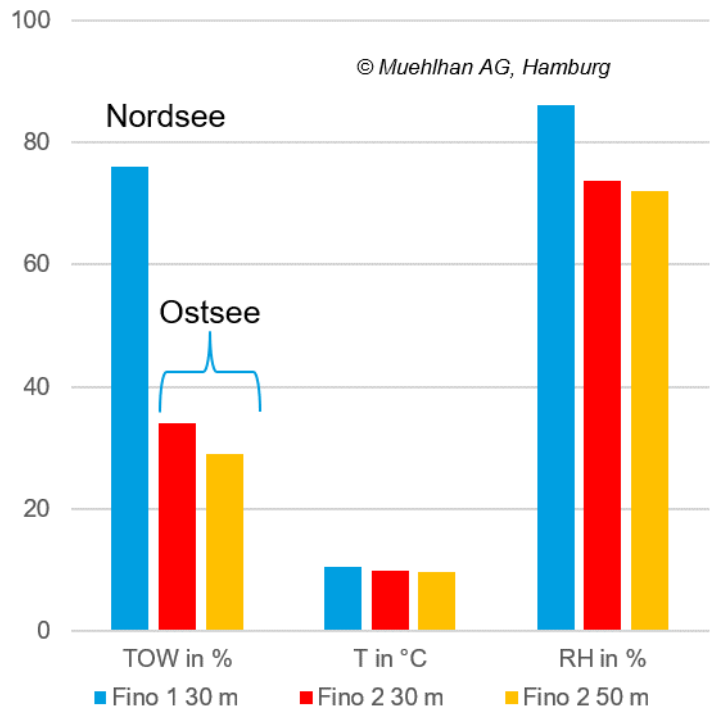

Figure 1: Data utilization and estimation of time of wetness in the North Sea and the Baltic Sea

The corrosive loads on structures are characterized through corrosivity categories, whereby offshore structures operate under the highest corrosivity category (CX) currently specified. This category is, however, specified based for one year of exposure only. The precise progress of corrosion over longer periods depend on environmental parameters. Most important primary parameters for the corrosion of steel in marine/offshore atmospheres (transition pieces, towers, nacelles) include air temperature, relative air humidity, and chloride deposition rate. Other parameters, however, have notable secondary effects and shall be considered as well. This includes precipitation (rain), wind speed and wind direction, wave height, and radiation (UV, solar).
Primary parameters for the progress of corrosion of immersed (under water) structural parts (foundations) include water temperature, dissolved oxygen, pH value, and water flow velocity. These parameters have also strong effects on the formation of fouling on immersed structures and on the design of cathodic protection

systems. New regulations for cathodic protection require the consideration of atmospheric (meteorological) parameters for the design of cathodic protection systems, namely wave height, tidal movement and water flow velocity.

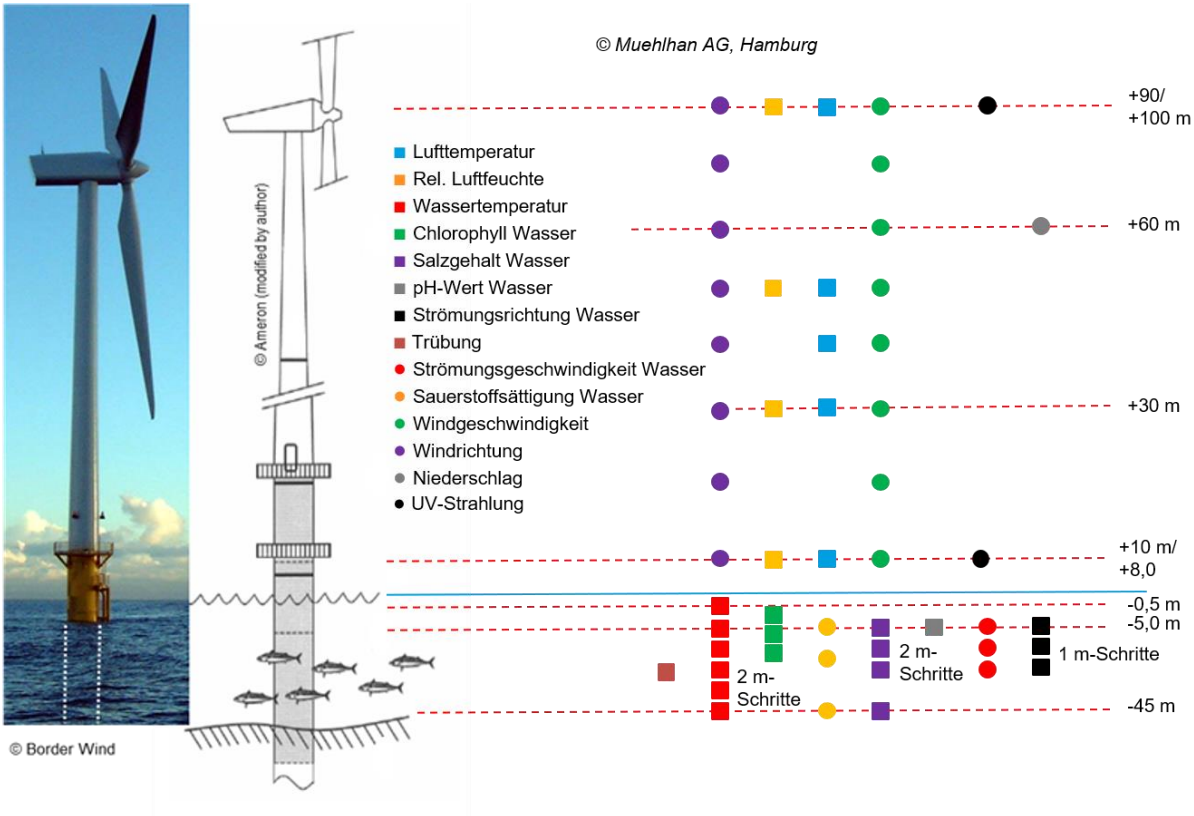

Figure 2: Sensor availability in the Baltic Sea.

Data are available for the majority of the above mentioned parameters, either from alpha ventus (RAVE) sensors or from the BSH sensor network in the North Sea and the Baltic Sea (including the FINO met platforms).

This presentation defines the requirements for sensor data to be included in two corrosion rate models, one for atmospheric offshore corrosion and one for seawater corrosion. The availability of the data is discussed along with the geographical and local situation of the respective sensors.

The utilization of big data (sometimes 300.000 data for a 6-months measurement period) requires particular treatment. An important step in using large amounts of automatically generated sensor data is data clearing-up. This step involves elimination of outliers, testing for data consistency, data interrelationships, interpolation of missing data.

Based on sensor data from alpha ventus and from the BSH sensor network, examples are presented for how to use this data for particular applications to corrosion assessment and cathodic protection design.

The results are obtained in the course of the project "ISyMOO" (Intelligente integrative Systeme für das Monitoring von Oberflächenschutzsystemen an Offshore-Windenergiekonstruktionen), which is funded by the German Federal Ministry of Economic Affairs and Energy.

Mini-Symposium: Research at Germany's First Offshore Wind Farm alpha ventus (II)

Marine Radar Wind and Wave Measurements for Short Term Forecasts

Jochen Horstmann*, Ruben Carrasco, and Michael Streßer
Helmholtz-Zentrum Geesthacht
*Presenting author

Keywords: marine radar | wind fields | wind gusts | extreme waves | short term forecast

Extracting the mean wind vector and spectral wave parameters (e.g. significant wave height and peak period) from marine radar data is well developed. However, determination of surface wind fields and individual waves in space and time is still a challenging topic, due to the complex nature of the radar modulation transfer function. Coherent marine radars measure in addition to the backscatter intensity the radial velocity of the scatterers, which is strongly related to surface wind, waves and currents. We will introduce new methodologies to retrieve ocean surface wind as well as individual wave fields using both the intensity as well as the Doppler information measured by the radar.

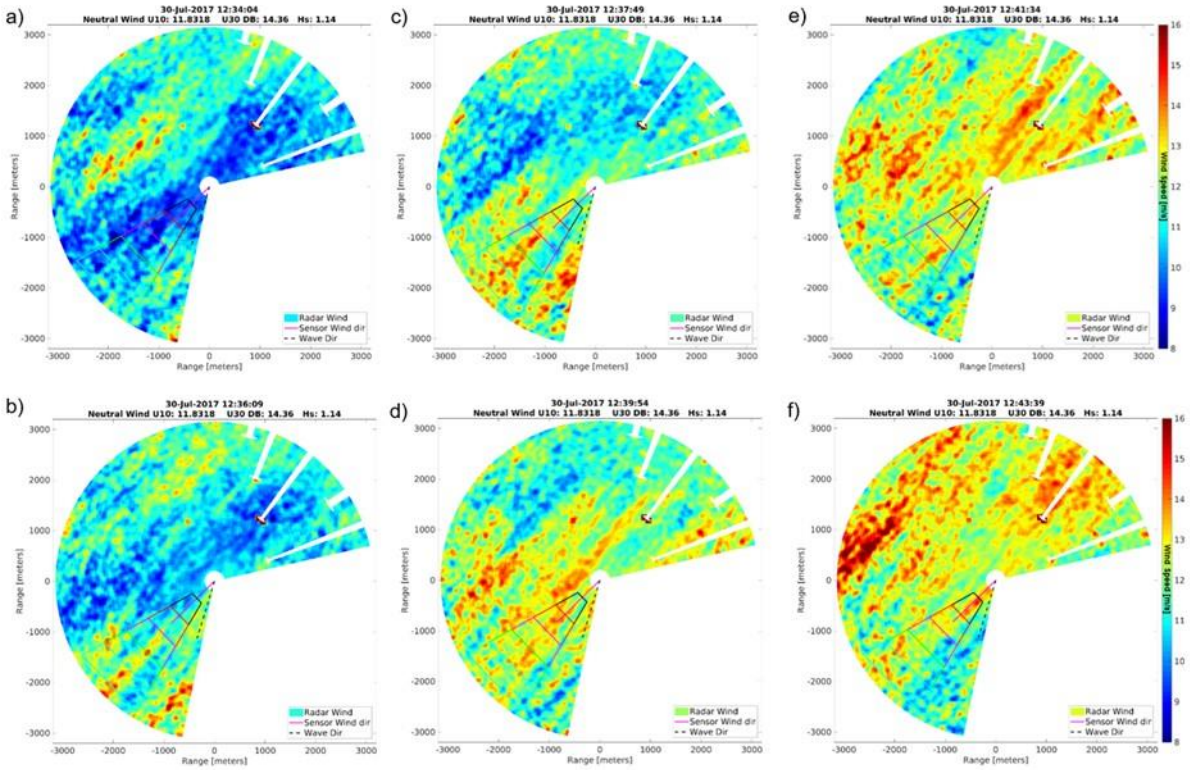

Figure 1: Radar retrieved wind field sequence from 30. July 2017 between 12:34 (a)) and 12:44 UTC (f)) at the off shore wind farm Dantysk in the German Bight of the North Sea. Every wind field represents the mean wind speed over 60 s and has a spatial resolution of 30 m. This example shows the potential of the radar retrieved wind fields for observing wind gust in space and time.

We will show results under various wind and wave situations and compare our resulting fields to in situ measurements. We will utilize these measurements for short term (30 to 60 s) forecast of wind gusts (Figure) and individual waves, which could help to improve the predictive control of wind farms as well as aviation operations (e.g. landing on vessels).

Wind conditions within the first fully developed offshore cluster N2 in comparison to long term trends – measurements at FINO1

Richard Frühmann*, Thomas Neumann 1, Juan Trujillo, Beatriz Canadillas, and Nick Hansen
UL International GmbH
*Presenting author

Keywords: Wind Measurements | FINO 1 | Scanning Lidar | Windpark-Cluster | Long-term Wind Measurement

This paper presents the long term wind statistics time series measured at FINO1, that now include data from the first year of operation within the now fully developed and operational wind farm cluster N2. The annual statistics, in particular for mean wind speed and turbulence intensity are compared with 4-year periods during different stages of construction and operation of the surrounding wind farms. For selected periods, conditions within the wind farm are compared with Lidar measurements conducted on the nearby light ships German Bight and TW Ems that represent as near as possible the undisturbed conditions.
Results show that the operating conditions for wind turbines in the offshore cluster (in particular for the oldest wind farm Alpha Ventus) have changed during the last years as a consequence of the increased number of wind turbines in operation. This is of particular interest for the direction and execution of research projects within RAVE, as the turbines are now exposed to conditions very different from those originally assumed in the design brief. On the larger scale, this finding is relevant to the design of new offshore wind turbines and the layout and planning of offshore wind farms.

Assessment of two wind field generation methods for the simulation of wake loads

Matthias Kretschmer, and Po Wen Cheng
University of Stuttgart

Keywords: wind farm loads | validation | fullscale measurements | alpha ventus

Wake effects inside offshore wind farms contribute significantly to the overall structural fatigue loads of the individual wind turbines. Therefore, it is crucial to address wake-induced loads properly in numerical calculation tools which are for example applied in the design of new wind farms or in lifetime extension efforts of existing wind farms.
In this study, we focus on two methods for calculating the structural loads of wind farms which are suggested in the IEC 61400-1 Ed. 4 standard: 1) The effective turbulence (ET) method (Frandsen, 2007), 2) the dynamic wake meandering (DWM) method (Larsen, 2008). Both methods are evaluated against measurement data from the wind farm alpha ventus focusing on the prediction of structural loads in single wake situations.
In a first step, environmental conditions acquired at the Fino 1 met mast are analyzed. The meteorological data are aggregated in a way that based on three atmospheric stability classes (unstable, neutral, stable) functions of turbulence intensity and vertical wind shear dependent on the wind speed are derived. Mann's method (Mann, 1994) is used as basis to generate three types of wind fields representing: 1) freestream conditions as reference, 2) wake conditions with the ET method, 3) wake conditions defined by the DWM method. The Mann wind field parameters (turbulence length scale L, shear parameter Γ) are adapted to match the aggregated meteorological conditions. Sea states are transferred to the simulations by using a JONSWAP spectrum fed by the measured significant wave height and mean wave period.

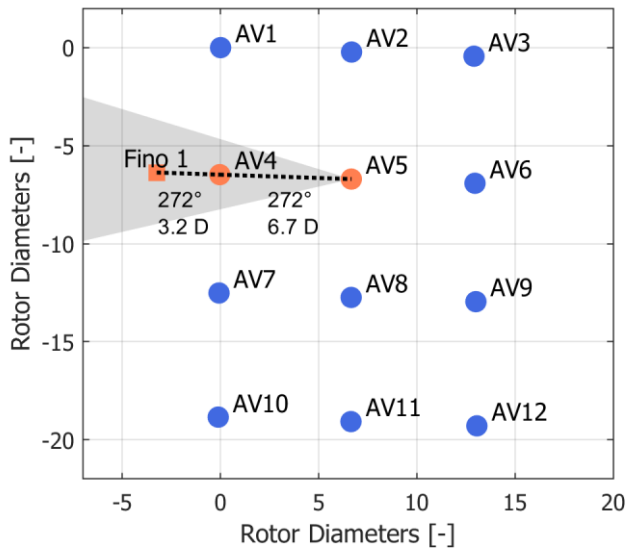

Figure 1: Wind farm layout of alpha ventus including Fino 1 met mast. North is pointing up. Shaded triangle indicates the considered wind direction sector 257–287 [deg] seen from AV5

In a next step, the considered turbines AV4 and AV5 of type Senvion 5M (see layout in Figure 1) are modelled in the software OpenFAST. The simulation models of both turbines are adjusted individually to account for asymmetries of the real wind turbines (e.g. pitch errors, mass imbalances).
Simulations are run with the turbine model AV4 for freestream conditions and AV5 for wake conditions. Metrics of turbine operational performance (e.g. power, blade pitch) as well as structural loads (bending

moments at blade root and tower base) are compared in terms of statistical data such as mean, standard deviation and damage equivalent loads.

Analysis of the results reveal good agreement of the DWM method with the measurement data. Trends of power deficit and structural loads distribution dependent on the wind direction are reproduced for wake conditions. The ET method gives only wake loads at one level which are not dependent on the wind direction and for instance do not include partial wake situations. Results show that the ET method gives conservative predictions of structural loads compared to the DWM method. It is found that the results are sensitive to the definition of atmospheric stability. In general, better agreement of simulations with measurements is observed for unstable and neutral conditions. The simulations with stable atmospheric stratification tend to underpredict the measured structural loads.

References:
S. Frandsen (2007) Turbulence and turbulence generated structural loading in wind turbine clusters, Risø report R-1188 Larsen, G.C., Madsen, H.Aa., Thomsen, K., and Larsen, T.J. Wake meandering – a pragmatic approach. Wind Energy, 11, 2008, p. 377–395
Mann, J.: The spatial structure of neutral atmospheric surface-layer turbulence, Journal of fluid mechanics, 273, 141–168, 1994.

Inter-disciplinary approach for sustainable offshore wind farm decommissioning

Vanessa Spielmann*, and Silke Eckardt
City University of Applied Sciences Bremen
*Presenting author

Keywords: offshore windfarm end-of-life process | decommissioning strategies | sustainable offshore decommissioning

At the end of their operational life, offshore wind farms need to be decommissioned. As large-scale energy production from offshore wind really established just over the last decade, only few experiences on decommissioning these structures are available. There are still major uncertainties, for example regarding suitable technology and feasibility of dismantling wind turbine foundation structures, reliability of cost and time estimations as well as impacts on the environment. Also, benefits and drawbacks of different scopes of decommissioning, regarding the removal of inner array cables, scour protection and wind turbine foundations, and their effects on overall decommissioning costs, marine environment and subsequent use of offshore wind farm areas are not known yet.
Within the research project "SeeOff - Development of efficient strategies for offshore windfarm decommissioning", we are developing a process-oriented and indicator-based approach for analysing decommissioning strategies with a holistic assessment. Technical, organisational and regulatory requirements as well as objectives for a sustainable decommissioning are compiled. Different options on technologies, logistics and scopes of decommissioning are investigated and combined to decommissioning scenarios. These scenarios cover the entire end-of-life process, from dismantling the structures offshore, processing the components onshore up to recovering secondary raw materials and secondary fuels. Thereafter, the scenarios are assessed using economic, environmental as well as social indicators and multi criteria decision analysis is applied in order to identify sustainable decommissioning strategies for the offshore wind farm under consideration.

Mini-Symposium: Machine Learning and big data applications in wind energy

Lars Landberg
DNV GL

Following on from last WESC's very succesful mini-symposium this year's mini-symposium will address all applications of machine learning (ML) in the wind energy space. Big data will be an important element too. The mini-symposium will emphasise the use of different machine learning and big data methods, and abstracts should address this.

The symposium will address the different ML techniques available, starting from simple perceptrons but the latest and most advanced models will also be described and discussed. A goal of this symposium is that the audience will get inspiration to not only how ML can be used in their own fields but also what are the drawbacks of the very wide range of methods available. Discussions about explainability are also envisaged, how can we prise valuable information out of these in principle black boxes? We will also discuss biases in training and testing data sets and how to avoid them, and finally reliability and applicability of the various methods should be discussed.

Mini-Symposium: Machine Learning and big data applications in wind energy (I)

Bayesian neural network model for estimating fatigue loads on wind turbines

Omole John Adetoyese[1,*], David Schlipf[2], Mike Ludde[1], and Anish Venu[1]
[1]DNV-GL
[2]Flensburg University of Applied Sciences
[*]Presenting author

Keywords: Bayesian Neural Network | Probabilistic Machine Learning | Fatigue Loads | Load Estimation | Blade Loads

The operation of wind turbines usually focuses on generating as much energy as possible over the lifetime while keeping the structural loads of mechanical components within their design limits. The loads are mainly caused by continuous change in mechanical stress levels due to stochastic variability of the turbine wind inflow. Thus, the monitoring of fatigue loads is very crucial for the operation and for possible lifetime extensions. However, continuous load measurements on each wind turbine is very expensive.
Recent studies have shown that fully connected layer neural networks can be valuable to extract useful insights from both measurement and simulated load data [1, 2]. The application of Artificial Neural Network (ANN) techniques on wind turbine historical data has proved to accurately estimate loads on the turbine structural components based on Supervisory Control and Data Acquisition (SCADA) data only or with additional acceleration sensor data. Load measurements are only needed for the training of the neural network.
The artificial neural network training optimizes the network parameters, i.e. bias and weight using maximum likelihood estimation method [3]. The ANN uses point estimation which is easy to compute but is prone to overfitting and overconfidence [4]. However, Bayesian Neural Network (BNN), introduced a probabilistic approach through the Bayesian Theorem in which the posterior distribution is modeled. The BNN uses probability distributions over possible values for the weights, rather than having a single value as the ANN, see Figure 1. Intuitively, the Bayesian neural network can then produce probabilistic guarantees on it's estimations and also generate the distribution of the parameters that it has learnt from the observations and fine-tune its learning from the data to action decision making [5].

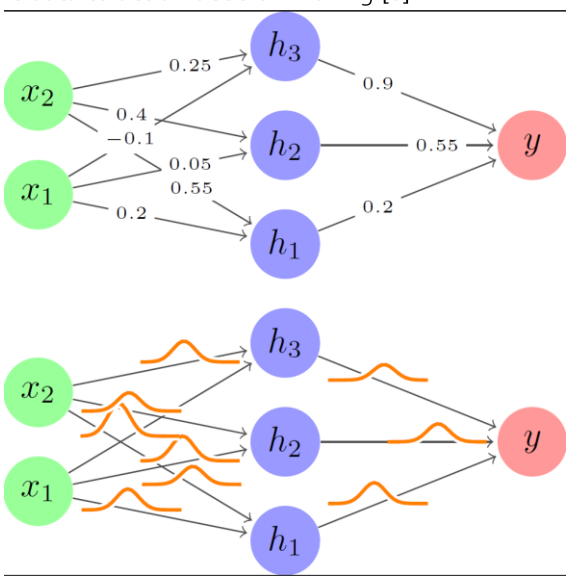

Figure 1: Scalar weights used for Artificial Neural Network (top) and probability distributions used as weights of the Bayesian Neural Networks (bottom), based on [5].

In this project, we consider an onshore wind farm, containing eight 2 MW wind turbines from which one is equipped with load and acceleration measurements. The fatigue loads used in this project are measured in accordance with IEC TS 61400-13. The input data for the BNN are the SCADA and acceleration data, the output considered in this work are the blade flapwise bending moments.
The raw data from the wind turbine undergoes several stages. First, the data is preprocessing which comprises the load calculation (Wöhler exponent of 12 for blades), data cleaning (removal of start-up and shut-down). Finally, a Principal Component Analysis is performed to avoid the curse of dimensionality and other problems mostly encountered in machine learning during training and prediction. The model initialization of the Bayesian neural network is done using a Gaussian distribution of the parameters. Then the probability distribution on the weights of the model is learned to give the predictive distribution of the outputs used in estimating the validation data.

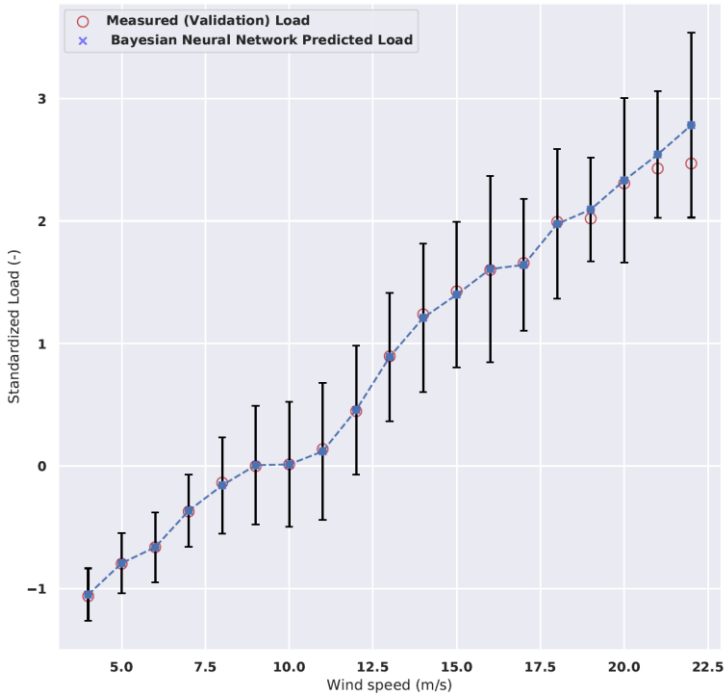

Figure 2: Blade flap-wise damage equivalent loads estimated from SCADA and acceleration data: Mean measured (red circle), mean estimated (blue dots), and uncertainties (black lines, +/-2 standard deviation of error between mean estimated and mean measured, providing a 95% confidence) over 0.5 m/s wind bins.

Here we used 50% of the data for training and 50% for validation. The BNN is able to provide a good estimate of the blade loads, see Figure 2. Overall, a coefficient of determination of 95.3% is reached.
The deviation of the estimated loads from the measured ones as well as the uncertainties increases with the wind speed due to the fewer data points.
In future work we will compare the results of the BNN to the ones from an ANN and quantify the uncertainty associated to the overall estimation by aggregating the model uncertainty with the measurement load uncertainty.

References:
[1] Nikolay Dimitrov, and Anand Natarajan 2019. From SCADA to lifetime assessment and performance optimization: how to use models and machine learning to extract useful insights from limited data. Journal of Physics: Conference Series, 1222, p.012032.
[2] Anish Venu, Mike Lüdde, and John Omole 2020. Prediction and Validation of Fatigue loads using Artificial Intelligence on Real World Measurement Data. Journal of Physics: Conference Series, 1618, p.022006.
[3] C. M. Bishop, Pattern Recognition and Machine Learning. Springer, 2006.
[4] C. Blundell, J. Cornebise, K. Kavukcuoglu, and D.Wierstra, "Weight uncertainty in neural networks," 2015.
[5] Laurent Valentin Jospin, Wray Buntine, Farid Boussaid, Hamid Laga, and Mohammed Bennamoun. (2020). Hands-on Bayesian Neural Networks – a Tutorial for Deep Learning Users.

Identification of Optimal Sensor Locations for Virtually Sensing Transmission Input Loads of a Wind Turbine using Machine Learning Techniques and Drivetrain Simulations

Baher Azzam*, Ralf Schelenz, and Georg Jacobs
Center for Wind Power Drives
*Presenting author

Keywords: Feature Selection | Virtual Sensor | Multivariate Data Analysis | Multibody Simulation | Artificial Intelligence

The ongoing trend of building larger wind turbines (WT) to reach greater economies of scale is contributing to the lowering cost of wind energy as well as the increase of WT drivetrain input loads into unchartered territories. The resulting intensification of the load situation within the WT gearbox motivates the need to monitor WT transmission input loads. However, due to the high costs of direct measurement solutions, more economical solutions such as virtual sensing of transmission input loads using stationary sensors mounted on the gearbox housing or other drivetrain locations are of interest. This research addresses this need by identifying optimal sensor locations for virtually sensing WT transmission input loads.
A model of the Vestas V52 WT was subjected to a simulated wind field in a virtual multibody simulation (MBS) environment [1]. The simulated wind fields were generated in accordance with design load cases from the IEC 61400 standard. During simulated operation, time-series data of the 6-degree of freedom (6-DOF) transmission input loads were extracted as well as signals from potential sensor locations covering deformations, misalignments, and rotational speeds at various drivetrain locations. These locations were selected based on an initial hypothesis of sensor locations suspected to be useful and practical for the envisaged transmission input load virtual sensor. Though, as the computational cost of adding sensors to the WT model in the simulation environment is relatively low, additional locations could be investigated.

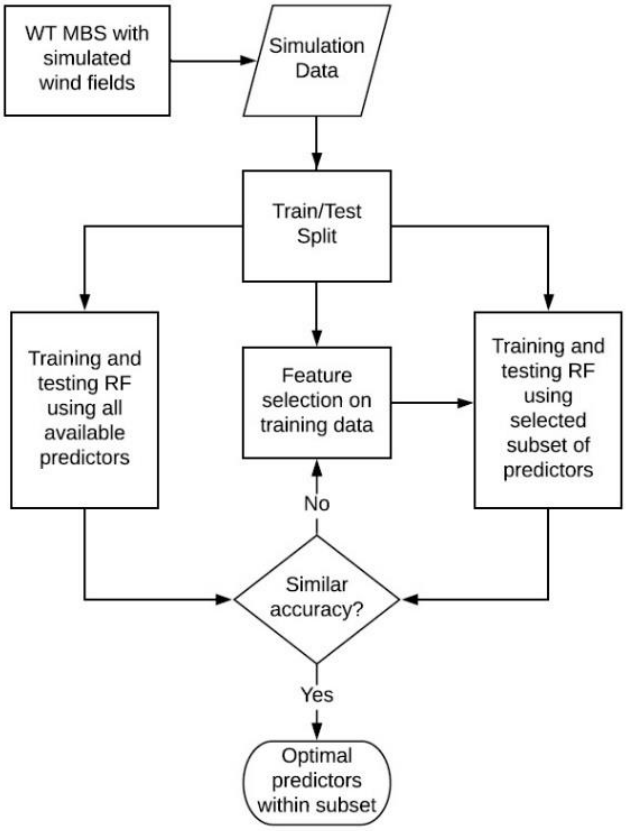

Figure 1: Overview of Methodology

Six Random Forest (RF) regression models were trained to estimate the respective 6-DOF transmission input loads, taking the chosen predictor variables as input. The available data from six simulated wind fields, each lasting 600 seconds, was used to train and test the RF models. The sampling frequency was 200 Hz. The data was split in half with 50% used for training the models and 50% used for testing. The RF models demonstrated varying levels of skill in estimating the target 6-DOF loads reaching R2 scores for moments about the x-,y-, and z-axes of 0.99, 0.96, and 0.99, respectively, and R2 scores for forces along the x-,y-, and z-axes of 0.86, 0.75, and 0.89, respectively.

In order to identify the most influential predictor variables on estimation accuracy, shuffled versions (shadows) of the predictors were added to the data, and a statistical test [2] was used to iteratively remove less important predictors in 6-DOF load estimation than the shadows. The process was applied for each of the 6-DOF transmission input loads. The results indicated that for each input load, a subset (roughly half) of available predictors are of particularly high importance on model accuracy.

In order to verify that this subset indicated the optimal sensor locations, RF models were trained using only the predictor variables within the subset. The resulting R2 scores for Moments about the x-, y-, and z-axes and Forces along the x-, y-, and z-axes were 0.99, 0.90, 0.92, 0.83, 0.71, and 0.86, respectively. Despite using close to half of the available predictors, the models were able to achieve similar accuracies (within 7%) as compared to the performance of the models using all available predictors. Figure 1 provides an overview of the methodology.

The authors aim to utilize the methodology presented in this paper to identify high potential sensor locations and types of an envisaged virtual sensor system for estimating WT 6-DOF transmission input loads.

References:

[1] Azzam, B., Schelenz, R., Roscher, B., Baseer, A. and Jacobs, G., 2021. Development of a Wind Turbine Gearbox Virtual Sensor using Multibody Simulation and Artificial Neural Networks. Manuscript submitted for publication.

[2] Kursa, M., Jankowski, A. and Rudnicki, W., 2010. Boruta – A System for Feature Selection. Fundamenta Informaticae, 101(4), pp.271-285.

Wind Turbine Localization in Satellite and Aerial Images

Daniel Gritzner[1,*], Hauke Hinrichs[1], Chris Stetter[2], Henrik Wielert[2], Michael H. Breitner[1], and Jörn Ostermann[1]
[1]Leibniz University Hannover
[2]Nefino GmbH
[*]Presenting author

Keywords: wind turbine localization | satellite images | aerial images | repowering | wind farms

Knowing the precise locations of wind farms and the turbines within is a prerequisite for many modern applications, studies and simulations in the field of wind energy. Examples include estimating the power or the noise produced by a wind farm or checking whether new turbines would comply with current regulatory distance restrictions when considering repowering a wind farm for increased capacity (Piel et al, 2019). However, aside from a few positive examples, there are no wellmaintained databases available which contain the necessary location information. Due to the high cost of manually building and maintaining such a database, an automated localization approach is desirable.

We explored the use of a state-of-the-art object detection model, Faster R-CNN (Ren et al, 2016, pp. 1137-1149), on high resolution satellite and aerial images provided by the Google Maps Static API to perform automatic wind turbine localization. This model is able to predict not only the location of objects in an image, but also their size in the form of a bounding box. Additionally, it assigns a class from an a-priori known set of classes to each prediction. We trained configurations with continuous and with discrete bounding box sizes which we assigned to each wind turbine based on its height and rotor diameter. We achieved F1 scores up to 91% and the average distance between the predicted locations and the ground truth locations varied between 5.3m and 13.4m. These results are visualized in Fig. 1. However, higher F1 scores are correlated with higher average distances. The model using discrete sizes of bounding boxes generally performed better. By also partitioning our test data into small wind turbines, medium-size wind turbines and large wind turbines we found that the model performance depends on the turbine size: larger turbines are easier to detect (high F1 score) while the small turbines are easier to locate precisely (low average distance).

Figure 1: Detection results of our best model in terms of F1 score. Predictions with their confidences are shown in red, ground truth is shown in blue.

We investigated whether a simplified version of the model, with a lowered computational cost and required training dataset size, already performs well. For the prescribed simulations and analyses, the center point of a wind turbine location is sufficient. However, removing the bounding box size predictions caused the model training to no longer converge. Furthermore, there is only a single class in our case. Removing the multi-class prediction component of the model caused it to make too many predictions. In the best configuration we achieved a recall of more than 90% but the best possible precision was only 60% (top F1 score was 72%). The multi-class prediction component is also able to reject initial predictions which were made erroneously, thus this component is necessary to achieve a high precision in addition to a high recall.
In a last experiment we also investigated the model's geographical limitations. We trained a model on data from Germany and applied it to data from Germany and the USA. It performed worse on the US data (best F1 score: 79%) than it did on the German data (best F1 score: 91%). While the F1 scores could be improved by fine-tuning the model on US data, the average distances also increased by about 4m in the process. This finding motivates exploring proper domain adaptation, such as Chen et al (2018, pp. 3339-3348), in future work.

References:

Chen, Y., Li, W., Sakaridis, C., Dai, D. and Van Gool, L., 2018. Domain adaptive faster r-cnn for object detection in the wild. In Proceedings of the IEEE conference on computer vision and pattern recognition (pp. 3339-3348).

Piel, J.H., Stetter, C., Heumann, M., Westbomke, M. and Breitner, M.H., 2019, May. Lifetime Extension, Repowering or Decommissioning? Decision Support for Operators of Ageing Wind Turbines. In Journal of Physics: Conference Series (Vol. 1222, No. 1, p. 012033). IOP Publishing.

Ren, S., He, K., Girshick, R. and Sun, J., 2016. Faster r-cnn: Towards real-time object detection with region proposal networks. IEEE transactions on pattern analysis and machine intelligence, 39(6), pp.1137-1149.

Mini-Symposium: Machine Learning and big data applications in wind energy (II)

How can machine learning be successfully used for wind speed vertical extrapolation under a round-robin approach?

Nicola Bodini*, and Mike Optis
National Renewable Energy Laboratory
*Presenting author

Keywords: machine learning | wind speed extrapolation | lidars

An accurate characterization of the wind resource available at hub height is required for an efficient and bankable wind farm project. However, direct measurement of wind speed at the constantly increasing height of the hub of commercial wind turbines is oftentimes challenging and expensive, so that it is common practice to vertically extrapolate the wind resource from lower and more easily accessible levels. Conventional techniques for wind speed vertical extrapolation include the use of a power law and a logarithmic profile. While simple, the limits in accuracy of these methods have been shown in various studies.
Recently, machine learning has been proposed as a new method to vertically extrapolate winds. All the published studies on the topic assess the performance of machine learning techniques in vertically extrapolating the wind resource at the same location where the algorithm has been trained. However, in real-world applications, the wind resource is measured at the instrument location, but it then needs to be extrapolated at hub height at the location of the wind turbines within the find farm. To be able to fully recommend the use of machine learning techniques over the simple power law and logarithmic law, the spatial variability of the performance improvements of the machine learning approaches needs to be assessed. Here, we propose a round-robin validation of a machine learning-based method for wind speed extrapolation. We use 20 months of lidar and sonic anemometer observations at four locations spanning a 100 km wide region at the Southern Great Plains (SGP) atmospheric observatory, in north-central Oklahoma.
At each location, we train a random forest to extrapolate 30-min average wind speed at heights relevant for wind energy production.

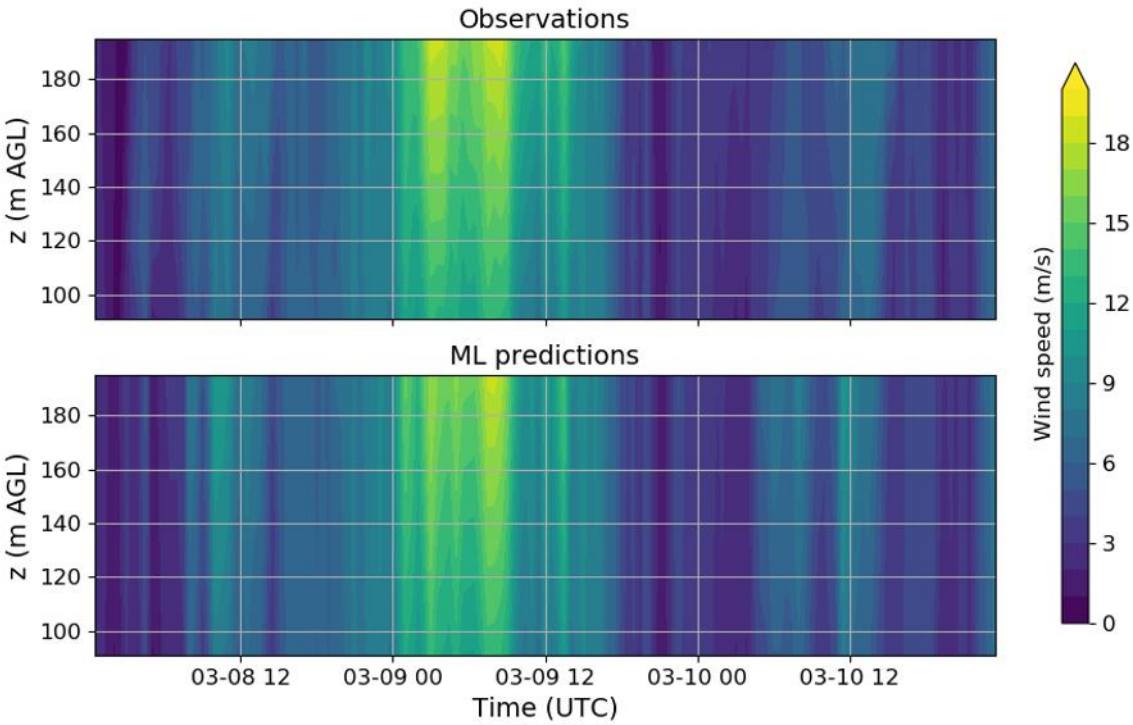

Figure 1: Time-height cross section of observed and machine-learning extrapolated wind speed during a LLJ event on 9 March 2018.

First, we perform a same-site comparison of the performance of the proposed random forest against the conventional techniques for wind speed extrapolation (namely power law and logarithmic profile, with widely accepted stability corrections). We find that the random forest outperforms the power law and logarithmic law in vertically extrapolating wind speed in all the considered stability regimes, with average error reductions over 30%.

Next, we propose a round-robin validation, to use the random forest trained at a specific site to extrapolate wind speed at the remaining instrument locations. We find that the performance of the random forest approach degrades when the algorithm is tested at a site different than the training one. However, even under those circumstances, the machine learning-based approach still outperforms the conventional techniques for wind speed extrapolation, with the largest benefits obtained under stable conditions.

Finally, as case study, we present the performance of the proposed extrapolation approach during low-level jet events (Figure 1), which cannot be fully captured by the conventional extrapolation methods. We find that the random forest can accurately predict wind speed during LLJs, with significant benefits for the prediction of wind energy production.

References:

Bodini, N. and Optis, M., 2020. The importance of round-robin validation when assessing machine-learning-based vertical extrapolation of wind speeds. Wind Energy Science, 5(2), pp.489-501.

Power and load prediction using lidar measurements and deep learning

Tuhfe Gocmen[1,*], Jens Visbech Madsen[1], Albert Meseguer Urbán[1], Antoine Larvol[2], and Jennifer Rinker[1]
[1]DTU Wind Energy
[2]Windar Photonics
[*]Presenting author

Keywords: LSTM for short-term forecasting | lidar-based power forecasting | lidar-based load forecasting | sequence modelling for power and loads

Nacelle-mounted lidars have the capability of providing a preview of the wind field in front of the rotor. Such a preview is beneficial when controlling the wind turbine to improve power performance and reduce structural loads. This study investigates the potential of using lidars and machine learning for short-term forecast of the power and blade root flap-wise bending moment on an 850kW Vestas V52 wind turbine. For that, both a 2-beam and a 4-beam lidar units are analysed and the added value of the latter instrumentation is quantified. It should be noted that the forecasts take lidar measurements as inputs exclusively as the operational condition of the turbine ahead of time is unknown.

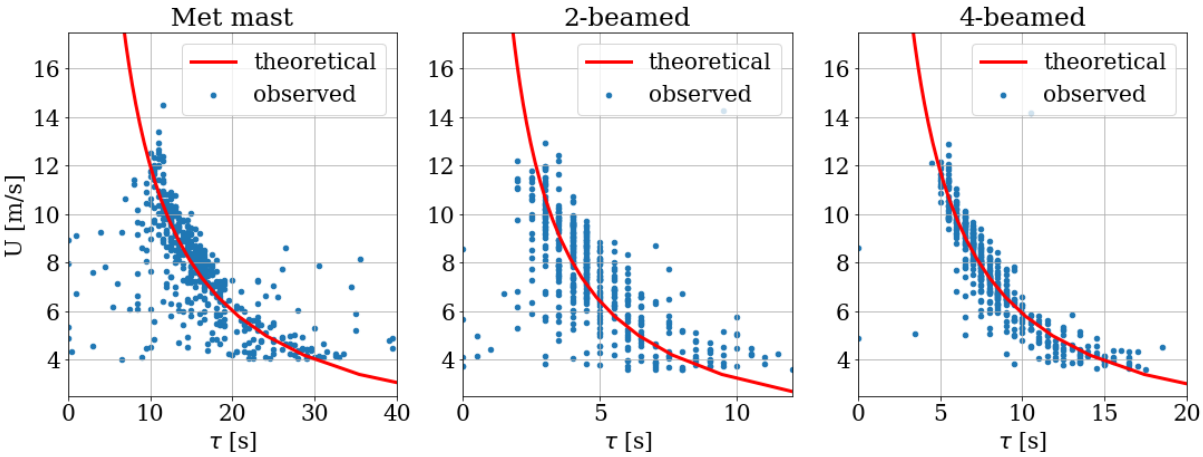

Figure 1: Wind speed, U, as function of time delay, tau, with highest correlation based N 10-minute time series. Note that the x-axes are different for the three plots whereas the y-axes are identical.

First, a time delay analysis is performed to assess the time scales of relevance for the forecast models. The analysis presented in Figure1 shows a good agreement between the actual time to impact and the expected time to impact based on relative distance from met-mast to turbine and lidar measurements to turbine pairs, as well as the corresponding average advection wind speed. The induction zone has the potential to slow down the measured advection wind speed but its effects were found to be negligible. Especially, the 4-beamed lidar is seen to be in very good compliance with the theoretical time to impact based on average advection speed and the relative distance between the lidar measurements and the turbine location.

For the selection of the forecasting algorithm, the most recent review concerning the deep learning applications in renewable energy forecasting [4] compares several architectures implemented in a number of case studies and shows that the deep recurrent neural networks (RNNs) outperform the others on root mean square error (RMSE) and mean absolute percentage error (MAPE) indices.

Accordingly, due to their capability of capturing dynamic behaviour, long-short-term memory (LSTM) approach [2] is implemented in this study so far, using the inflow measurements via the 2-beam and 4-beam lidars separately. As the common benchmark, the persistence model is used as the baseline to evaluate the forecast error for different horizons. The mean absolute error is used as the validation metric as it is commonly used for control algorithms, which are the end-user of the generated forecasts.

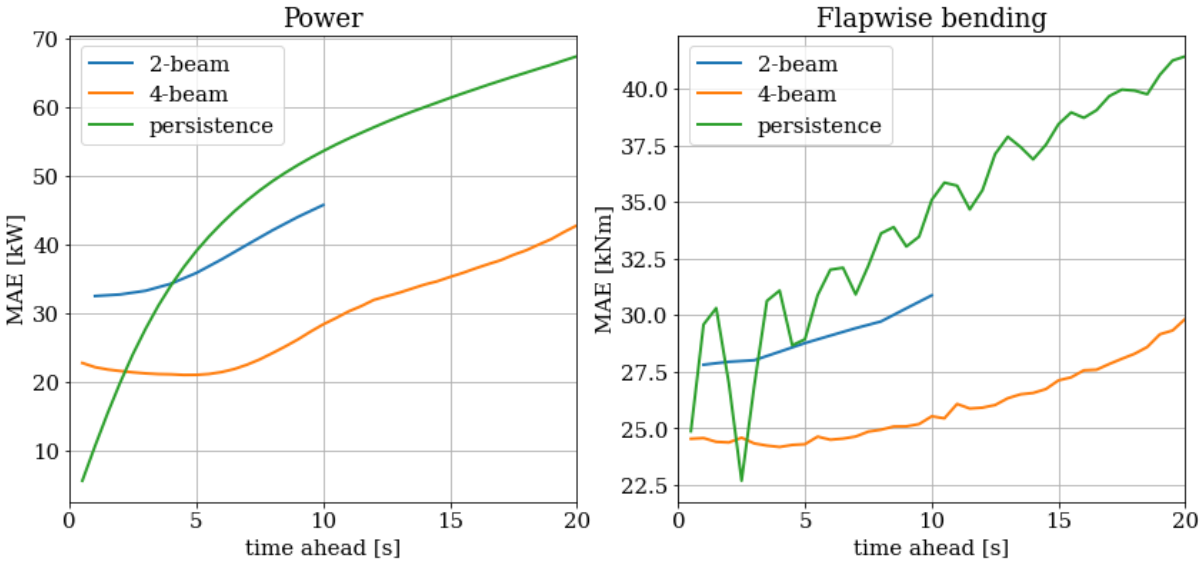

Figure 2: Mean absolute error (MAE) comparison of the LSTM-based power and flap-wise bending moment forecasts using 2-beam and 4-beam lidar measurements for different horizons.

Figure 2 shows that the networks developed in this study are capable of predicting short-term electrical power and blade flap-wise bending moment based on lidar measurements and provides better forecasts than persistence already after 2-seconds horizon. In general, the models are able to capture the overall trends with low biases ahead of time, but are seen to be insufficient in reproducing relatively high-frequent fluctuations of the blade flap-wise bending moment. The blade is exposed to asymmetrical loading which is highly influenced by the rotational speed of the turbine and the rotor-local wind, which are not represented in the training of the networks. The LSTMnetworks based on inputs from the 4-beamed lidar shows a significantly better performance than the 2-beamed lidar with up to 35% lower MAE for power and 13% for the flap-wise bending moment.

For the final presentation, the study will be extended to benchmark other sequential modelling architectures for the defined forecast cases such as gated recurrent units (GRUs)[1], which is the other state-of-the-art RNN, and a relatively new approach to capture the timely dependencies in sequences: Attention based transformer[3].

References:

[1] Cho, K., Van Merri ̈enboer, B., Gulcehre, C., Bahdanau, D., Bougares, F., Schwenk, H., and Bengio, Y. (2014). Learningphrase representations using RNN encoder-decoder for statistical machine translation. InEMNLP 2014 – 2014 Conferenceon Empirical Methods in Natural Language Processing, Proceedings of the Conference.

[2] Hochreiter, S. and Schmidhuber, J. (1997). Long Short-Term Memory.Neural Computation.

[3] Vaswani, A., Shazeer, N., Parmar, N., Uszkoreit, J., Jones, L., Gomez, A. N., Kaiser,Ł., and Polosukhin, I. (2017).Transformer: Attention is all you need.Advances in Neural Information Processing Systems 30.

[4] Wang, H., Lei, Z., Zhang, X., Zhou, B., and Peng, J. (2019). A review of deep learning for renewable energy forecasting.Energy Conversion and Management, 198:111799.

Region-Based Convolutional Neural Network for Wind Turbine Wake Characterization in Complex Terrain

J.A. Aird[1,*], Eliot Quon[2], R.J. Barthelmie[1], Mithu Debnath[2], Paula Doubrawa[2], and S.C. Pryor[1]
[1]Cornell University
[2]National Renewable Energy Laboratory
[*]Presenting author

Keywords: Convolutional Neural Network | Complex Terrain | Wakes | Machine Learning

Knowledge of wake trajectory, geometry, and orientation is pertinent to wind resource assessment, power output analysis, and fatigue analyses. Wake identification and characterization methods have been introduced to quantify wake geometries in both simulation output and measurements (Quon et al., 2020; Doubrawa et al., 2016). Some methods approximate the location and area of the wake's center through fitting Gaussian curves to velocity deficits, implementing contour-based methods utilizing momentum flux, or using a velocity deficit and turbulence profile method (Vollmer et al., 2016; Quon et al., 2020; Panossian et al., 2018). However, results from these methods vary. Most methods exhibit difficulties in distinguishing the wind turbine wake from local turbulent flows (España et al., 2011). Furthermore, methods to identify wakes from observational data (such as Lidar campaigns) are commonly dependent on turbine or experimental parameters such as rotor diameter, atmospheric stability, and data resolution (Aitken et al., 2014; Herges et al., 2017). Limitations of current wake identification methods in flat terrain also apply in cases of complex terrain, although complex terrain introduces enhanced wake splitting (in which the wake splits into two or more pieces and propagates throughout the flow field) and asymmetry. An automated wake detection algorithm has shown success in identifying one turbine wake in complex terrain (Barthelmie and Pryor, 2019). However, wake identification for multiple wakes in complex terrain remains unexplored.

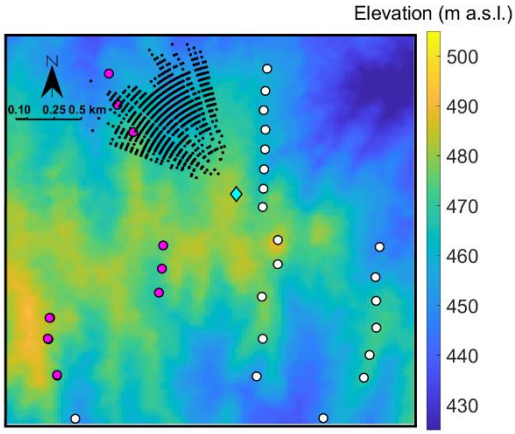

Figure 1. Elevation map of scanning site with target turbines (pink) and all turbines captured (white) over the course of the scan campaign. Lidar location is indicated by the light blue diamond. Spatial scan coverage (black) for the scan example displayed in Figure 2.

Convolutional neural networks (CNN) are commonly used for image processing and object detection. A CNN analyzes images and characterizes objects within them according to object type, quantity, and location. Improving upon the capability of traditional CNNs, the R-CNN implements a region-proposal network to detect multiple instances of objects in varying positions and aspect ratios (Girshick et al., 2015). Mask R-CNN, an extension of the R-CNN, outputs image segmentation masks (a mask is a binary pixel matrix representing object geometry) for detected objects (He et al., 2017). Due to its computational efficiency and accuracy in object segmentation and classification, the Mask R-CNN is a robust option for addressing common limitations in wake identification and characterization, particularly in complex terrain.

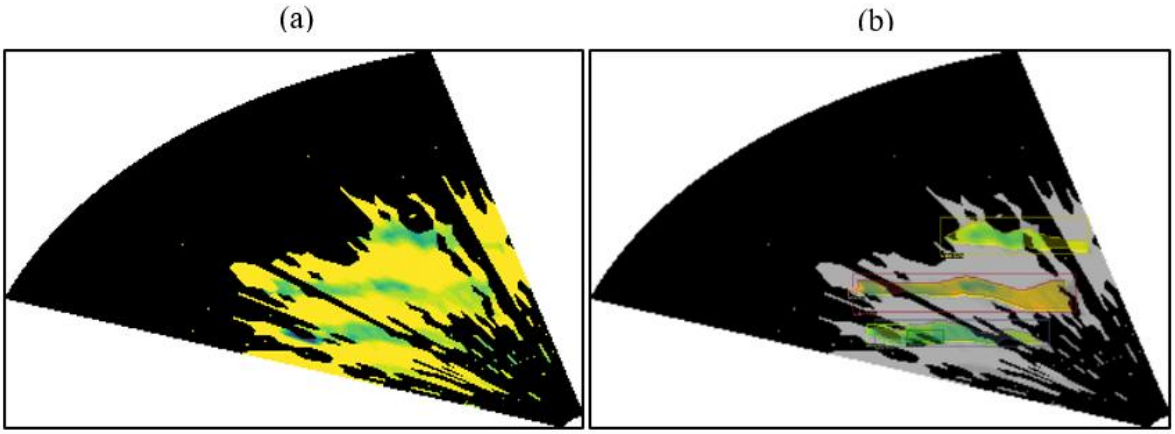

Figure 2. Comparison of (a) PPI scan image input to Mask R-CNN and (b) Mask R-CNN output when identifying wakes in spatially disjoint regions (due to CNR filtering). Colors in (b) are unique for each wake identified. The colored wake masks represent binary pixel arrays for wakes within the image; the spatial geometry of the wakes is known through a conversion from pixels to meters.

The Mask R-CNN is applied to a subset of Lidar PPI scan images from a wind farm in the US Pacific Northwest in complex terrain to present a proof-of-concept analysis of Mask R-CNN for wind turbine wake characterization (Figure 1). Examples and accuracy/precision rates exhibit that the Mask R-CNN identifies and characterizes wakes in: scans with varying resolutions and geometries, spatially disjointed flow fields due to SNR/CNR filtering (thus the complete wake geometry is obscured; Figure 2). The Mask R-CNN also identifies and characterizes: asymmetric wakes, segments of turbine wakes as they dissipate and split, and multiple wakes simultaneously. In each case, the exact geometry and spans of the wakes are also shown to be characterized successfully through Mask R-CNN output. This wake characterization approach may be applied in current and future field campaigns to enhance understanding of wind plant aerodynamics and enable automated and efficient wake detection under a variety of conditions.

References:
Aitken, M.L., Banta, R.M., Pichugina, Y.L. and Lundquist, J.K., 2014. Quantifying wind turbine wake characteristics from scanning remote sensor data. Journal of Atmospheric and Oceanic Technology, 31(4), pp.765-787.
Barthelmie, R.J. and Pryor, S.C., 2019. Automated wind turbine wake characterization in complex terrain. Atmospheric Measurement Techniques (Online), 12(6), pp.3463-3484.
Doubrawa, P., Barthelmie, R.J., Wang, H., Pryor, S.C. and Churchfield, M.J., 2016. Wind turbine wake characterization from temporally disjunct 3-d measurements. Remote Sensing, 8(11), p.939.
España, G., Aubrun, S., Loyer, S. and Devinant, P., 2011. Spatial study of the wake meandering using modelled wind turbines in a wind tunnel. Wind Energy, 14(7), pp.923-937.
Girshick, R., Donahue, J., Darrell, T. and Malik, J., 2015. Region-based convolutional networks for accurate object detection and segmentation. IEEE transactions on pattern analysis and machine intelligence, 38(1), pp.142-158.
He, K., Gkioxari, G., Dollár, P. and Girshick, R., 2017. Mask r-cnn. In Proceedings of the IEEE international conference on computer vision (pp. 2961-2969).
Herges, T.G., Maniaci, D.C., Naughton, B.T., Mikkelsen, T. and Sjöholm, M., 2017. High resolution wind turbine wake measurements with a scanning lidar. In Journal of Physics: Conference Series (Vol. 854, p. 012021).
Panossian, N., Herges, T.G. and Maniaci, D.C., 2018. Wind Turbine Wake Definition and Identification Using Velocity Deficit and Turbulence Profile. In 2018 Wind Energy Symposium (p. 0514).
Quon, E.W., Doubrawa, P. and Debnath, M., 2020. Comparison of Rotor Wake Identification and Characterization Methods for the Analysis of Wake Dynamics and Evolution. In Journal of Physics: Conference Series (Vol. 1452, p. 012070).
Vollmer, L., Steinfeld, G., Heinemann, D. and Kühn, M., 2016. Estimating the wake deflection downstream of a wind turbine in different atmospheric stabilities: an LES study. Wind Energy Science, 1, pp.129-141.

Mini-Symposium: Demystifying Complex Terrain

Andrew Clifton
WindForS

Wind energy is increasingly being deployed in complex mountainous and forested terrain and near to people and settlements. Such areas often have better wind resources but the terrain brings new technical challenges in modeling and measuring wind conditions, and understanding how wind turbines perform. There are also complex interactions with local stakeholders, for example because of disturbance during construction, visual impact and sound emission from operating turbines, or effects on birds and bats. Together these factors can make wind energy deployments in complex terrain challenging and expensive. However, in order to help reach local, regional, and national goals for low-carbon energy, these challenges need to be mitigated so that wind turbines can be built in such locations. This mini symposium explores how the wind energy community can bring together information across multiple disciplines to better understand operating conditions, stakeholder interactions, and other factors to achieve efficient, accepted wind farms in complex terrain. We welcome papers on any tools, techniques, methods, measurement methods or other developments that help illuminate the conditions for wind energy in complex terrain and help make informed actions that benefit all stakeholders.

Model-based parameter study on the main influencing factors on lidar errors in complex terrain

Tobias Klaas*
Fraunhofer IEE
*Presenting author

Keywords: lidar | complex terrain | forest | wind energy

Wind energy will significantly contribute to renewable power generation in the future. Much of the onshore wind energy potential is located at complex and forested sites. Remote sensing, in particular, light detection and ranging (lidar), has become a valuable technology to assess the wind resource at hub height of modern wind turbines.
However, common wind profile Doppler lidars suffer from errors at complex terrain sites because of their measurement principle that assumes homogeneous flow between the measurement points.
The presentation sums up the work of a non-dimensional model-based parameter study on the estimation of wind speed errors of wind profile Doppler lidars in complex terrain that has been carried out within the doctoral thesis of the author.

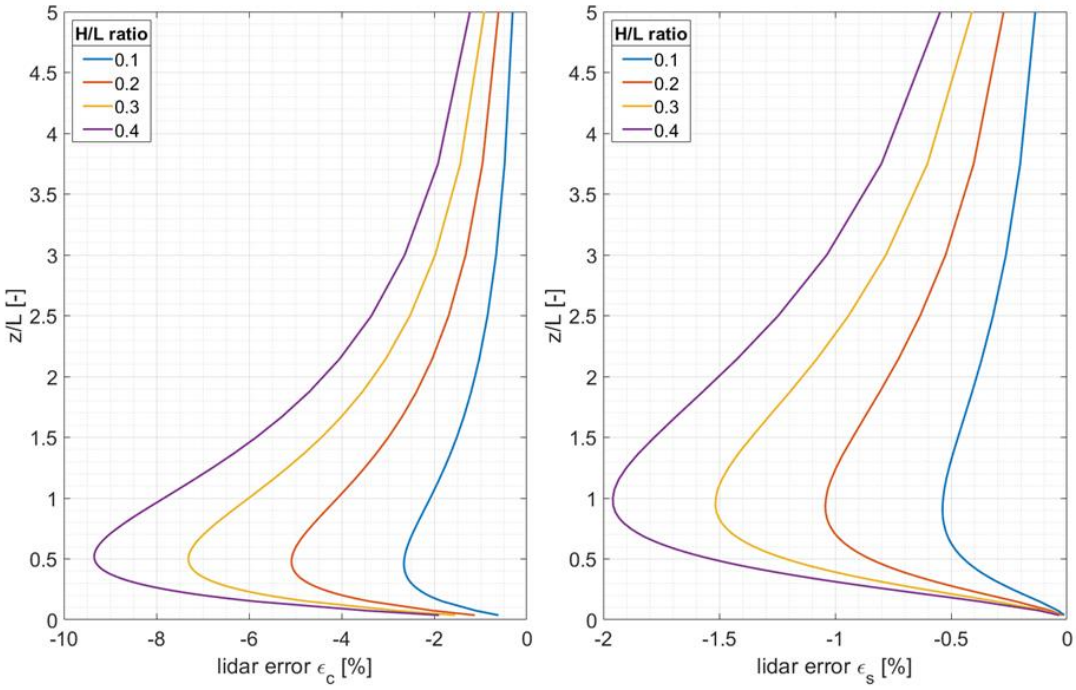

Figure 1: Lidar error epsilon_c (left) and epsilon_s (right) in dependence of the ratio H/L between z/L ratios from 0 to 5. Results are based on the potential flow model. Note the different scaling of the x-axes.

The study uses analytic and numerical models of different complexity to simulate the flow over diverse two-dimensional Gaussian hill geometries with increasing hill height to hill half-width ratios H/L. It provides an analysis of the influence of orographic complexity, measurement height, surface roughness and vegetation, atmospheric stability and half-cone opening angle ϕ on the resulting lidar error.
Results for the lidar error ε are presented against the non-dimensional ratio of measurement height over hill half-width z/L. A novel approach is introduced that subdivides error into a part epsilon_c resulting from flow curvature and a part epsilon_s resulting from speed-up between the probe volumes and the measurement location. Separating the lidar error shows that, depending on the actual hill geometry, speed-up effects cause up to 30 % of the total lidar error. Neglecting these effects will therefore introduce a significant uncertainty to the lidar error estimation.

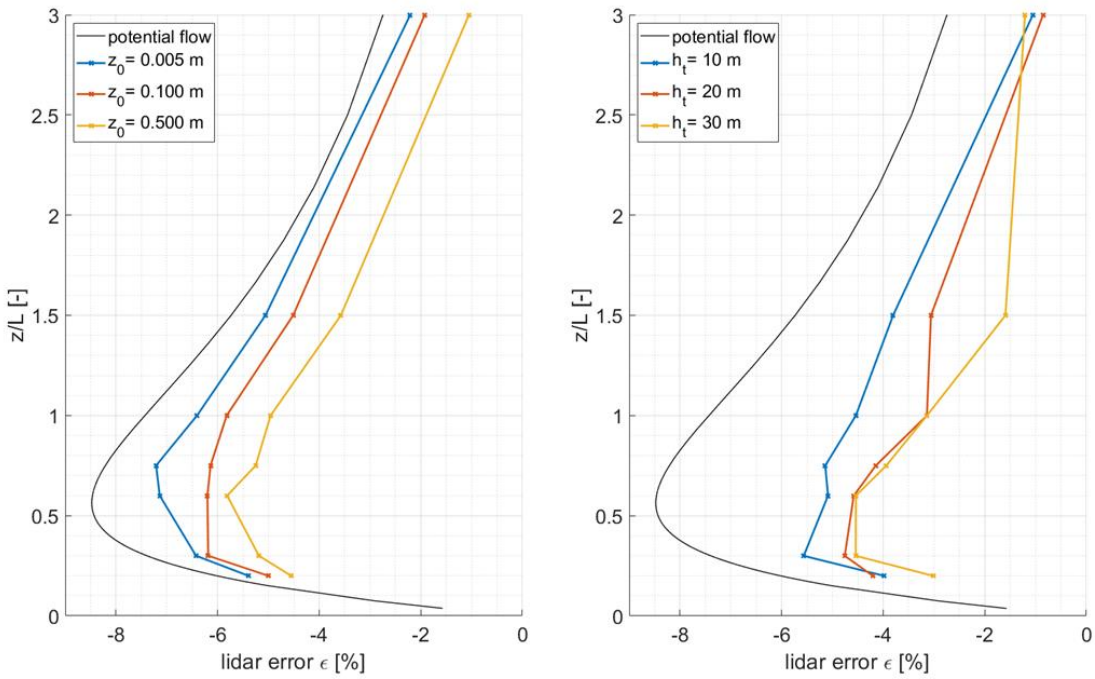

Figure 2: Lidar error epsilon in dependence of the roughness length z_0 (left) and in dependence of tree heights h_t (right) between z/L ratios from 0 to 3. Results are based on Meteodyn WT (colored) and the potential flow model (black) for an H/L ratio of 0.3.

The lidar error is mainly influenced by orographic complexity. However, its magnitude is dependent on z/L. It reaches a maximum at z equal to 50-60 % of L and significantly decreases for smaller and higher ratios (Figure 1). In situations of asymmetric or detached flow, as they occur above steep hills with high surface roughness or forest, the lidar error is significantly reduced (Figure 2).

Splitting up the total lidar into epsilon_c and epsilon_s reveals contrary effects of reduced ϕ, which explain the small differences in the total lidar error for symmetric flows described in the literature. However, under certain asymmetric flow conditions (e.g., forested hills), the half-cone opening angle can significantly affect the magnitude of the lidar error.

It is therefore highly recommended to use e.g., a RANS CFD model in conjunction with appropriate forest modeling to account for these effects. Simple potential flow or linearized models will overestimate the lidar error in these cases. Furthermore, the influence of atmospheric stability is significant, particularly for stable stratification. If atmospheric stability variation at a measurement site plays a vital role, it should also be considered in the modeling.

Wind field and performance measurements of vertical axis wind turbines on modelled buildings

Yannick Jooss[1,*], Roberto Bolis[2], R. Jason Hearst[1], and Tania Bracchi[1]
[1]Norwegian University of Science and Technology
[2]Politecnico Milano
[*]Presenting author

Keywords: urban wind energy | complex terrain | wind tunnel measurements | performance measurements

In response to the world's growing energy demand (IEA 2020), it becomes increasingly important to explore complex terrain as potential sites for wind energy. A proper assessment of the urban wind resource was found to be one of the main aspects requiring further investigation to advance the potential usage of urban wind energy (KC et al. 2019). Significant analysis on this was conducted numerically, often employing the Reynolds-averaged Navier-Stokes equations. Furthermore, most studies do not involve an actual turbine in their analysis, but rather rely on the available power in the wind. Neglecting the impact of the wind turbine on the flowfield through e.g. upstream blockage effects (Medici et al. 2011) can lead to significant discrepancies in the estimation of the available power.

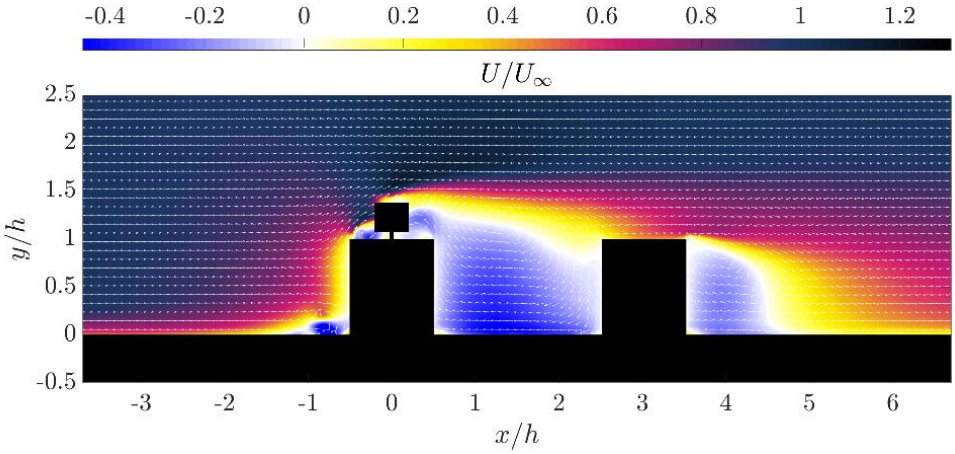

Figure 1: Mean wind field with wind turbine positioned centrally on the upstream cube showing the suppression of the recirculation zone on top of the cube. Note that all velocities are normalized with the incoming velocity upstream of the cubes at turbine height.

In this study this is addressed experimentally in a wind tunnel for two idealized buildings. Two cubes were placed in a tandem arrangement, i.e. in line with each other, on an artificial floor. The distance between the two cubes was fixed at two cube heights (h). Vertical axis wind turbines of the Savonius type were placed at six different streamwise positions on the roofs of the two cubes. This setup enabled the study of a building relatively unaffected by its surroundings as well as a building directly in the wake of another building. The flowfield was measured with particle image velocimetry along the centerline. Performance measurements were carried out following the method proposed by Bastankhah and Porté-Agel (2017), using a brushed DC motor to measure the electromagnetic torque and an optical sensor to record the rotational velocity.

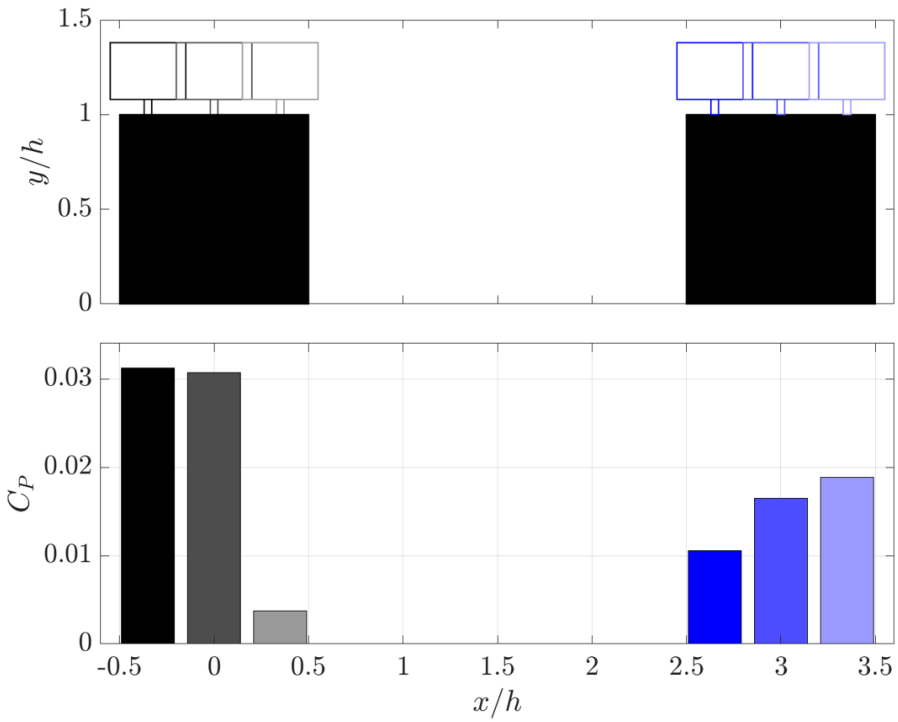

Figure 2: Power coefficient of wind turbines at different positions. Note that the velocity used to calculate the power coefficients was the incoming velocity upstream of the cubes at turbine height, resulting in generally low values. Using the same reference velocity allows a comparison between the different positions.

An analysis of the flowfield with and without the wind turbines was carried out and compared to the measured performance of the turbines at different positions. Figure 1 shows the flowfield for the wind turbine placed centrally on the upstream cube. It was found that the wind turbines had a significant impact on the flowfield and thus on the available wind power, especially at positions where they were partly submerged in the recirculation zone on top of the upstream cube. The power coefficients at all positions are shown in figure 2. The upstream cube was found to yield higher power outputs overall. The optimal position differed between the upstream and downstream cube. On the upstream cube the optimal performance was measured at the most upstream position on the cube, whereas for the downstream cube the most downstream position resulted in the highest energy extraction. This is due to differing flow patterns on top of the two cubes. At the windward edge of the upstream cube the flow separates and creates a growing area of recirculating flow. With increasing distance from the windward edge, the performance of the wind turbine was more and more affected by this. On the roof of the second cube the flow reattaches, and the wake of the upstream cube recovers with increasing downstream distance, leading to improved performance. It was thus concluded that for this specific configuration the outside positions, farthest from the neighbouring building, are to be preferred. Based on these results the ideal position of a roof-mounted wind turbine in general will be discussed.

References:
Bastankhah, M. and Porté-Agel, F. (2017) A New Miniature Wind Turbine for Wind Tunnel Experiments. Part I: Design and Performance, Energies, 10(7):908.
IEA. (2020) World Energy Outlook 2020 - Analysis.
KC, A., Whale, J., and Urmee, T. (2019) Urban wind conditions and small wind turbines in the built environment: A review, Renewable Energy, 131:268-283.
Medici, D., Ivanell, S., Dahlberg, J.-Å. and Alfredsson, P. H. (2011) The upstream flow of a wind turbine: blockage effect, Wind Energy, 14(5):691–697.

The effect of surface roughness on the wake of a wind turbine sited on a cliff

Arslan Salim Dar*, and Fernando Porté-Agel
École Polytechnique Fédérale de Lausanne
*Presenting author

Keywords: topography | wakes | surface roughness | particle-image velocimetry

Onshore wind energy is currently one of the cheapest available sources of energy (IRENA). While wind turbine wakes in flat terrain have been extensively studied in the past, wind turbines are often sited on topographical features such as hills or escarpments (Porté-Agel et al.). The flow characteristics in such terrains are significantly influenced by the geometrical details of the topography. In addition, the surface roughness determined by the land-cover at a particular site can affect the flow induced by the topography as well.
In the current work, we perform wind tunnel experiments using stereoscopic particle-image velocimetry on the flow over a cliff and its interaction with the wake of a wind turbine sited on it.
Two cases of surface roughness are studied, with the increase in the aerodynamic roughness by a factor of 22 between the smooth and the rough surfaces. The turbulence upstream of the cliff is higher in the rough surface case, which results in smaller leading-edge flow separation and lesser mean flow shear compared to the smooth surface. The streamwise turbulence intensity on the cliff has a contribution from two sources: the turbulence in the upstream flow and the turbulence generated by the leading edge flow separation. Therefore, even though the shear induced by the flow separation is reduced with the increase in surface roughness, the streamwise turbulence intensity is still higher away from the surface in this case.

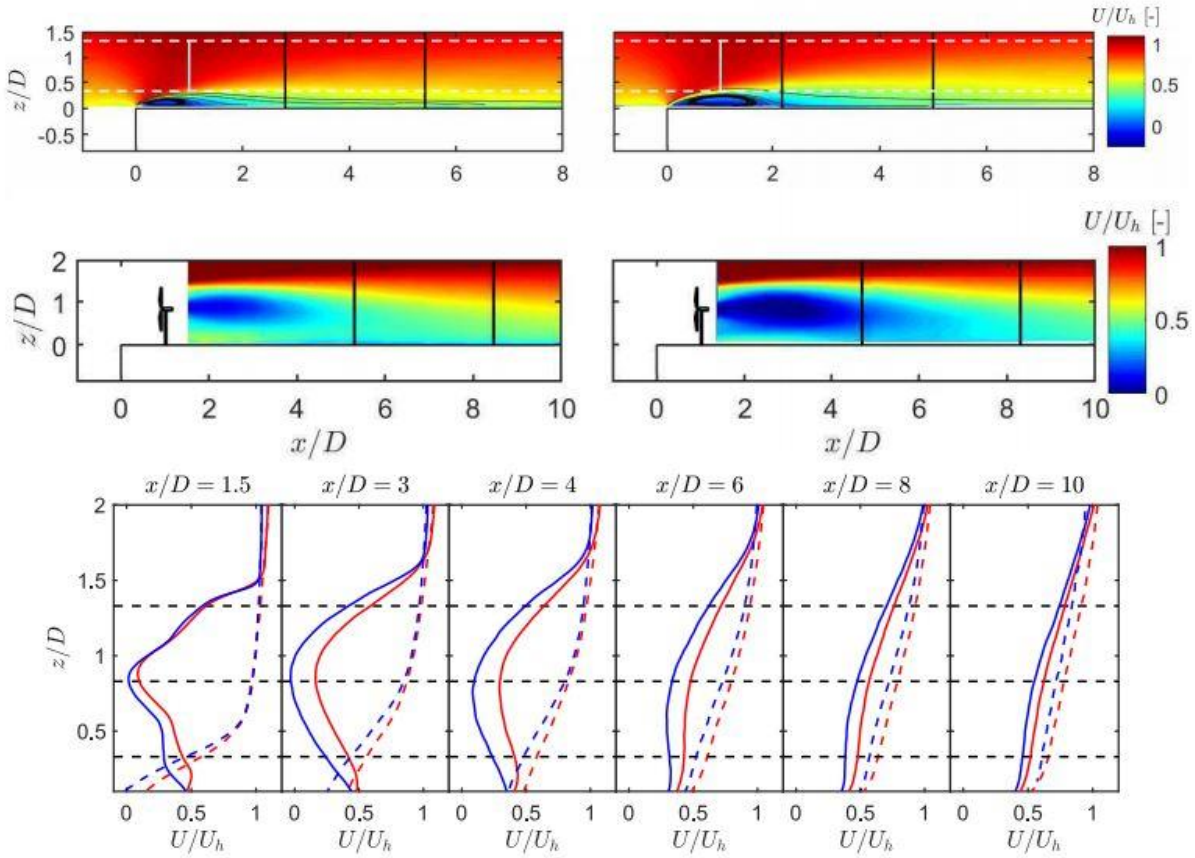

Figure 1: Normalized averaged streamwise velocity component in the base and wake flow

The streamwise velocity deficit in the turbine wake initially shows a comparatively faster recovery for the rough surface, before converging to the same value around 7 rotor diameters downstream of the turbine. Compared to related works in flat terrain (Wu & Porté-Agel, Barlas et al.), differences in the streamwise wake

velocity deficit between the two roughness cases disappear at shorter downstream distance from the turbine on the topography. This is consistent with the turbulence characteristics in the wake, which only differ at relatively shorter downstream distances. The added streamwise turbulence intensity is found to be the same in both roughness cases, which is in contrast with what is reported in the flat terrain (Wu & Porté-Agel). This is because the proportional change in the streamwise turbulence intensity between the base (without turbine) and wake flow is similar in the two roughness cases which results in similar added turbulence intensity. The higher turbulence in the base flow for the rough surface also results in an increased meandering and higher expansion rate of the wake in this case compared to the smooth one.

Figure shows the contours of the normalized averaged streamwise velocity component in the base (top row) and wake (middle row) flow for the rough (left panel) and smooth (right panel) surface cases. Vertical profiles at different streamwise locations are also plotted, where red and blue lines represent the rough and smooth surface cases, respectively. The solid and dashed lines represent profiles in the wake and base flow, respectively. The horizontal dashed black lines represent the rotor tips and hub locations.

References:

IRENA. (2020). Renewable Power Generation Costs in 2019. International Renewable Energy Agency, Abu Dhabi.

Porté-Agel, F., Bastankhah, M. and Shamsoddin, S. (2020). Wind-Turbine and Wind-Farm Flows: A Review. Boundary-Layer Meteorology, 174(1), 1-59.

Wu, Y. T. and Porté-Agel, F. (2012). Atmospheric turbulence effects on wind-turbine wakes: An LES study. Energies, 5(12), 5340-5362.

Barlas, E., Buckingham, S. and van Beeck, J. (2016). Roughness effects on wind-turbine wake dynamics in a boundary-layer wind tunnel. Boundary-Layer Meteorology, 158(1), 27-42.

Reducing the uncertainty of Wind Resource Assessments through a new complex flow scoring system

Sarah Barber[1], and Andrew Clifton[2]
[1]Eastern Switzerland University of Applied Sciences
[2]University of Stuttgart

Keywords: Wind resource assessment | Complex terrain | Classification | Wind modeling

For a given Wind Resource Assessment (WRA), the modeller is faced with a difficult choice of simulation tools and calculation steps with varying accuracies and costs. The most cost-effective choice is expected to be a compromise between performance and cost. This choice is dependent on the characteristics of the site. To help with this choice, wind energy sites are usually classified as "complex" or "not complex" to help assess whether the flow modeling tool WAsP can be applied with high confidence or not. This is done by calculating the average RIX and DRIX values (Mortensen et al., 2008) at the site using WAsP. RIX values > 0 are taken as the start of "complex terrain" (Mortensen et al., 2011). For terrain above this threshold, other, more complete flow models are generally recommended (EMD International, 2021). However, this strict definition makes it difficult for wind energy project planners to confidently assess the uncertainties associated with their WRAs. A classification on an analogue scale or with a number of different categories related to the flow complexity – and more importantly the consequences of this classification – would be help modellers choose the most appropriate tool for their site.

Site	Germany	Portugal	Norway	Spain
Organisation 1	38.89	53.00	38.89	32.22
Organisation 2	40.00	52.00	40.00	42.22
Organisation 3	40.00	43.00	40.00	50.00
Organisation 4		47.00		
Organisation 5		67.00		
Organisation 6		71.00		
Organisation 7		46.67		
Average	**39.63**	**54.24**	**39.63**	**41.48**
Max. deviation from av. (%)	**1.87%**	**33.74%**	**1.87%**	**18.69%**

Figure 1. Overall scores estimated by each different modeller for each of the four sites.

In this work, a first investigation into a new complex flow scoring system is carried out for four different sites. This is done by asking the modellers carrying out WRAs at these sites to fill out a survey to estimate the relative value of certain parameters on a scale of 0-100. These parameters are defined based on previous work on terrain classification related to lidar measurements (Clifton, 2015). This splits complex flow into the following categories: (a) Complex terrain (e.g. from IEC 61400-12-1 (IEC, 2017)); (b) Surface roughness (e.g. forested land, changes in ground cover); (c) Presence of obstacles (e.g. buildings, towers and wind turbines); (d) Local meteorology (e.g. low-level jets, divergent flows and fronts). The parameters used for this work should not be too difficult or time-consuming to calculate, and the site classification given in IEC 61400-12-1 and 61400-12-2, for example, are too complex for this application. A full list of parameters can be found in S. Barber et al. (2020) and on Figure 2.

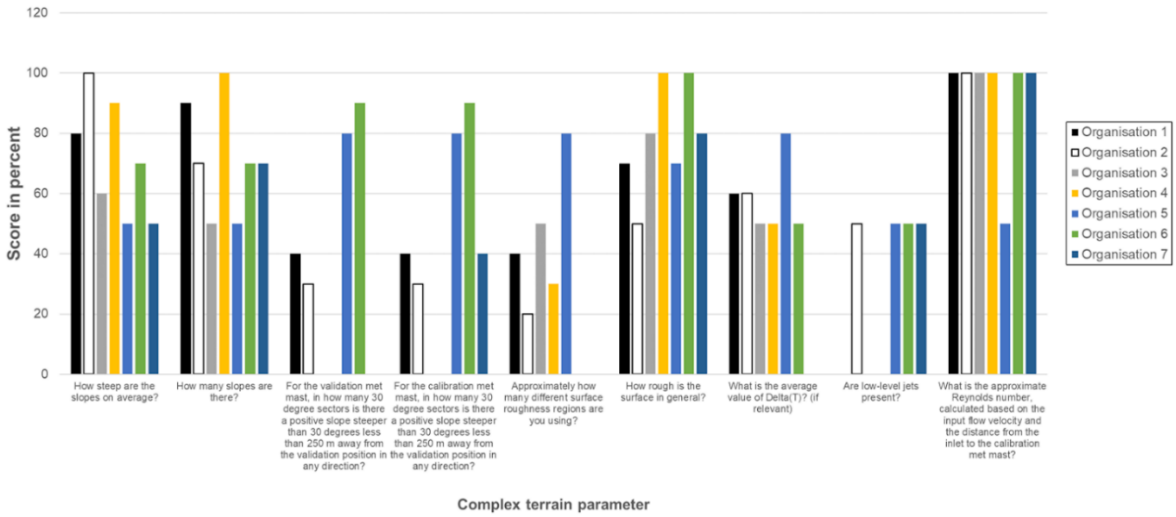

Figure 2: Variation in answers to all the questions between modellers for the site in Portugal.

In this study, these parameters are all weighted equally and then averaged in order to get a single flow complexity score. Figure 1 shows the overall scores estimated by each different modeller for each of the four sites. Although a statistically significant number of samples is not yet available, the results are promising. It is interesting that the sites with higher complexity scores also have a higher variation from the average. The individual scores provide more insight into the suitability of the method, as shown for the site in Portugal in Figure 2. It can be seen that the variation in answers between modellers varies between question. The answers to the questions "For the validation/calibration met mast, in how many 30 degree sectors is there a positive slope steeper than 30 degrees less than 250 m away from the validation position in any direction?" seem to be particularly inconsistent. Further investigation lead to the conclusion that the participants did not all read the question properly. Further studies are underway in order to improve the method and associate the scores with concrete recommendations for WRAs.

References:
S. Barber, M. Buehler and H. Nordborg (2020), IEA Wind Task 31: Design of a new comparison metrics simulation challenge for wind resource assessment in complex terrain Stage 1, Journal of Physics Conference Series 1102:012002
A. Clifton (2015), Remote sensing of complex flows by Doppler wind lidar: Issues and preliminary recommendations; technical report NREL/TP-5000-64634
EMD International (2021), WAsP CFD in WindPRO. http://www.emd.dk/files/windpro2.9/WindPRO_and_WAsPCFD.pdf
IEC International Electrotechnical Commission (2017). Wind energy generation systems - part 12-1: Power performance measurements of electricity producing wind turbines, 03.03.2017
N.G. Mortensen, D.N. Heathfield, O. Rathmann and M. Nielsen (2011), Wind Atlas Analysis and Application Program: WAsP 10 Help Facility. Roskilde: DTU Wind Energy. Belgium
N.G. Mortensen, A. Tindal, A. and L. Landberg, (2008), Field validation of the RIX performance indicator for flow in complex terrain. Paper presented at 2008 European Wind Energy Conference and Exhibition, Brussels

Insights into the realization of the Wind Science and Engineering Test Site "WINSENT" in Complex Terrain

Andreas Rettenmeier*, Florian Haizmann, Frank Musiol, Maayen Wigger, and Maike Schmidt
Center for Solar Energy and Hydrogen Research (ZSW)
*Presenting author

Keywords: test site | complex terrain | field testing | nature conservation | research

Both industry and research institutions strive to reduce wind turbine costs, to increase availability and energy yield and to further develop technologies. For this reason, a number of research test sites with accessible, open-source research wind turbines already exists in flat terrain, e.g. NREL (USA). In contrast, WINSENT, the research platform of WindForS, focuses on research questions in in complex terrain (Rettenmeier et al, 2016). In parallel to the technology developments, the WINSENT test site supports answering questions regarding social acceptance of wind energy and to align wind energy with nature conservation.
The presentation will give insights into the realization of the WindForS research platform, which is currently under construction in the joint research project WINSENT. Two sub-projects serve the detailed characterization of the site and of the research wind turbines. In the sub project "Mikroklima", the site is investigated regarding the wind conditions, soil-air interaction and ecological implications in the period before and after installing the turbines. The measurement equipment consists presently of two meteorological masts, synchronized scanning lidar systems, eddy-covariance systems, ceilometer, measurement drones, bird radar and bat microphones etc. The measured data are used amongst others for the development and validation of a simulation chain, which couples mesoscale and microscale domains using WRF, LES and detailed CFD simulation (El Bahlouli et al, 2020 and Letzgus et al., 2020). In parallel to "Mikroklima", numerical wind turbine models have been created at different levels of accuracy in the second subproject "FoWEA". Hence, models of simple aero-elastic codes up to FSI-coupled or multi body codes of the research turbines are available (Bucher et al., 2019). A new baseline turbine controller has been developed which is used for the site-specific type certification and will be open to any research institution after the completion of the test site. The turbines are of open-access and have modifications to facilitate the work of researchers . The machines are heavily equipped with sensors to gather data of mechanical loading from tower bottom up to the blade tip, various turbine parameters and seismic vibrations in the surrounding.

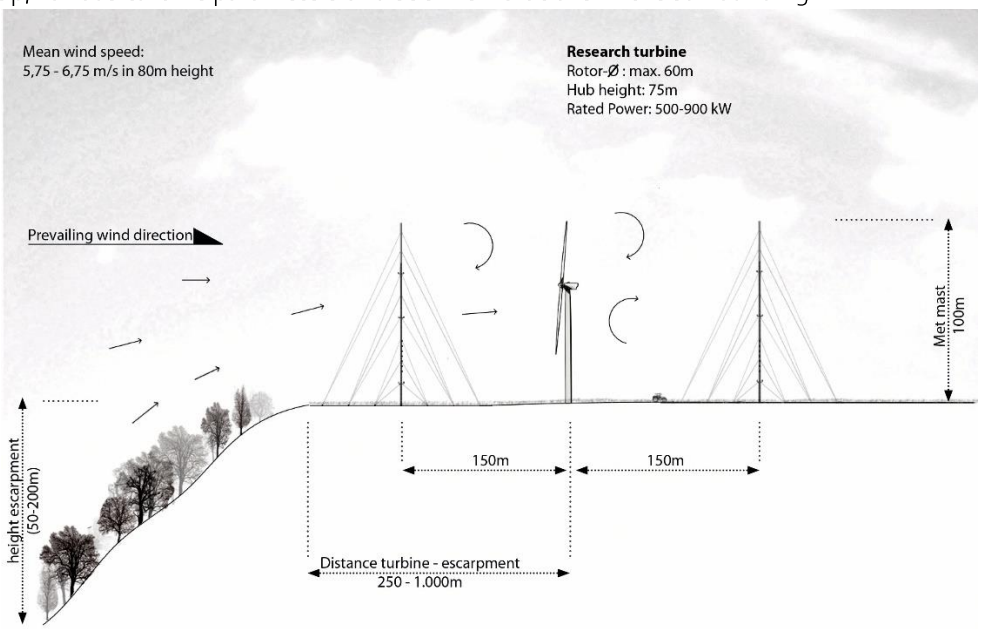

Figure 1: Illustration of test site layout: two research wind turbines in forest-free terrain near a slope and meteorological masts upstream and downstream [source: TUM-LAREG].

The location of the test site is forest-free close to a steep slope. The two turbines will have hub heights of 73m and a rotor diameter of 54m and thus an overall height of 100m. Their electrical power output is 750kW each. This turbine size still allows transferring knowledge of parameters such as loads, controller settings and turbine behavior to larger wind turbines as the different detailed and validated simulation models exist. The turbines will be erected side by side to have the possibility to directly compare the behaviors of the modified turbine and the reference turbine. The met masts are positioned in front of and behind each research turbine. The top anemometer is as high as the top blade tip position of the turbines. The masts are equipped with various meteorological sensors as well as with bat microphones and bird detection cameras (Rettenmeier et al, 2019). The turbines will be installed in autumn 2021 and the impact on birds and bats is accompanied in the project NatForWINSENT.

Figure 2: Installation of the northeastern met mast in September 2018 [source: WindForS].

Acknowledgement

The project WINSENT (No. 0324129A-F) is funded by the German Federal Ministry for Economic Affairs and Energy (BMWi).

The project NatForWINSENT II (No. FKZ 3518 86 0100) is funded by the German Federal Agency for Nature Conservation (BfN).

References:

Rettenmeier, A., Anger, J. and Cheng, P.W. (2016). Southern German Wind Energy Test Site in Complex Terrain and Associated Research Opportunities, Euromech Colloquium 576, Stockholm, Sweden

Bucher, P., Guma, G., Wuchner, R., Lutz, T. and Bletzinger K.-U..(2019). High-Fidelity aeroelastic analysis of Wind-Turbines in complex terrain - Structural Model and FSI-Coupling. IASS Annual Symposium 2019, Barcelona, Spain

Rettenmeier, A. Haizmann, F., Anger, J., Musiol, F. and Schmidt, M. (2019). Das WindForS-Forschungstestfeld in bergigkomplexem Gelände, Meteorologentagung DACH, Garmisch-Partenkirchen, Germany

El Bahlouli, A.; Leukauf, D.; Platis, A.; zum Berge, K.; Bange, J. and Knaus, H.(2020.) Validating CFD Predictions of Flow over an Escarpment Using Ground-Based and Airborne Measurement Devices. Energies 2020, 13, 4688

Letzgus, P., El Bahlouli, A., Leukauf, D., Hofsäß, M., Lutz, T. and Krämer, E. (2020). Microscale CFD Simulations of a Wind Energy Test Site in the Swabian Alps with Mesoscale Based Inflow Data. J. Phys.: Conf. Ser. 1618 062021

Mini-Symposium: IEA Wind Task 32: Wind Lidar

Andrew Clifton
WindForS

Since 2012 IEA Wind Task 32 has built a strong community that works together to identify and mitigate the barriers to adoption of wind lidar for wind energy applications. We do this by providing a structured forum for international collaborations between researchers, vendors, and users to exchange needs, ideas, and experience. The Task focuses on producing tangible results such as recommended practices that can be used by practitioners. And, Task 32 continues to work in collaboration with other IEA Wind Tasks and related industry and academic groups to help encourage scientific investigations and align them with users' needs. We welcome new participants and invite anyone interested in the Task to take part in this MS. This Mini Symposium will provide an update on the Task's activities around wind lidar use for wind resource assessment, power performance testing, lidar-assisted controls, offshore wind, and other applications. We will also give a brief overview of some of the open-source software tools and projects that are enabling a collaborative community and supporting research and development in this area.

Mini-Symposium: IEA Wind Task 32: Wind Lidar (I)

Lidar applications and methods – where next?

Vasilis Pettas*, Ines Würth, Oliver Bischoff, Yiyin Chen, Francisco Costa Garcia, Holger Fürst, Martin Hofsäß, and Po Wen Cheng
University of Stuttgart
*Presenting author

Keywords: wind lidar | remote sensing | applications of wind lidar

Stuttgart Wind Energy (SWE) is a research institute dedicated to wind energy research. The research carried out covers a wide spectrum of topics including simulations, controls, floating and wind sensing in the turbine and farm level. One of the core topics is research on wind lidar, ranging from lidar hardware/software developments, to diverse measurement campaigns and development of application methods. This contribution aims to present to the community the lidar applications and methods we are working on in order to enhance knowledge exchange and enable future collaborations. For each application or method, we demonstrate what they do and how they can be included in other researchers' workflows and invite constructive feedback.
The main advantages of using a wind lidar, compared to using a meteorological mast for wind energy, are 1) its ability to measure wind speeds remotely over a large range of directions and distances, 2) portability, and 3) cost. Its limitations are 1) availability, depending on atmospheric conditions and the hardware and software involved, and 2) the measurement uncertainty due to the requirement for wind field reconstruction (since it measures on a single direction), and volume averaging (Clifton2018). In this presentation, we want to discuss with the community the topics we currently focus on in order to leverage these advantages and overcome the challenges.

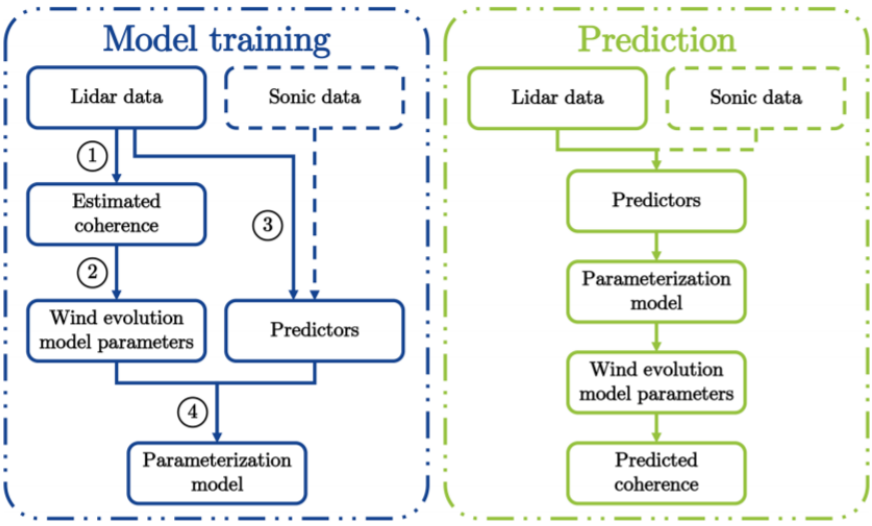

Figure 1: Procedure to calibrate a wind evolution model using lidar data

Due to limited space, we will mention the main points in a list:
•Modelling wind evolution (Chen2021): Leveraging the long-range capabilities of lidars and the possibility for simultaneous measurements in multiple distances, we can model how the turbulent structures are transported and changed travelling downstream. Using machine learning techniques parametrized wind evolution models are enhanced, calibrated and validated using the lidar information (fig.1). This topic is most relevant to lidar assisted control.

•Estimate lidar uncertainty budget: In order to increase confidence on lidar measurements, uncertainty of measurements must be assessed. We develop an uncertainty model allowing us to assess measurement uncertainties for profiling and nacelle-mounted lidars, before a device is built.
The outcome is an open-source python-based tool called Qlunc (Quantification of lidar uncertainties) aiming to estimate lidar uncertainty, considering hardware and data processing methods.

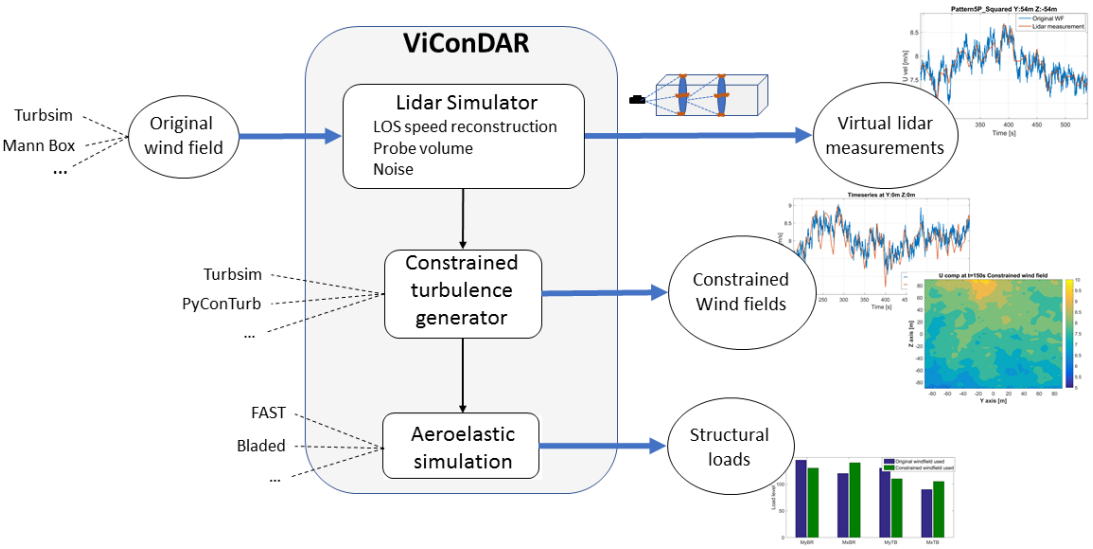

Figure 2: Overview of the ViConDAR framework for simulating lidar measurements and constraining windfields for numerical simulations

•Using lidar to improve aereoelastic simulations: Using lidar measured time series instead of statistical values to create constrained numerical wind fields for aeroelastic simulations in both wake and free flow conditions can reduce the uncertainties and costs of such procedures. For these purposes we developed an open-source modular framework (fig.2) that can simulate lidar measurements and use different constrained turbulence methods to produce wind fields for aeroelastic codes like FAST (Pettas2020).
•Forecasting power production (Würth2019): In order to accommodate the grid integration of wind energy and reduce production uncertainty we use wind lidars to measure the upstream flow of a wind farm. Different methodologies are investigated in order to have minute-scale forecasts of power production with quantified uncertainty.
•Reducing the cost of offshore resource assessment using floating lidars (Bischoff 2018): We have developed numerical tools to simulate a floating lidar in order to assess the uncertainties and limitations of such devices.
Development of a new generation scanning pulsed lidar: We are developing a new device that has a high sampling rate and accuracy while being robust, small and freely programmable. This short range lidar will be useful for all research applications requiring an accurate representation of the wind field.

References:
Chen, Y., Schlipf, D. and Cheng, P. W. (2021) 'Parameterization of wind evolution using lidar', Wind Energy Science, 6(1), pp. 61–91. doi: 10.5194/wes-6-61-2021.
Clifton, A. et al. (2018) 'IEA Wind Task 32: Wind Lidar Identifying and Mitigating Barriers to the Adoption of Wind Lidar', Remote Sensing, 10(3), p. 406. doi: 10.3390/rs10030406.
Pettas, V. et al. (2020) 'A numerical framework for constraining synthetic wind fields with lidar measurements for improved load simulations', in AIAA Scitech 2020 Forum. Reston, Virginia: American Institute of Aeronautics and Astronautics, pp. 1–6. doi: 10.2514/6.2020-0993.
Würth, I. et al. (2019) 'Minute-Scale Forecasting of Wind Power—Results from the Collaborative Workshop of IEA Wind Task 32 and 36', Energies, 12(4), p. 712. doi: 10.3390/en12040712.
Bischoff, O. et al. (2018) 'Validating a simulation environment for floating lidar systems', Journal of Physics: Conference Series, 1037, p. 052036. doi: 10.1088/1742-6596/1037/5/052036.

Comparison of uncertainties in measurements from cup anemometers and lidar systems

David Schlipf[1], Feng Guo[1], and Yiyin Chen[2]
[1]Flensburg University of Applied Sciences
[2]University of Stuttgart

Keywords: lidar | uncertainty | power performance | wind field reconstruction | wind evolution

Nacelle-based lidar systems are cost-effective alternatives to conventional wind measurements with cup anemometers on meteorological masts [1]. For power performance testing of wind turbines, the knowledge of the uncertainties in the measurement is crucial. Traditional cup anemometers measure the horizontal wind speed directly. On contrary, lidar systems need to estimate the horizontal wind speed from the measured line-of-sight wind speeds using wind field reconstruction methods assuming a wind flow model. Therefore, the uncertainty in lidar measurements is often assumed to be higher than the one from cup anemometers, which is justified when focusing on a point measurement.
For power performance testing, however, it is important to obtain a precise value of the wind speed not only at a single point, but representing the effect of the wind flow over the full rotor disc, e.g. by using several cups on different heights [2]. The relevance of this approach is reported to depend also on turbine dimensions and wind shear [3]. In this work, we extend the modeling of lidar uncertainties to capture the rotor-effective wind speed based on spectral wind models [4] with recent knowledge from wind evolution investigations [5] and apply the same approach to cup anemometers to compare both devices.
We considered a wind turbine with a rotor diameter D = 130 m [6]. In this first investigation, the turbine is assumed to be always perfectly aligned with the mean wind direction. For the comparison, the nacelle-based lidar is modelled as a commercial, pulsed lidar measuring with 4 beams, a probe volume of 30 m, and a horizontal/vertical opening angle of 30/10 deg in 2.5 D (see Figure 1). Further, the cup anemometer is assumed to be installed at hub height on a meteorological mast 2.5 D north of the wind turbine.

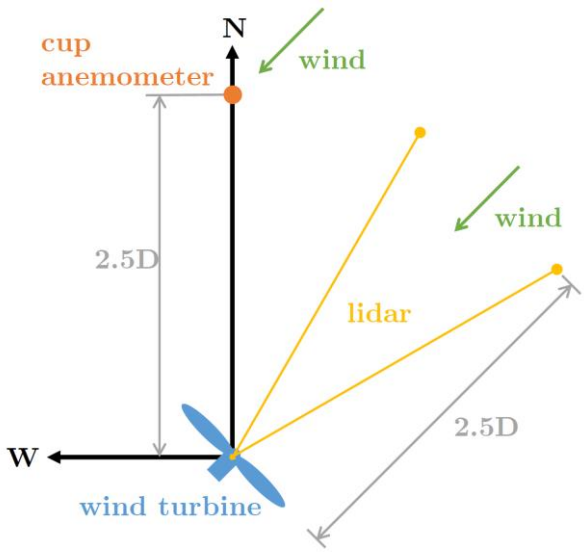

Figure 1: Considered setup: The cup anemometer is located on a met mast in 2.5 rotor diameter (D) from the turbine, which is assumed to yaw perfectly into the wind. A 4-beam lidar system installed on the nacelle is measuring at 2.5 D distance in front of the rotor. The paper compares the uncertainties in capturing the rotor-effective wind speed for both devices.

Usually, homogeneous flow over the rotor is assumed to reconstruct the wind speed from lidar line-of-sight wind speeds. However, wind is not constant in all measurement points as assumed, but turbulent as defined by spectral models. This leads to uncertainties in both lidar and cup measurements, when relating the

measurement to the rotor-effective wind speed, which here is assumed to be the mean of the longitudinal wind speed over the rotor.

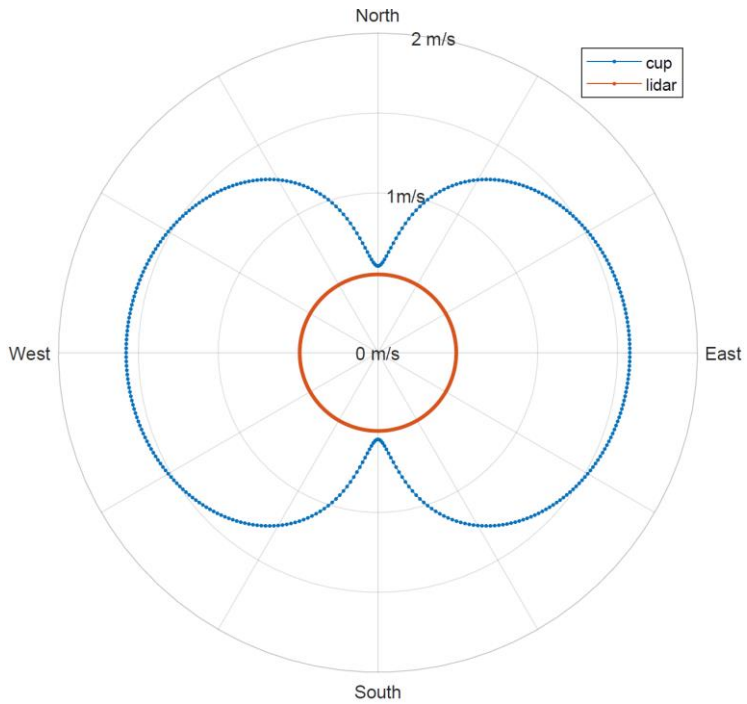

Figure 2: Comparison of uncertainties (2σ=95% confidence interval) to measure the rotor-effective wind from cup and lidar depending on the wind direction. While the lidar uncertainty is constant due to installation on the nacelle, the cup uncertainty is best when turbine and met mast are aligned. Wake effects, shear, yaw misalignment, measurement errors etc. are neglected in this first investigation.

The uncertainty of the lidar wind speed estimate is modelled via the auto- and cross-spectra as well as the frequency representation of a 10 minute moving average [4]. With a mean wind speed of 16 m/s, a IEC Kaimal spectral model, and a medium wind evolution decay parameter of 2 [5], the uncertainty is determined to be 0.5 m/s, independent of the wind direction (see Figure 2). The uncertainty of the cup anemometer is calculated with the same approach. The result is comparable to the uncertainty of the lidar, when cup and turbine are aligned (northerly as well as southerly wind, since no wake effects are considered). For east and west wind however, the uncertainty is more than 3 times higher due to the large lateral turbulence coherence decay. Similar effects on scatter in power curves has been reported in [1].

In future work, we will extend the uncertainty model with additional effects such as error propagation, Mann turbulence, and yaw misalignment. We further plan to investigate how lidar scans can be optimized to reduce the uncertainty.

References:

[1] R. Wagner, T.F. Pedersen, M. Courtney, I. Antoniou, S. Davoust, R.L. Rivera, Power curve measurement with a nacelle mounted lidar, Wind Energy, vol. 17, no. 9, pp. 1441-1453, 2014, DOI: 10.1002/we.1643.

[2] R. Wagner, M. Courtney, J. Gottschall, P. Lindelöw-Marsden, Accounting for the speed shear in wind turbine power performance measurement, WindEnergy, vol. 11, no. 8, pp. 993-1004, 2011 , DOI: 10.1002/we.509.

[3] W.G.J.H.M. Van Sark, H.C. Van der Velde, J.P. Coelingh, W.A.A.M. Bierbooms, Do we really need rotor equivalent wind speed?, Wind Energy, vol. 22, no. 6, pp. 745-763, 2019, DOI: 10.1002/we.2319.

[4] D. Schlipf, M. Koch, S. Raach, Modeling Uncertainties of Wind Field Reconstruction Using Lidar, NAWEA conference, Amherst, MA, USA, October 2019, Journal of Physics: Conference Series, DOI: 10.1088/1742-6596/1452/1/012088.

[5] Y. Chen, D. Schlipf, P.W. Cheng, Parameterization of wind evolution using lidar, Wind Energy Science, 6, 61–91, 2021, DOI: 10.5194/wes-6-61-2021.

[6] P. Bortolotti, H. Canet Tarres, K. Dykes, K. Merz, L. Sethuraman, D. Verelst, F. Zahle. IEA wind task 37 on systems engineering in wind energy - WP2.1 reference wind turbines. Technical report, International Energy Agency, 2019.

Limitations of LIDAR-based systems for power capture enhancement al low wind speeds : a theoretical framework

Irene Miquelez[1,*], Asier Diaz[2], and Jorge Elso[1]
[1]Universidad Pública de Navarra
[2]Siemens Gamesa Renewable Energy
[*]Presenting author

Keywords: Wind turbine | Power capture | LIDAR | Below rated | Control

Optimizing power production is one of the main objectives of the control strategies for wind turbines. More specifically, for below rated wind speeds, the generator torque input is used to place the wind turbine in its optimal operation point and thus, extract the maximum available energy for each wind speed.
The most well-known control strategy for below rated operation is the Indirect Speed Control (ISC).
By using a nonlinear feedback of the generator speed, ISC achieves a perfect tracking of the maximum power point in the steady state. Although an increase in power capture with respect to ISC is promised by some authors (Rajendran & Jena 2014), studies based on simulation show that the possibility of greater power capture is too small to be profitable, even with good wind measurements such as the ones provided by LIDAR sensors (Schlipf et al. 2011). Consequently, efforts should concentrate on reducing yaw misalignment (Zhang & Yang 2020) or improving parameter identification to ensure ISC works optimally (Fingersh & Carlin 1998).

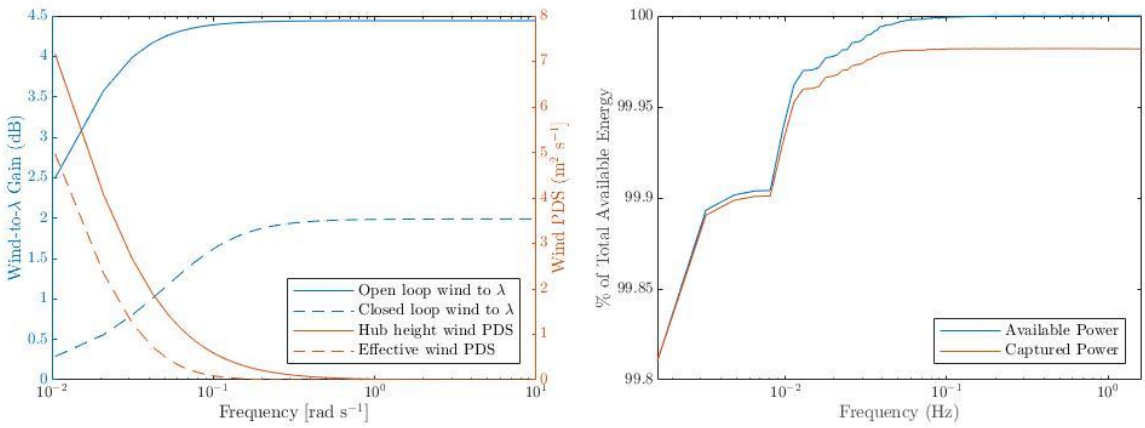

Figure 1: (a) In blue linearisation of the closed loop system, in red wind power density. (b) Captured power and available power.

To clarify this point, a theoretical approach to the evaluation of power capture enhancement has been carried out, based on the linear model of NREL's 5MW wind turbine. The first step consists in a revision of the criteria for determining an increase on captured power. When evaluating the characteristics of a wind field in terms of power production, the input time series used for calculations should be the rotor effective wind speed, instead of the hub height wind, as the latter presents components at much higher frequencies, and would therefore generate a different response when acting on a system.
Besides, a linearization of the wind turbine is obtained, that includes the ISC block. Frequency domain analysis shows good disturbance rejection precisely at all the relevant frequencies of the effective wind, which is an indicator of the small improvement possibility.
For a better understanding, a nonlinear relation has been established between effective wind and maximum available energy and between effective wind and captured energy. The comparison of both results show a close-to-optimal energy capture. Simulations match the theoretical results and confirm that it is not possible to improve the ISC significantly, even with an ideal LIDAR-based reconstruction of effective wind speed.
Figure 1a shows the disturbance rejection of the simplified wind turbine model with and without ISC and the wind spectra for a single point and for the rotor effective wind speed. Plot 1b represent a frequency distribution of the available and captured power.

Figure 2: G97 2MW SGRE wind turbine.

A collaboration between Public University of Navarre (UPNA) and Siemens Gamesa Renewable Energy (SGRE) have supported the work presented in this document. Figure 2 shows a G97 2MW SGRE wind turbine where future LIDAR based control algorithms which developed during this collaboration will be field tested.

References:
Rajendran, S., and Jena, D. 2014. Control of variable speed variable pitch wind turbine at above and below rated wind speed. Journal of Wind Energy, 2014.
Schlipf, D., Kapp, S., Anger, J., Bischoff, O., Hofsäß, M., Rettenmeier, A., and Kühn, M. 2011. Prospects of optimization of energy production by lidar assisted control of wind turbines.
Zhang, L., and Yang, Q. 2020. A Method for Yaw Error Alignment of Wind Turbine Based on LiDAR. IEEE Access, 8, p.25052–25059
Fingersh, L., and Carlin, P. 1998. Results from the NREL variable-speed test bed. In 1998 ASME Wind Energy Symposium (pp. 50).

4D wind fields for aeroelastic simulations of wind turbines with lidars

Yiyin Chen[1,*], Feng Guo[2], David Schlipf[2], and Po Wen Cheng[1]
[1]University of Stuttgart
[2]Flensburg University of Applied Sciences
[*]Presenting author

Keywords: stochastic wind field simulation | lidar-assisted control | unfrozen turbulence

Lidar-assisted control (LAC) of wind turbines is a control concept that takes advantage of a nacellemounted lidar (a remote sensing device) to measure upstream wind of a turbine and enables a preact to incoming turbulence (see, e.g., Schlipf, 2015; Simley, 2015). Because the turbine will not be exposed to the identical disturbances as that measured by the lidar in advance, wind evolution must be involved in generating wind fields for simulating a LAC system, and thus the 3D wind field simulation methods (Mann, 1998; Veers, 1988) usually used in aeroelastic simulations are no longer sufficient in this case. For this reason, some attempts have been made to determine the longitudinal coherence (see, e.g, Chen, Schlipf and Cheng, 2021; Schlipf et al., 2015; Simley and Pao, 2015) and integrate it into wind field simulations (see, e.g., Bossanyi, 2013; Laks, Simley and Pao, 2013).

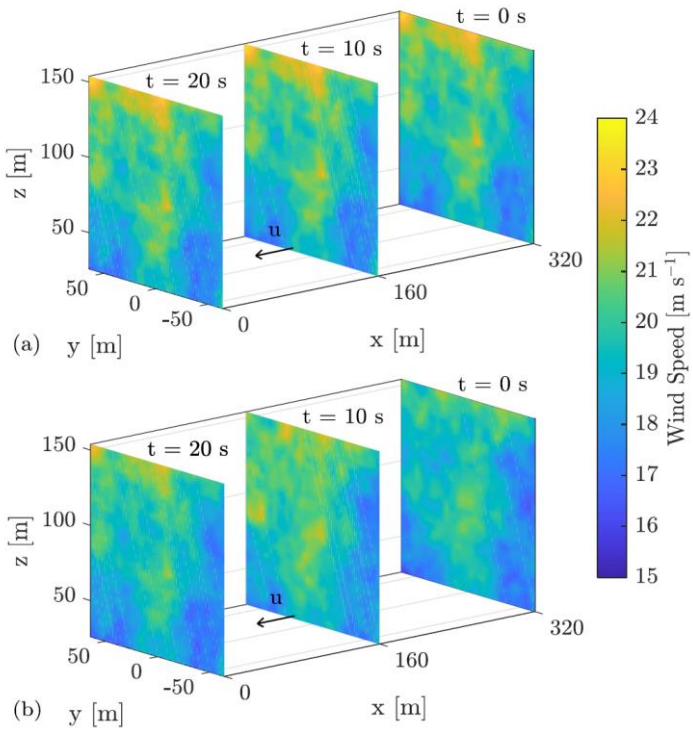

Figure 1: Example plots of (a) frozen and (b) unfrozen turbulent wind fields. Turbulence properties: mean wind speed = 16 m/s, turbulence intensity = 0.16, shear constant = 0.2. Generated with Mann turbulence generator.

In this work, we aim to extend the Veer's (1988) method of 3D stochastic wind field simulation to 4D by including the longitudinal coherence. We first give a derivation of our 4D method. Based on this, a two-step Cholesky decomposition method is proposed to factorize the matrices of the lateral-vertical coherence and the longitudinal coherence, respectively, to pursue a better computational performance. This method also makes it possible to generate 4D wind fields by combining multiple independent 3D wind fields. It is verified that our 4D method can produce a synthetic wind field in which the time series data of wind speeds at any two points in a 3D space can preserve the predefined lateral-vertical and longitudinal coherence (see Figure 1).

To facilitate practical application of our 4D method, we will implement it as an open-access tool on Github (accessible in Matlab and Python). This tool takes 3D wind fields generated using standard wind field simulation tools --- TurbSim or Mann turbulence generator, so that the longitudinal coherence can be introduced in synthetic wind fields without changing any other turbulence properties. The tool can be further integrated into aeroelastic simulations of wind turbines, e.g., OpenFAST (see Figure 2).

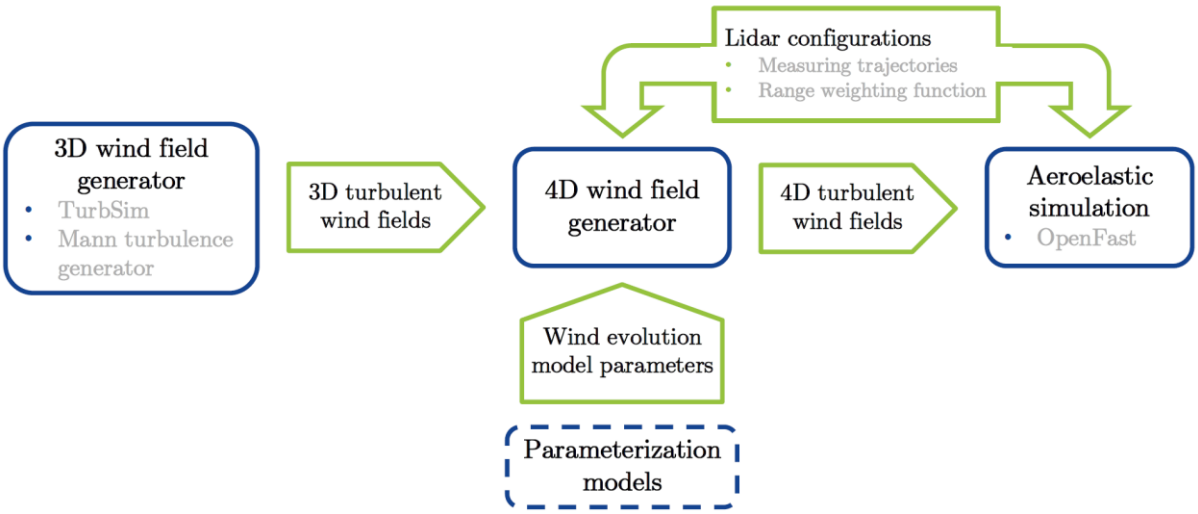

Figure 2: Concept for integrating the 4D wind field simulator into the aeroelastic simulation of wind turbines.

Furthermore, since the 4D wind field simulation is supposed to be applied in couple with lidar simulations, it is expected to generate wind speeds for a 3D grid, and thus the size of simulation points as well as the computational effort will be much larger than that of the 3D method. Therefore, we further look into the possibility to reduce the size of simulation grid. For this purpose, we first derive the analytical expressions of the lidar-estimated auto-spectrum and coherence as the reference for comparison. Then, we analyze the influence of the discretization of the lidar range weighting function, settings of the simulation grid, and the interpolation of wind speeds on the spectral properties of synthetic wind fields using our simulation tool.
To summarize, we will introduce a 4D wind field simulation method based on the extension of the Veer's method and provide it as an open-access tool which allows users to simulate 4D wind fields using TurbSim or Mann turbulence generator. This approach extends previous work (see, e.g., Bossanyi, 2013; Laks, Simley and Pao, 2013) from single-distance lidar measurements to multidistance systems. By studying the impact of the discretization in simulations using this tool, we can provide some insights about optimizing the simulation configurations to obtain good simulation results.

References:
Bossanyi, E. (2013) 'Un-freezing the turbulence: Application to LiDAR-assisted wind turbine control', IET Renewable Power Generation, 7(4), pp. 321–329. doi: 10.1049/iet-rpg.2012.0260
Chen, Y., Schlipf, D. and Cheng, P.W. (2021) 'Parameterization of wind evolution using lidar', Wind Energy Science, 6(1), pp. 61–91. doi: 10.5194/wes-6-61-2021
Laks, J., Simley, E. and Pao, L. (2013) 'A spectral model for evaluating the effect of wind evolution on wind turbine preview control', 2013 American Control Conference, 2013 American Control Conference (ACC), Washington, DC, 17-19 June: IEEE, pp. 3673–3679. doi: 10.1109/ACC.2013.6580400
Mann, J. (1998) 'Wind field simulation', Probabilistic Engineering Mechanics, 13(4), pp. 269–282. doi: 10.1016/S0266-8920(97)00036-2
Schlipf, D. et al. (2015) 'Detection of Wind Evolution and Lidar Trajectory Optimization for Lidar-Assisted Wind Turbine Control', Meteorologische Zeitschrift, 24(6), pp. 565–579. doi: 10.1127/metz/2015/0634
Schlipf, D. (2015) Lidar-assisted control concepts for wind turbines. Dissertation.
Simley, E. and Pao, L.Y. (2015) 'A longitudinal spatial coherence model for wind evolution based on large-eddy simulation', 2015 American Control Conference (ACC), 2015 American Control Conference (ACC), Chicago, IL, USA, 1/7/2015 - 3/7/2015: IEEE, pp. 3708–3714. doi: 10.1109/ACC.2015.7171906
Simley, E.J. (2015) Wind Speed Preview Measurement and Estimation for Feedforward Control of Wind Turbines. PhD thesis.
Veers, P.S. (1988) Three-Dimensional Wind Simulation. Albuquerque, New Mexico (SAND88-0152 UC-261).

Mini-Symposium: IEA Wind Task 32: Wind Lidar (II)

Smart Lidar Systems for Floating Offshore Wind Turbines

Florian Thomas[1,*], David Schlipf[2], and Steffen Raach[1]
[1]sowento GmbH
[2]Flensburg University of Applied Sciences
[*]Presenting author

Keywords: smart lidar | motion compensation | lidar data processing | floating wind turbine | lidar-assisted control

Lidar-assisted control (LAC) has been so far successfully tested for onshore wind turbines and shows promising potential to reduce the LCOE of large offshore wind turbines [Canet et al., 2020]. This approach is also considered promising for floating offshore wind turbines (FOWT) [Schlipf et al., 2015]. However, due to the high motion of the whole system and the blockage of laser beams by the blades, the baseline lidar data processing (LDP) algorithms currently implemented on lidar devices provide a highly disturbed wind speed preview signal. This work aims to outline the possibilities of smart lidar systems on FOWT and show the benefits of an improved LDP algorithm including motion compensation and blade ghost avoidance.
The work is conducted within the VAMOS project, a German-French research project for deep-water offshore wind energy. The main objective of this project is to close knowledge gaps in the measurement and simulation of FOWT systems for commercial use.
As lidar devices only detect the relative velocity, the measurements are affected by the movement of the system itself due to waves and wind [Kelberlau et al., 2020]. In order to compensate the influence of this motion on the measured line-of-sight velocities, data from an inertial measurement unit (IMU) located in the turbine's nacelle is used. First, in order to derive the correct longitudinal wind component, the actual lidar measurement location is calculated using the Euler angles of the IMU. Second, this information is combined with the velocity measurements from the IMU in order to deduct the velocity induced by the turbine motion from the measured line-of-sight wind velocity [Schlipf et al., 2020].

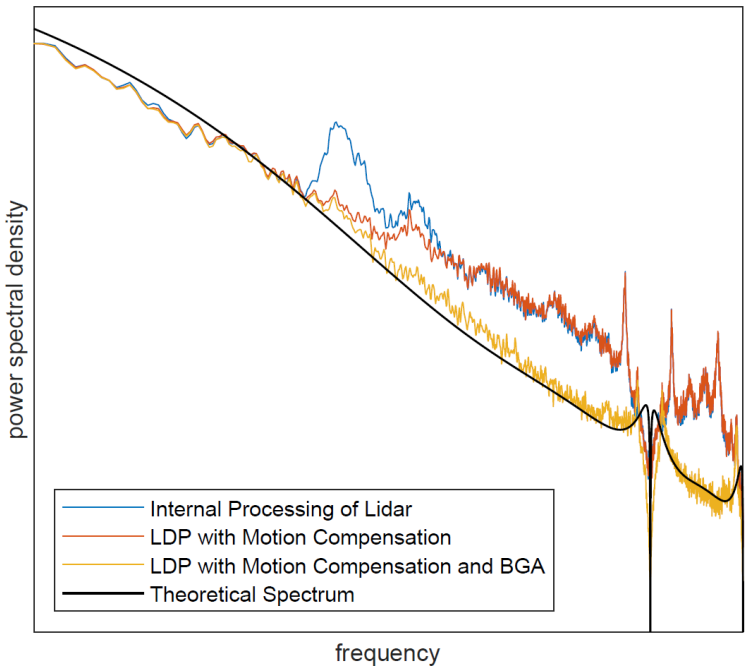

Figure 1: Auto-spectra of lidar estimates of the rotor-effective wind speeds based on the lidar measurements of the first range at 50 m from 5 h measurement data on 26 January 2021 with a mean wind speed of 11.3 m/s: baseline processing of the lidar device (blue), advanced processing with motion compensation (red) and advanced processing with motion compensation and blade ghost avoidance (yellow), compared to the theoretical spectrum (black).

Subsequently, the consecutive measurements of one full scan are combined to one estimate of the rotor-effective wind speed (REWS). If one or more measurements of the current scan are unavailable, the averaging becomes unbalanced. As nacelle-based lidar systems are mainly located on top of the nacelle behind the rotor plane, the main source of unavailability is the blockage of the lidar beams by the bypassing rotor planes, causing interferences, which we named the blade ghost effect. In this work the LDP has been extended by a blade ghost avoidance algorithm, which uses an interpolated or previous value of the same beam, if the measurement from the current scan is unavailable [Schlipf et al., 2019].
The described algorithms are implemented on an additional PC in the nacelle, processing Dynamic Link Libraries which can be also loaded in aero-elastic tools [Schlipf et al., 2020], following the "Smart Lidar" concept, see Figure 2.

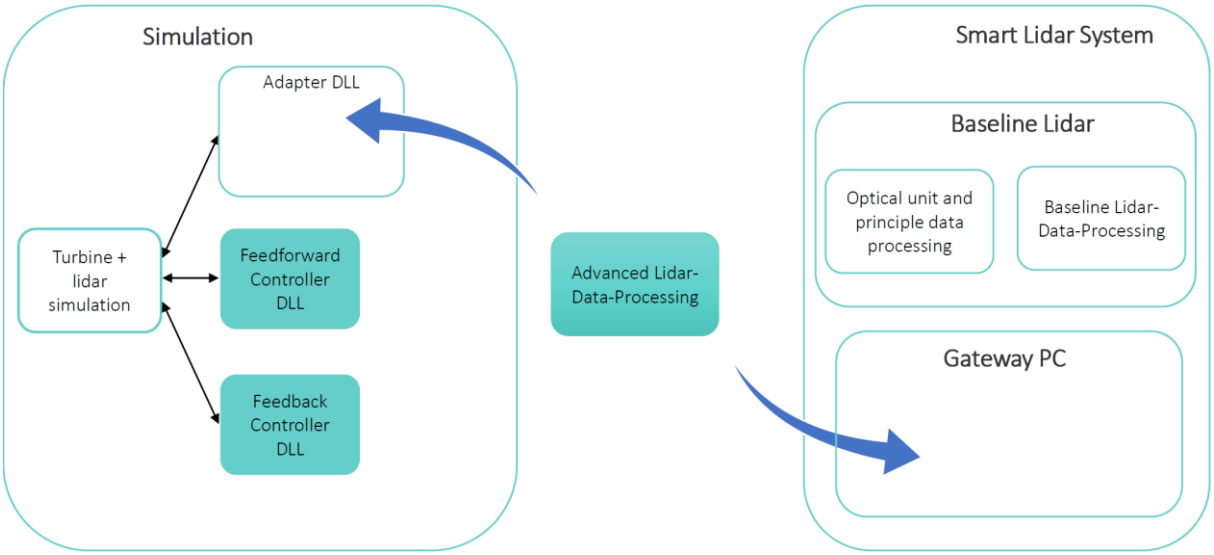

Figure 2: Smart Lidar Concept: Algorithms can be loaded into aero-elastic simulations as Dynamic Link Libraries (DLLs) and on the smart lidar system, which simplifies testing and certification. In this evaluation, the system still consists of a baseline lidar device and an additional PC. Future systems are expected to be a single device.

Results demonstrate that the influences of the blade ghost effect and the movement of the system could both be significantly reduced. Figure 1 shows the autospectra of the lidar estimates of the REWS for different algorithms based on real lidar and IMU measurement data. The motion compensation almost completely eliminates the wave-induced peak in the spectrum of the raw REWS estimate. The blade ghost avoidance additionally leads to a significant reduction of interferences in higher frequencies. Overall, the spectrum of the final signal fits well to the theoretical lidar spectrum based on turbulence models, indicating that it mostly contains wind information and can be used for LAC.
Further works will include the application of an extended multi-distance LDP algorithm and the inclusion of these measurements in the turbine's control loop by a feed-forward controller.

References:
H. Canet, S. Loew, and C. L. Bottasso. What are the benefits of lidar-assisted control in the design of a wind turbine? Wind Energy Science Discussions, 2020:1–23, 2020. doi:10.5194/wes-2020-131.
F. Kelberlau, V. Neshaug, L. Lønseth, T. Bracchi, and J. Mann. Taking the motion out of floating lidar: Turbulence intensity estimates with a continuous-wave wind lidar. Remote Sensing, 12(5), 2020. doi:10.3390/rs12050898.
D. Schlipf, E. Simley, F. Lemmer, L. Pao, and P. W. Cheng. Collective pitch feedforward control of floating wind turbines using LIDAR. Journal of Ocean and Wind Energy, 2(4):440–447, July 2015. doi:10.17736/jowe.2015.arr04.
D. Schlipf, S. Raach, and F. Haizmann. Control system for controlling a turbine, method for controlling a turbine, and wind turbine, 2019. Patent WO2019097092A2.
D. Schlipf, F. Lemmer, S. Raach, et al. Multi-variable feedforward control for floating wind turbines using lidar. In The 30th International Ocean and Polar Engineering Conference. International Society of Offshore and Polar Engineers, 2020. doi:10.18419/opus-110

Lidar taxonomy for modular lidar designs

Francisco Costa[1,*], Andrew Clifton[1], and Nikola Vasiljevic[2]
[1]University of Stuttgart
[2]Technical University of Denmark
*Presenting author

Keywords: Ontology | Open Science | Controlled vocabulary | Open Lidar

Introduction

Open science can help us share and leverage the results from each others' research and speed up innovation. However, experience shows that this can also lead to a "wild west" situation with uncoordinated activities that don't lead to progress.

One way to mitigate this lawless free-for-all is to create frameworks for research and provide the tools for others to contribute within those frameworks. This can lead to modular tools and processes that can be improved module-by-module.

In this work the first essential step is to agree on a common terminology by creating a controlled vocabulary (CV), which is a list of terms for a specialized purpose [1]. In the second step relations between terms are defined and established (e.g., hierarchical relations) and thus a CV is uplifted to an ontology. Generally speaking, controlled terminologies such as CVs and ontologies must be always under continuous update, guaranteeing that established relationships are up to date and reflects the current domain of knowledge.

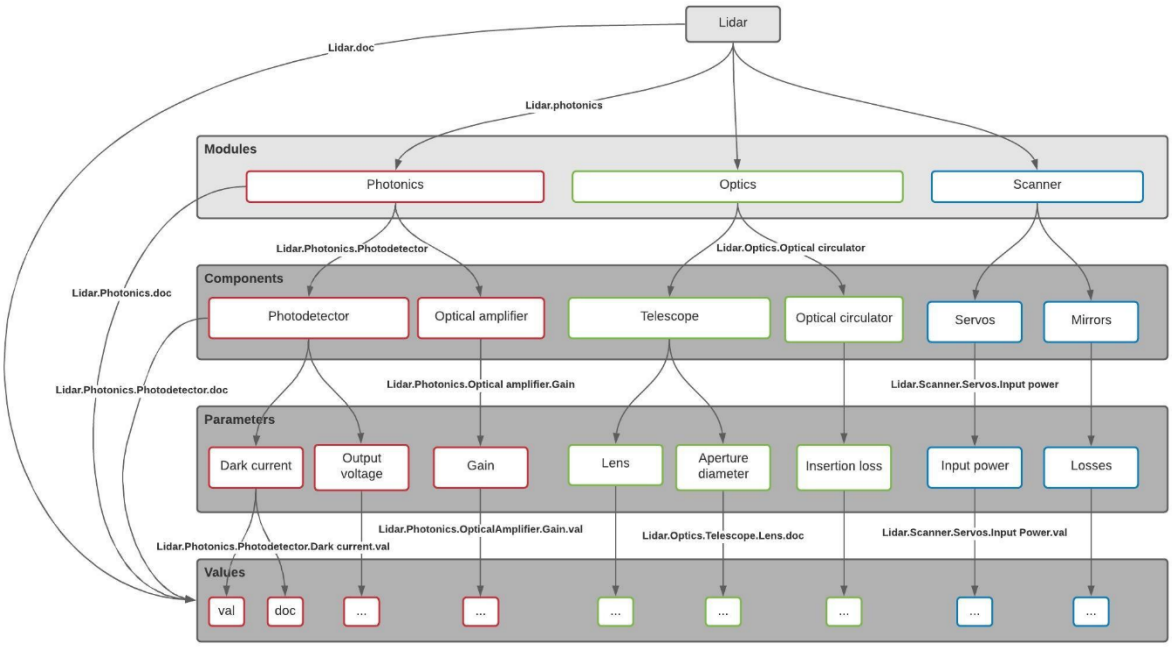

Figure 1. Example of tree-like structure used to describe a lidar (modules and components) configuration.

Objectives

Here, we introduce the concept of modular wind lidar. This is enabled by a common ontology that defines the many aspects of a wind lidar. We show how it can be used to define and describe the different modules and their interactions, and how it can be used to help transfer data, tools, and knowledge (e.g., by simplifying the process of creating input files for simulations).

Methodology

The wind lidar ontology is developed and managed using sheet2rdf [2] and OntoStack [3]. sheet2rdf is an automatic workflow executed by means of GitHub actions, that contains underlying shell and python scripts,

which converts specifically formatted Google sheet to machine-actionable and FAIR ontology, in a RDF format. Terms are lexicalized using the Simple Knowledge Organization System (SKOS), deploying an ontology. OntoStack is a set of orchestrated micro-services configured and interfaced such that they can intake ontologies and serve to humans and machines.

Table 1. Lidar controlled vocabulary and labelling. num states for numerical value and doc states for documentation. By using dot notation can access to lidar components information, either parameter values or describing documentation.

Device	Module	Component	Subcomp.	Paramet	Value	SKOS label
Lidar	Optics	--------	-------	----------	doc	Lidar.Optics.doc
Lidar	Optics	Telescope	Lens	Curvature	doc	Lidar.Optics.Telescope.Lens.Curvature.doc
Lidar	Photonics	Photodetector	------	Dark Current	num	Lidar.Photonics.Photodetector.DarkCurrent.num

The derived ontology includes vertical (broader/narrower and parent/child) and horizontal (transitive) relationships between terms, as well as notes about origins of terms and their description. The implementation of the above-described tooling is accessible at https://github.com/IEA-Wind-Task-32/wind-lidar-glossary, while the derived ontology is served at the OntoStack implementation of DTU Wind Energy at http://data.windenergy.dtu.dk/ontologies/view/IEATask32Glossary.

We've aligned the wind lidar ontology with the existing best practice and the e-WindLidar and Open Lidar initiatives. The Open Lidar initiative [4] defines the most common modules and components a lidar is made of. The e-WindLidar initiative [5] has been pursuing the goal of including expert lidar knowledge in tools that will facilitate the application of lidar technology.

From top to bottom in a hierarchical dependence, parameters are related with their corresponding components and each component, as well, with their corresponding module. Combining tree-like structure with parent-child dependencies between parameters, components and modules we can obtain very readable, easily understandable and flexible lidar ontology. We can consider the lidar device as the top level element or concept in the hierarchical list. Going down through existing levels (which represent modules and components) up to the value we want to know, considered as the bottom element, one can label each lidar component. The use of highly descriptive labels will ease tracking components' relationships along the lidar structure.

Here we provide an overview of the idea and its implementation, and show how the wind energy community can benefit from it.

References:

[1] M. Zaharee, "Building Controlled Vocabularies for Metadata Harmonization." [Online]. Available: https://asistdl.onlinelibrary.wiley.com/doi/epdf/10.1002/bult.2013.1720390211 [Accessed: 06-Nov-2020].

[2] N. Vasiljevic, "sheet2rdf," First release (version v0.1), 2021. [Online]. Available: https://zenodo.org/record/4432136#.YABPOhZ7nb0. [Accessed: 13-Jan-2021].

[3] N. Vasiljevic, "OntoStack," 2021. [Online]. Available: http://data.windenergy.dtu.dk/ontologies/view/en/. [Accessed: 14-Jan-2021].

[4] A. Clifton, I. Würth, F. Haizmann, S. Raach, N. Vasiljevic, and J. F. Newman, "OpenLidar : A Collaborative Wind Lidar Platform."

[5] N. Vasiljevic et al., "e-WindLidar : making wind lidar data FAIR," no. January, 2018, doi: 10.5281/zenodo.2478051.

Wind lidar technology development and transfer

Andrew Clifton[1], David Schlipf[2], and Ines Würth[3]
[1]Stuttgart Wind Energy (SWE)
[2]Flensburg University of Applied Sciences
[3]University of Stuttgart

Keywords: wind lidar | technology transfer | certification | systems engineering | wind resource assessment

Wind lidar is one of the biggest changes to occur in wind energy in recent decades. The use of lasers to measure wind vectors remotely has enabled many new developments, including lidar-assisted control of wind turbines and wind plants, and has directly contributed to the growth of offshore wind [see Clifton et al, 2018]. In this contribution we consider several case studies of how wind lidar technologies were developed or adapted for new applications, and commercialised.

Figure 1: The IEA Wind Task 32 2020 logo

These case studies include:
- Vertical profiling wind lidar for ground-based resource assessment. Initially launched as a commercial product in the mid 2000's, wind lidar were initially seen as research devices that could measure up to the rotor tip, reducing the need for wind profile extrapolation and thus reducing uncertainty. Early adopters sought to standardise their use for resource assessment (i.e., vertically resolved wind speed and direction profiles) through IEA Wind Task 11. In 2011 IEA Wind Task 32 started developing a Recommended Practices document that was adopted in 2013. In 2017 an IEC Standard (IEC 61400-12-1) provided a framework for their use in some applications. Since then, the "Consortium for the advancement of remote sensing" (CFARS) has been actively promoting the use of wind lidar, backed up with evidence from industry users. Now, in 2021, wind lidar are widely accepted for use in flat terrain. The focus over the past few years has shifted to the potential for wind lidar to completely replace met masts. As a result, there is great interest in their ability to measure turbulence, and in their ability to be used in all terrain. These remain the major themes of research at this time.
- Forward-looking lidar for wind turbine control offers the potential to reduce turbine loads and fatigue, and would enable larger wind turbines in future. Lidar-assisted controls may also be key to improve the control performance of floating offshore wind turbines. And, due to collaboration between multiple stakeholders the advantages of designing a wind turbine with feed-forward lidar control are becoming clearer. Despite their potential benefits, the adoption of wind lidar for feedforward control has been slower than other applications; this stems from the general complexity and difficulty of reliably and safely integrating a wind lidar into the wind turbine control system in such a way that the turbine can still be certified. Work continues to generate evidence for the safe and reliable deployment of lidar for this application [see e.g., Schlipf et al, 2018].
For each case study we identify some of the main drivers for the adoption of wind lidar, some of the challenges that were experienced on the way, and discuss what steps remain. Our goal is to familiarise the wind energy research and development community with the process of technology transfer and the various actors that are involved.

References:
Clifton, A., Clive, P., Gottschall, J., Schlipf, D., Simley, E., Simmons, L., Stein, D., Trabucchi, D., Vasiljevic, N., Würth, I., 2018. IEA Wind Task 32: Wind Lidar Identifying and Mitigating Barriers to the Adoption of Wind Lidar. Remote Sensing 10, 406.
Schlipf, D., Hille, N., Raach, S., Scholbrock, A. and Simley, E., 2018. IEA Wind Task 32: Best Practices for the Certification of Lidar-Assisted Control Applications. Journal of Physics: Conference Series, 1102, p.012010.

Mini-Symposium: Advances in High-Performance Computing for Wind Energy Applications

Mohsen Lahooti
Imperial College London

Bruno Carmo
University of Sao Paulo

Numerical simulation plays a critical role in modern wind turbine design. It gives detailed information of the expected response and performance of wind farms, wind turbines or individual subcomponents under different operating and design conditions. High-resolution computer simulations are essential in our understanding of atmospheric turbulent flows and wind farm wakes to enable farm optimization for increased power extraction. They are also now increasingly necessary to describe the dynamics of very long flexible blades interacting with turbulent flow structures, which can result in vortex-induced vibrations and power output degradation. Therefore, high performance advanced numerical algorithms and computational tools with excellent scalability, which can address such simulations robustly and efficiently, play an important role in future wind turbine design. This mini symposium is aiming at sharing the state-of-the-art advances in numerical methods, mathematical models and computational techniques in the application of high-performance computing to wind energy. It seeks contributions on applications including, but not limited to, turbulence and atmospheric flow, aeroelasticity and fluid-structure interaction, wake and farm modelling. It will survey the landscape of current HPC technology and will aim to identify existing bottlenecks for the adoption of exascale computing by the wind energy community.

Actuator line modeling: efficiency improvements and code comparisons

Luoqin Liu[1], Lucas Franceschini[2], Daniel Francisconi Oliveira[2], Flavio Cesar Cunha Galeazzo[3], Bruno Souza Carmo[2], and Richard Stevens[1]
[1]University of Twente
[2]University of Sao Paulo
[3]University of Stuttgart

Keywords: Actuator line modeling | High performance computing | Code comparison

Large-eddy simulations (LES) have recently become a prominent tool for performing high-fidelity simulations of wind turbine wakes and wind farm flows. LES can capture the three-dimensional, unsteady character of the flow past wind turbines and predict their performances. However, the flow around the rotating turbine blades with body-fitted grids or immersed boundary methods is not feasible yet because of the high computational cost. Therefore, the actuator line model (ALM) is commonly used to model wind turbines in atmospheric flows [1]. The ALM is based on the blade element theory using tabulated aerofoil data but with the velocities computed from computational fluid dynamics. The ALM is known to represent the blade movement and the associated flow details more accurately than the actuator disk model but at the expense of a much higher computational cost.

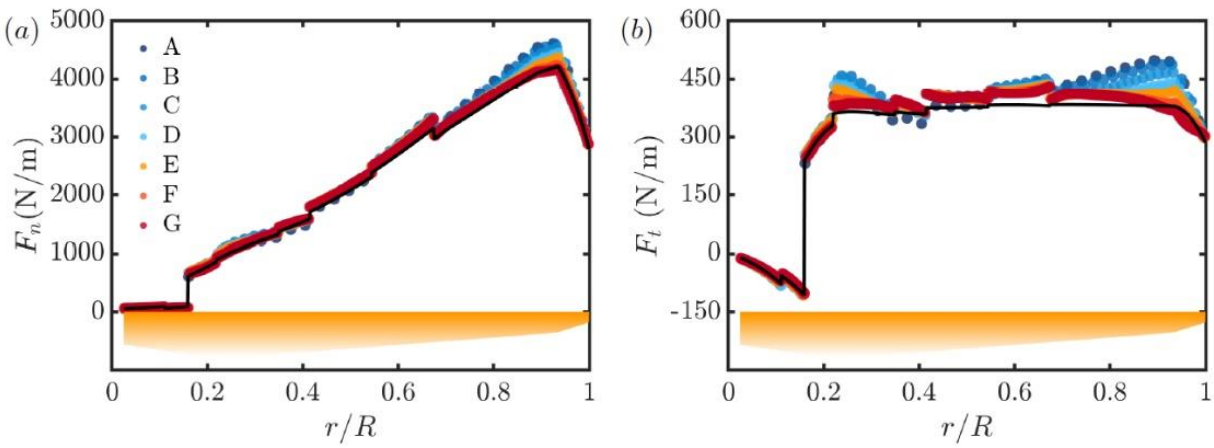

Figure 1: Comparison between the results obtained from the ALM simulations with different grid resolution (increasing from A to G) and the BEM method. (a) Axial force and (b) tangential force per unit span along each blade. Filled symbols: the ALM simulations; solid line: the BEM results.

In the ALM, the body forces are calculated using tabulated airfoil data employing the local angle of attack along the blades. The local angle of attack is defined from the local relative velocity determined at each time step while running a simulation. After determining the local forces, they are projected from the lines representing the rotor blades to the CFD grid points. The force projection method requires numerical stability but forms a computational bottleneck. Typically this force project is performed using an isotropic Gaussian function.

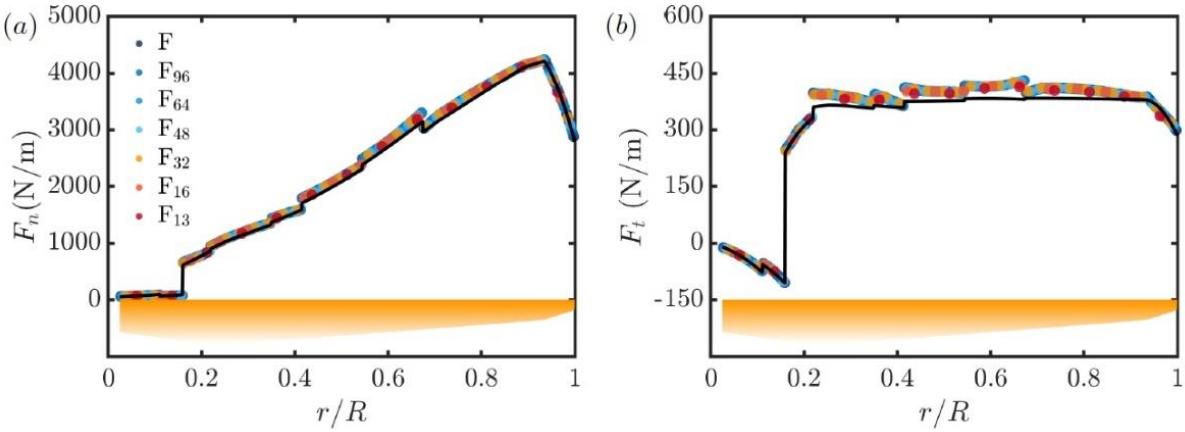

Figure 2: Comparison between the results obtained from the ALM simulations with different number of actuator points N with BEM results. (a) Axial force and (b) tangential force per unit span along each blade. Filled symbols: the ALM simulations; solid line: the BEM results.

In this work, we perform a one-to-one comparison between simulations of the NREL 5MW [6] turbine performed using two large-eddy simulation codes, i.e., the LES code used at the University of Twente [4,5] and the Winc3D [2]. We find perfect agreement between the two codes. We perform a detailed comparison of the ALM results with Blade Element Momentum (BEM) predictions by performing different resolution simulations. Figure 1 shows that the results from high-resolution simulations converge to the BEM [3] results when a high resolution for the flow solver is used. Figure 2 shows that the number of actuator points has only a limited effect on the obtained solution. We conclude that the accuracy of wind turbine simulations performed using ALM is limited by the resolution of the flow solver and not by the number of actuator points.

From comparing the different resolution simulations with the BEM results, we formulate guidelines for the optimal number of actuator points to be used in ALM simulations when a given accuracy is desired. This results in a meaningful reduction of the used actuator points. This decreases the computational overhead of ALM computations. To further reduce the computational overhead of the ALM, we introduce a compact, smooth function to replace the Gaussian force projection method that is commonly used. The results obtained using the new force projection method are identical to the commonly employed Gaussian method but at a much lower computational cost. The guidelines and updated force projection method allow for much more efficient usage of the ALM model in large scale high-performance simulations. A detailed analysis of the performance benefits will be presented in an accompanying presentation.

References:

[1] Sorensen, J.N. and Shen, W.Z., 2002. Numerical modeling of wind turbine wakes. J. Fluids Eng., 124(2), pp.393-399.

[2] Deskos, G., Laizet, S. and Palacios, R., 2020. WInc3D: A novel framework for turbulence-resolving simulations of wind farm wake interactions. Wind Energy, 23(3), pp.779-794.

[3] Glauert, H., 1983. The elements of aerofoil and airscrew theory. Cambridge University Press.

[4] Liu, L. and Stevens, R.J., 2020. Wall modeled immersed boundary method for high Reynolds number flow over complex terrain. Computers & Fluids, p.104604.

[5] Gadde, S.N., Stieren, A. and Stevens, R.J., 2020. Large-Eddy Simulations of Stratified Atmospheric Boundary Layers: Comparison of Different Subgrid Models. Boundary-Layer Meteorology, pp.1-20.

[6] Jonkman, J., Butterfield, S., Musial, W. and Scott, G., 2008. Definition of a 5-MW Reference Wind Turbine for O shore System Development, TP 500-38060. National Renewable Energy Laboratory.

Assessment of a heterogeneous computing CFD code in wind farm simulations

Bruno López*, Andrés Guggeri, Martín Draper, and Gabriel Usera
Facultad de Ingeniería, UdelaR
*Presenting author

Keywords: Wind energy | Heterogeneous computing | Graphics Processing Unit (GPU) | Large Eddy Simulation | Actuator Line Model

In the last decade, the introduction of heterogenous architectures for parallel computing programs allowed a considerable increase of performance in High-Performance Computing (HPC), compared to parallel applications executed on homogenous architectures, based on Central Processing Units (CPU). At present, the most extended heterogenous computing platforms combine CPUs with Graphics Processing Units (GPU), which have been generalized for data-parallel computationintensive tasks (Cheng, Grossman & McKercher, 2014).

Recently, scientists have assessed the use of CPU-GPU architectures for solving Computational Fluid Dynamics (CFD) problems, obtaining important improvements in the computational performance of the codes (Niemeyer & Sung, 2014; Afzal et al., 2017; Fernandez et al., 2020). These works also show that the redesign of code programming strategies is needed to maximize the benefits of the GPU architecture. The exploration of heterogenous computing in wind energy applications is incipient.

Wind turbines simulations using the lattice Boltzmann method performed on GPU architecture are presented in (Asmuth, Olivares-Espinosa & Ivanell, 2020). The turbines rotor is represented using the Actuator Line Model (Sorensen & Shen, 2002). The GPU accelerated code used in this work achieved simulations performance close to real time. In (Liu et al., 2021) control vibration strategies in onshore wind turbines are analysed using an aeroelastic model developed for GPU architecture, using Python and CUDA C programming languages. These strategies are based on mass damper technics which are tuned using the GPU accelerated code, through massive parallel computation. The wind speed time series are generated using LES simulations and taken as input for the aeroelastic model to compute the equivalent fatigue loads.

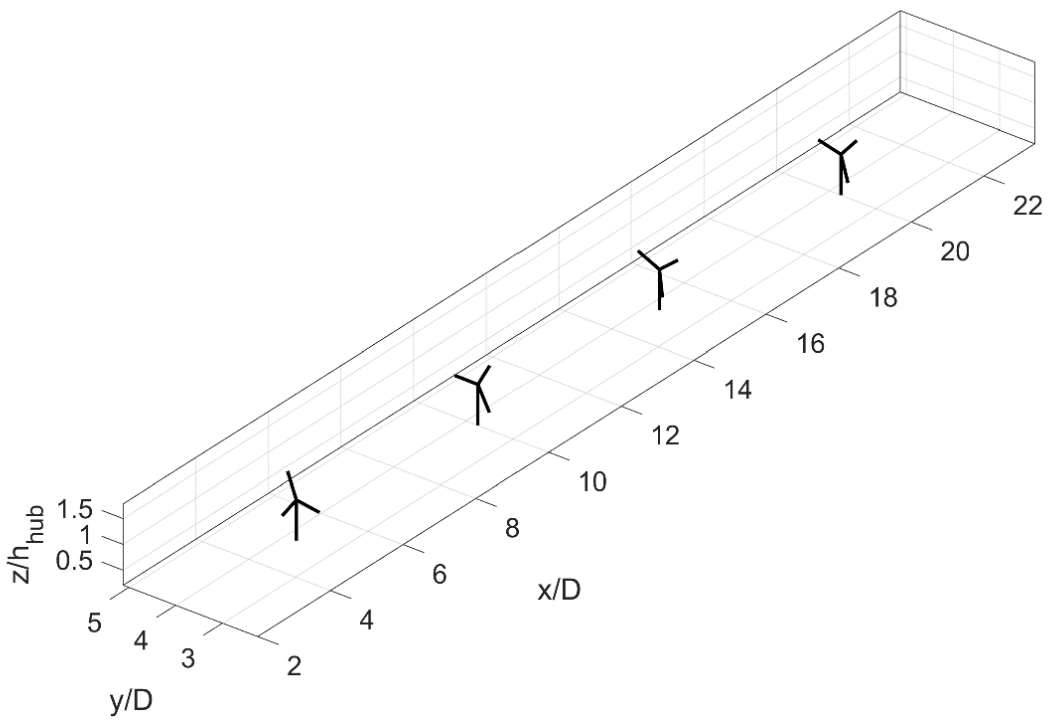

Figure 1: Real onshore wind farm setup used to assess GPU-based code performance.

The aim of this work is to assess the performance of a general purpose CFD open-source code in wind energy applications. The code has been recently migrated from in-house open-source code caffa3d (Usera et al., 2008; Mendina et al., 2014) to a heterogeneous architecture based on CPU and GPU, to analyse the pollution dispersion in an urban environment (Fernandez et al., 2020). The code implements the finite volume method for solving incompressible flows. The discretization strategy follows a fully implicit scheme with second order accuracy in both space and time. In the context of this work, the Fortran 90 programming modules of caffa3d, oriented to wind turbines simulations, had to be extended with CUDA C Kernels for GPU computations. The new code combines the use of GPU and the communication protocol Message Passing Interface (MPI) to handle different levels of parallelisms and benefit from massive parallel computing platforms.
The original homogeneous code caffa3d have already been validated for wind farm simulations through Large Eddy Simulations (LES) coupled with an implementation of the Actuator Line Model for representing the wind turbines rotor (Guggeri & Draper, 2019). In this work, the performance of both codes are compared while performing the same simulation scenarios in a wind farm. The results show that faster computations and larger simulation domains are achievable using the CPU-GPU based code.

References:

Afzal, A., Ansari, Z., Faizabadi, A.R. and Ramis, M.K., 2017. Parallelization strategies for computational fluid dynamics software: state of the art review. Archives of Computational Methods in Engineering, 24(2), pp.337-363.
Asmuth, H., Olivares-Espinosa, H. and Ivanell, S., 2020. Actuator line simulations of wind turbine wakes using the lattice Boltzmann method. Wind Energy Science, 5(2), pp.623-645.
Cheng, J., Grossman, M. and McKercher, T., 2014. Professional CUDA c programming. John Wiley & Sons.
Fernandez, G., Mendina, M. and Usera, G., 2020. Heterogeneous Computing (CPU–GPU) for pollution dispersion in an urban environment. Computation, 8(1), p.3.
Guggeri, A. and Draper, M., 2019. Large Eddy Simulation of an Onshore Wind Farm with the Actuator Line Model Including Wind Turbine's Control below and above Rated Wind Speed. Energies, 12(18), p.3508.
Liu, Z., Wang, Y., Nyangi, P., Zhu, Z. and Hua, X., 2021. Proposal of a novel GPU-accelerated lifetime optimization method for onshore wind turbine dampers under real wind distribution. Renewable Energy, 168, pp.516-543.
Mendina, M., Draper, M., Soares, A.P.K., Narancio, G. and Usera, G., 2014. A general purpose parallel block structured open source incompressible flow solver. Cluster Computing, 17(2), pp.231-241.
Niemeyer, K.E. and Sung, C.J., 2014. Recent progress and challenges in exploiting graphics processors in computational fluid dynamics. The Journal of Supercomputing, 67(2), pp.528-564.
Sorensen, J.N. and Shen, W.Z., 2002. Numerical modeling of wind turbine wakes. J. Fluids Eng., 124(2), pp.393-399.
Usera, G., Vernet, A.N.T.O.N. and Ferré, J.A., 2008. A parallel block-structured finite volume method for flows in complex geometry with sliding interfaces. Flow, Turbulence and Combustion, 81(3), p.471.

Wall-resolved FSI simulation of modern turbine blades: Assessment of fidelity on the aerodynamic forces and deformation of the blade

Mohsen Lahooti[1,*], Rodolfo Curci Puraca[2], Bruno Souza Carmo[2], Rafael Palacios[1], and Spencer Sherwin[1]
[1]Imperial College London
[2]University of Sao Paulo
[*]Presenting author

Keywords: FSI | wind turbine blade | LES, URANS | wall resolved simulation | HPC

Modern wind turbine blades feature long blades to increase the harvesting capacity of the turbine. However, with increasing the size of the blades, comes the flexibility which introduces new design aspects for modern wind turbines and requires aeroelastic and vortex-induced vibration (VIV) simulations to be considered in the design process. High-fidelity fluid-structure interaction (FSI) simulation of such blades is computationally challenging due to the combined effect of large deformations on the blade and the presence of locally or globally separated flows at high Reynolds numbers. Hence, distinct levels of fidelity are required when targeting various aspects of design such as the effect of flexibility in power generation or VIV of blades in parked conditions.

This work presents an assessment of the effect of fidelity on the captured flow features and predicted deformation of a highly deformable slender structure representing the typical turbine blades. Comparisons are made between the results of two FSI solvers, Nektar++/SHARPy FSI framework [1] and OpenFoam/Calculix FSI solver.

Nektar++/SHARPy FSI solver is an open-source code developed in Nektar++ [2] framework where a quasi-3D sectional approach, thick strip method [1,3] is used for representing the full 3D domain with a series of smaller domains distributed over the structural span. Each of these strips has a finite thickness in spanwise direction to enable capturing the local 3D turbulent wake near the structure while reducing the computational cost. Incompressible Navier-Stokes equations are discretized and solved using high-order spectral/hp element method with the Fourier expansion in the spanwise direction in each strip. Navier-Stokes equations are solved in a non-inertial body-fitted frame to avoid dynamic remeshing due to high deformation of the structure. Large-Eddy simulation is used to resolve turbulent structures in fluid flow. Large-deformation dynamics of the structure is modelled using a geometrically-exact nonlinear composite beam finite-element model [4]. A demonstrative example of Nektar++/SHARPy FSI simulation result is shown in Figure (1).

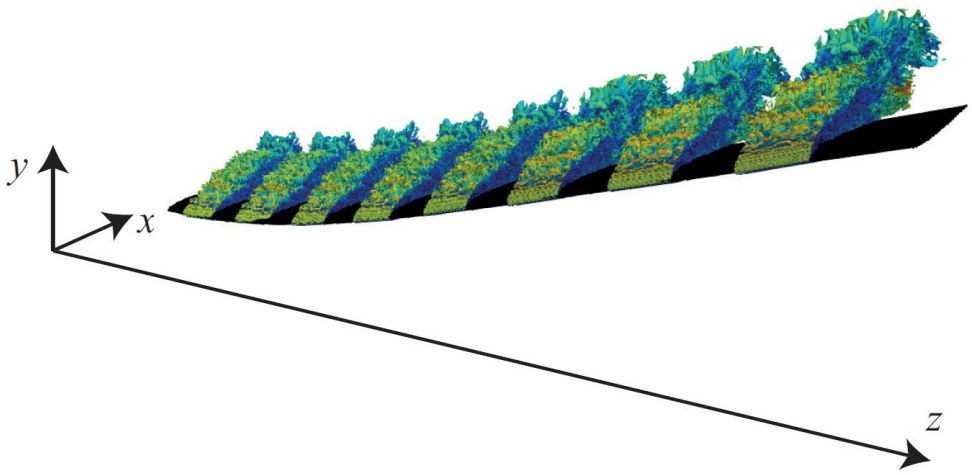

Figure 1: Q-criterion iso-contour coloured by velocity magnitude over the deformed structure with flow Reynolds number Re=1.56e5 and initial angle of attack alpha=16 degree. The contour range for velocity is in [0-2] with blue colour for lowest value and red correspond to the highest contour level. Simulation is performed by Nektar++/SHARPy FSI framework.

The OpenFoam/CalculiX FSI solver is developed in OpenFoam 2006 library [5] where the OpenFoam native flow solver is used for solving flow equations and structural dynamics are dealt with using CalculiX FEM package [6]. The two solvers are coupled using the PreCiCE coupling package [7].

Unsteady Reynolds-Averaged Navier-Stokes equations (URANS) are used for the full 3D simulation of turbulent flow, where a second-order spatial and temporal discretization is adopted with transient PISO method for pressure-velocity coupling. Second-order solid elements are used in CalculiX and proper material values are calculated to model the simulated object structural characteristics.

Both solvers will be first validated against the UVLM-based simulations at low angle of attack and simulation results of the two FSI solvers at below-rated conditions are compared for a highly deformable slender structure. Effect of simulation fidelity, i.e. large-eddy simulation and URANS, are investigated on the turbulent flow structure near the blade and final deformation of the blade.

Moreover, the effect of quasi-3D approach versus full 3D simulation is discussed and recommendations on the range of applicability of each FSI approach are made.

References:

Lahooti, M., Palacios, R. and Sherwin, S.J., 2021. Thick Strip Method for Efficient Large-Eddy Simulations of Flexible Wings in Stall. In AIAA Scitech 2021 Forum (p. 0363).

Moxey, D., Cantwell, C.D., Bao, Y., Cassinelli, A., Castiglioni, G., Chun, S., Juda, E., Kazemi, E., Lackhove, K., Marcon, J. and Mengaldo, G., 2020. Nektar++: Enhancing the capability and application of high-fidelity spectral/hp element methods. Computer Physics Communications, 249, p.107110.

Bao, Y., Palacios, R., Graham, M. and Sherwin, S., 2016. Generalized thick strip modelling for vortex-induced vibration of long flexible cylinders. Journal of Computational Physics, 321, pp.1079-1097.

del Carre, A., Muñoz-Simón, A., Goizueta, N. and Palacios, R., 2019. SHARPy: A dynamic aeroelastic simulation toolbox for very flexible aircraft and wind turbines. Journal of Open Source Software, 4(44), p.1885.

OpenFoam. The open source CFD toolbox. January, 2021. Available: https://www.openfoam.com

Dhondt, G., Wittig, K. CalculiX: A Free Software Three-Dimensional Structural Finite Element Program. July, 2020. Available: http://www.calculix.de

preCICE. The coupling library for partitioned multi-physics simulations. January, 2021. Available: https://www.precice.org

On the scalability of a single wind turbine simulation using the code WInc3D

Flavio Cesar Cunha Galeazzo[1,*], Lucas Franceschini[2], Bruno Carmo[2], and Andreas Ruopp[1]
[1]University of Stuttgart
[2]University of Sao Paulo
*Presenting author

Keywords: high-fidelity simulation | LES | high-perfomance computing

Wind energy is one of the fastest-growing energy sources worldwide. Computer models and simulations support many aspects of wind energy exploitation, ranging from wind turbine design and wind resource assessment to wind farm layout optimization and operation, with extensive use of High-Performance Computing (HPC). At the same time, HPC hardware is experiencing a massive growth in parallelization, which requires the simulation codes to show a good strong scalability – the ability to perform well using an increasing number of processor cores.

WInc3D is an open-source wind farm simulation code that allows detailed wake analyses. It is based on Incompact3D (Laizet and Lamballais, 2009), which is a high-order finite-difference numerical solver. WInc3D uses the Large-eddy simulations (LES) approach, which is an outstanding tool for performing high-fidelity simulations of wind farms and wind turbine wakes. With LES the turbulent, three-dimensional, unsteady flow past wind turbines can be accurately predicted and their performance can be evaluated. The turbine blades are modelled using the actuator line model (ALM), which is based on the blade element theory and uses tabulated aerofoil data. The ALM implemented in WInc3D has been validated using both wind tunnel data (Deskos et al 2019) and supervisory control and data acquisition (SCADA) measurements from a utility-scale offshore wind farm.

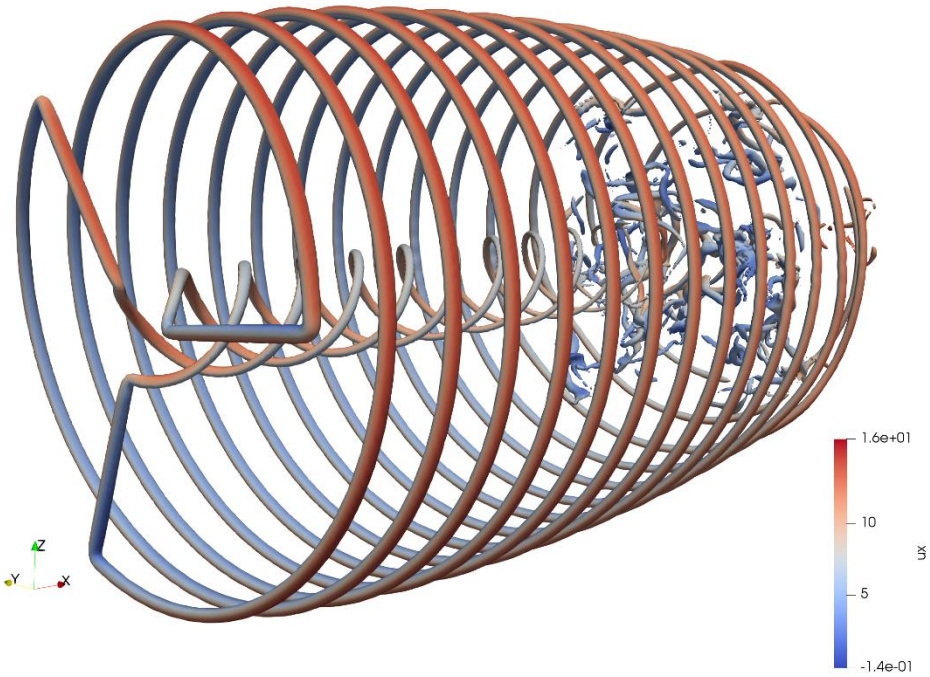

Figure 1: Contour plot of the vorticity generated by wind turbine blades, colored by the horizontal velocity component in m/s.

To study the scalability of WInc3D, a test case with a single NREL 5MW turbine is used. The NREL 5MW wind turbine is a conventional three-bladed upwind variable-speed variable blade-pitch-to feather-controlled turbine, with a rotor diameter (D) of 126 m. The tower is omitted in the present simulations. The (imposed) tip-speed ratio is 7.017. The domain spans 5D x 5D x 8D, corresponding to a flow blockage of about 3%. The turbine is placed 2D downstream the inflow, leading to the same distance between any point of the turbine and a border of the domain. The inflow velocity is constant with a value of 11.4 m/s.

Each blade of the NREL 5MW turbine is composed of 17 sections with 8 different airfoil shapes and is discretized using 71 blade elements. Uniform grids with different resolutions are tested. The temporal discretization is accomplished using a third-order Runge-Kutta and the spatial discretization uses is a fourth-order finite difference scheme. The Poisson equation for the pressure is solved in spectral space using a Fast Fourier Transform (FFT).

The supercomputer Hawk of the High-Performance Computing Center Stuttgart (HLRS) is used for the scalability tests. It is among the fastest high-performance computers in the world and the fastest general-purpose machine for industrial production in Europe by the time of the installation. Hawk has 5,632 nodes with two AMD EPYC 7742 processors each.

The results show the influence of the ALM model and the different grid resolutions on the scalability of WInc3D.

References:

Deskos, G., Piggott, M. D., & Laizet, S. (2019). Development and validation of the higher-order finite-difference wind farm simulator, WInc3D. Advances in Renewable Energies Offshore - Proceedings of the 3rd International Conference on Renewable Energies Offshore, RENEW 2018, April 2019, 721–728.

Laizet, S., & Lamballais, E. (2009). High-order compact schemes for incompressible flows: A simple and efficient method with quasi-spectral accuracy. Journal of Computational Physics, 228(16), 5989–6015.

Mini-Symposium: Digital Twin Technology

Carlo L. Bottasso
TU Munich

Anton Kaifel
Zentrum für Sonnenenergie- und Wasserstoff-Forschung Baden-Württemberg (ZSW)

Stefan Hauptmann
Mesh-Engineering

Christoph M. Hackl
Munich University of Applied Sciences

Digital twins represent one of the most important and innovative technologies to empower the future energy system to achieve the 'Energy Transition' by an intelligent, decentralized and sustainable energy conversion, storage, transmission and use. In combination with intelligent sensors, control, machine learning and data analysis, digital twins provide powerful and enhanced capabilities to the component, plant and system level such as e.g. condition monitoring, fault detection and optimal operation. Nevertheless, there does not yet exist a holistic framework to exploit the full potential of digital twins in the overall energy system. This mini symposium wants to bring together interested players in this field from academia, industry and society by giving (i) an overview of the state-of-the-art of digital twins and (ii) to highlight new trends in their use. Therefore, we cordially invite authors to share and present recent advances in this interdisciplinary research field with particular focus on but not limited to: * Advanced control strategies, fault-tolerant control * Fault detection and condition monitoring * Lifetime extension, prediction, decision support * Virtual sensors, estimation technology * Flexible grid connection/integration (grid-supporting/-feeding/-forming, black start), * Economic and market analysis.

Mini-Symposium: Digital Twin Technology (I)

A holistic view on digital twins in the future energy system

Abhinav Anand[1], Joaquìn Klee Barillas[2], Carlo L. Bottasso[1], Robert Braunbehrens[1], Christoph M. Hackl[3,*], Stefan Hauptmann[4], Anton Kaifel[2], Omar Kamel[4], Birger Luhmann[4], Kay Ohnmeiß[2], Jonas Petzschmann[2], Christian Roos[4], Zhao Song[3], Katharina Strecker[2], and Andre Thommessen[3]
[1]Technical University of Munich
[2]Zentrum für Sonnenenergie- und Wasserstoff-Forschung Baden-Württemberg
[3]Munich University of Applied Sciences
[4]Mesh-Engineering
[*]Presenting author

Keywords: digital twins | PV | wind | inverters | power grid

Digital twins are one of the key enabling technologies for the "Energiewende", as they facilitate the transition from a centralized fossil-fuel-based power generation to a decentralized and distributed renewable-energy-based power conversion. Digital twins will allow to enhance functionality, safety / security and reliability of the future energy system across all system and integration levels such as generation, distribution, conversion, storage and consumption.
In this introductory talk of the WESC 2021 - Mini Symposium on "Digital Twin Technology", we will introduce the collaborative research project "e-TWINS – Holistic digital twins for the energy system" funded by the German Federal Ministry for Economic Affairs and Energy (BMWi) and present first results and ideas. The goals of the project are design, implementation, application and demonstration of a holistic software platform and system theoretical methods to support the holistic application of digital twins to the future energy system, taking into account scalability, modularity, extensibility and conversion to large trans-regional systems.

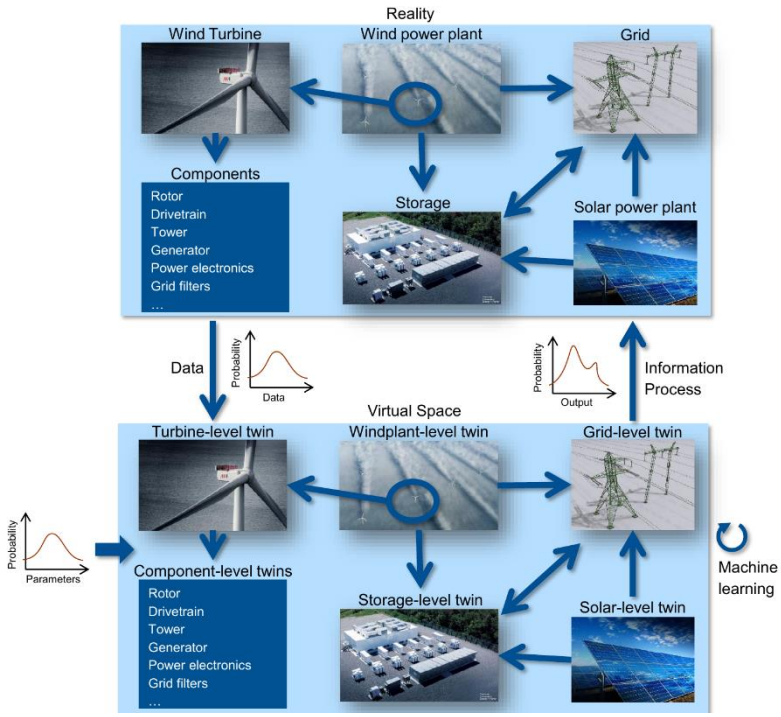

Figure 1: Reality versus virtual space and their interconnection.

In particular, our vision on digital twins for systems of systems and its possible implementation / framework should pave the way for such a distributed and meshed utilization of digital twins across all hierarchical

system levels (e.g. component, generating unit, storage, plant, transmission, consumer / load) of the future energy system. In our talk, we focus on the electrical energy system only (see Fig. 1); however, the presented ideas can also be extended to other energy systems such as gas or heat / cold, which is crucial as in future all these energy systems will be coupled.

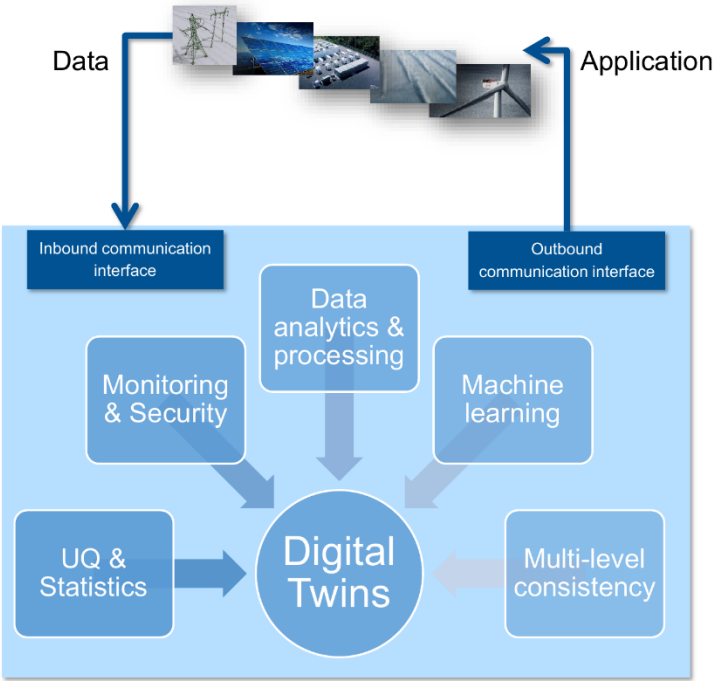

Figure 2: Holistic software platform with communication interface(s) enabling interaction, communication and distributed services of the digital twins for systems

In Fig. 1, the concept of digital twins for systems of systems is illustrated for parts of the electrical energy system. Each system level is equipped with individual digital twins which (i) are fed by data measured in real time at the system level time resolution, and (ii) exchange crucial information between each other and with reality. All aspects of these multi-level interconnected system are affected by uncertainties, whose effects are assessed with modern Uncertainty Quantification (UQ) tools. The interconnected digital twins are (i) self-learning agents using e.g. adaptive and / or modelbased methods or machine-learning techniques, and (ii) implemented in a distributed manner on the respective real-time system. To exploit the full features of these interconnected digital twins on the different system levels and to enhance the behavior of the future energy system, a holistic software platform (see Fig. 2) with adequate communication interface(s) must be designed and implemented to allow for communication, data exchange, analytics & processing and multi-level consistency (e.g. synchronicity by time stamps). This platform is the basis for the featured services such as UQ, statistics, monitoring (e.g. condition monitoring and / or fault-detection), security and machine learning.

A Holistic Software Framework for Digital Twins in the Energy Sector

Christian Roos, Stefan Pfeifer, Omar Kamel, Birger Luhmann, and Stefan Hauptmann
MesH Engineering GmbH

Keywords: Digital Twins | Internet of Things | Energy System | Software Framework

Digital twins (DTs) are one of the most important technologies provided by the digital revolution (Tao et. al., 2019). In parallel there is a fast transition of the energy sector with respect to renewable energies. The electrical energy system is transformed into a complex, decentralized system of energy producers with a high percentage of renewable energies. Due to enhancements in the fields of sensor technology, system theory, machine learning and data analysis digital twins provide a large number of possibilities to improve and accelerate the energy transition by realtime monitoring, fault detection and service optimization (Brunton and Kutz, 2019; Nelles, 2001).

Existing monitoring and optimization services, which to some extend include DT-enriched data, are mostly implemented as a customer specific software solution (Damjanovic-Behrendt and Behrendt, 2019). At the same time, connectivity of physical and numerical entities has become significantly more standardized by the advances of the Internet of Things. Currently there is no existing technological approach which allows to apply the digital twin technology to the overall energy system, including producers, consumers, and their economic interests.

In order to fill this gap MesH Engineering is developing a holistic software framework for the application of digital twin technology to a distributed energy system. The target is to enable a scalable, modular, and extendable integration of digital twins for the future energy system. The development takes place as part of the joint project eTWINS, which is funded by the German Ministery of Economics and Energy ("Bundesministerium für Wirtschaft und Energie").

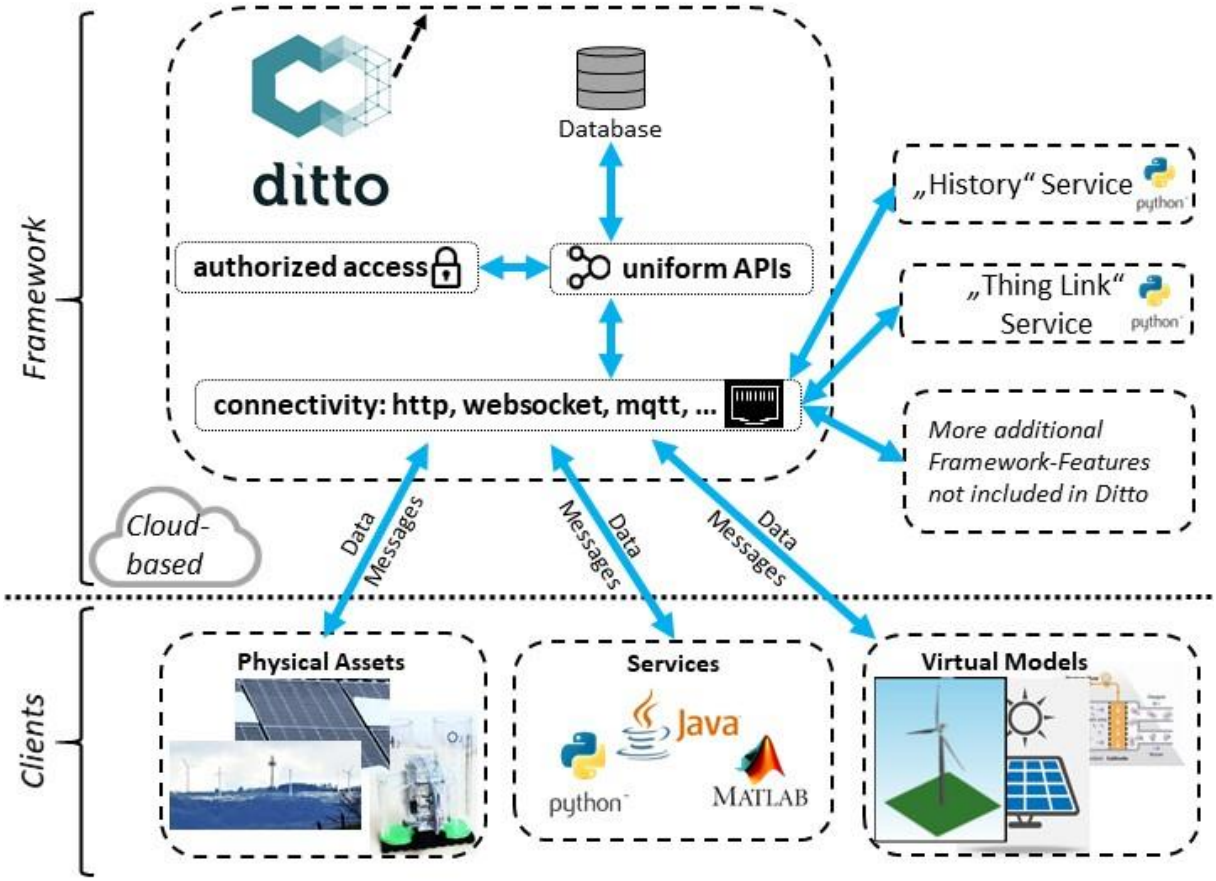

Figure 1: Structure of the Software Framework

A good starting point to meet the requirements following the intended functionalities is the software Eclipse Ditto. It is a software for IoT projects to manage digital twins. Ditto provides standardized APIs on a database via various protocols commonly used in the IoT field, such as websocket, mqtt and others (Practical Guide IoT, 2019). In this database the state-data of connected assets are stored in nested key-value structures, the so called "Things". Authorized access to each key can be granted for dedicated users. Subscribed clients are informed about changes made to data stored in the Things. Interaction between the connected clients is also possible by exchanging messages, which are distributed via Things.

In addition to the integrated functionalities of Eclipse Ditto there are more features necessary to meet the required functionalities of the framework, which are not directly provided by Eclipse Ditto, e.g. the handling of time series data. These functionalities are developed by MesH in order to extend Ditto.

This structure, which is also shown in the attached figure, provides several advantages for a large variety of use cases. Interactions, like data exchange or configuration of a service, are performed via the same entry point and the same APIs for each connected client. Digital Twin functionalities, such as machine learning or uncertainty quantification, can be implemented accessibly for IoT devices.

Already existing functions can be easily integrated using the provided common protocols in the IoT field. The concept of connecting all functionalities via internet-based protocols allows the adaption to different requirements with regard to scalability, multi-fidelity, location-independency and modularization.

The abilities of the framework are demonstrated for different challenging physical and economical scenarios. An example is given for an electrical system containing a wind-, photovoltaic- and battery device. In addition to the software solution physical hardware demonstrator assets are implemented.

References:

Brunton, S.L. and Kutz, J.N. (2019) ‚Data-driven science and engineering machine learning, dynamical systems, and control', Cambridge University Press, Online ISBN: 9781108380690, doi: https://doi.org/10.1017/9781108380690

Nelles, O. (2001) Nonlinear System Identification. Berlin, Heidelberg: Springer Berlin Heidelberg. Available at: http://link.springer.com/10.1007/978-3-662-04323-3

Practical Guide IoT (2019): A Practical Guide for Connecting LabVIEW to the Industrial IoT (2019). Available at https://www.ni.com/de-de/innovations/white-papers/17/a-practical-guide-for-connecting-labview-to-the-industrialiot.html (Accessed 29 January 2020).

Tao, F.; Zhang, H.; Liu, A. and Nee, A.Y.C. (2018) ‚Digital Twin in Industry: State-of-the-Art', IEEE Transactions on Industrial Informatics (Volume: 15, Issue: 4, April 2019), pp. 2405 – 2415. doi: 10.1109/TII.2018.2873186

Eclipse Ditto. 2020. Version 1.5.0. Eclipse Foundation Inc., Ottawa, CA

Java®. 2020. Sun Microsystems, Inc., Santa Clara, CA, USA

Matlab®. 2020. The MathWorks, Inc., Natick, MA, USA

Python. 2020. Python Software Foundation, DE, USA

Digital Twin Workflow Development Framework in the context of Fluid Structure Interaction

Yuriy Marykovskiy[1,2,*], Thomas Clark[3], Sarah Barber[2], and Eleni Chatzi[1]
[1]ETH Zürich
[2]Ost - Eastern Switzerland University of Applied Sciences
[3]Octue Ltd.
*Presenting author

Keywords: Digital Twin | Fluid Structure Interaction | Workflow | Software integration and management

Digital Twin (DT) is a relatively new concept of creating a virtual counterpart (digital object) to a physical system, initially introduced in the context of manufacturing by Grieves. Since its introduction the term "Digital Twin" has been used rather broadly, leading to the distinction by Kritzinger et al. (2018) of Digital Model and Digital Shadow based on the degree of automation in data flow between the physical and digital objects. Meanwhile, Wagg et al. (2020) introduced the concept of the hierarchy of digital twins based on the operational capabilities. The common feature of various definitions is a continuous feedback loop between virtual and physical system, often with a scope of achieving a higher accuracy of predictive capabilities and more rapid and informed decision-making (Van der Valk et al., 2020).

Capability	General Workflow Steps
Supervisory (Digital Shadow)	Measurement Information/ Visual Data
Operational (Digital Shadow)	Measurement Information/Visual Data Operator Decision
Predictive (Digital Shadow/ Digital Twin)	Measurement Simulation / Surrogate Model Predicted Information/Visual Data Operator Decision
Self-Improving (Digital Shadow/ Digital Twin)	Measurements Evaluation of uncertainties on the state variables of the system Multi-Fidelity Simulation / Surrogate Model Uncertainty propagation/Data fusion/ Statistical Inference Predicted state with quantified uncertainty Operator Decision
Self-Managing (Digital Twin)	Same as for Self-Improving, with the digital system actively controlling/changing physical object

Figure 1. Digital twin hierarchy based on the system capabilities

In the context of wind energy, digital twins are seen mainly as a tool for more effective asset management such as lifetime prediction (Tao et al., 2018; Branlard et al., 2020). However, DT technology can offer much wider potential applications ranging from design phase to specific operational improvements such as noise reduction, rotor imbalance or yaw misalignment detection.

While individual existing technologies such as Finite Element Analysis (FEA), Computational Fluid Dynamics (CFD), Machine Learning (ML), Bayesian methods, Multi-fidelity approaches already enable the tasks required of a DT such as verification and validation, physics-based modeling, dataaugmented modelling and uncertainty quantification (Peherstorfer et al.,2018; Xiao and Cinnella, 2019; Renganathan et al., 2020), one of the main open challenges is the creation of a system that enables the interaction between the above-mentioned components (Wagg et al., 2020). Such a system is usually referred to as workflow.

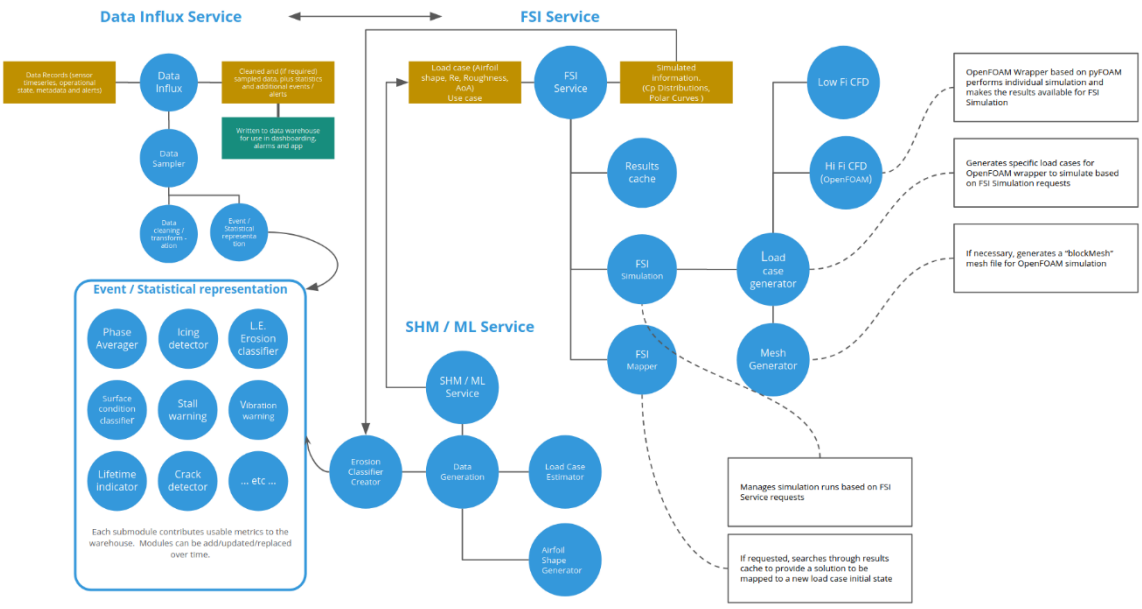

Figure 2. Example network of FSI Digital Twin modules, used to monitor leading edge erosion of wind turbine blades.

Unlike the majority of current wind turbine DTs that rely on existing SCADA data and strain gauge sensors, the twin discussed in this work integrates the data from pressure and acoustic sensors significantly expanding the possible use cases. Practical realisation of Supervisory and Operational pre-Digital Twins (Figure 1) is straightforward with current software tools, meanwhile the development of full DTs is particularly dependent on availability and usability of fluid-structure interaction (FSI) simulation software packages with other components of the DT such as measurement system, machine learning modules, etc.

In terms of IT infrastructure, several commercial packages such as ANSYS Workbench enable automation of FSI simulations and subsequent creation of DTs via ANSYS Twin Builder, while there is lack of well developed open-source alternative available to the researches. A possible solution is the integration of packages such as OpenFOAM, OpenFAST, XFOIL via louse coupling into the workflow through so-called wrappers. These wrappers can be seen as individual twin modules. In this regard, Octue platform offers a clear framework that specifies what each module can and/or must contain, as well as functions to validate incoming data and outputs, in addition to functions to check that a module itself is valid. Moreover, this framework deals with the task of combining individual modules together in hierarchies and networks, such as one in Figure 2. Further research in academic setting clearly necessitates the development of open-source libraries specifically facilitating implementation of DTs that incorporate FSI simulations. Moreover, realisation of logical frameworks such as the ones presented by Abdallahet al. (2017) and Bi and Zhao (2004) will be crucial for the development of Self-Improving and Self-Managing Digital Twins.

References:

Branlard, E., Jonkman, J., Dana, S., and Doubrawa, P.: A digital twin based on OpenFAST linearizations for real-time load and fatigue esti-mation of land-based turbines, Journal of Physics: Conference Series, 1618, 022 030, https://doi.org/10.1088/1742-6596/1618/2/022030,https://doi.org/10.1088%2F1742-6596%2F1618%2F2%2F022030, 2020.

Fuller, A., Fan, Z., Day, C., and Barlow, C.: Digital Twin: Enabling Technologies, Challenges and Open Research, IEEE Access, 8, 108 952–108 971, https://doi.org/10.1109/ACCESS.2020.2998358, 2020

Grieves, M.: Origins of the Digital Twin Concept, https://doi.org/10.13140/RG.2.2.26367.61609, 2016.

Kritzinger, W., Karner, M., Traar, G., Henjes, J., and Sihn, W.: Digital Twin in manufacturing: A categorical literature review and classifica-tion, IFAC-PapersOnLine, 51, 1016–1022, https://doi.org/10.1016/j.ifacol.2018.08.474, 2018.

Peherstorfer, B., Willcox, K., and Gunzburger, M.: Survey of Multifidelity Methods in Uncertainty Propagation, Inference, and Optimization,SIAM Review, 60, 550–591, https://doi.org/10.1137/16M1082469, 2018.

Renganathan, S. A., Harada, K., and Mavris, D. N.: Aerodynamic Data Fusion Toward the Digital Twin Paradigm, AIAA Journal, 58,3902–3918, https://doi.org/10.2514/1.J059203, https://doi.org/10.2514/1.J059203, 2020.

Tao, F., Zhang, M., Liu, Y., and Nee, A.: Digital twin driven prognostics and health management for complex equipment,CIRP Annals, 67, 169 – 172, https://doi.org/https://doi.org/10.1016/j.cirp.2018.04.055, http://www.sciencedirect.com/science/article/pii/S0007850618300799, 2018.
van der Valk, H., Haße, H., Möller, F., Arbter, M., Henning, J.-L., and Otto, B.: A Taxonomy of Digital Twins, 2020.
Wagg, D. J., Worden, K., Barthorpe, R. J., and Gardner, P.: Digital Twins: State-of-the-Art and Future Directions for Modeling and Simulation in Engineering Dynamics Applications, ASCE-ASME J Risk and Uncert in Engrg Sys Part B Mech Engrg, 6, https://doi.org/10.1115/1.4046739, https://doi.org/10.1115/1.4046739, 030901, 2020.
Xiao, H. and Cinnella, P.: Quantification of model uncertainty in RANS simulations: A review, Progress in Aerospace Sciences, 108, 1 – 31, https://doi.org/https://doi.org/10.1016/j.paerosci.2018.10.001, http://www.sciencedirect.com/science/article/pii/S0376042118300952, 2019.
Abdallah, I., Dertimanis, V., and Chatzi, E.: DATA–DRIVEN IDENTIFICATION, CLASSIFICATION AND UPDATE OF DECISIONTREES FOR MONITORING AND DIAGNOSTICS OF WIND TURBINES, pp. 55–65, https://doi.org/10.7712/120217.5351.17092, 2017.
Bi, H. and Zhao, J.: Applying Propositional Logic to Workflow Verification. Henry H. Bi, J. Leon Zhao. 2004. Information Technology and Management (1385-951X). 5(3-4): 293-318. https://doi.org/10.1023/b:item.0000031583.16306.0f, Information Technology and Management, 5, 293–318, https://doi.org/10.1023/B:ITEM.0000031583.16306.0f, 2004.

A holistic open source framework to help scientists create data services like Digital Twins

Thomas Clark*
Octue Ltd
*Presenting author

Keywords: twined | framework | digital | twin | schema

The open-source Twined framework provides the scientific community with the building blocks for creating data services like Digital Twins.

Introduction

Twined is a fledgling framework (https://twined.readthedocs.io) that emerged from the "Simulation for Asset Lifetime Extension" and "Turbulence In Marine Environments" projects, undertaken with the UK's Offshore Renewable Energy Catapult and Carbon Trust respectively. The need to manage a diverse range of data sources and analysis services across many stakeholders revealed a clear need for a framework that:

- Allows Digital Twins to be modularised, shared between stakeholders, and assembled into larger models.
- Allows access to both underlying data and services built on top to be permission-controlled in a granular way.
- Enables and encourages FAIR data (Wilkinson et. al. 2018, Vasiljevic et. al. 2018) and the GEMINI principles (Lamb, 2019) for digital twins.

Above all, the aim is to eliminate an emergent problem - that Researchers with a specific specialty must also become Computer Scientists and DevOps engineers, simply to share their work and for others to validate and build upon it - let alone accelerate that research into industrial use.

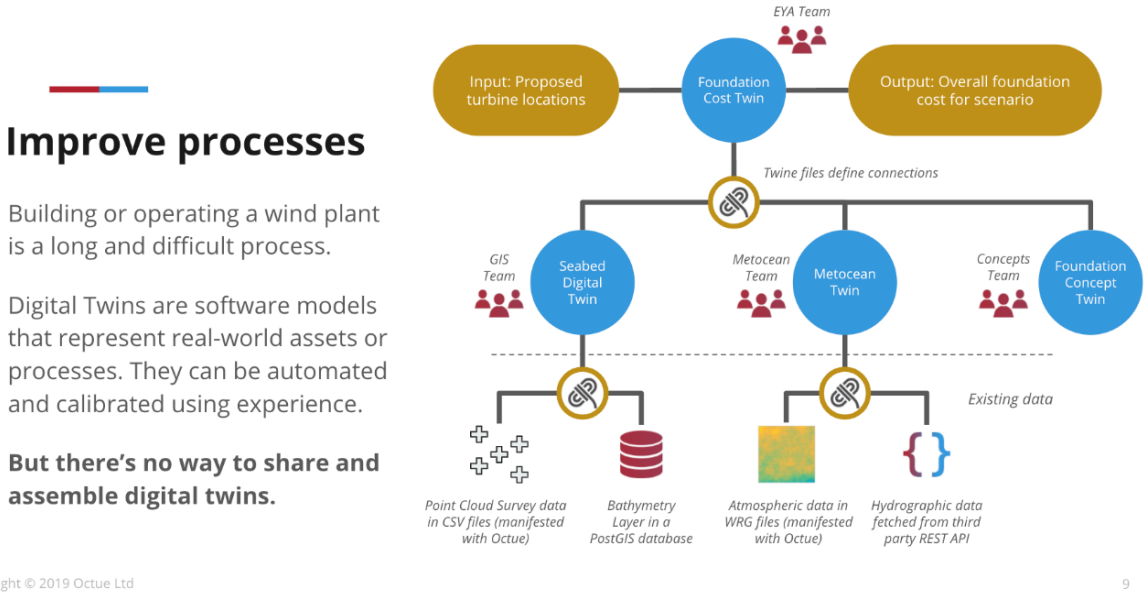

Figure 1. Assembly of digital twins in a modular fashion enables specialist teams to focus on their concerns whilst avoiding extreme overhead integrating different services.

Framework Design

Twined aims to be holistic in providing "all the ingredients" and incorporates a range of related tools and libraries to help Researchers create, describe and share their data services. We will briefly introduce the following elements of Twined:

- A method for describing data input/output when building a Digital Twin, based on a combination of JSONSchema and taagging syntax for file manifesting.

- A modular approach to connection and assembly of digital twins, using a Directed Acyclic Graph algorithm (See Figure 1).
- A validation library (the Twined core) to help Researchers fetch and validate data.
- Realistic example "apps" to help Researchers get started building data services and Digital Twins.
- A pre-configured server and automated DevOps, to turn Researchers' code into production-grade data services.
- ElasticSearch, PubSub and PostgreSQL integrations enabling digital twins to find and communicate with one another.
- A frontend application to monitor live digital twins.
- Frontend components, built in React, enabling web developers to quickly build applications that utilise outputs from Researchers' Digital Twins.

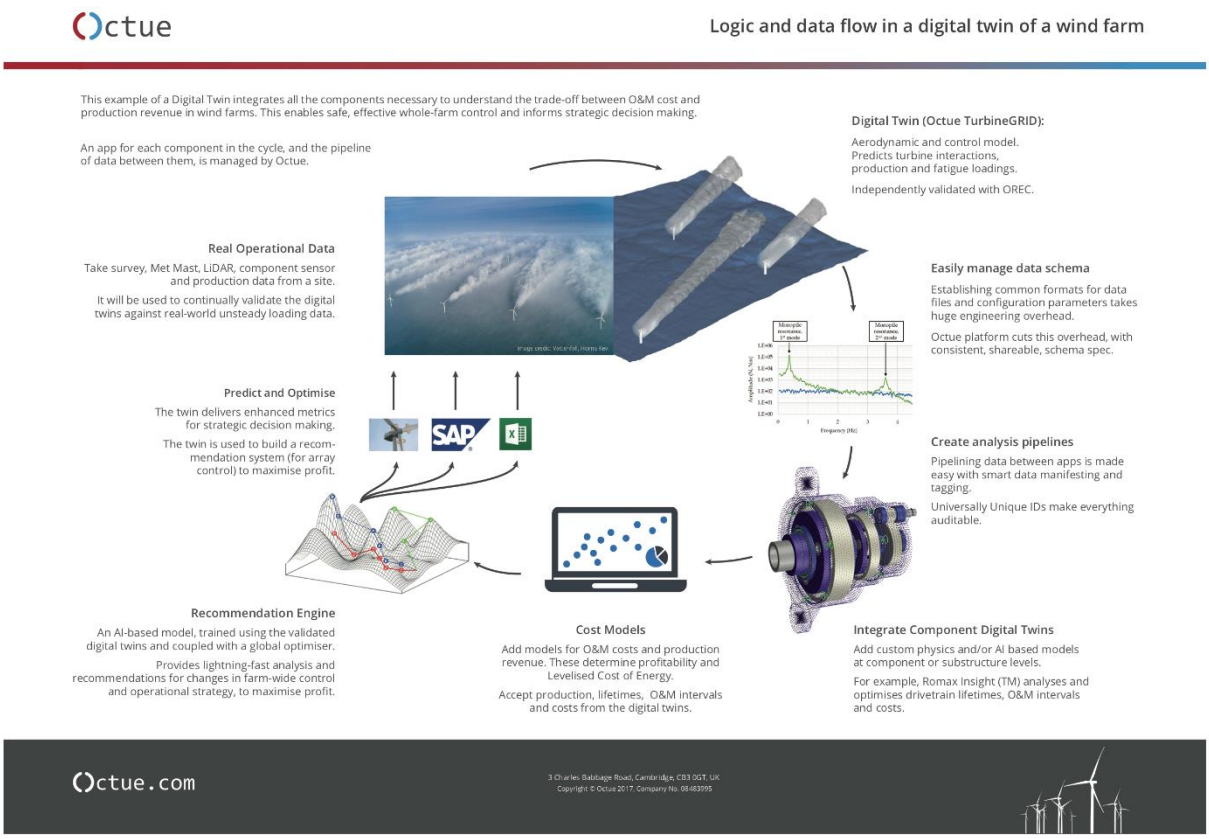

Figure 2. Building complex digital twins - particularly when tackling for whole-farm simulation and analysis, requires a multidisciplinary approach; and without a clear framework, integration of the different parts becomes prohibitively difficult.

Usage

Having outlined the framework, we will look at its use in an application for wind farm design, in which wake models, turbine digital twins and environmental models are integrated to provide realtime feedback on site performance during the design process.

We will present, in particular, the conceptual architecture (the "tree" of digital twins used) and how they interact, followed with a more detailed example of one aspect of the site evaluation process, an elevation model which draws on ESA/NASA's Earthdata set to provide a digital twin representing the planet surface. By expression of the granular building blocks, we will demonstrate how they assemble into much more complex wind farms models such as that of Figure 2.

Twined is also used in the Aerosense research project, in which it is used to connect a network of modules for real-time measurement and analysis of turbine blade aerodynamics. Other abstracts submitted to WESC will cover the Aerosense digital twins and architecture.

References:
Wilkinson M., Dumontier M., Aalbersberg I. J., Appleton G., Axton M., Baak A., Blomberg N., Boiten J., Bonino da Silva Santos L., Bourne P., Bouwman J., Brookes A., Clark T., Crosas M., Dillo I., Dumon O., Edmunds S., Evelo C., Finkers R. and Mons B. (2016). The FAIR Guiding Principles for scientific data management and stewardship. Scientific Data. 3. 10.1038/sdata.2016.18.
Vasiljevic N. (2018) Exploring the FAIR data principles across disciplines: Case DTU Wind Energy. DOI 10.5281/zenodo.1493874
Lamb K., (2019) Principle-based digital twins: a scoping review. Centre for Digital Built Britain https://www.cdbb.cam.ac.uk/files/scopingreview_dec20.pdf

Mini-Symposium: Digital Twin Technology (II)

Wind speed estimator for a vertical-axis wind turbine

Livia Brandetti*, Yichao Liu, Jan-Willem van Wingerden, Simon Watson, and Carlos Simao Ferreira
Delft University of Technology
*Presenting author

Keywords: vertical-axis wind turbine | wind speed estimation | identification

Wind turbines as a renewable energy source have always been part of public debate. On-shore horizontal-axis wind turbines (HAWTs) represent a cost-effective solution to meet the electricity demand (Tripanagnostopoulos et al., 2004) but their public acceptance is still a problem as in the case of the NIMBY (Not In My Back Yard) effect. A promising alternative to the HAWT is represented by the vertical-axis wind turbine (VAWT) which results more visually appealing and less noisy (Pearson, 2013). Furthermore, the inherent omnidirectionality of VAWTs makes them suitable for the installation into urban environments, where the turbulence levels are high and the wind direction variations are larger (Eriksson, Bernhoff and Leijon, 2008). However, the variation with the azimuth angle of the perceived velocity and of the angle of attack make the VAWT's performance and the wind speed acting on the rotor difficult to predict (Simão Ferreira et al., 2009).
To address this lack of knowledge, the current study proposes a wind speed estimator for a VAWT. The Immersion & Invariance (I&I) identification technique (Ortega, Mancilla-David and Jaramillo, 2013) and an Extended Kalman filter (EKF) (Knudsen, Bak and Soltani, 2011) are proposed to solve the rotor-effective wind speed estimation problem while a Repetitive estimator (RE) based on blade load measurements will be used to estimate the blade-effective wind speed on the individual blades (Liu et al., under review). Wind speed estimators are designed on the basis of a first-order model of a realistic 1.5 m two-bladed H-Darrieus VAWT (LeBlanc and Simão Ferreira, 2018). The aerodynamic input data are determined with the use of the Actuator Cylinder model (Madsen, 1982).

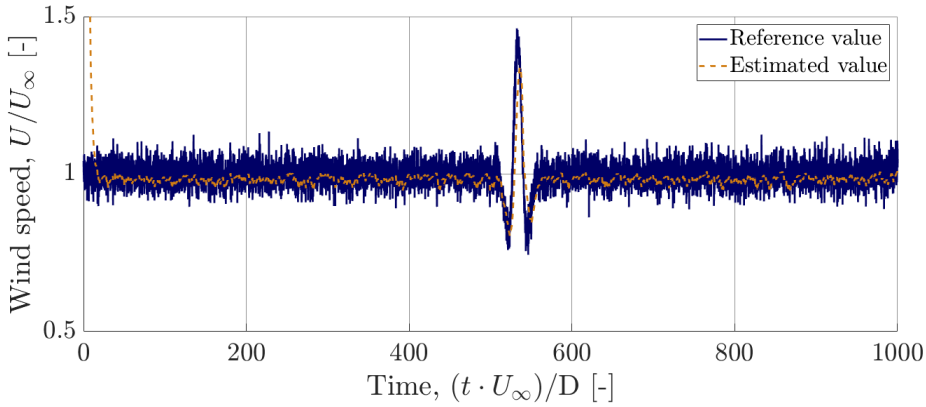

Figure 1: Performance of the I&I estimator to a Mexican hat gust for the rotor-effective wind speed.

The performance of the system is tested simulating step changes in the wind speed. Simulations are also carried out adding noise to the wind speed to emulate wind gusts. Preliminary results show that the error between the estimated and the actual rotor-effective wind speed is minimal. The performance of the I&I estimator to a Mexican hat gust is presented in Figure 1. The rotor-effective wind speed, U, is non-dimensionalized by the wind speed, U_∞ = 2 m/s, while the time, t, is nondimensionalized by U_∞ and the diameter of the VAWT, D = 1.5 m. The simulation is executed using the MATLAB-Simulink (Documentation, 2020) software package. The I&I gain, γ = 0.6, is selected as a trade-off between convergence speed and noise

filtering (Ortega, Mancilla-David and Jaramillo, 2013). Overall, a good agreement between the reference and the estimated rotor-effective wind speed is found both in terms of trend and absolute values.
A comparison study between the I&I estimator, the EKF estimator and the RE will be performed. The approach will be demonstrated with the help of experimental data as well as with simulations performed with mid-fidelity aero-servo-elastic model (i.e. Qblade (Marten, 2020)).

Acknowledgments
This research is part of the Arkom-Tulyp Wind project and is sponsored by RVO, the Netherlands Enterprise Agency, under a Hernieuwbare Energie (Sustainable Energy) subsidy.

References:
Eriksson, S., Bernhoff, H. and Leijon, M. (2008) 'Evaluation of different turbine concepts for wind power', Renewable and Sustainable Energy Reviews, 12, pp. 1419–1434. doi: 10.1016/j.rser.2006.05.017.
Knudsen, T., Bak, T. and Soltani, M. (2011) 'Prediction models for wind speed at turbine locations in a wind farm', Wind Energy, 14(7), pp. 877–894. doi: 10.1002/we.
Liu, Y. et al. (no date) 'Blade Effective Wind Speed Estimation: A Subspace Predictive Repetitive Estimator Approach', in European Control Conference 2021 (under review)
Madsen, H. A. (1982) The Actuator Cylinder - A Flow Model for Vertical Axis Wind Turbines. Aalborg University Centre. doi: 10.13140/RG.2.1.2512.3040
Marten, D. (2020) QBlade : A Modern Tool for the Aeroelastic Simulation of Wind Turbines
Ortega, R., Mancilla-David, F. and Jaramillo, F. (2013) 'A globally convergent wind speed estimator for wind turbine systems', INTERNATIONAL JOURNAL OF ADAPTIVE CONTROL AND SIGNAL PROCESSING, 27, pp. 413–425. doi: 10.1002/acs
imão Ferreira, C. J. et al. (2009) 'Visualization by PIV of dynamic stall on a vertical axis wind turbine', Experiments in Fluids, (46), pp. 97–108. doi: 10.1007/s00348-008-0543-z
Pearson, C. (2013) Vertical Axis Wind Turbine Acoustics. Corpus Christi College Cambridge University Documentation, S., (2020). Simulation and Model-Based Design, MathWorks. Available at: https://www.mathworks.com/products/simulink.html
Tripanagnostopoulos, Y. et al. (2004) 'Practical aspects for small wind turbine applications', Proc. in Int. EWEC 2004 Conf., Track, 7.
LeBlanc, B. and Simão Ferreira, C. (2018) 'Overview and Design of PitchVAWT : Vertical Axis Wind Turbine With Active Variable Pitch For Experimental and Numerical Comparison', in 2018 Wind Energy Symposium. Kissimmee, Florida, pp. 1–11.

Novel hybrid gearbox signal model development for condition monitoring

Kayacan Kestel*, Cédric Peeters, Timothy Verstraeten, and Jan Helsen
Vrije Universiteit Brussel
*Presenting author

Keywords: condition monitoring | signal processing | wind turbines

The growing utilization of wind energy for its environmental benefits comes paired with the need for condition monitoring of the mechanical components. Condition monitoring can be effectively employed to reduce maintenance costs and optimize productivity by the early detection of faults.

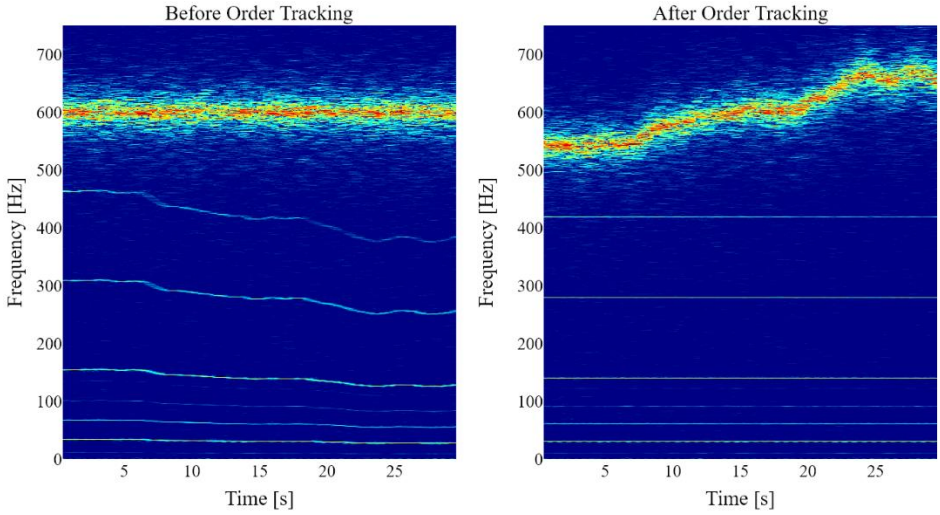

Figure 1. Spectrogram of the synthesized signal before and after order tracking

This surveillance of the turbine's health can become highly complex given that wind turbines are comprised of an immense number of components. Dynamic wind and weather conditions further complicate the already intricate the task, hence it requires a multi-disciplinary approach. The present study aims to synthesize physical and data-driven methods in order to simulate realistic wind turbine gearbox vibration signals which represent measurements on real-world machines. The signal model must be adaptive to varying operating conditions and is based on characteristic vibration signatures of individual components of a wind turbine gearbox, i.e., gears, shafts, and bearings. While part of the signal parameters can be estimated through pre-processing experimental data, a substantial portion of parameters remains unknown to these approaches. These unknown parameters are then estimated by employing data-driven methods like Bayesian networks or neural networks to process the vast amount of data measured on wind turbine gearboxes. Finally, the signal model permits us to track anomalies by comparing it with real measurement data. It also allows us to validate novel signal processing techniques in a controlled environment as well as to comprehend the variation of faulty signatures of distinct gearbox components in varying dynamic conditions. Fig. 1 demonstrates the spectrogram of a synthetic signal representing a vibration measurement from a gearbox that is comprised of 3 shafts, 2 helical gear-pinion couple and a single faulty bearing. Most prominent peaks of the spectrum are related with the gear meshing and shaft orders and their harmonics, which are synthesized based on a deterministic model [1]. On the other hand, the signal model of an unhealthy roller bearing with outer race damage introduces randomness, due to the slippage phenomenon [2].

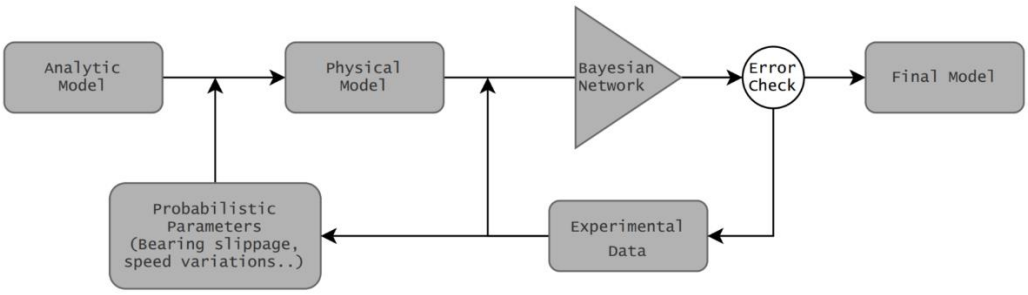

Figure 2. Overview of the signal simulation methodology

Furthermore, as in the real case, all the components are synchronous with varying rotational speed of the input shaft. Combining all the constituents of the signal in a coherent manner necessitates knowledge of the amplitudes of prominent orders relative to the white noise as well as of the damage signature of the bearing in varying conditions. An automated order detection method is employed to determine the harmonic families in the measurements. The certainty of order detection estimation is enhanced by exploiting large numbers of available data sets. The method flow of the present study is demonstrated in Fig. 2. Further steps will focus on minimizing the error of the physics-based signal model to the experimental measurements by using Bayesian statistics to estimate the model parameters and by exploiting the large amount of available measurement data.

References:
[1] Fan, X. & Zuo, M.J., 2006. Gearbox fault detection using Hilbert and wavelet packet transform. Mechanical Systems and Signal Processing, 20(4), pp.966–982. Available at: http://dx.doi.org/10.1016/j.ymssp.2005.08.032.
[2] Antoni, J. & Randall, R.B., 2002. Differential Diagnosis of Gear and Bearing Faults. Journal of Vibration and Acoustics, 124(2), pp.165–171. Available at: http://dx.doi.org/10.1115/1.1456906.

A digital twin concept for fatigue estimation of fixed-bottom offshore wind turbines

Emmanuel Branlard, and Kelly Clevenson
National Renewable Energy Laboratory

Keywords: digital-twin | offshore wind | Kalman filter | fatigue

Introduction and motivations

The offshore wind industry is challenged by the high costs of operation and maintenance (O&M), which accounts for approximately 35\% of the life-cycle costs. Predicting component failures would significantly reduce these costs, but with current technology, this requires the installation of numerous and expensive measuring devices.

Is it possible to obtain the fatigue of individual wind turbine components with a limited number of measurements and physical inspections? We address this question by developing a physics-based digital twin technology. Current digital twin technologies rely on available measurements, whereas our concept provides online prediction of signals that are otherwise not measured, using a limited set of reliable measurements and a physics-based model. The predicted signals can be used in applications with direct cost benefits: 1) real-time estimation of the fatigue consumption of key components; 2) root cause analyses and failure detections; 3) lifetime reassessments; and 4) improvements to follow-on designs.

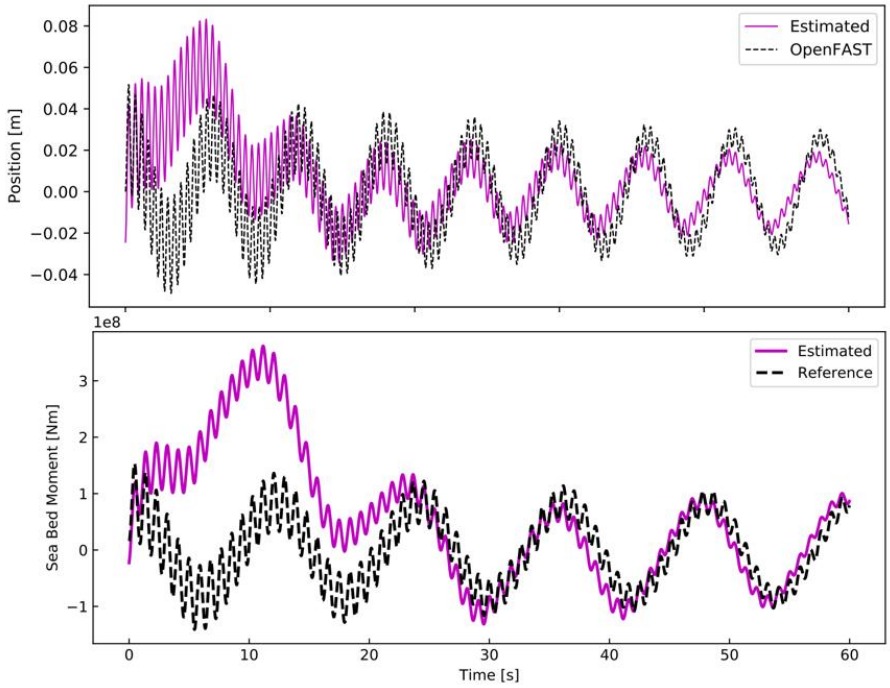

Figure 1: Tower top displacements and sea bed moments as estimated by the digital twin and compared with a reference OpenFAST simulation for a monopile at standstill under a regular wave

Methods

Our digital twin uses an extended Kalman filter (Lourens, 2012) to combine measurements with a linear model of the system. The Kalman filter provides optimal estimates of unknown states, accounting for model and measurement uncertainties. This technique was previously demonstrated by NREL for onshore applications (Branlard et al., 2020). In this work, we extend the technique to fixed bottom offshore structures.

Our model consists of a wind speed and thrust estimator a linear time invariant model of the turbine which we obtained in two ways: from first principles, or, using OpenFAST. In the former case, we use a shape function approach and simplified Morison equations to obtain an expression of the generalized wave loading. The main concept and components of the digital twin are shown in Figure 1.

The main challenge for this work is the estimation of the generalized wave loading with few nacellebased sensors. Recent work achieved such estimations using an extended Kalman filter (Davis, 2020). We improve the method by introducing an additional filter to narrow down the frequency and spectral amplitude range of the wave loading. The filtered wave loading is included in the state vector and combined with the linear model of the turbine.

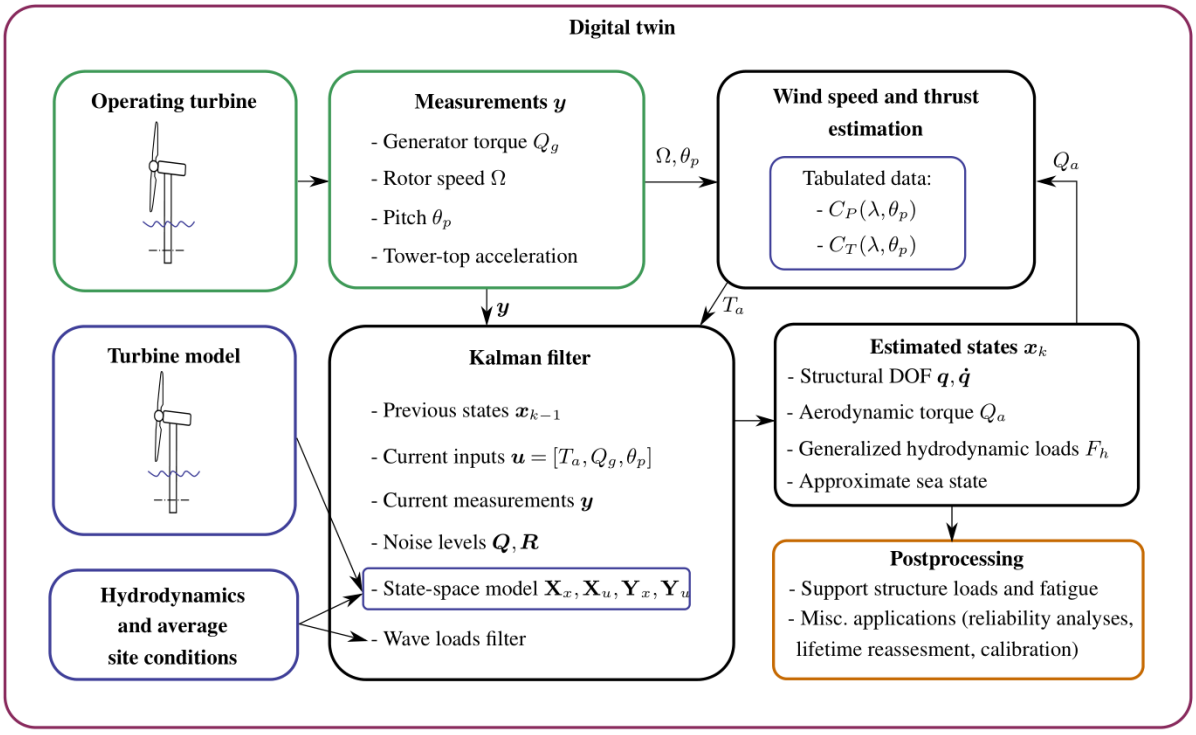

Figure 2: Workflow and main concepts of the digital twin. Measurements from the turbine and a linear model are combined within a digital twin to estimate loads and structural states.

Presentation

In the presentation, we will introduce our methods and present results obtained with our digital twin for standstill and normal conditions. OpenFAST simulations will be used as reference. We will focus on the estimation of the section loads in the support structure, from tower-top to sea-bed (sample results are shown in Figure 2), but will also present results for the tower-top position, wind speed and thrust estimates. We will report damage equivalent loads of the support structure as estimated by the digital twin and simulated by OpenFAST to indicate how well the digital twin can predict the fatigue consumption of the support structure.

References:

Davis, A. (2020) State Estimation and Wave Excitation Force Estimation and Prediction for Wave Energy Converters Using Extended Kalman Filters, PhD Thesis, University of Washington

Lourens, E., Reynders, E., Roeck, G. D., Degrande, G., and Lombaert, G. (2012) An augmented Kalman filter for force identification in structural dynamics, Mechanical Systems and Signal Processing, 27, 446–460.

Branlard, E., Giardina, D., and Brown, C. S. (2020) Augmented Kalman filter with a reduced mechanical model to estimate tower loads on an onshore wind turbine: a digital twin concept, Wind Energy Science, 1, 2020.

Mini-Symposium: Airborne Wind Energy System Modelling, Control and Optimisation

Roland Schmehl
TU Delft

Lorenzo Fagiano
Politecnico di Milano

Airborne wind energy systems use tethered flying devices for harvesting wind energy. The tethered connection to the ground introduces a large number of degrees of freedom which, on the one hand, require continuous control and present severe challenges for complete automation and reliability, but, on the other hand, also offer many opportunities for optimizing the design and operation of the systems. For example, using a tether drastically reduces the material effort of wind energy harvesting compared to conventional turbines and allows accessing higher altitudes while continuously adjusting to the available wind resource. As a result achievable capacity factors are considered to be higher than for turbines with fixed operational height. Driven by the commercial development of airborne wind energy systems, many computational tools and experimental techniques have emerged over the last decade.

This mini-symposium focuses on contributions in the areas of system modeling, control and optimization of airborne wind energy systems. Covered are also tools for system and component design, reference designs and simulation models, methods for reliability and safety engineering, wind resource modeling, performance analysis, aerodynamic characterization of kites, aeroelasticity as well as operational aspects such as launching and landing. Both theoretical and experimental contributions are welcome.

Mini-Symposium: Airborne Wind Energy System Modelling, Control and Optimisation (I)

Airborne Wind Energy Power Cycle Simulation of a Multi-Megawatt 6DoF Reference Kite with Rigid Wing

Dylan Eijkelhof*, and Roland Schmehl
Delft University of Technology
*Presenting author

Keywords: Airborne Wind Energy | Reference System | Dynamic Simulation | 6DoF | Tether Dynamics

Currently developed airborne wind energy (AWE) systems have reached sizes of up to several hundred kilowatts [1, 2, 3]. For the next scaling step towards megawatts, computational tools for the simulation of the entire AWE system covering all relevant physics will be indispensable. A detailed description of a large-scale AWE reference framework is given in [4, 5]. The kite design is inspired by Ampyx Power AP-3/4 with a 150 m2 surface area [6]. The framework couples kite dynamics, aerodynamic and brake forces, flight controller, tether dynamics, ground station dynamics and control, and wind physics to simulate consecutive pumping cycles. In [5] the kite is represented as a point mass, which the present study complements by a more accurate 6 degree of freedom (DoF) model of the kite dynamics. Standard 6 DoF rigid body equations of motion [7] are assumed with the additional tether force term in the sum of forces of the three translation equations. The tether is attached at the centre of gravity, thus, does not appear in the three rotational equations.
The present study further introduces a quasi-static tether model [8], which allows using a very stiff tether material (Dyneema®) while keeping a reasonably large time step and thus reducing the computational effort. The essence of this model is to neglect potential high-frequency elastic responses along the tether, because resolving these dynamic phenomena requires a very small time step, while their effect on the overall simulation result is negligible. The quasi-static approach computes the steady-state tether shape and corresponding tensile force distribution by means of a shooting process [8]. This shape is the result of an equilibrium between centrifugal forces caused by the tether rotation and external forces. The dominating external forces acting on the tether segments are assumed to be gravity and drag. The deployed length of the tether, wind speed at each tether segment, kite velocity and position are known at each time step. A Trust-Region Dogleg Method, based on the approach given in [9], iteratively adjusts the tether force and direction at the ground station until the tether end point coincides with the kite position.

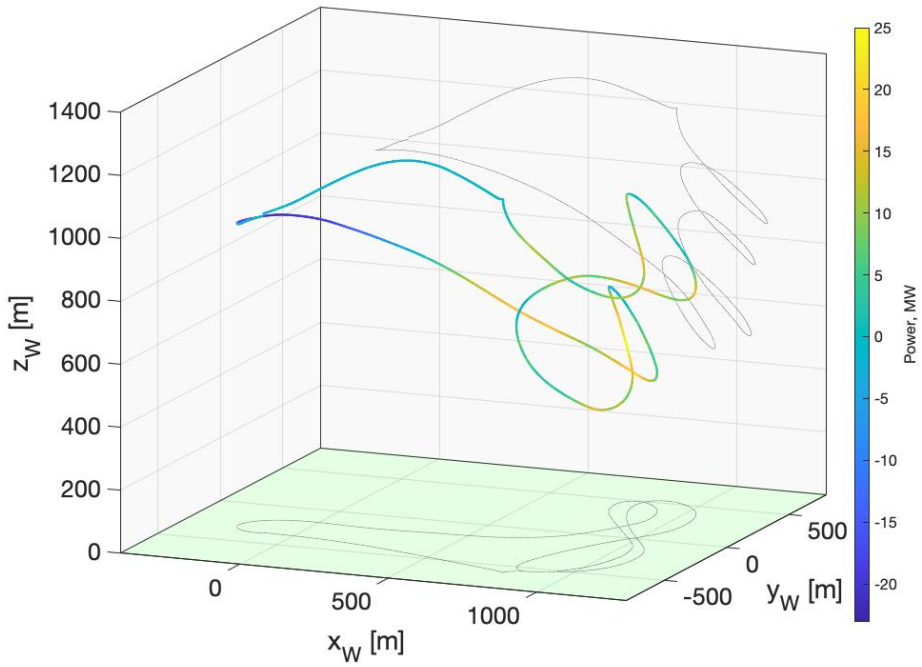

Figure 1: Power cycle flight path at an average wind speed of 24.3 m/s (varies with altitude according to a loglaw).

Figure 1 shows a computed flight path with an average mechanical power of 3.95 megawatts, while Figure 2 shows the evolution of the instantaneous power during this particular pumping cycle. The flight path can be varied by the CMA-ES optimisation algorithm [10]. As a result, it allows for a different number of figure-of-eight manoeuvres during the traction phase, for example.

A common trend found during optimisations is for the retraction flight path, a circular shape directed upwards back to the ground station is preferred over a straight downwards slope. A tether force is maintained to stabilise the overall kite-tether interaction. This is necessary to prevent a sudden force peak when transitioning back from retraction to traction phase, which can cause tether rupture.

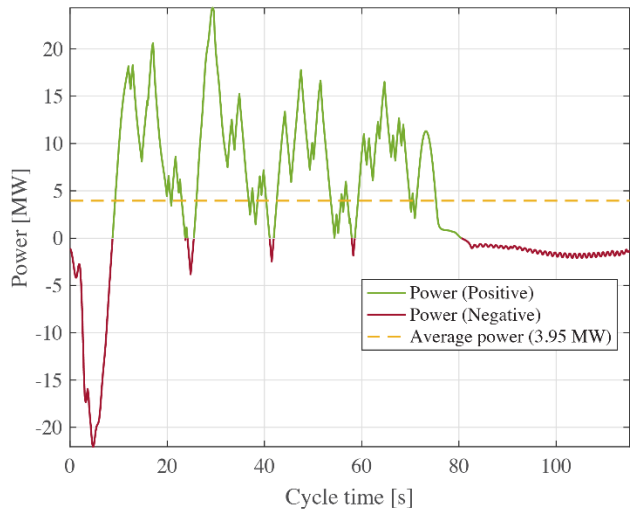

Figure 2: Instantaneous mechanical power versus pumping cycle time.

In this study we investigate phenomena that govern the dynamic behaviour of large-scale AWE systems and that cannot be observed at smaller scale. Future optimisations with this dynamic simulation framework can give useful insights into flight path planning during the early design process. The implementation of the quasi-static tether model is a big step towards more realistic and faster tether shape and force computations, ideal for optimisation purposes.

References:
[1] P. Jamieson. Innovation in Wind Turbine Design. John Wiley & Sons, Hoboken, NJ, 2 edition, 2018. ISBN 978-1-119-13790-0.
[2] V. Nelson. Innovative Wind Turbines: An Illustrated Guidebook. CRC Press, Boca Raton, FL, 2019. doi: 10.1201/9781003010883.
[3] R. Schmehl and O. Tulloch, editors. The International Airborne Wind Energy Conference 2019: Book of Abstracts. University of Strathclyde — Delft University of Technology, Glasgow, United Kingdom, 2019. doi: 10.4233/uuid:57fd203ce069-11e9-9fcb-441ea15f7c9c.
[4] D. Eijkelhof. Design and optimisation framework of a multi-MW airborne wind energy reference system. Master's thesis, Delft University of Technology & Technical University of Denmark, 2019. URL http://resolver.tudelft.nl/uuid:e759f9ad-ab67-43b3-97e0-75558ecf222d.
[5] D. Eijkelhof, S. Rapp, U. Fasel, M. Gaunaa, and R. Schmehl. Reference design and simulation framework of a multimegawatt airborne wind energy system. In Journal of Physics: Conference Series, volume 1618, page 032020, 2020. doi: 10.1088/1742-6596/1618/3/032020.
[6] M. Kruijff and R. Ruiterkamp. A roadmap towards airborne wind energy in the utility sector. In R. Schmehl, editor, Airborne Wind Energy – Advances in Technology Development and Research, Green Energy and Technology, pages 643–662. Springer, Singapore, 2018. doi: 10.1007/978-981-10-1947-0 26.
[7] Brian L Stevens, Frank L Lewis, and Eric N Johnson. Aircraft control and simulation: dynamics, controls design, and autonomous systems. John Wiley & Sons, 2015.
[8] P. Williams. Cable modeling approximations for rapid simulation. Journal of guidance, control, and dynamics, 40(7):1779–1788, 2017. doi: 10.2514/1.G002354.
[9] MATLAB. Documentation R2019b: Equation Solving Algorithms. The MathWorks Inc., Natick, Massachusetts, 2019.
[10] A. Auger and N. Hansen. A restart CMA evolution strategy with increasing population size. In 2005 IEEE Congress on Evolutionary Computation, volume 2, pages 1769–1776 Vol. 2, 2005. doi: 10.1109/CEC.2005.1554902.

An entrainment-based model for annular wakes, with applications to airborne wind energy

Sam Kaufman-Martin*, Nicholas Naclerio, Pedro May, and Paolo Luzzatto-Fegiz
University of California
*Presenting author

Keywords: Airborne Wind Energy | Wake Model | Entrainment | Turbulent Wake

Several airborne wind energy (AWE) designs consist of a tethered kite that flies transverse to the wind in a closed loop (Cherubini et al 2015). A commonly considered operating mode involves flying along a circular path, thereby generating a wake with an annular cross-section (Mcleod & Nordstrom 2019). These annular wakes are qualitatively different from the wakes with circular cross-sections generated by conventional wind turbines and by compact obstacles, as demonstrated by recent large eddy simulations of Haas & Meyers (2017). While circular wakes have been modelled extensively in the literature on wind turbine wakes (Jensen 1983; Frandsen et al. 2006; Bastankhah & Porté-Agel 2014), there appear to be no theoretical models of annular wakes, to the best of our knowledge. This makes it impossible to efficiently estimate the array performance of AWE devices.

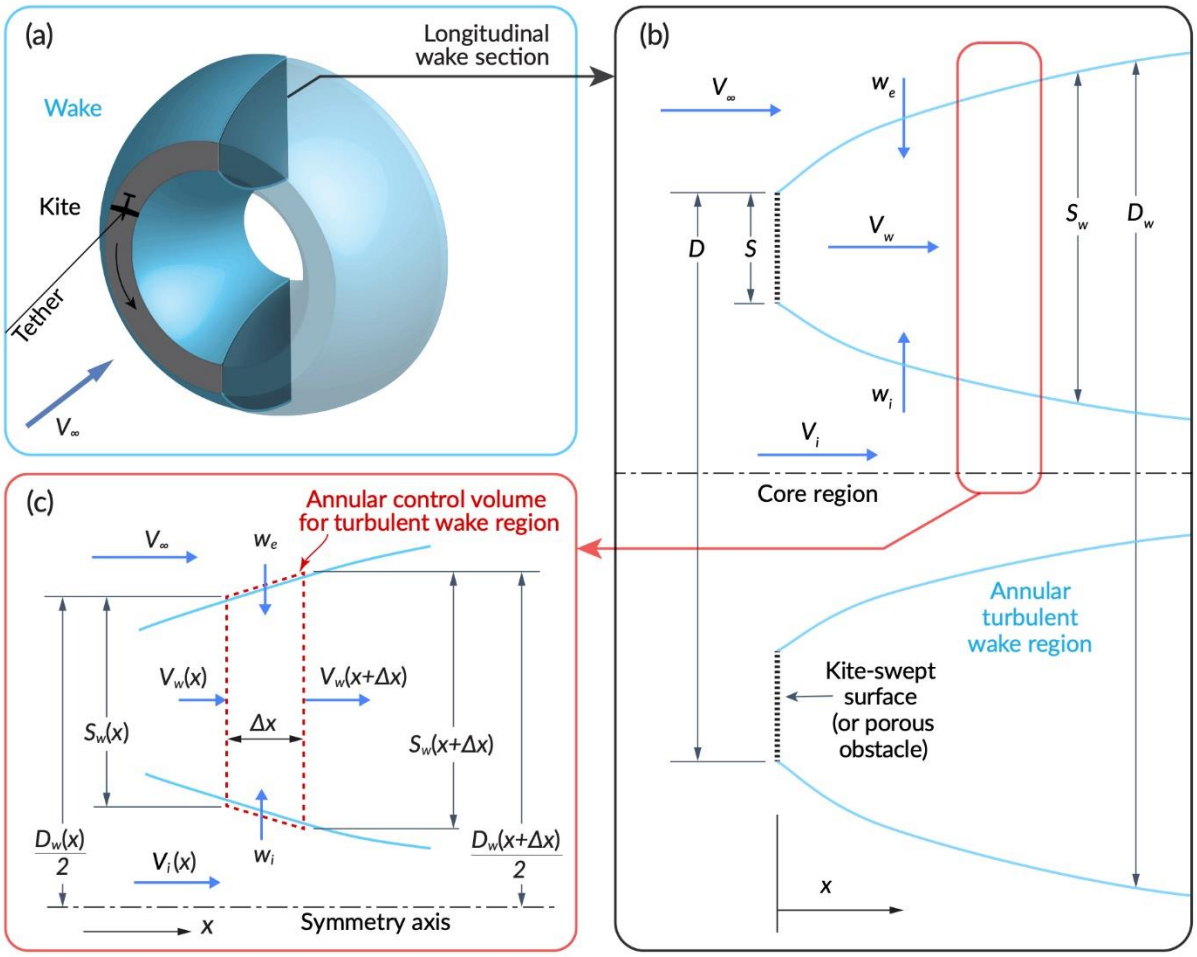

Figure 1 (a) Schematic of the development of an annular wake behind a porous obstacle or kite flying on a circular path. (b) Annular-wake cross-section, showing definitions for the entrainment model. (c) Cross-section of the annular control volume used for the turbulent wake region; for clarity, only the top portion is shown. A similar control volume analysis is used for the core region.

In this conference contribution, we develop two reduced-order models for the shape and speed of an annular wake as a function of distance behind an annular obstacle. Our annular wake models are derived by applying a control volume approach to mass and momentum conservation in an annular wake (see Figure 1). In order

to model the effects of turbulent entrainment, we employ the well-established "entrainment hypothesis," first introduced by G.I. Taylor in the context of modelling turbulent plumes (Morton et al. 1956). In brief, the entrainment hypothesis assumes that the fluid surrounding a turbulent plume, jet, or wake is entrained with a radial velocity that is proportional to the difference in streamwise velocities across the interface. This model of turbulent entrainment has been applied extensively in geophysical and industrial flow problems including plumes (Scase & Dalziel 2006), jets and wakes with circular cross sections (Morton 1961), natural ventilation (Coomaraswamy & Caulfield 2011), and wind turbines (Luzzatto-Fegiz 2018).

Both of the models that we obtain conserve mass and mass and momentum in the annular wake region. The first model also conserves mass and momentum in the core region at the center of the annulus, and consists of three ordinary differential equations, which we solve numerically. The second model is obtained by assuming that the annular wake does not drift radially, which allows us to obtain mathematical closure without accounting for conservation in the core region. This reduces the problem to only two differential equations, which we solve analytically. Details of the solution are reported in Kaufman-Martin et al. (2021).

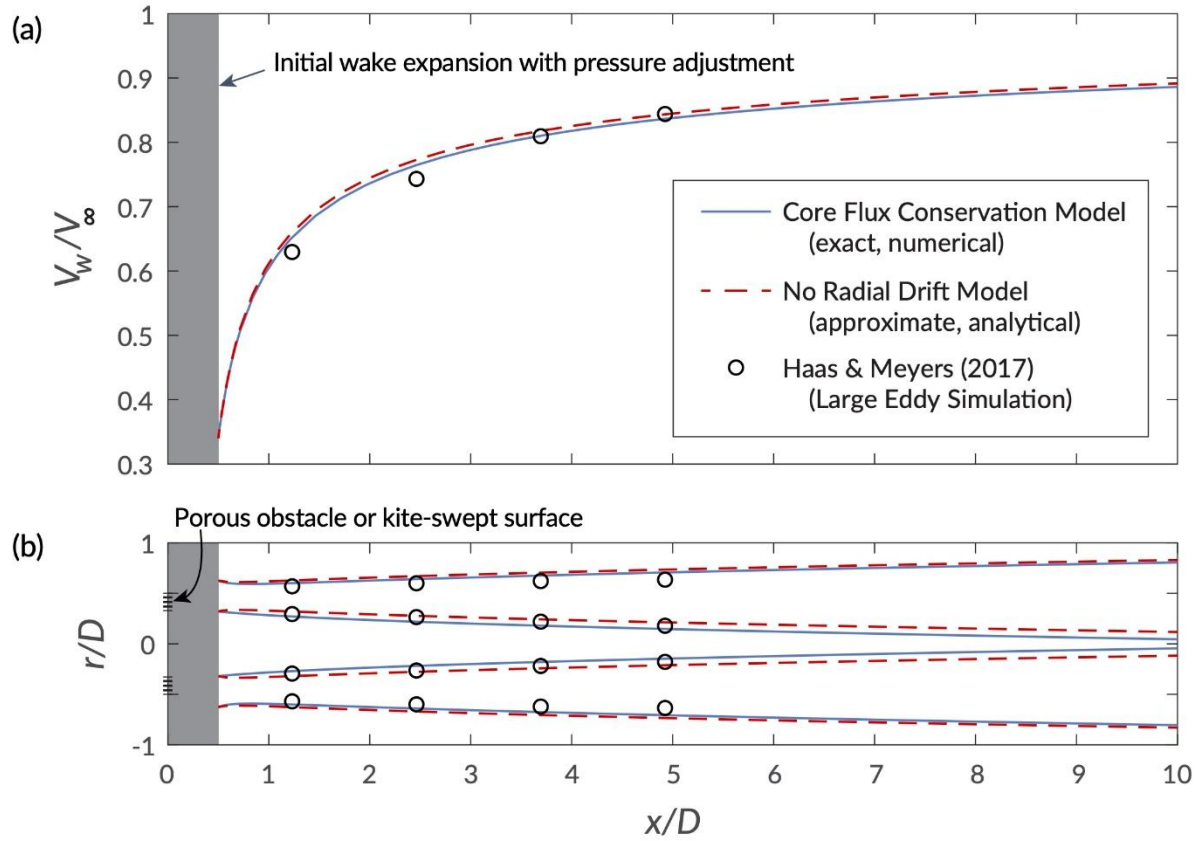

Figure 2. Laminar inflow case, comparing entrainment wake models and the simulation of Haas & Meyers (2017). (a) Wake velocity. (b) Wake boundary.

We compare our annular wake models with the large eddy simulations of Haas & Meyers (2017), who considered both laminar and turbulent inflow conditions. In the region of the wake for which the entrainment hypothesis is valid (x/D 1), the velocity predictions of both models show good agreement with the simulation data for both inflow conditions. For brevity, Figure 2 in this abstract shows the laminar inflow case; the turbulent inflow case is reported in Kaufman-Martin et al. (2021).

If supported by additional data from experiments or simulations, the models described here would enable the modeling of AWE kite wakes at a much lower computational cost than existing methods. This would greatly facilitate the planning of AWE wind farms, which in turn could enable society to harvest previously untapped, energy-dense wind resources.

References:
Bastankhah, M. and Porté-Agel, F. (2014) 'A new analytical model for wind-turbine wakes', Renewable Energy, 70, pp. 116–123.
Cherubini, A. et al. (2015) 'Airborne Wind Energy Systems: A review of the technologies', Renewable and Sustainable Energy Reviews, 51, pp. 1461–1476.
Coomaraswamy, I. A. and Caulfield, C. P. (2011) 'Time-dependent ventilation flows driven by opposing wind and buoyancy', Journal of fluid mechanics, 672, pp. 33–59.
Frandsen, S. et al. (2006) 'Analytical modelling of wind speed deficit in large offshore wind farms', Wind Energy, 9(1-2), pp. 39–53.
Haas, T. and Meyers, J. (2017) 'Comparison study between wind turbine and power kite wakes', Journal of physics. Conference series, 854(1), p. 012019.
Jensen, N. O. (1983) A note on wind generator interaction. RISØ-M-2411. Risø National Laboratory. Available at: http://orbit.dtu.dk/files/55857682/ris_m_2411.pdf.
Kaufman-Martin, S. et al. (2021) 'An entrainment-based model for annular wakes, with applications to airborne wind energy', arXiv [physics.flu-dyn]. Available at: http://arxiv.org/abs/2003.10521.
Luzzatto-Fegiz, P. (2018) 'A one-parameter model for turbine wakes from the entrainment hypothesis', Journal of physics. Conference series. doi: 10.1088/1742-6596/1037/7/072019.
Mcleod, D. and Nordstrom, C. (2019) 'Lessons Learned from Testing Makani's Energy Kite Offshore'. Airborne Wind Energy Conference 2019, 15 October.
Morton, B. R. (1961) 'On a momentum-mass flux diagram for turbulent jets, plumes and wakes', Journal of fluid mechanics, 10(1), pp. 101–112.
Morton, B. R., Taylor, G. I. and Turner, J. S. (1956) 'Turbulent gravitational convection from maintained and instantaneous sources', Proceedings of the Royal Society of London. Series A, Mathematical and physical sciences, 234(1196), pp. 1–23.
Scase, M. M. and Dalziel, S. B. (2006) 'Internal wave fields generated by a translating body in a stratified fluid: an experimental comparison', Journal of fluid mechanics, 564, p. 305.

Simulation of utility-scale airborne wind energy farms: Investigation of wake interaction and power extraction

Thomas Haas*, and Johan Meyers
Katholieke Universiteit Leuven
*Presenting author

Keywords: airborne wind energy | large-eddy simulations | wake interaction

The large-scale deployment of airborne wind energy (AWE) will yield the emergence of parks of AWE systems operating in the multi-megawatt range (Kruijff and Ruiterkamp, 2018). The operation of large-scale AWE systems in the atmospheric boundary layer (ABL) generates wind velocity deficits and increases turbulence in the wake of the system (Haas et al, 2019). When clustered in parks, the cumulative effects of individual wakes impact the operation and the power performance of the complete AWE farm. An efficient farm operation therefore requires a profound understanding of the interaction between the wind resource and the AWE farm. To that end we have developed a computational framework combining large-eddy simulations and optimal control techniques, which consists of the coupled simulations of ABL flow dynamics and AWE system dynamics. We consider large-scale AWE systems based on a generic design procedure that allows to investigate different power-generation modes and easily adapt system dimension and performance to different wind conditions. The AWE system is modelled as a tethered wing system using a mass-point model and its dynamics are optimized for power generation and trajectory tracking using the open-source toolbox awebox (awebox, 2020). The flow simulations are performed by means of large-eddy simulations with the in-house solver SP-Wind developed at KU Leuven. The coupling of AWE system and ABL flow dynamics is performed in the large-eddy simulations by using actuator techniques such as actuator line and actuator sector methods. The AWE system response to the local flow conditions is controlled using a model predictive controller to ensure the stable tracking of the optimized flight path. Finally, A high-level controller supervises the power extraction
of the AWE farm by adapting the reference flight path of each system to the transient wind conditions of the atmospheric boundary layer, such as turbulence- and wake-induced wind speed fluctuations.

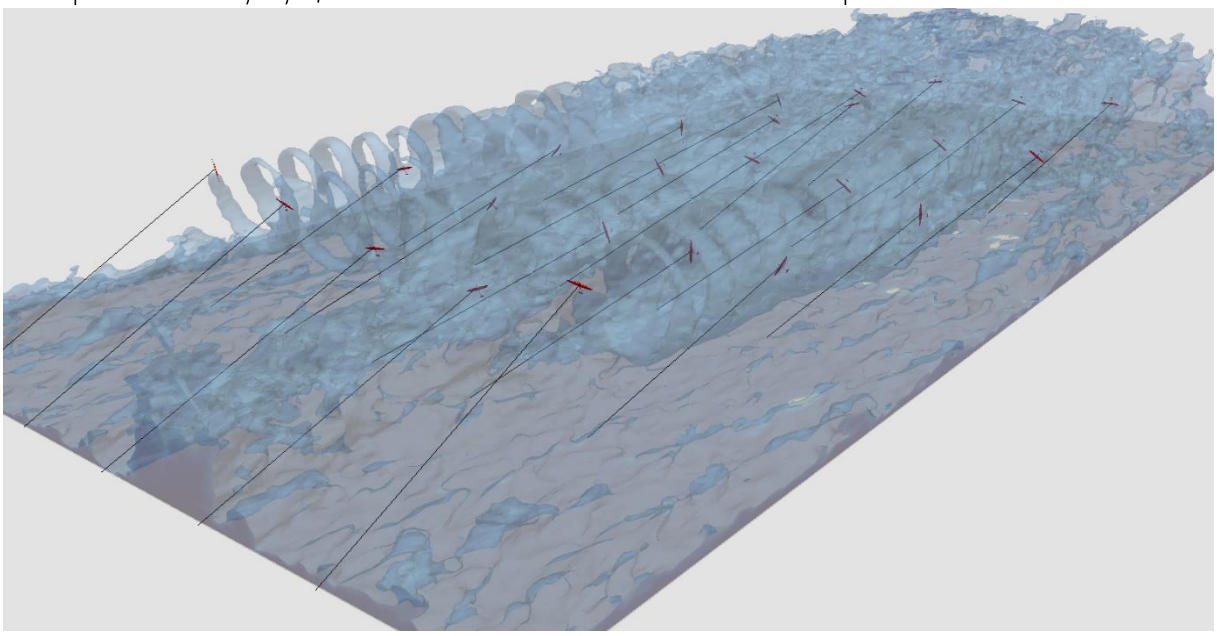

Figure 1: Visualization of ABL flow structures in a 5x5 farm of on-board generation AWE systems. The figure depicts the instantaneous wake-induced velocity deficit by means of iso-volumes of the axial wind speed component.

We consider large AWE farms operating with ground-based and on-board generation AWE systems and investigate the effects of farm layout and power density on the power extraction at both systemand farm-

level. We pay particular attention to the effects of ABL turbulence and upstream wakes on the operation of individual systems as they adapt the tracked flight path for different wind speeds inside the farm. Furthermore, we look at the effects of the different operation modes of the AWE systems on the dynamics of the boundary layer in terms of wake development and recovery.

Preliminary results show that the wake-induced power decrease through the AWE farm is smaller than for conventional wind farms. An example of wake interaction in a large farm of AWE systems is shown in Figure 1. The AWE farm consists of 25 utility-scale AWE systems with on-board power extraction designed to generate up to 5MW of power at rated wind speed.

References:

awebox. (2020). 'Modelling and optimal control of single- and multiple-kite systems for airborne wind energy'. https://github.com/awebox

Haas T. et al (2019). 'Wake characteristics of pumping mode airborne wind energy systems'. In J. Phys.: Conf. Ser. 1256 012016

Kruijff M. and Ruiterkamp R. (2018). 'A Roadmap Towards Airborne Wind Energy in the Utility Sector'. In: Schmehl R. (ed) Airborne Wind Energy. Green Energy and Technology. Springer, Singapore

Computational fluid dynamics simulations of a multi-megawatt airborne wind energy reference system

Niels Pynaert*, Jolan Wauters, Guillaume Crevecoeur, and Joris Degroote
University of Ghent
*Presenting author

Keywords: Airborne wind energy | Computational fluid dynamics | Reference model

Airborne wind energy (AWE) is an emerging technology that aims at converting wind energy by flying crosswind patterns with a tethered aircraft. It has the potential to increase wind energy yield by capturing wind energy at locations and heights unreachable for conventional wind turbines. Recently, Makani, the first company to fly an offshore AWE system, released all their data on the design and insights of their AWE system. In their report, it is indicated that understanding the behavior of unsteady aerodynamics and the effect of turbulence on the aircraft is key to the viability of AWE [1].

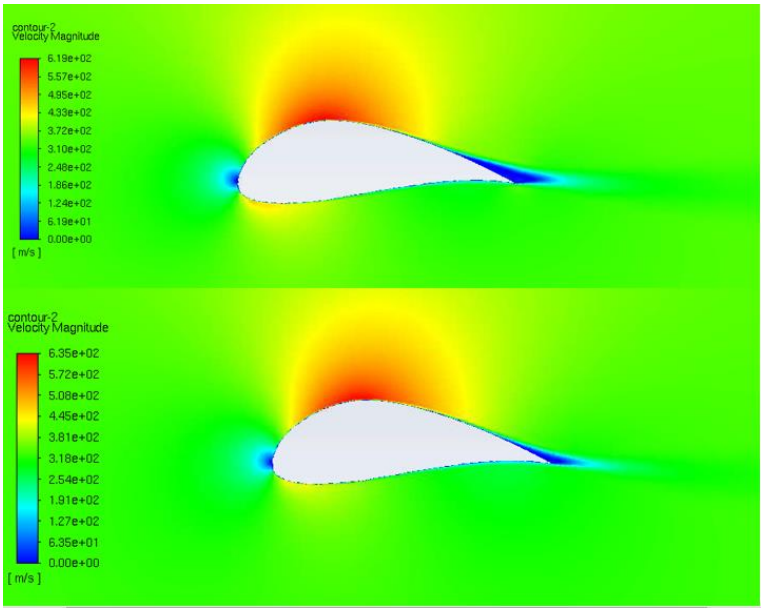

Figure 1: Visualization of the velocity magnitude using SST k- ω model (above) and k-ε model (below) at 0 angle of attack for the 2D reference airfoil (Reynolds number: 2.41e7, velocity: 356 m/s).

To resolve the issues indicated by Makani, there is a need for high fidelity tools that can be used to analyze the effects of environmental conditions. The availability of high fidelity models would permit the optimization of design and control trajectories that would enable the physical realization of AWE systems.
This research makes a first step towards high fidelity modeling by setting up computational fluid dynamics (CFD) simulations of the reference model introduced in Eijkelhof et al. [2]. The wing is examined by means of steady and incompressible Reynolds Averaged Navier-Stokes (RANS) simulations at a Reynolds number of 2.41e7 and different angles of attack. A comparison between k-ω SST and k-ε turbulence models showed large differences in terms of separation. For example, the k- ω SST model predicts separation at the trailing edge at low angles of attack. As opposed to the k- ε model which predicts a more attached flow (Figure 1). This emphasizes the complexity of accurate flow field predictions of the reference model. Due to the presence of trailing-edge separation, the lift curve slope is found less steep than given in Eijkelhof et al. [2]. The offset can be explained by the assumptions made using the latter's lower fidelity model, which undermines the physical prediction of flow separation. This furthermore illustrates the importance of high fidelity assessment of AWE systems. The maximum lift coefficient of 1.85 is found at an angle of attack of 13 degrees. After which a gradual decrease of lift is observed, corresponding to a trailing-edge stall.

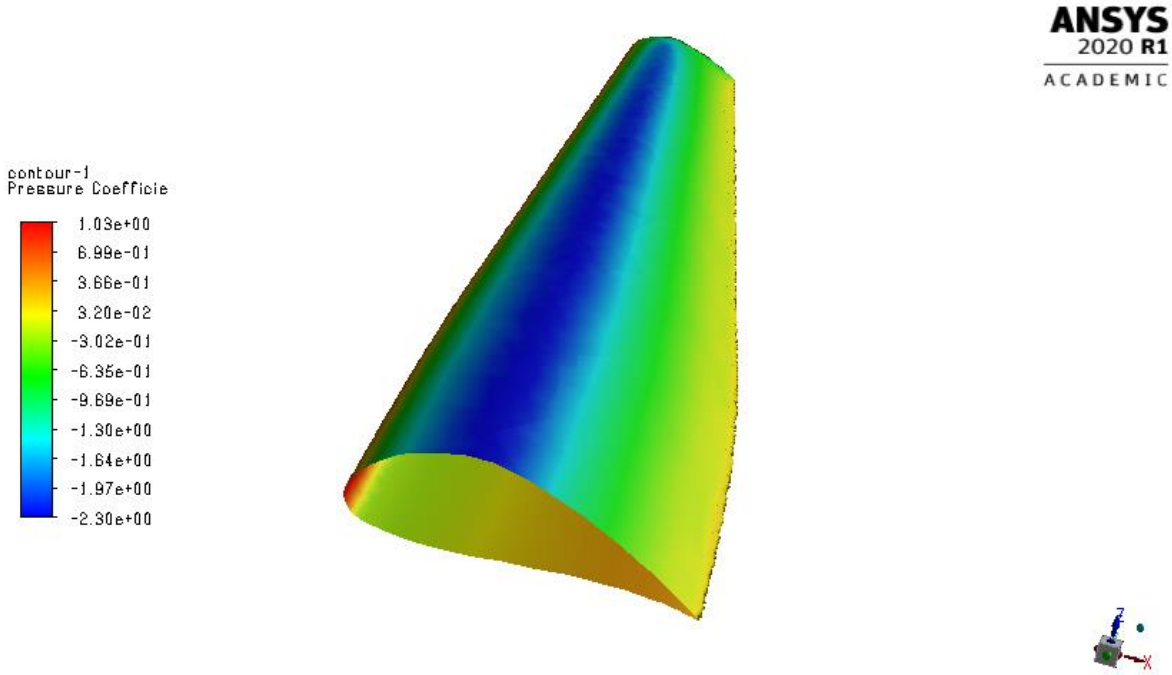

Figure 2: Visualization of the pressure coefficient on the 3D reference wing (velocity 80m/s).

In future work, fluid-structure interaction (FSI) will be included by coupling the wing CFD model with a FEM model using the in-house code CoCoNuT. The final goal of this research is to model the effects of unsteady aerodynamics and atmospheric turbulence on the AWE system. To include the unsteady aerodynamics, an unsteady RANS model of an AWE system will be developed, including a representation of the atmospheric boundary layer at its inlet. The motion of the AWE system will be dealt with by overlaying a moving body-fitted mesh attached to the AWE system over a Cartesian stationary background mesh. Connectivity between both meshes will be provided by the Chimera overset technique, which has been proven successful for a horizontal axis wind turbine [3].

Challenges for applying this technique to an AWE system are the need to consider the variable path and control in the simulation. The movement of the aircraft, location and speed of the wing will be dictated by the dynamics of the system, given by the reference simulation model [2].

References:

[1] Echeverri, P., Fricke, T., Homsy, G. and Tucker, N. (2020). The Energy Kite: Selected Results From the Design, Development and Testing of Makani's Airborne Wind Turbines.

[2] Eijkelhof, D., Rapp, S., Fasel, U., Gaunaa, M. and Schmehl, R. (2020). Reference Design and Simulation Framework of a Multi-Megawatt Airborne Wind Energy System. Journal of Physics Conference Series. 1618. 32020. 10.1088/17426596/1618/3/032020.

[3] Santo, G., Peeters, M., Van Paepegem, W., and Degroote, J. (2019). Dynamic Load and Stress Analysis of a Large Horizontal Axis Wind Turbine using Full Scale Fluid-Structure Interaction Simulation. Renewable Energy. 140. 10.1016/j.renene.2019.03.053.

Particle Swarm Optimization for Synchronizing Multiple Pumping-Cycle AWES and the Implications on Wind Park Area, Energy Storage Systems and Power Electronics Requirements for Grid Integration

Bakr Bagaber*, Xinlan Wang, and Axel Mertens
Leibniz University Hannover
*Presenting author

Keywords: Pumping-cycle AWES | Electrical grid integration | Optimum time shift | Energy storage | Wand park area

Pumping-cycle AWES are characterized by their motor/generator phases as well as their low inertia, a combination that results in highly fluctuating output power. This property brings new challenges to conformity with electrical grid codes and the collective operation of multiple units in a wind park scenario. In this work, an optimum synchronization approach for multiple pumping-cycle units is investigated to improve the collective output power quality of a wind park. Additionally energy storage systems (ESS) are investigated for additional peak shaving.

The basic concept available in literature relies on operating the pumping-cycle units with corresponding phase shifts to compensate for the power fluctuations of each single Kite. Particle Swarm Optimization (PSO) algorithm is used in this investigation to find the optimum phase shifts.

Two objective functions for the optimization are tested; the first is the maximum difference over one flight period in the time domain, while the second is the sum of amplitudes of harmonic components, based on the Fast Fourier Transform (FFT). Both optimization results show that the optimal phase shift between the kites is equal to the cycle period of a single kite divided by the number of kites if ideal constant wind conditions are assumed, and all kites are experiencing the same wind speed. Fig. 1 depicts the fluctuation in output power as a function of wind speed and the number of kites, each kite is modeled using an average mathematical model of the output power.

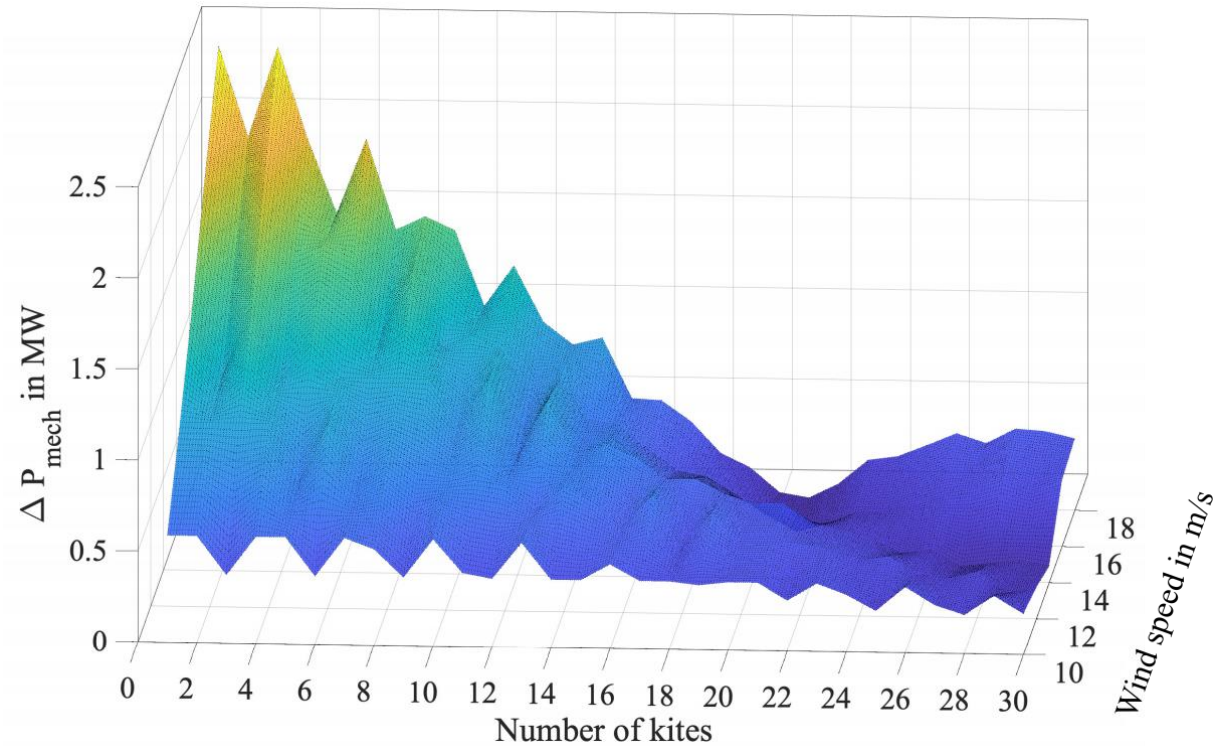

Fig. 1: Maximum power difference ΔPmech produced by different AWES numbers with constant wind velocities from 10 m/s to 18 m/s.

However, our results show that for more realistic scenarios of turbulent wind fields, this simple mathematical relation does not necessarily hold true anymore. Using MATLAB Simulink, the dynamics and control of several AWES systems were simulated using the wind data in [1]. A PSO algorithm is again used to find the optimum phase shift of each unit in real time based on the data collected from the previous cycle; the results for three AWES systems are depicted in Fig. 2. It is clear that PSO can find a better optimum value of the phase shifts regardless of the selected objective function. This is eventually reflected in the lower power spikes, which reduces the requirements for power electronics, filters and transformers at the point of common coupling (PCC) with the grid. It could also reduce the impact of the wind park on the frequency stability of the grid.

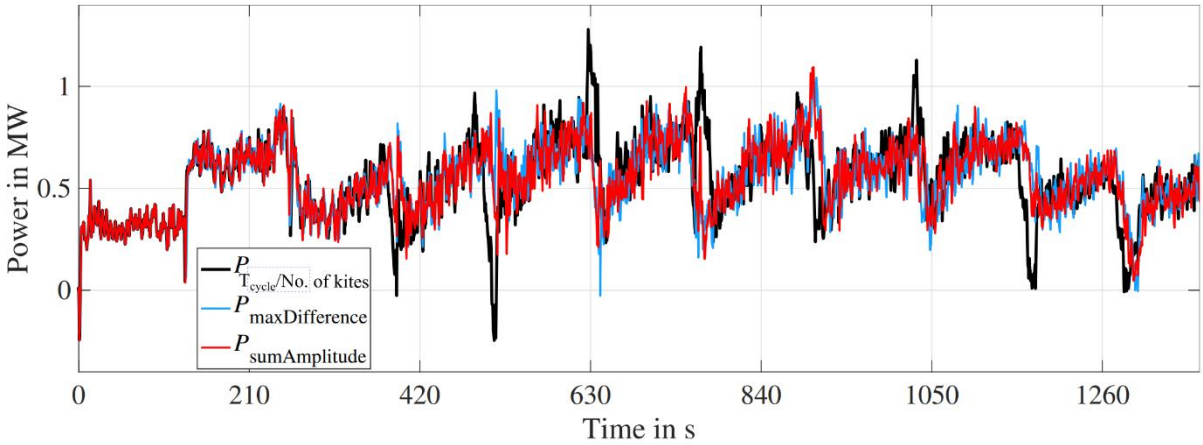

Fig.2: Total output power of 3 kites wind park using different time shifts.

For wind parks with less than six kites, an ESS is further investigated to even reduce the output power variations. The ESS is also optimally sized using PSO under the constraints of minimum energy storage capacity and power handling capability, the dimensioning is based on the average power model of the kite system. The results show that the power handling capacity of the ESS depends mainly on the wind conditions rather than the number of kites, whereas the required energy storage capacity is more correlated to the number of kites. Finally, the wind park area requirement if the output power fluctuation is optimized (strategy I) is compared against another method [2] optimized for reducing the wind park area (strategy II). It is found that for 9 kites, the minimum distance between two kites required for strategy II can be reduced to twice that required for strategy I, while the maximum power difference of strategy II is less than 1/3 of strategy I.

References:
http://awesco.eu/
FAGGIANI, PIETRO AND SCHMEHL, ROLAND: Design and Economics of a Pumping Kite Wind Park. Version: 2018. http://dx.doi.org/10.1007/978-981-10-1947-0{_}16. In: SCHMEHL, Roland (Hrsg.): Airborne Wind Energy: Advances in Technology Development and Research. Singapore : Springer Singapore, 2018. – DOI 10.1007/978–981–10–1947–0_16. – ISBN 978–981–10–1947–0, S. 391–411

Mini-Symposium: Airborne Wind Energy System Modelling, Control and Optimisation (II)

AirWing, a self-regulating control system for kites

Ingo Mewes[1,2,*]
[1]HfS "Ernst Busch", Berlin
[2]AirWing
[*]Presenting author

Keywords: Airborne Wind Energy | Flight Control | Steering | Gust Alleviation | Self Regulation

One of the key challenges of reliable and safe operation of kites is flight control. In this study I present an innovative control concept which is suitable for wind-assisted ship propulsion as well as airborne wind energy harvesting. Compared to the existing steering systems, my development differs in three main points:
1. Simple and robust mechanical structure, the basic functionality can also be guaranteed without current.
2. Only one winch is required for take-off, landing and cyclical energy generation.
3. A kite control pod is not required.

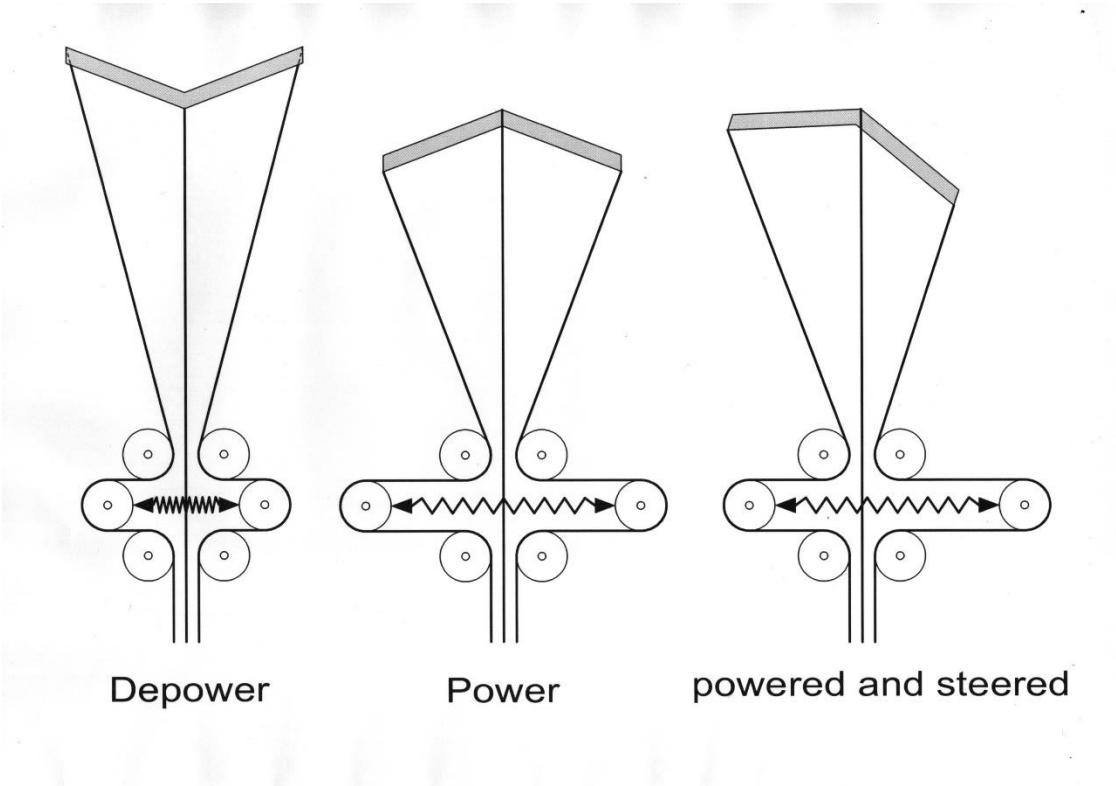

Figure 1, schematic representation of the function

As can be seen in Figure 1, AirWing is part of the ground station. It essentially consists of 6 pulleys, 4 of which are fixed and 2 are movable with a central spring element. The main tether connect the kite directly with the not illustrated winch, while the less stressed control lines are guided around the spring element. A delta-shaped kite with 3 lines is shown as an example, but the system works on principle with all kites with four-line control.
By spreading the control lines and moving the spring element horizontally, the kite can be trimmed and steered. The specified spring force limits the maximum tension of the control lines; with higher pulling forces on the control lines, these are automatically extended. That leads to immediately depower of the kite in the

event of temporary overload. The whole system can be operated safe at its performance limit, even in gusty winds, which can improve efficiency.

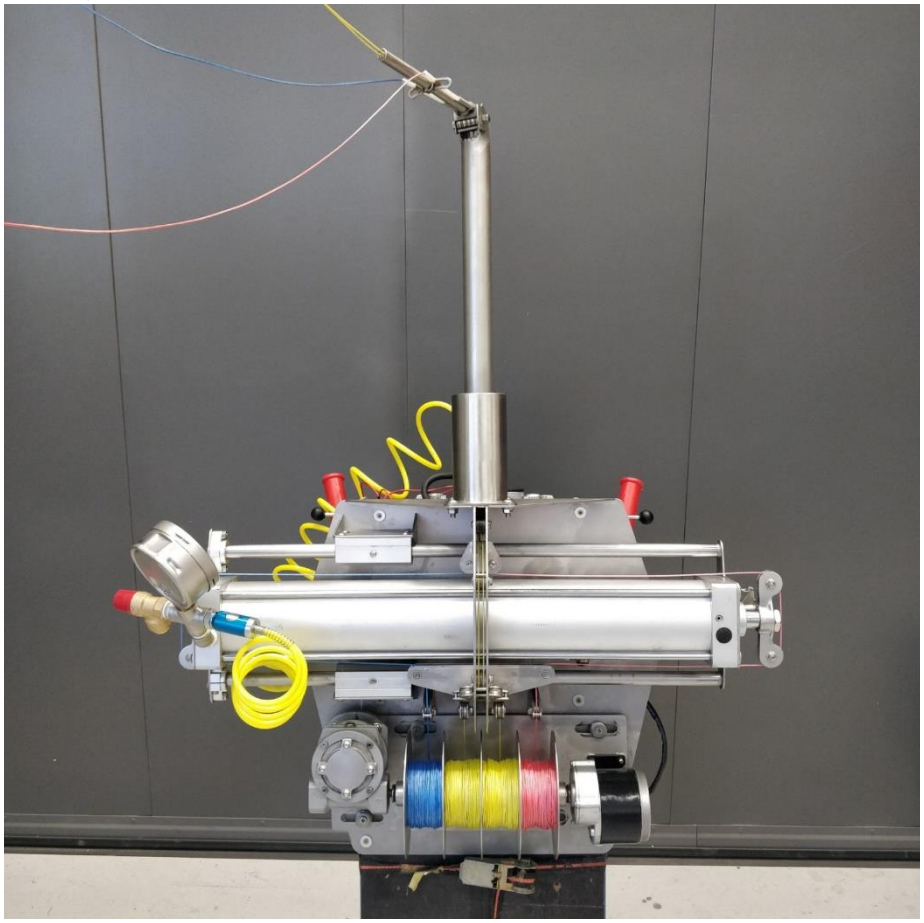

Figure 2, first prototype

Figure 2 shows a first prototype with a linear guided and self-centering pneumatic cylinder as the spring element. There is an compressor, electric winch and on top a small pylon integrated. The relation between power and depower (trimming) and the regulating force of the steering lines can be adjusted by cylinders filling level. The oscillating winch is constructed only for the orderly handling of the 330 feet each dyneema lines, not for current generation. This first prototype was able to show the basic functioning of the technology, but it still has decisive weaknesses:

1. The trim and cut-off force cannot be set independently of each other.
2. The counter pressure has an exponential effect, which can lead to system overloads.

A new prototype in preparation will no longer have these weaknesses. It will be based on gas springs, no compressor will be needed, and a linear regulation force is guaranteed. A separate device will adjust the stroke of the gas springs for manual trimming. It will initially only be suitable for manual steered towing a 34 ft. boat. At the WESC, I plan to present the existing status in order to find suggestions and possibly partnerships for the next work steps.

It is my goal to find out, how AirWing can be integrated into automated energy generation and whether its integration can result in long-term benefits.

References:

Bormann A., Ranneberg M., Kövesdi P., Gebhardt C., Skutnik S.: Development of a Three-Line Ground-Actuated Airborne Wind Energy Converter. In: Ahrens U., Diehl M., Schmehl R. (eds) Airborne Wind Energy. Green Energy and Technology. Springer, Berlin, Heidelberg. 2013. https://doi.org/10.1007/978-3-642-39965-7_24

Mewes, I.: Steuereinrichtung für ein seilgebundenes Fluggerät, Verfahren zur Steuerung und Fluggerät. Patent File number: 10 2020 131 131.1. , www.airwing.de

Robust Automatic Pumping Cycle Operation of Airborne Wind Energy Systems

Sebastian Rapp*, Roland Schmehl, and Gerard van Bussel
Delft University of Technology
*Presenting author

Keywords: airborne wind energy | robust flight control | reliability | safety

Airborne wind energy (AWE) is a novel technology that aims at accessing wind resources at higher altitudes which cannot be reached with conventional wind turbines. This technological challenge is accomplished using tethered aircraft, or kites, in combination with either onboard or ground-based generators. In the former case, the kinetic energy of the air flow is transformed into electricity and transmitted via a conductive cable to the ground. In the latter case, the aerodynamic force of the aircraft or kite is translated into tether tension. The pulling force uncoils the tether from a drum which turns a generator and hence transforms the mechanical torque into electrical power on the ground. In this case two operational modes are required: In the first mode, the tether is reeled out until the maximum length is reached. It follows a reeling in phase where the aircraft or kite glides back towards the ground station and a fraction of the generated power is used to wind the tether again onto the drum of the winch. The cycle restarts as soon as the minimum tether length is reached. These two modes combined constitute a so-called pumping-cycle.
Reliability is a key system property that will decide over the success of AWE as a commercially feasible technology. To reach this goal, a well designed control system is required that can achieve the nominal control objectives as well as handle disturbances such as atmospheric turbulence and mismatches between the model used for control design and the real plant. In light of these challenges, the presented work, which concludes the PhD research of the first author [1], aims at making a contribution to bring AWE closer to commercial success. A systematic design workflow of a modular control architecture for a rigid wing AWE system operated in pumping-cycle mode is presented. Models of different fidelity are introduced, that are either directly used for the controller synthesis or in order to verify if the designed controller is able to meet its objectives. A quasistationary analysis is performed to describe the operational flight envelope and to derive linear state space models for the longitudinal and lateral flight controller synthesis. A generic outer loop controller is designed independent of the specific aircraft actuation which guides the system along the traction and retraction phase reference flight paths. A ground based winch controller is used to track the tether tension and hence the radial motion of the aircraft. To track the outer loop guidance commands several linear and nonlinear inner loop flight controllers are proposed. All controller designs are verified in detail using Monte Carlo simulations. The resulting distributions of critical metrics are used to quantify performance as well as robustness of the controllers in presence of stochastic variations in the wind field and model uncertainties (Figure 1).

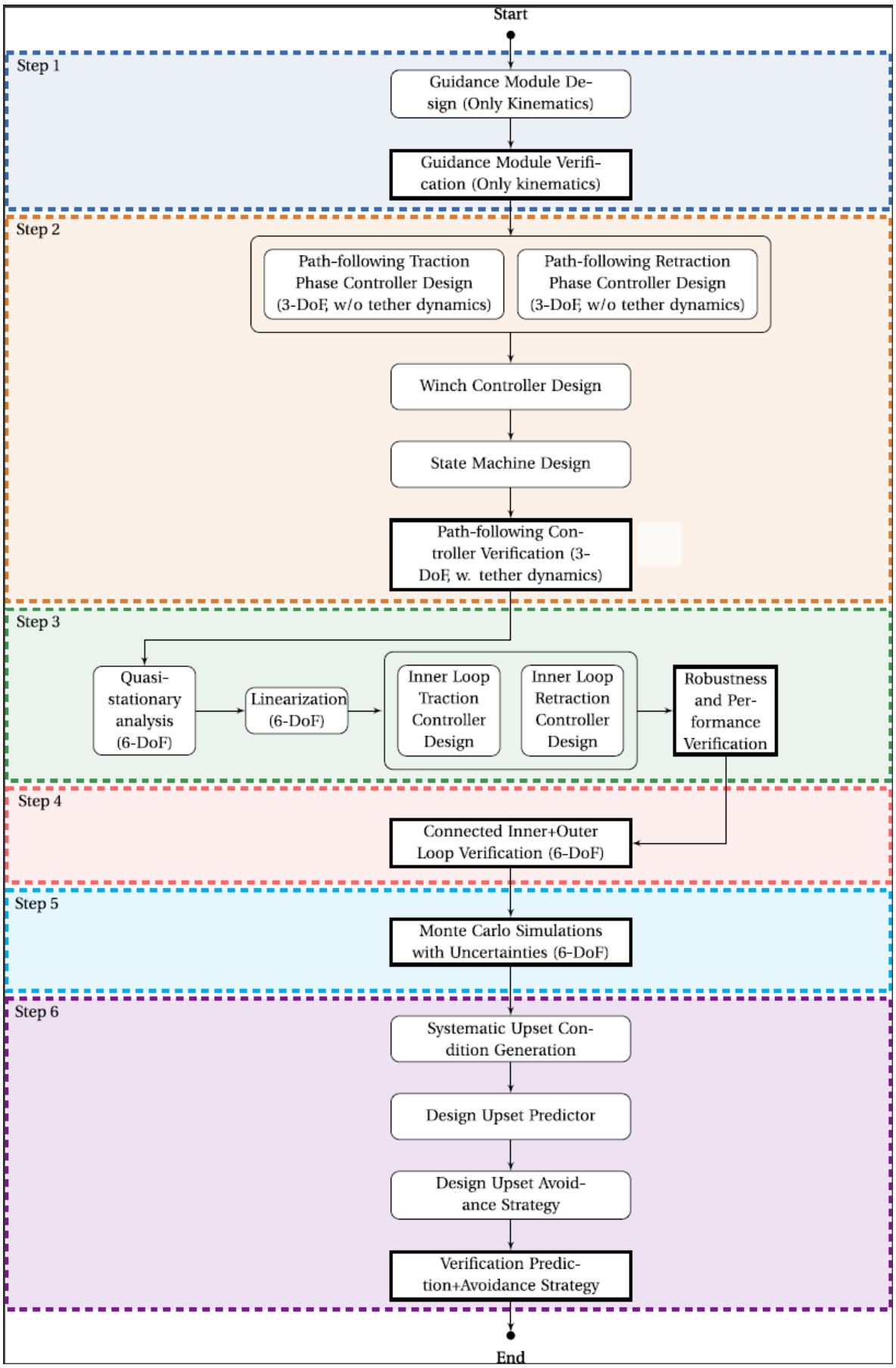

Figure 1: Control design and verification workflow using models with appropriate fidelity. Possible design iterations are not displayed for visualization purposes. Blocks with round corners indicate design tasks, sharp corners indicate verification tasks. Illustration taken from [1].

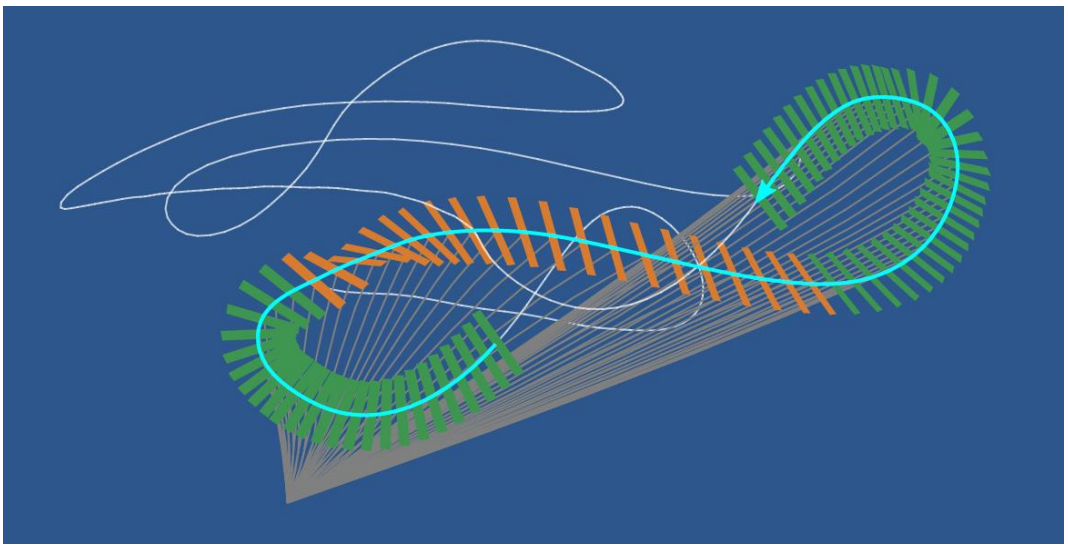

Figure 2: Flight path and aircraft orientation during a pumping-cycle with tether rupture avoidance maneuver. Illustration taken from [1].

We propose a methodology to systematically generate conditions in which the AWE control system is failing. The generated knowledge can be leveraged to create an analytic model that is able to predict during operation a critical flight state and can trigger a mitigation maneuver to avoid it (Figure 2).
Different prediction strategies are presented and eventually the methodology is specifically applied to the case of tether rupture condition generation, prediction and avoidance.

References:
[1] Rapp, S.: Robust Automatic Pumping Cycle Operation of Airborne Wind Energy Systems. PhD dissertation, Delft University of Technology, 2021. https://repository.tudelft.nl/

Experimental Results on drone-based Take-Off and Landing of an AWE System

Audrey Schanen*, Ahmad Hably, Jonathan Dumon, and Nacim Meslem
Univ. Grenoble Alpes
*Presenting author

Keywords: Take-off and landing | Experimental | Airborne Wind Energy System | Tethered drone

Modeling, control and optimization problems of AWE system have been extensively studied in the literature: theoretically, in numerical environments and through infield experiments. However, several urgent aspects should be addressed to validate their technical feasibility and to ensure their commercial success.
One of such aspects is the take-off and landing of the airborne platform, especially for on-ground production systems with rigid airfoils. During the Airborne Wind Energy Conference (AWEC 2017), the authors of [1] have presented three approaches for launching and landing of an AWE system:
Vertical take-off, catapult, and rotating arm. In [2], a theoretical analysis of different concepts for only the take-off phase of AWE systems based on rigid wings and on-ground power conversion are presented.
In this work we study the control design of a vertical take-off and landing of a rigid-wing airborne wind energy system using a multicopter.

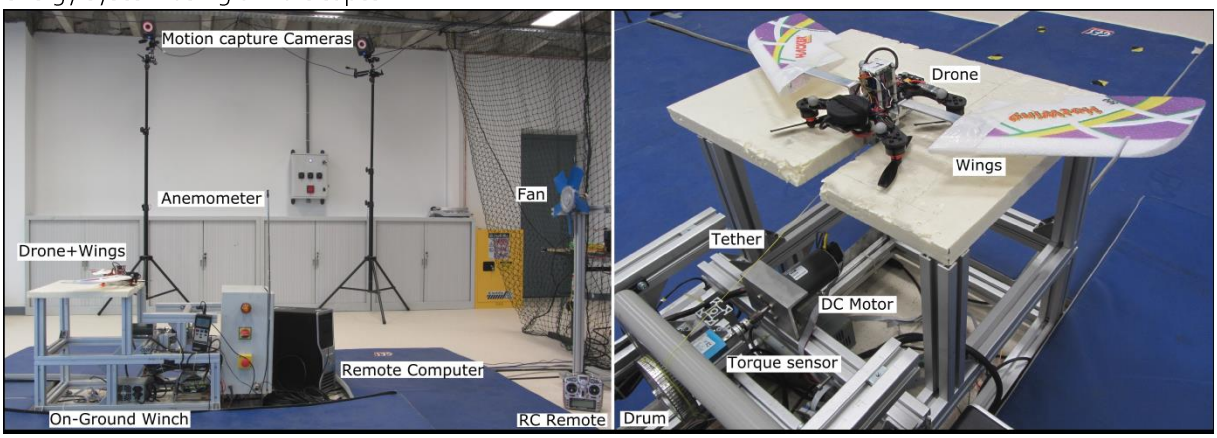

Fig 1 : Experimental bench is composed of wings attached to a drone, linked to an on-ground winch with a tether. A motion capture system tracks the drone position and send it to an on-ground computer that controls the winch and the drone.

A first step has been focused on the development of a 2D model and the design of a controller using an output feedback linearization method. The aim is to transform the nonlinear tracking problem to a linear stabilisation problem. Then, an intermediate linear control law is computed to ensure the asymptotic stability of the tracking error. The position of the drone is controlled thanks to both winch torque and lateral force of the drone, while the tension in the tether is controlled with the radial force of the drone [3].
The control algorithm was then applied on an indoor bench composed of wings fixed on a tethered drone linked to an on-ground winch. Since an extension in 3D was necessary, the azimuth angle of the system, as well as yaw angle of the drone has to be controlled. An additional control law for the azimuth angle using roll angle of the drone was therefore designed. On the other hand, in order to stay as much as possible equivalent to the 2D problem, the yaw is chosen to have the drone always pointing to the ground station.
To validate this control strategy, an experimental bench uses a motion capture system that tracks the drone position and send it to an on-ground computer using ROS middle ware to control the winch and the drone has been developed. Moreover, to consider the effect of the wind disturbance on the system a fan is used (see Fig 1).

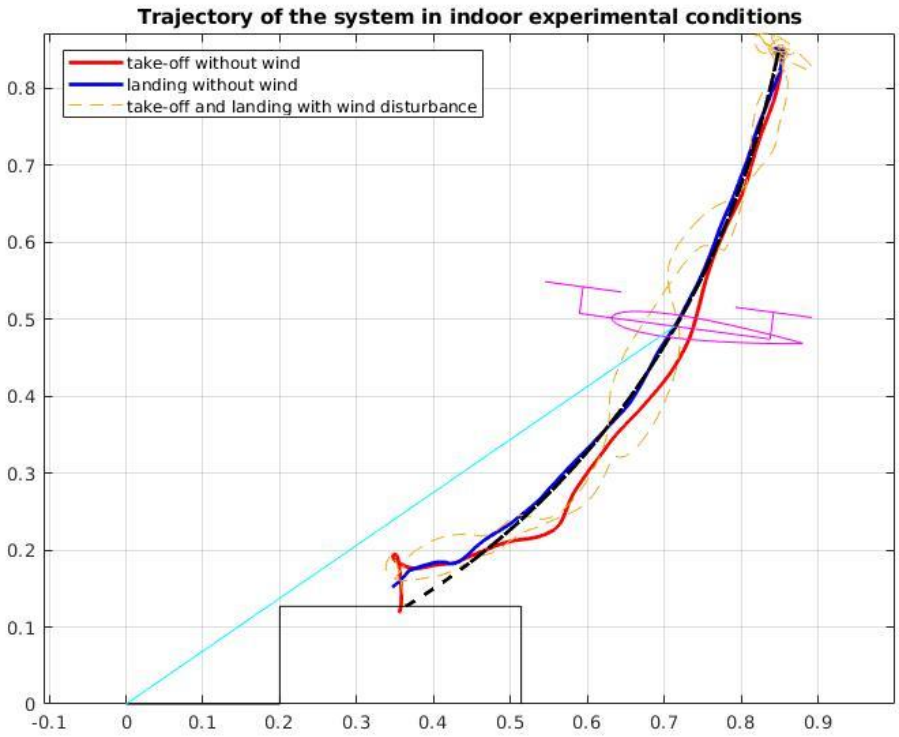

Fig 2 :Trajectory of the system in indoor experimental conditions under a wind disturbance around 2 m/s

Then, the control law is tested on different scenarios including a take-off and a landing. Results show that the higher the wind speed is more the trajectory is disturbed but over all its cycle it follows well the reference and it never gets in a critical zone where the system could crash (see Fig 2).
Further development are in progress to take into account aerodynamic forces in the design of the control law to be more robust regarding wind disturbances and to adapt the commands send to the drone.

References:
[1] Rieck, B., Ranneberg, M., Candade, A., & Bormann, A. (2017). Comparison of Launching & Landing Approaches.
[2] Fagiano, L., & Schnez, S. (2017). On the take-off of airborne wind energy systems based on rigid wings. Renewable energy, 107, 473-488.
[3] Schanen, A., Dumon, J., Meslem, N., & Hably, A. (2020, July). Take-off and landing of an AWE system using a multicopter. In 2020 American Control Conference (ACC) (pp. 3846-3851). IEEE.

Airborne Wind Energy: Trajectory Tracking Controller Design of a Tethered Aircraft

Anıl Sami Önen*, and Prof. Ozan Tekinalp
Middle East Technical University
*Presenting author

Keywords: Airborne Wind Energy | Crosswind Flight | Quater. based nonlinear attitude control

Airborne wind energy has been intensely studied by the researchers, especially in the last decade (Ahrens, Diehl and Schmehl, 2014). It stems from the crosswind flight concept that was originally introduced by Loyd (1980). The improvements in the micro-computer and sensor technology, helped designers use complex control algorithms and paved the path to the development of airborne wind energy concept as an alternative to the conventional wind turbines. This new concept is advantageous when compared to the classical wind turbines since it can be used in higher altitudes that have a bigger wind energy potential. Moreover, due to not needing a concrete construction it is an applicable concept in offshore as well. Although there are different types and various design philosophies behind, using a flying object that is connected to the ground by a tether in this evolving technology is common.

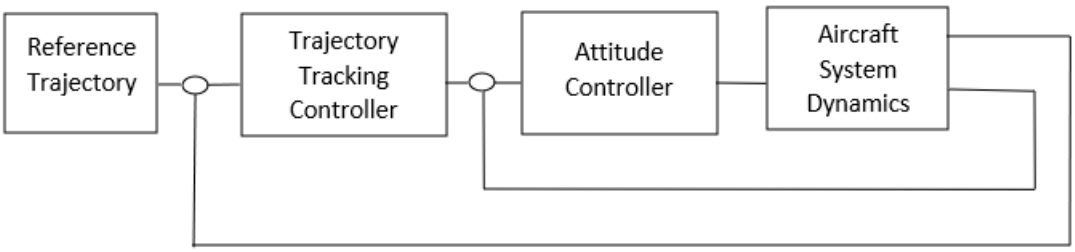

Figure 1: Trajectory Tracking Problem – Control Architecture

In this study, a winged airplane is used as an energy supplier. The mathematical model of the airplane is constructed that is composed of aerodynamic, environmental, gravitational sections and nonlinear equations of motion. (Önen, 2015) The mathematical model uses the aerodynamic control surfaces such as ailerons, elevator and rudder. In constructing the aerodynamic model, variation of the nondimensional force and moment coefficients according to varying angles of attack, sideslip angle and control surface deflections are analyzed and obtained using an analysis software. The maximum power that can be generated according to varying wind speed conditions is calculated. The control problem of the crosswind flight is addressed in the paper which is fundamental to the control architecture of airborne wind energy systems. There are two main approaches in controlling airborne systems. First approach is based on online optimization of the power output of the system, employing nonlinear model predictive control (NMPC) (Ilzhöfer, Houska and Diehl, 2007; Houska and Diehl, 2010; Canale, Fagiano and Milanese, 2007; Canale, Fagiano and Milanese, 2008). In the second method a trajectory tracking control methodology is preferred that separates the optimal trajectory estimation and control problem from each other. The second methodology is used in this paper and the trajectory tracking problem is formed as shown in Figure 1. The trajectory tracking controller is producing the angle commands by using the difference between the actual position of the aircraft and the desired trajectory and is mainly based on geometrical considerations. (Jehle, 2012, p.28) The quaternion based nonlinear attitude controller is designed, producing steering commands by using the difference between the angle command that is produced by the tracking controller and the actual attitude of the aircraft. By expressing the current attitude and the desired attitude with quaternions, the attitude control is realized by using the so called "to-go" quaternions. (Ariyibi and Tekinalp, p.6) The optimal trajectory estimation that is necessary to produce the maximum amount of power is not addressed in this study and left as a future work. The response of the controller is tested in a simulation environment by using a pre-defined trajectory.

References:
Ahrens, U., Diehl, M. And Schmehl, R. (eds.) (2014) Airborne Wind Energy. Heidelberg: Springer-Verlag Berlin
Ariyibi, S., Tekinalp, O. (2020) 'Quaternion-based nonlinear attitude control of quadrotor formations carrying a slung load', Journal of Aerospace Science and Technology, 105.
Canale, M., Fagiano, L. and Milanese, M. (2007) 'Power Kites for Wind Energy Generation – Fast Predictive Control of Tethered Airfoils', IEEE Control Systems Magazine, pp. 25-38.
Canale, M., Fagiano, L. and Milanese, M. (2009) 'KiteGen: A revolution in wind energy generation.' The International Journal Energy, 34 (3), pp. 355-361.
Houska, B., Diehl, M. (2010) 'Robustness and Stability Optimization of Power Generating Kite Systems in a Periodic Pumping Mode', IEEE International Conference on Control Applications, pp. 2172-2177.
Ilzhöfer, A., Houska, B. and Diehl, M. (2007) 'Nonlinear MPC of kites under varying wind conditions for a new class of largescale wind power generators', Journal of Robust and Nonlinear Control, 17(17), pp.1590-1599.
Jehle, C 2012, Automatic Flight Control of Tethered Kites for Power Generation, Munich Technical University, Munich.
Loyd, M. (1980) 'Crosswind Kite Power', Journal of Energy, 4(3), pp.106-111.
Önen, A.S 2015, Modeling and Controller Design of a VTOL Air Vehicle, Middle East Technical University, Ankara.

Fault-tolerant Control of Airborne Wind Energy Systems with Multicopter/Fixed-Wing UAV Configuration

Tareg Mohammed*, and Lorenzo Fagiano
POLIMI
*Presenting author

Keywords: Airborne Wind Energy | Fault-Tolerant Control | Quad-rotor Fixed-wing Hybrid UAV

Airborne Wind Energy (AWE) is the technology of harvesting electrical power from the wind blowing at an altitude higher than the conventional wind turbine height (Ahrens U., Diehl, M., Schmehl, R., 2013). A recent study (Bechtle et al., 2019) shows that AWE can provide power with a density higher than the conventional wind turbine by a factor of two and with a time availability of 95\%. Yet, no commercial usage of the technology has been recorded. One of the commercialization barriers that need to be overtaken is improving the system reliability and ensuring operation safety (DirectorateGeneral for Research and Innovation (European Commission), ECORYS, 2018).
In AWE system reliability and safety, a recent study (Salma, 2020) points out that the majority of failure mitigation measures for AWE can be performed by fault detection and isolation techniques. Taking into consideration different plant types used in AWE (Fagiano, L. and Milanese, M., 2012) (Cherubini et al., 2015) a study (Fagiano, L et al., 2018) state that the qualitative feature like small required land area, low cost, repeatability, and robustness could be a significant technological bottleneck for AWE technology. One candidate configuration that can compete with these features is the quad-rotor fixed-wing hybrid unmanned aerial vehicle (UAV). Such UAVs can achieve superior flying qualities, and at the same time, offer redundancy in the control system (Gunarathna et al., 2018). In this study, a Hybrid UAV prototype from Kitemill is selected (see figure), the required modeling data and plant specification are provided by (Rapp, Sebastian, et al., 2019).

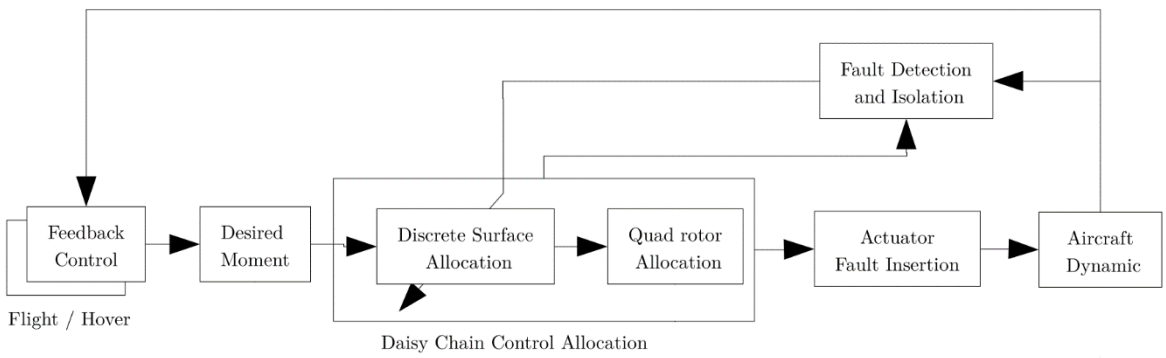

Figure 1: Proposed control scheme for multicopter/Fixed-Wing UAV for AWE application

Fault-tolerant control (FTC) can be defined as methods used to preserve a system's operational objectives in case of one or multiple component/sensor failure (Aviziens, 1976). Active fault-tolerant control (AFTC) incorporates one of the Fault Detection and Diagnoses (FDD) methods and actively reconfigure the plant controller to accommodate the failure. One open research question is how best to mate an FDD method with another re-configurable controller. In practice, a tailored FTC scheme is needed for each particular system or application. In aircraft control systems, FTC has been widely used. Most studies consider fixed-wing aircraft (Fekih, Afef, 2014); in contrast, for quad-rotor, fixedwing hybrid UAV, no FTC publication could be mentioned. This research suggests an AFTC tailored for quad-rotor fixed-wing hybrid UAV for AWE application.
This presentation discusses ongoing research activities to apply FTC for AWE tethered flight. First, it introduces a control scheme dedicated to quad-rotor fixed-wing hybrid UAV (see attached figure).

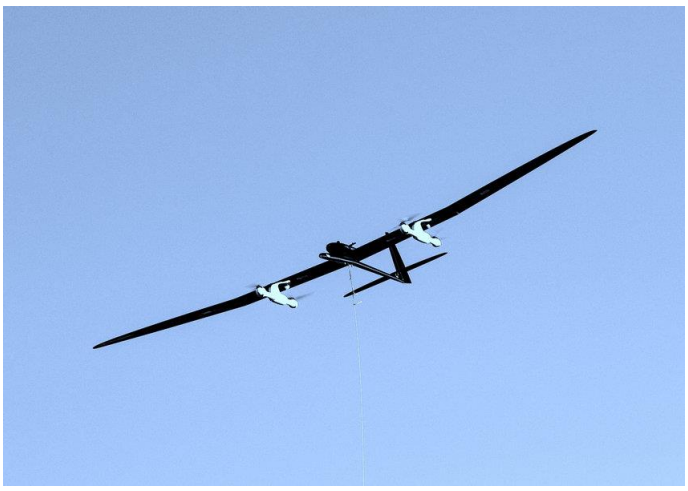

Figure 2: 5 kW prototype of Kitemill AS with vertical takeoff-and landing capabilities

The suggested scheme uses daisy chain control allocation (Dale E. at al., 1994), which can react instantly in the cause of actuator saturation; this is highly demanded in AWE for a robust continuous autonomous operation. The second contribution upgrades the before mentioned scheme to AFCT by introducing a quantitative model-based FDD scheme and introduce a new parameter that links between a command control signals and a system state; in particular, it gives the command signal contribution ratio in a specific dynamic mode, the new parameter is used to assist residual generator in identifying the faulty actuator. This contributes a new idea to analytical redundancy methods, which may overcome false alarms and improve fault-tolerance measures for the AWE system.

References:
Aviziens, A., 1976. Fault-Tolerant Systems. IEEE Transactions on Computers, C-25(12), pp. 1304--1312.
Bechtle et al, 2019. Airborne wind energy resource analysis. Renewable Energy, 141(0960-1481), pp. 1103--1116
Blanke, M et al., 2001. Concepts and methods in fault-tolerant control. Proceedings of the 2001 American Control Conference. (Cat. No.01CH37148), 4(0743-1619)
Cherubini et al., 2015. Airborne Wind Energy Systems: A review of the technologies. Renewable Sustainable Energy Rev., 51(1364-0321), pp. 1461--1476
Dale E. at al., 1994. Dynamic inversion: an evolving methodology for flight control design. International Journal of Control, Volume 59, pp. 71-91.
Directorate-General for Research and Innovation (European Commission) , ECORYS, 2018. Study on challenges in the commercialisation of airborne wind energy systems. [Online] Available at: https://op.europa.eu/en/publication-detail/-/publication/a874f843-c137-11e8-9893-01aa75ed71a1/language-en [Accessed 13 1 2021]
Fagiano, L et al., 2018. Autonomous Takeoff and Flight of a Tethered Aircraft for Airborne Wind Energy. IEEE Trans. Control Syst. Technol., 26(1558-0865), pp. 151--166.
Fekih, Afef, 2014. Fault-tolerant flight control design for effective and reliable aircraft systems. Journal of Control and Decision, 1(2330-7706), pp. 299--316
Gunarathna et al., 2018. Development of a Quad-rotor Fixed-wing Hybrid Unmanned Aerial Vehicle. 2018 Moratuwa Engineering Research Conference (MERCon), pp. 72--77
Rapp, Sebastian et al., 2019. Cascaded Pumping Cycle Control for Rigid Wing Airborne Wind Energy Systems. Journal of Guidance, Control, and Dynamics, Volume 42, pp. 1—18 Guidance, Control, and Dynamics, Volume 42, pp. 1--18. Salma, V. a. o., 2020. Improving reliability and safety of airborne wind energy systems. Wind Energy, 23(1095-4244), pp. 340--356.
Ahrens U., Diehl, M., Schmehl, R., 2013, Airborne Wind Energy, Springer-Verlag Berlin Heidelberg. (1865-3529).

Mini-Symposium: Airborne Wind Energy System Modelling, Control and Optimisation (III)

A Model for the Dynamic Simulation of Rotary Airborne Wind Energy Machines

Alvaro Cerrillo-Vacas[1,*], Christof Beaupoil[2], and Gonzalo Sánchez Arriaga[1]
[1]Universidad Carlos III de Madrid
[2]SomeAWE Labs S.L
[*]Presenting author

Keywords: Rotary Airborne Wind Energy Machine | Cosserat Theory | Modelling AWE Machine

Rotatory airborne wind energy (RAWE) machines are a sub-family of airborne wind energy systems that, unlike conventional aerogenerators, harvest energy from the wind by using aircraft. A RAWE machine typically involves a rotor, made of rigid blades or a set of kites, that transforms the kinetic energy of the wind into a rotatory motion that is directly transmitted to an on-ground generator by a structure. Since very light and with a high torsional stiffness, tensile rotatory structures are currently used in RAWE prototypes (see Fig. 1), thus proving their suitability for this application. Typical tension force, transmitted torque, and spinning velocity are in the order of 200 N, 25 Nm, and 120 rpm, respectively, for actual prototypes [1]. However, experimental tests revealed that tensile rotatory structures can collapse if some of these variables overpass critical thresholds [2]. For this reason, having access to dynamic simulators to study and find the operational boundaries of tensile rotatory structures is a topic of major importance for RAWE developers.
The rotatory structure of a RAWE machine has been modelled in the past by a chain of masses linked by springs [3]. This works proposed an alternative approach based on Cosserat Theory (see Ref. [4] and reference therein). Since the structure is slender, i.e. its length is much larger than the characteristic dimensions of its cross-section, one just needs to compute for practical applications the dependence on time (t) and the unstretched arc-length (s) of the position vector of the central line r(s,t) and an angle $\alpha(s,t)$ that orientates the unshearable cross-section. Under sensible assumptions, a set of partial differential equations for r(s,t) and angle $\alpha(s,t)$ was obtained. They capture axial deformation, bending, and twisting of the tensegrity structure.

Figure 1: Rotary Airborne Wind Energy Machine by SomeAWE Labs S. L..L.,

A numerical scheme based on finite element method was developed and used to integrate the equations of motion in relevant configurations for RAWE applications. In this preliminary study, the detailed dynamics of the rotor is ignored, and its effect just appears as boundary conditions for the tensegrity structure, which is the core of the study.

Laboratory testing activities were performed to determine experimentally the axial, bending, and torsional stiffness of the tensegrity structure of SomeAWE's RAWE machine. These physical characteristics of the structure, which naturally appears in the equations of motion in the Cosserat Theory, depend on the tension force exerted on the structure. This experimental data was used as input in the numerical tool and simulations were carried out to study and understand the dynamics of the tensegrity structure for typical operation conditions of the RAWE machine. The results of the simulations were compared with the experimental data obtained during a flight-testing campaign of the RAWE machine. Future works and the main applications and limitations of the proposed model are discussed.

References:
Beaupoil, C. (2019), Practical Experiences With a Torsion Based Rigid Blade Rotary AWE System With Ground Based Power Generation, Airborne Wind Energy Conference, Glasgow.
SomeAWE Labs S.L video. https://www.youtube.com/watch?v=p8Hfj7L7d_w
Tulloch, O., Amiri, A. K., Yue, H., Feuchtwang, J. and Read, R. (2020), Tensile rotary power transmission model development for airborne wind energy systems, Journal of Physics Conference Series. 1618, 032001, doi:10.1088/17426596/1618/3/03200.1.
Villaggio,. P. (2005), Mathematical Models for Elastic Structures. Cambridge University Press, 2005.

Flight dynamic and aerodynamic characterization of a softkite with suspended robotic control unit

Roland Schmehl*, and Arthur Roullier
Delft University of Technology
*Presenting author

Keywords: airborne wind energy | kite | flight dynamics | aerodynamics

Several concepts for airborne wind energy conversion and ship propulsion are based on inflatable membrane wings with suspended, remote-controlled cable robots [1]. Prominent examples are the leading edge inflatable (LEI) tube kites of Kitepower [2] or the ram-air kites of Skysails [3], which both have reached sizes of 100 m2 and larger. Especially the lightweight construction and compact packing volume makes these kites attractive for applications where low costs and high mobility are important. In contrast to rigid wing kites, an inflatable membrane wing can be regarded as a single morphing control surface, actuated by the robotic control unit via the bridle line system. For this reason, softkites are generally much better maneuverable [4].
In this study, we used a large data set provided by Kitepower, comprising 128 pumping cycles totalling a flight time of 4:25 hours, to analyze the flight dynamic and aerodynamic characteristics of the pre-commercial LEI kite shown in Figure 1. Compared to its predecessor, the V3 kite, which was investigated in a previous study [5], this kite is structurally reinforced to fly at a higher wing loading.

Figure 1: LEI kite V3.25B with 25 m2 wing surface area (Photo courtesy of Kitepower B.V.). The design of the V3 kite series dates back to March 2012.

The mass of the control unit is a few kilograms higher than that of the wing (12 kg) because it is already designed for larger wings with higher pulling forces. Next to the position and orientation of the wing, the steering actuation, and the tether force and reeling speed at the ground station are measured at a sampling rate of 20 Hz, as well as the apparent wind speed va at the kite, including its direction. The data analysis includes several models and filtering techniques to separate the effects of the aerodynamic drag on the bridle line system, the control unit and the tether, the inertia of the control unit, and different flight modes such as turning maneuvers, straight flight and retraction. The analysis confirms the linear relation between steering input us and the flight dynamic response of the kite, the yaw rate. This turn rate law [6] is illustrated in Figure 2 (left) and indicates that even in straight flight a small amount of steering is required to compensate for the effect of gravity. The flight data further revealed a time lag between the steering actuation and the actual turning of the kite, as well as a significant effect of the suspended control unit on the dynamics of the kite.

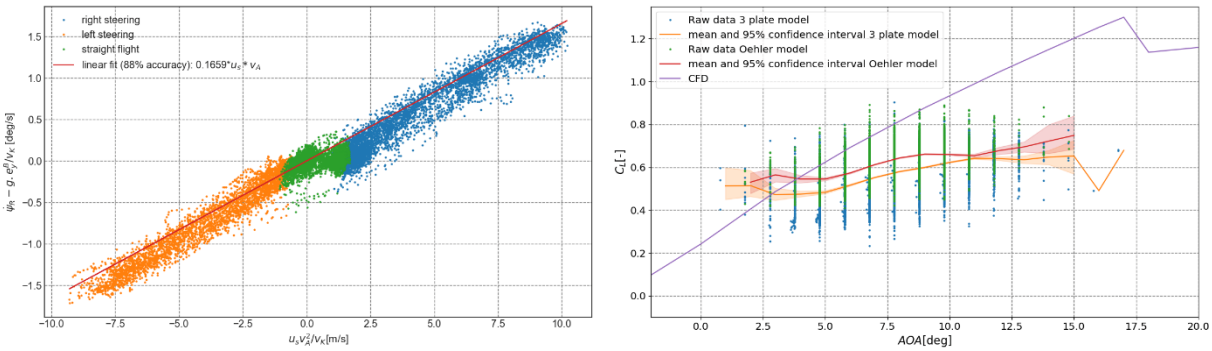

Figure 2: Turn rate law (left) and aerodynamic lift coefficient as a function of the angle of attack (right). The flight data from 8 October 2019 includes only the figure-of-eight maneuvers, which, in this case, are downloops. Diagrams taken from [9]

During turning maneuvers, the centrifugal force pulls the relatively heavy unit away from the turning axis and by that induces a roll of the entire kite towards the axis. The tilted lift vector balances a part of the centrifugal force of the kite – the other balancing contribution is the aerodynamic side force generated by the aeroelastic twisting of the wing as a result of the steering actuation [4]. The effect of the induced roll on the overall performance of the kite was found to be negligible, as only 1 to 2% of the lift force is used for this compensation. The aerodynamic properties of the wing were computed from the experimental data with a three-plate aerodynamic model [7] and Oehler's model [5] and compared to a CFD analysis of the design shape of the wing [8]. This comparison is shown in Figure 2 (right). The study provides interesting insights into the flight behavior of LEI kites.

References:
[1] R. Schmehl, O. Tulloch (eds.): The International Airborne Wind Energy Conference 2019: Book of Abstracts. University of Strathclyde & Delft University of Technology, 164 pages, 15-16 October 2019. doi:10/dcjm
[2] Kitepower: https://kitepower.nl (Accessed 17 January 2021)
[3] Skysails: https://skysails.info (Accessed 17 January 2021)
[4] J. Breukels: A methodology for kite design. PhD thesis, Delft University of Technology, 2011. http://resolver.tudelft.nl/uuid:cdece38a-1f13-47cc-b277-ed64fdda7cdf
[5] J. Oehler, R. Schmehl: Aerodynamic characterization of a soft kite by in situ flow measurement. Wind Energy Science, Vol. 4, pp. 1-21, 2019. doi:10.5194/wes-4-1-2019
[6] C. Vermillion, M. Cobb, L. Fagiano, R. Leuthold, M. Diehl, R. S. Smith, T. A. Wood, S. Rapp, R. Schmehl, D. Olinger, M. Demetriou: Electricity in the Air: Insights From Two Decades of Advanced Control Research and Experimental Flight Testing of Airborne Wind Energy Systems. Annual Reviews in Control, accepted, 2021.
[7] U. Fechner, R. van der Vlugt, E. Schreuder, R. Schmehl: Dynamic Model of a Pumping Kite Power System. Renewable Energy, Vol. 83, pp. 705-716, 2015. doi:10.1016/j.renene.2015.04.028
[8] G. Lebesque. Steady-state RANS simulation of a leading edge inflatable wing with chordwise struts. MSc thesis, Delft University of Technology, 2020. http://resolver.tudelft.nl/uuid:f0bc8a1e-088d-49c5-9b77-ebf9e31cf58b
[9] A. Roullier: Experimental analysis of a kite system's dynamics. MSc thesis, École polytechnique fédérale de Lausanne, 2020.

Enhanced parameterisation of the pumping cycle flight path in the quasi-steady model

Mark Schelbergen, Mihkel Talmar, and Roland Schmehl
Delft University of Technology

Keywords: Airborne Wind Energy | Performance Modelling | Optimal Control

Motivated by the vivid development of technology demonstrators, there is a high demand for performance models to assess the power output of airborne wind energy (AWE) systems and their potential contribution to the energy transition. We classify performance models as computationally cheap models that include the flight mechanics, but do not touch upon the control system, and are primarily used for high-level purposes, such as power output calculations. We distinguish between two types of performance models: quasi-steady and dynamic models. In contrast to dynamic models, quasi-steady models (QSMs) [1] do not yield the flight path as output, but take it as input and move the kite along this path. These paths are usually generated using a flight path parameterisation.
Dynamic models [2] take control sequences as input, e.g., the time series of the kite's control surface deflections. Both models have their strengths and weaknesses. QSMs are simple and robust making them relatively easy to use in power optimizations to find the optimal flight path parameters.
However, they provide little information on the ability of the kite to fly the corresponding flight paths. The flight paths that result from dynamic simulations do not need to conform to a parameterisation and thus enable a higher degree of freedom of the kite's motion. Also, they are well suited to assess the feasibility of flight paths. On the other hand, applying a dynamic model in an optimization requires more complex optimal control techniques. Solving these optimization problems is more challenging. For instance, finding a suitable initial guess can be problematic.

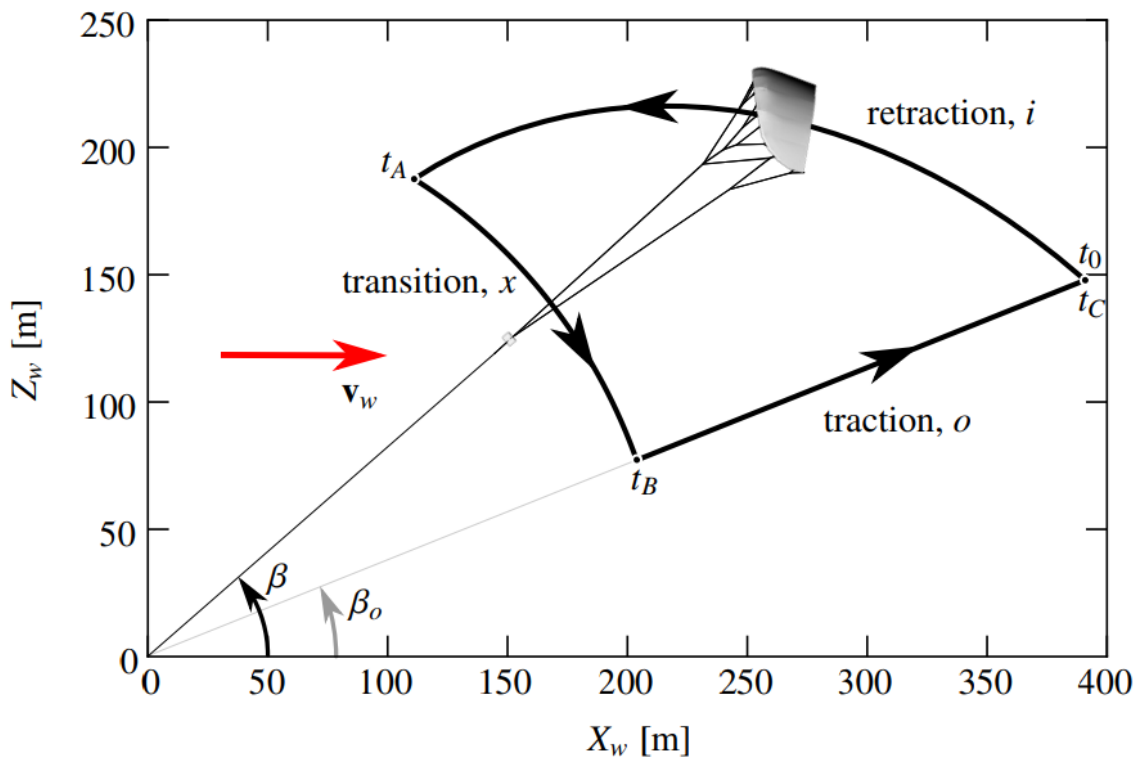

Figure 1: Abstract flight path parameterisation of a pumping cycle [1]

This study uses both modelling approaches next to each other, combining the best of both. We present an enhanced pumping cycle flight path parameterisation for a flexible kite in the QSM. Using flight data is a

sensible approach for deriving a realistic parameterisation. However, the availability of flight data is limited and covers only a small range of wind conditions. An alternative approach is used to determine flight paths for wind conditions other than those occurring during the flight tests.
As done previously in [3], power output optimizations are used to find the optimal flight path parameters for a large spectrum of wind conditions. The latter study uses an abstract flight path parameterisation. Here, we aim for a more realistic parameterisation. Once validated using the flight data, dynamic models are used to assess the feasibility of the realistic flight paths that follow from the optimizations. The findings are then used to enhance the parameterisation iteratively. Moreover, the dynamic models are used in an optimal control problem to find optimal flight paths of each phase of the pumping cycle without the restriction of a flight path parameterisation and thereby allowing for finding even higher power outputs. Also these findings are used as feedback for improving the flight path parameterisation.

References:
R. van der Vlugt, A. Bley, M. Noom, R. Schmehl: "Quasi-Steady Model of a Pumping Kite Power System". Renewable Energy, Vol. 131, pp. 83-99, 2019. doi: 10.1016/j.renene.2018.07.023
Malz, E., Koenemann, J., Sieberling, S., and Gros, S.: A reference model for airborne wind energy systems for optimization and control, Renewable Energy, Vol. 140, pp. 1004–1011, 2019. doi: 10.1016/j.renene.2019.03.111
M. Schelbergen, P. C. Kalverla, R. Schmehl, S. J. Watson: "Clustering wind profile shapes to estimate airborne wind energy production". Wind Energy Science, Vol. 5, No. 3, pp. 1097-1120, 2020. doi: 10.5194/wes-5-1097-2020

Flight stability of rigid wing Airborne Wind Energy Systems

Filippo Trevisi, and Alessandro Croce
Politecnico di Milano

Keywords: Flight stability | Airborne Wind Energy | Linearized equations of motion

Airborne Wind Energy Systems (AWESs) are tethered flying devices, which harvest power from the wind. To become a viable alternative to conventional wind turbines, AWESs flying crosswind need to prove reliable operations for long periods. Thus, all the design sub-problems should to be solved aiming at a robust system with respect to external disturbances and failures. Keeping this in mind, this presentation focuses on a methodology to approach the flight mechanics of rigid wing AWESs.
The flight mechanics problem of AWESs is fundamentally different from the one of conventional aircrafts for mainly three reasons: the presence of the wind, needed for the power generation, the presence of the tether, which transfers the thrust force to the ground, and the AWES continuous flight maneuvers.
It is therefore clear that conventional design techniques assuming straight and level flight can hardly be used for AWESs. Makani power, before the shutdown, started investigating the possibility of designing the flight path and the AWES aerodynamic derivatives to achieve passive stability [1,2].

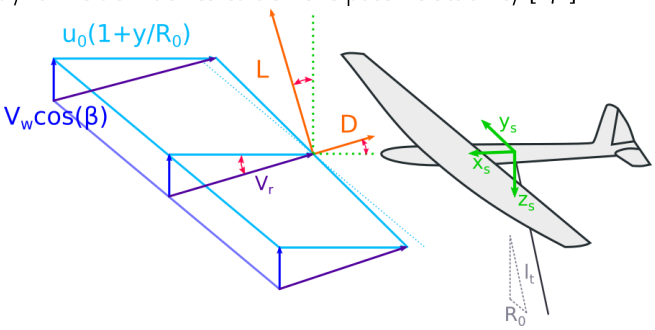

Figure 1: Relative wind velocity and aerodynamic forces

Stable AWESs would maintain the flight path with the least amount of control inputs. To achieve stability, the flight path should be properly chosen: a circular path makes the problem axial-symmetric and it exists one turning radius, for a given system with considerable mass, which ensures maximum thrust force on the tether [3]. This flight path is selected for this investigation (Figure 1). The AWES aerodynamic design should then help, as much as possible, the control system to stay in the chosen path.
In this presentation, an analytical modelling approach to study flight stability is shown. The 6 d.o.f equations of motion are linearized about the steady state motion of the AWES in the circular path.

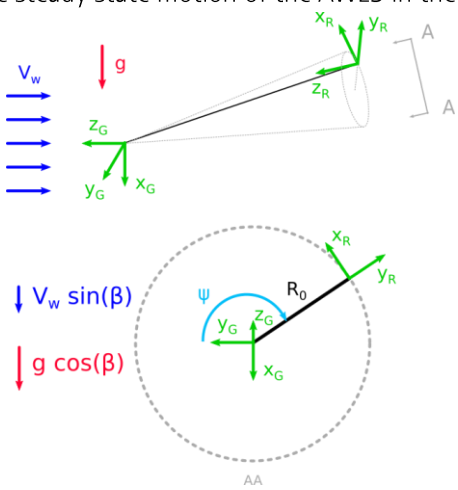

Figure 2: Reference systems and flight path

The steady state motion is computed by considering all the fluctuating terms as disturbances. In this analysis, the inertial velocity is varying linearly along the main wing, as shown in Figure 2, making aerodynamic loads to vary consequently. The derivatives of external forces and moments are finally taken, to study the dynamic response of the linear system.

This linear model allows for a simplified investigation of the influence of a) tether attachment position b) main wing geometry (position, shape, sweep, dihedral) c) main wing aerodynamics d) control surfaces geometry (position, shape) e) control surfaces aerodynamics f) steady flaps g) tether elasticity and h) gravitational force on the flight stability. First, no power generation will be considered, to study the free flight of rigid wing AWESs. Later, the feature of the two generation types (tether reel-out velocity and on-board wind turbines) will be included in the analysis, to study their influence on the flight stability.

This model, still under development, could give guidelines for the aerodynamic design of rigid wing AWESs, be coupled with design and optimization tools and used for simplified control laws derivation.

References:

[1] Geo Homsy. (2020). Oktoberkite and the MX2. in Echeverri P., Fricke T., Homsy G., Tucker N. (eds.) The Energy Kite Part I. pp. 7-89

[2] Jerome Sicard, Geo Homsy, Michael Abraham (2020) Kite Stability in Crosswind Flight. in Echeverri P., Fricke T., Homsy G., Tucker N. (eds.) The Energy Kite Part II. pp. 223-232

[3] Filippo Trevisi, Mac Gaunaa and Michael Mcwilliam (2020) The Influence of Tether Sag on Airborne Wind Energy Generation. Journal of Physics: Conference Series, Volume 1618, 032006. Available at: doi:10.1088/17426596/1618/3/032006

Mini-Symposium: Airborne Wind Energy System Modelling, Control and Optimisation (IV)

Computational Fluid Dynamic Analysis and Optimisation of a Multi-Element Airfoil

Gianluca De Fezza*, and Sarah Barber
OST - Eastern Switzerland University of Applied Sciences
*Presenting author

Keywords: Airborne Wind Energy Systems | Airfoils | CFD | Fluid-Structure Interaction | Optimisation

Airborne wind energy systems have the potential to play an important role in the today's energy transition (Cherubini, Papini, Vertechy, & Fontana, 2015). The Swiss start-up Skypull SA is an ambitious developer of such airborne concepts (Skypull's technology, 2018). Its drone has a double wing design to maximise lift with reduced wingspan. Each wing is made of a multi-element airfoil as shown in Fig. 1(a). In this work, the aerodynamic performance of this multi-element airfoil is analysed using steady-state 2D simulations using the Computational Fluid Dynamics (CFD) code OpenFOAM (OpenFOAM, 2020). Then the geometry is optimised to maximise the Loyd's Power Ratio (LPR), CL3/CD2 (CL = lift coefficient, CD = drag coefficient) (Loyd, 1980).

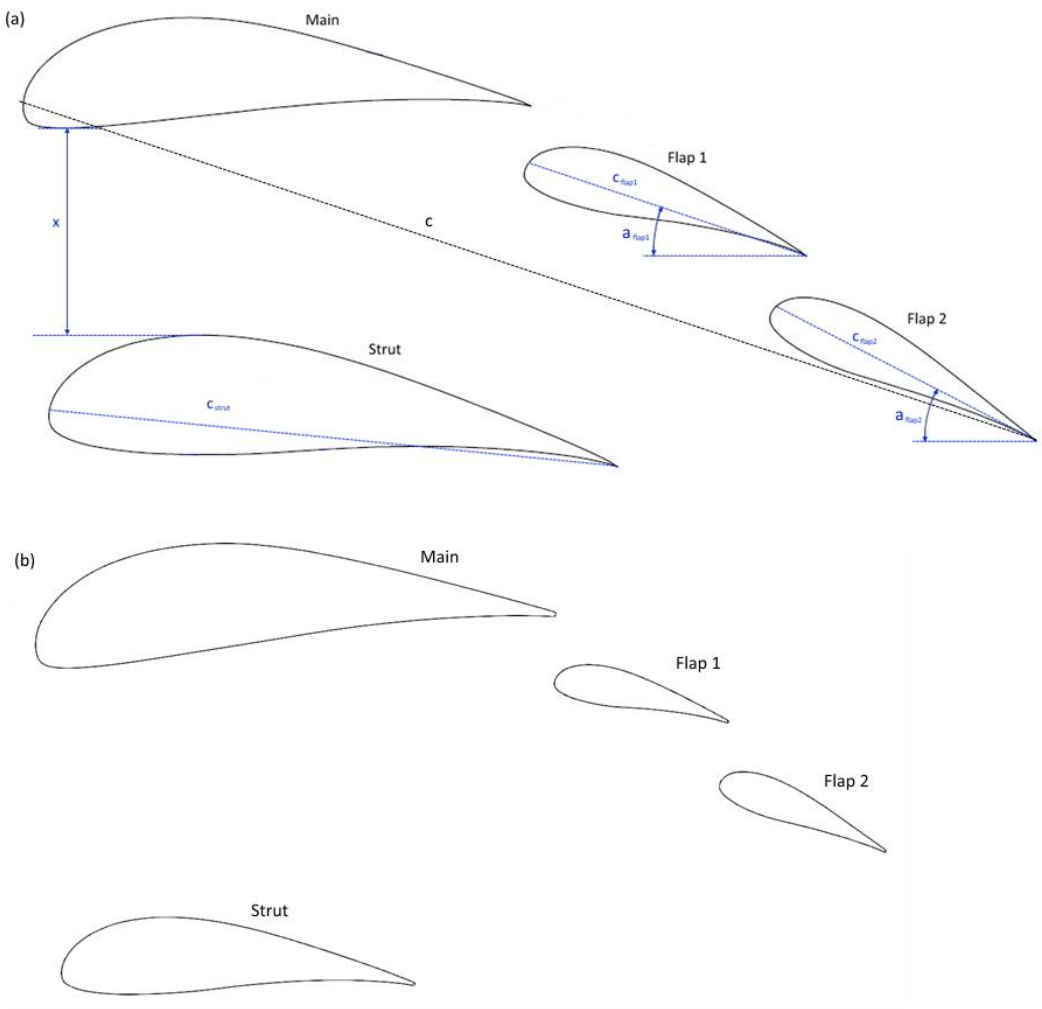

Figure 1: (a) The original multi-element airfoil with geometric parameters; (b) The optimised multi-element airfoil.

Following a grid dependency study, a hexahedral grid consisting of 50'000 cells is chosen, which gives a y-plus value of 30 with the nutUSpalding wall function. A range of turbulence models are tested for a Reynolds number of 1.5e6 and angles of attack (AoA) ranging from 0° to 30°. The Spalart-Allmaras model (Spalart–allmaras turbulence model, 2019) is chosen because there are no significant differences in the results between different turbulence models and the one-equation is comparatively more efficient. The resulting LPR vs. AoA is shown in Fig. 2(a). The coefficients are calculated using the chord length c marked on Fig. 1(a). The optimal AoA to maximise LPR is 17°.

Having found the ideal AoA, a geometric optimisation is carried out. For this, the following geometric parameters are altered as marked on Fig. 1(a): front and rear flap chord length cflap1 and cflap2 (from 60%-140% of original size), strut chord length cstrut (20%-140%), angle of flaps aflap1 and aflap2 (±10°), vertical distance x between main airfoil and strut (65%-265%). Changes in chord length are always accompanied by equal changes in airfoil thickness in order to preserve the airfoil shape. At the same time, the distance between the leading and trailing edges of neighbouring airfoils are preserved. The geometric optimisation limits are provided by Skypull based on structural and manufacturing constraints.

The results show that the flap scaling and angles do not have a great impact on the LPR: changes of ±40% in flaps chord length and ±10° in flaps angle only affect LPR by ±5% and ±13.7%, respectively (Fig.2(b)). However, these two plots indicate that the behaviour of LPR is not entirely linear, and local maxima do exist.

Increasing x increases LPR by 7.5%. The largest improvement is found by reducing cstrut: an 80% reduction brings an improvement in LPR of 39.1%. Altering the chord length of the flaps (-40%) and the strut (-60%) at the same time results in the largest improvement in LPR of 43.4%. This represents the new, optimised geometry shown in Fig. 1(b). The relative effects of the geometry changes on the LPR are summarised in Fig. 2(c).

Further work includes creating an automated optimisation strategy allowing the altering of all parameters at the same time, in order to ensure that no local maxima have been missed, as well as integrating the results into Skypull's mechanical system model.

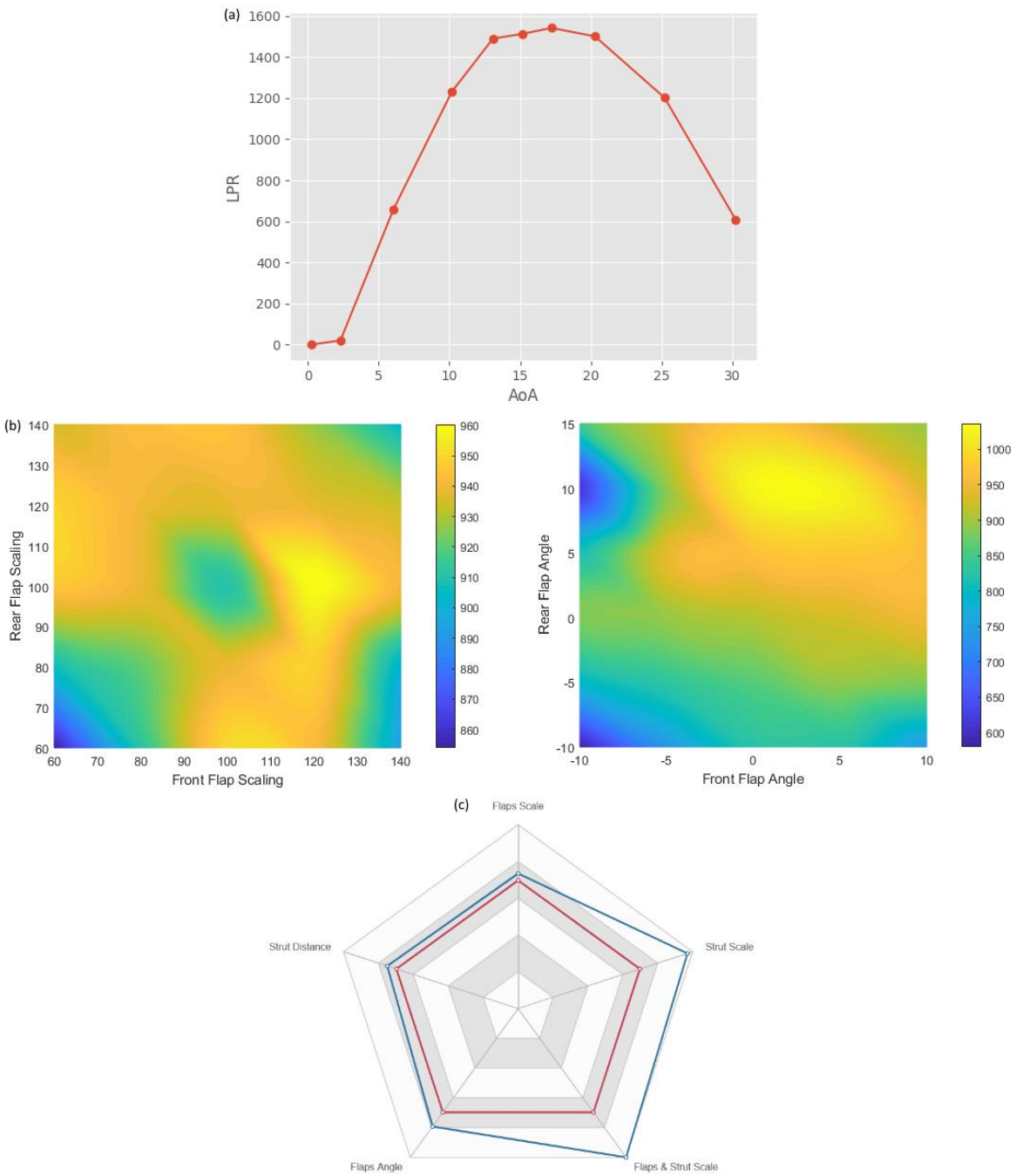

Figure 2: Geometry optimisation results: (a) LPR vs AoA; (b) 3D map of LPR by plotting front flap scale vs rear flap scale and front flap angle and rear flap angle; (c) Relative effect of geometry changes on LPR.

References:
Cherubini, A., Papini, A., Vertechy, R., & Fontana, M. (2015). Airborne wind energy systems: A review of the technologies. Renewable and Sustainable Energy Reviews, 51, 1461-1476.
Loyd, M. L. (1980). Crosswind kite power (for large-scale wind power production). Journal of energy, pp. 106-111.
OpenFOAM. (2020). Available at: https://openfoam.org/ [Accessed 15.12.2020]
Skypull's technology. (2018). Available at: https://www.skypull.technology/tech [Accessed 15.12.2020]
Spalart–allmaras turbulence model. (2019). Available at: https://en.wikipedia.org/wiki/Spalart–Allmaras_turbulence_model [Accessed 15.12.2020]

Three-Dimensional Unsteady Aerodynamic Analysis of a Rigid-Framed Delta Kite applied to AWES

Iván Castro Fernández[1,*], Ricardo Borobia Moreno[2], Rauno Cavallaro[1], and Gonzalo Sánchez Arriaga[1]
[1]University Carlos III de Madrid
[2]National Institute of Aerospace Technology, Spain
[*]Presenting author

Keywords: Delta Kite Aerodynamics | Flight Testing | Dynamic Simulation | Unsteadiness | Dynamic Stall

Reliable aerodynamic models have become essential for the development of AWE Systems because their characterization and optimization are key to increase the delivered power. The topic is currently an active field of research and well-known aerodynamic numerical tools have been recently adapted to study AWES (Candade, Ranneberg and Schmehl, 2020, p. 20; Fasel et al, 2019, p. 13). At preliminary design stages, fast and medium-fidelity models like Vortex Lattice Methods (VLM) are more convenient than high-fidelity and computationally expensive methods such as Reynolds-Averaged Navier-Stokes (RANS) and Direct Numerical Simulations (DNS). The present work is focused on the aerodynamic analysis of a Rigid-Framed Delta (RFD) HQ Fazer XXL kite, a two-line traction kite of 3.6 m of span and 1.86 m2 of surface. The study has been performed with an in-house Unsteady Panel Method UPM (Cavallaro, Nardini and Demasi, 2015, p. 27), which captures both threedimensional and unsteady effects. These two properties are important due to the dynamic character of the energy production maneuvers, typically made of figures-of-eight combined with tether reel-in and reel-out, and the aspect ratio of the kite (AR of 7). Within this research, the aerodynamic surface of the kite is modeled with thin surfaces, whereas the wake is modeled as free-force and experiences roll-up. Wake modeling is important to account for non-stationary effects since it contains the time history of circulation.

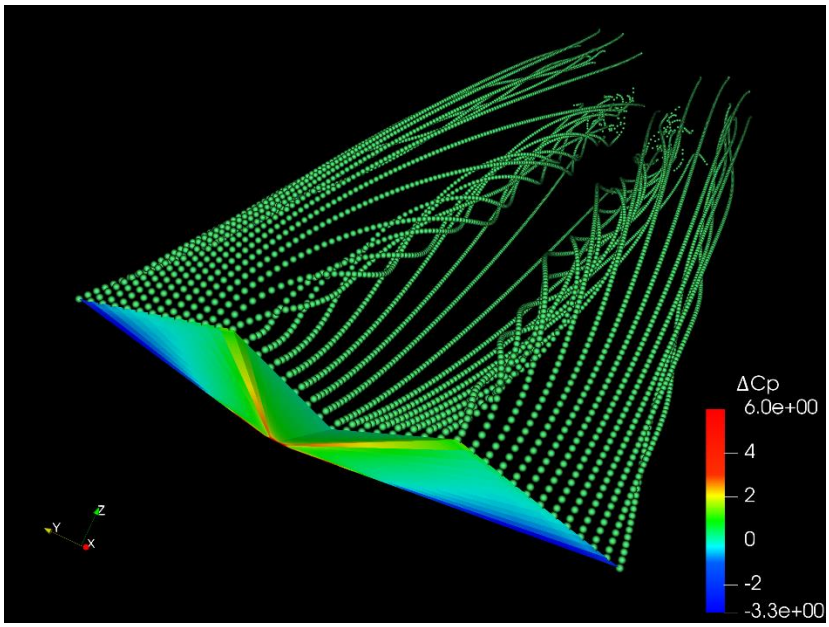

Figure 1: RFD kite aerodynamic visualization

The UPM code has been used to carry out two types of analyses. In the first place, we considered the experimental data recently obtained in a flight-testing campaign with the Fazer XXL, where the full state vector of the kite, including kinematic, dynamic, and aerodynamic coefficients, was obtained during the full flight by combining real flight data with an Extended Kalman Filter and Estimation Before Modeling techniques (Borobia-Moreno et al, 2021, p. 13). The experimental kinematic and environmental conditions

recorded during the flight are used as inputs to UPM that is then used to obtain theoretical aerodynamic coefficients (force and torque about the center of mass of the kite).

Although UPM is based on potential theory, good agreement between the experimental and theoretical aerodynamic coefficients is found in a wide range of angles of attack and side-slip angles.

The second part of the analysis is carried out with KiteAcrobat (Sánchez-Arriaga, García-Villalba and Schmehl, 2017, p. 14), which is the two-line kite simulation package of the open-source Lagrangian Kite Simulator LAKSA (Sánchez-Arriaga et al, 2018, p. 11). The simulator has been fed with the control law implemented in the figure-of-eight maneuvers of the flight-testing campaign of (Borobia-Moreno et al, 2021, p. 13) and the aerodynamic model provided by UPM. The outputs of the simulator, including the kite trajectory and tether tensions, are compared with the experimental data. The results of the two analyses together with the advantages and limitations of unsteady and threedimensional aerodynamic models based on potential theory are discussed. Other models and future works to bridge the gap between AWE experiments and simulations, like viscous-inviscid and semiempirical dynamic stall models, are proposed.

References:

Borobia-Moreno, R., Ramiro-Rebollo, D., Schmehl, R. and Sánchez-Arriaga, G. (2021). Identification of kite aerodynamic characteristics using the estimation before modeling technique. Wind Energy.

Candade, A.A., Ranneberg, M. and Schmehl, R. (2020). Structural analysis and optimization of a tethered swept wing for airborne wind energy generation. Wind Energy.

Cavallaro, R., Nardini, M., Demasi, L. and Santarpia, E. (2015). Amphibious PrandtlPlane: Preliminary Design Aspects Including Propellers Integration and Ground Effect. 56th AIAA/ASCE/AHS/ASC Structures, Structural Dynamics, and Materials Conference.

Fasel, U., Tiso, P., Keidel, D., Molinari, G. and Ermanni, P. (2019). Reduced-Order Dynamic Model of a Morphing Airborne Wind Energy Aircraft. AIAA Journal, 57(8), pp.3586–3598.

Sánchez-Arriaga, G., García-Villalba, M. and Schmehl, R. (2017). Modeling and dynamics of a two-line kite. Applied Mathematical Modelling, [online] 47, pp.473–486.

Sánchez-Arriaga, G., Pastor-Rodríguez, A., Borobia-Moreno, R. and Schmehl, R. (2018). A constraint-free flight simulator package for airborne wind energy systems. Journal of Physics: Conference Series, 1037, p.062018.

Steady-state RANS simulation of a leading edge inflatable wing with chordwise struts

Axelle Viré*, Geert Lebesque, Mikko Folkersma, and Roland Schmehl
Delft University of Technology
*Presenting author

Keywords: airborne wind energy | leading-edge inflatable wing | steady-state RANS | struts | flow with sideslip

The size and height of conventional wind turbines keeps increasing, to harness increasingly larger amounts of energy at higher efficiencies. This trend however brings structural challenges to the design of future wind turbines. One of the alternatives to access wind at higher altitudes is to use flying devices that are tethered to the ground. There are different concepts and modes of operation of such airborne wind energy (AWE) devices [1,4]. A prominent example is to fly a wing crosswind and tether it to a drum-generator module on the ground. The pulling force of the wing reels the tether off the drumand the connected generator converts the torque and rotational motion into electrical power. Although these AWE devices present several advantages compared to conventional wind turbines, they still face a number of challenges for large-scale commercial deployment. This work addresses persisting lack of aerodynamic reference data for AWE systems based on inflatable membrane wings.

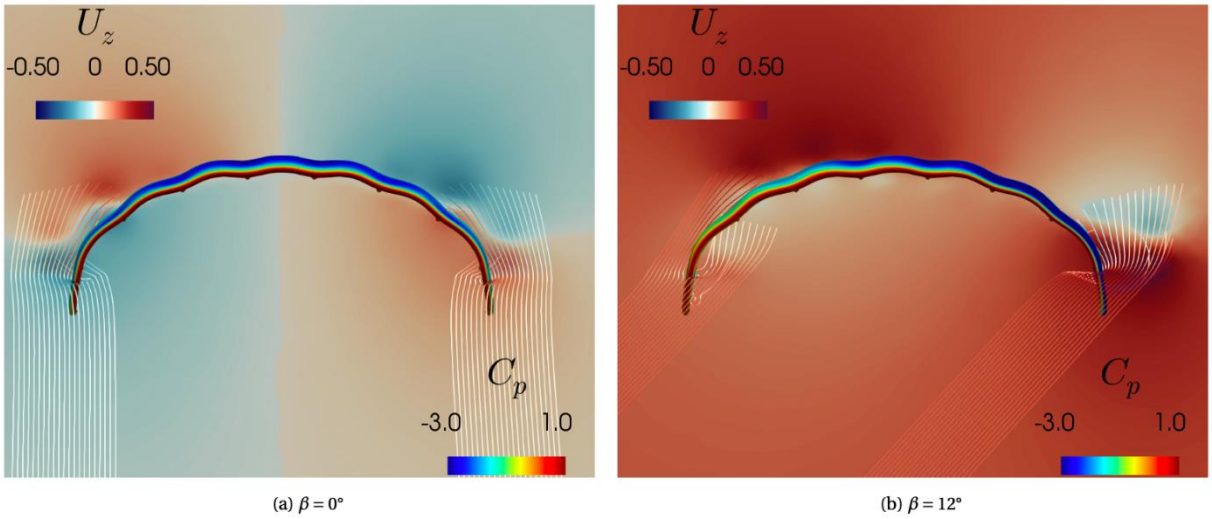

Fig. 1 Spanwise component of the velocity field, as well as the pressure coefficient on the wing, without (left) and with (right) sideslip angle. Taken from [3].

The investigated wing is a leading edge inflatable (LEI) tube kite, which is characterised by a leading edge tube connected to a thin canopy and supported by chordwise strut tubes. A wide range of flow conditions, with varying Reynolds number Re, angle of attack α and sideslip angle β is considered.
Although in practice the wing will deform in flight, here it is assumed to have a constant shape. This is because the pure aerodynamics of LEI wings with geometrical details has not yet been studied and is important to further improve the design of these wings. The effect of wing deformations on its aerodynamics is outside the scope of this work. Here, we build on recent studies that performed Reynolds-averaged Navier-Stokes (RANS) simulations with a k-ω SST turbulence model and a γ-Reθ transition model, first for a two-dimensional LEI airfoil [2], and then for a complete LEI wing without struts [5].
Figure 1 shows the spanwise component of the velocity field, as well as the pressure coefficient on the wing, without (left) and with (right) sideslip angle β. The inflow with sideslip angle leads to a pronounced asymmetry of the flow field. The lift coefficient of the wing (not shown here) decreases whilst the drag coefficient increases with the sideslip angle. Also, as expected, the lift coefficient increases and the drag coefficient

decreases for increasing Reynolds number.

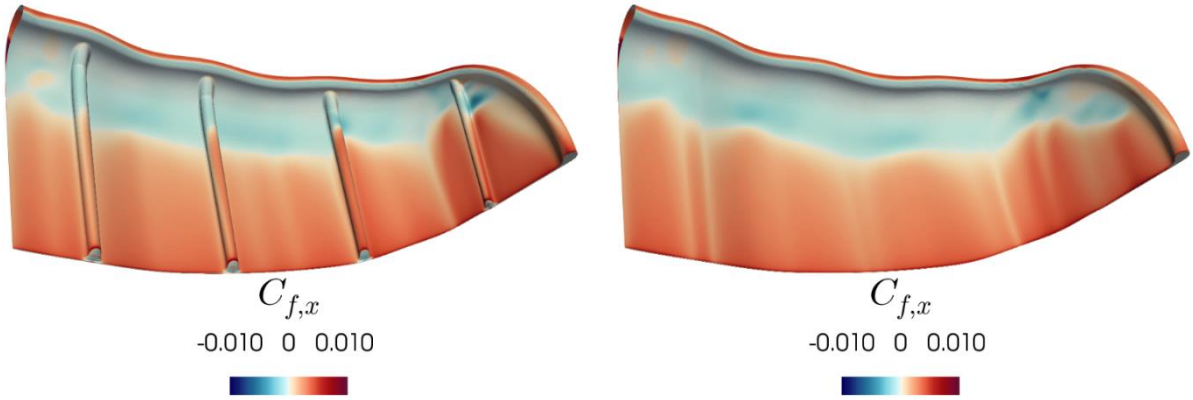

*Fig. 2 Streamwise component of the friction coefficient on the pressure side with (left) and without (right) struts at Re=3 x 106, **α**=12° and **β**=0°. Taken from [3].*

The study also shows that the effect of the struts on the force coefficients for both zero and non-zero sideslip angles is minimal over the whole ranges of considered Reynolds numbers and angles of attack. Figure 2 shows the changes in friction coefficient on the pressure side of the wing with (left) and without (right) struts.
The study provides interesting insights into the aerodynamics of LEI wings, and in particular the role of geometrical features on the overall aerodynamic performances.

References:
[1] A. Cherubini, A. Papini, R. Vertechy, and M. Fontana. Airborne wind energy systems: A review of the technologies. Renewable and Sustainable Energy Reviews, 51:1461–1476, 2015
[2] M. Folkersma, R. Schmehl, and A. Viré. Boundary layer transition modeling on leading edge inflatable kite airfoils. Wind Energy, pages 1–14, 2019
[3] G. Lebesque. Steady-state RANS simulation of a leading edge inflatable wing with chordwise struts. MSc thesis, Delft University of Technology (2020)
[4] R. Schmehl, editor. Airborne wind energy: advances in technology development and research. Springer, 2018
[5] A. Viré, P. Demkowicz, M. Folkersma, A. Roullier, R. Schmehl. Reynolds-averaged Navier-Stokes simulations for flow past a leading edge inflatable wing for airborne wind energy applications. Journal of Physics: Conference Series 1618:032007 (2020)

Computational simulation of the aeroelastic behavior of a ram-air kite for airborne wind energy applications

Paul Thedens[1,2,*], Mikko Folkersma[2], Axelle Viré[2], and Roland Schmehl[2]
[1]SkySails Power GmbH
[2]Delft University of Technology
[*]Presenting author

Keywords: airborne wind energy | ram-air kite | fluid-structure-interaction | aeroelasticity | tensile membrane structure

Ram-air kites are cellular membrane structures that are inflated by the flight-induced ram-air pressure through openings on the leading edge [1,2]. The distributed aerodynamic load on the membrane skin of the wing is collected by membrane ribs, from where it is transmitted to the tether via a bridle line system [3]. Ram-air wings are characterized by a strong coupling of flight dynamics, aerodynamics and structural dynamics, with the result that the shape of the wing during flight can deviate substantially from its design shape [4]. Measuring the deformation of large wings (25-100 m2 or larger) is challenging, because full-scale wind tunnel tests are expensive or infeasible and downscaling is not possible because ram-air pressure and Reynolds number do not scale similarly.

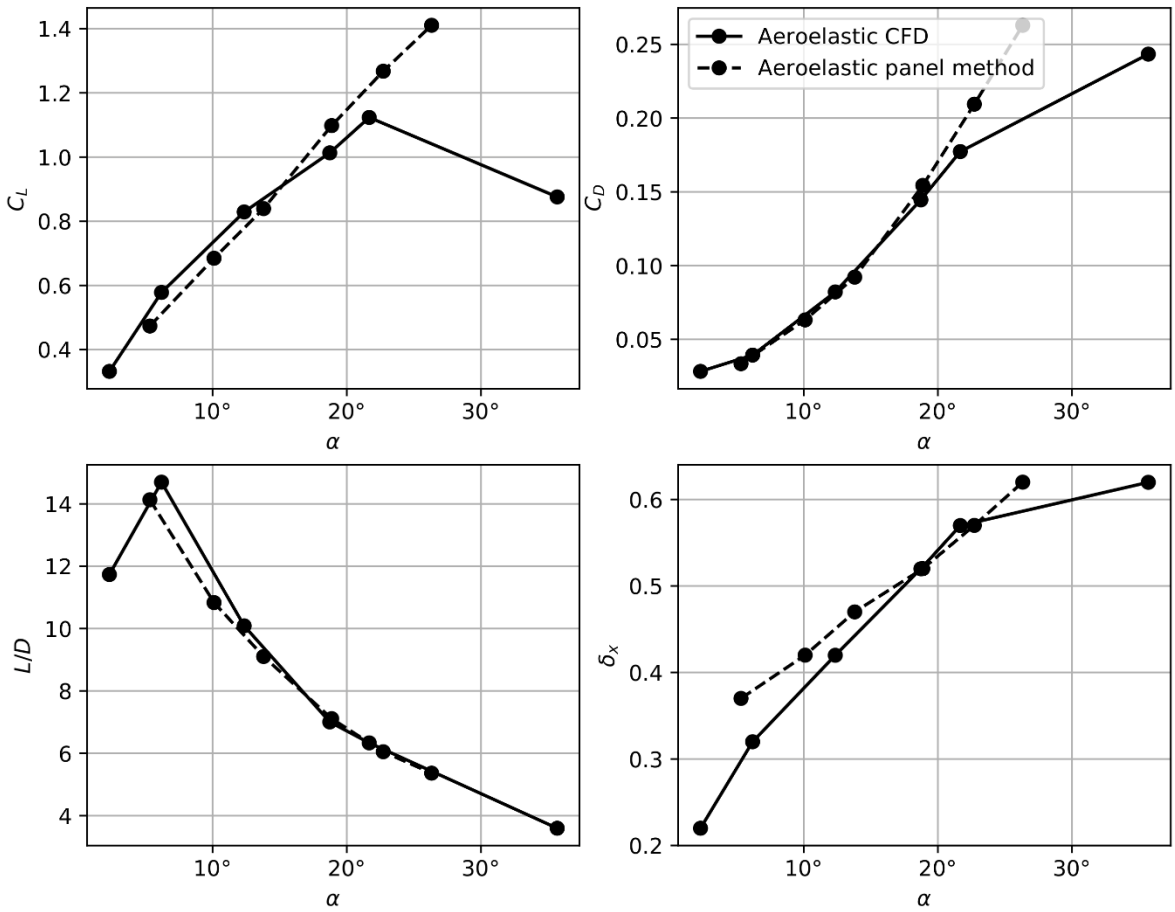

Figure 1: Streamlines along the suction side of the kite and vorticity component ωx on a plane normal to the streamwise direction at x = 1.5c and α = 10°. Bridle lines not visualized for clarity of illustration. Computed CFD-FSI result taken from [8].

We use two different numerical approaches to determine the static shape and aerodynamics of a ram-air kite in a specific flight condition. Both approaches use the open source finite element (FE) solver mem4py [5] and the coupling library preCICE [6]. The FE model of the bridled wing structure includes a wrinkling model and

uses dynamic relaxation to find the deformed static shape. The exterior flow field and aerodynamic load distribution is either determined with the vortex panel solver Apame [7] or with a Reynolds-averaged Navier-Stokes (RANS) method using OpenFOAM, employing an SST turbulence model [8]. To account for the two-way coupling, the structural and aerodynamic problems are alternatingly solved within an iterative scheme. All components of the framework, including the meshing tools and the coupling library, are available in open source. The simulation procedure comprises four steps: (1) generating the FE mesh of the design geometry, (2) pre-inflation, applying a uniform pressure on the inside, (3) generating the panel mesh on the exterior surface (Apame) or the finite-volume mesh around the wing surface (OpenFOAM), and (4) activating the exterior flow and two-way coupling iterations.

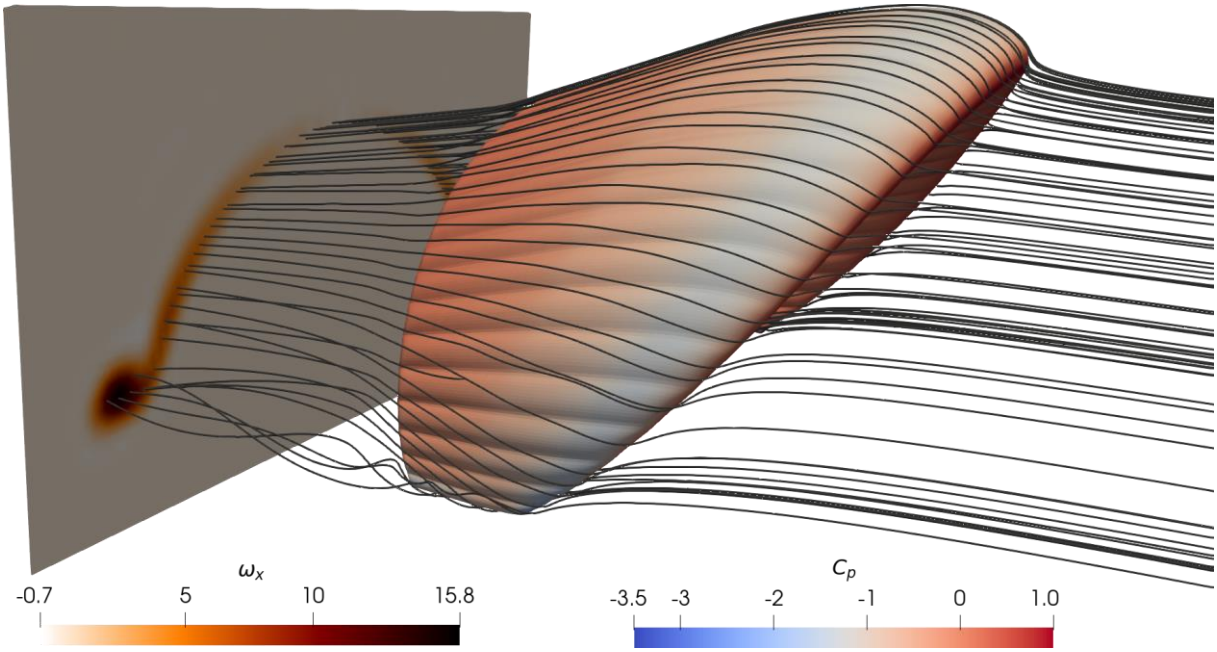

Figure 2: Computed aerodynamic lift coefficient CL, drag coefficient CD, lift-to-drag ratio L/D and trim δx as functions of the angle of attach of the wing.

The test case is a ram-air kite with a total wing surface area of 160 m2 and a projected span of 15.2 m, exposed to a relative wind speed of 30 m/s which is representative for crosswind flight operation.
The inflow is in the symmetry plane of the kite and the kite is not steered, such that the resulting shape deformation is symmetric. The lengths of the bridle lines are kept constant for each simulation, however, to vary the static angle of attack α of the wing, the trim δx of the unloaded kite is varied along the simulations. This geometric parameter is defined as the projected distance of the bridle point from the leading edge. The position of this point, where all bridle lines connect to the tether, affects the lengths of all bridle lines. The flow field and shape of the wing computed with the coupled FE-CFD solver is illustrated in Figure 1. Clearly visible is the wing tip vortex and the vortex layer that is shed from the trailing edge of the wing. Figure 2 compares the aerodynamic geometric properties computed with both approaches, indicating a good match except for high angles of attack, where the panel method cannot resolve flow separation.
We recommend the presented test case and simulations as a reference framework for ram-air kite simulation tools.

References:
[1] S. Dunker. Ram-air wing design considerations for airborne wind energy. In U. Ahrens, M. Diehl, R. Schmehl, editors, Airborne Wind Energy, Green Energy and Technology, chapter 31, pages 517-546, Springer, Berlin Heidelberg, 2013. https://doi.org/10.1007/978-3-642-39965-7_31
[2] X. Paulig, M. Bungart, and B. Specht. Conceptual design of textile kites considering overall system performance. In U. Ahrens, M. Diehl, and R. Schmehl, editors, Airborne Wind Energy, Green Energy and Technology, chapter 32, pages 547-562. Springer, Berlin Heidelberg, 2013. https://doi.org/10.1007/978-3-642-39965-7_32
[3] P. Thedens, G. de Oliveira, R. Schmehl: Ram-air kite airfoil and reinforcements optimization for airborne wind energy applications. Wind Energy, Vol. 22, No. 5, pp. 653-665, 2019. https://doi.org/10.1002/we.2313

[4] A. de Wachter: Deformation and Aerodynamic Performance of a Ram-Air Wing. MSc Thesis, Delft University of Technology, 2008. http://resolver.tudelft.nl/uuid:786e3395-4590-4755-829f-51283a8df3d2
[5] P. Thedens: mem4py - A membrane finite element solver based on kinetic dynamic relaxation. https://github.com/pthedens/mem4py (Accessed 31 January 2020)
[6] H. Bungartz, F. Lindner, B. Gatzhammer, M. Mehl, K. Scheufele, A. Shukaev, and B. Uekermann. PreCICE - a fully parallel library for multi-physics surface coupling. Computers and Fluids, Vol. 141, pp. 250-258, 2016. https://doi.org/10.1016/j.compfluid.2016.04.003
[7] Filković, D.: Apame – Aircraft 3D Panel Method. https://www.3dpanelmethod.com (Accessed 31 January 2021)
[8] M. Folkersma, R. Schmehl, A. Viré: "Steady-state aeroelasticity of a ram-air wing for airborne wind energy applications". Journal of Physics Conference Series, Vol. 1618, pp. 032018, 2020. https://doi.org/10.1088/1742-6596/1618/3/032018

Mini-Symposium: Performance Metrics and Technology Assessment of Airborne Wind Energy Systems

Jochem Weber
NREL

Robert Thresher
NREL

Airborne wind energy systems are at various pre-commercial stages of technology development and a diversity of technology archetypes, operational principles and designs are under development. As for many resource intensive technology development challenges and especially where a multitude of solution concepts and technological implementations are possible it is critical to acquire a clear, holistic and solution-agnostic formulation of the problem statement in form of stakeholder and functional requirements for all operational modes and over the life-cycle of the system. In order to progress the technology development towards successful realization a multitude of relevant performance characteristics need to be monitored and improved to satisfy the requirements. These may vary from simple performance metrics, through more complex compound trade-offs to comprehensive technology assessment methods and tools which are supported by simulation tools, validation and testing at component, subsystems and systems levels as well as by guided expert judgement. This mini symposium will reflect on the state of the art of performance metrics and technology assessment of airborne wind energy systems, identify gaps and address further options to support successful, cost, time and risk effective technology development processes.

Realistic and effective Airborne Wind Energy Performance Assessment Criteria for successful Technology Development

Jochem Weber
National Renewable Energy Laboratory

Keywords: airborne | metric | technology assessment | key performance indicators

The assessments of airborne wind energy systems, especially at early and intermediate stages of development and across a variety of archetypes, designs and operational concepts is challenging and at the same time critical for directing the research and technology development towards success.
Similar to other technology domains such as ocean wave energy criteria may be grouped in evaluation areas, figure 1 (Hudges et al. 2021).

Figure 1: Evaluation Areas, (Hudges et al. 2021)

Technology assessment criteria are often referred and reduced to key performance indicators and/or metrics, whereby the idealized wish list of the characteristics of technology assessment criteria and systems thereof may include but is not limited to the following:
Criteria ideally should/be: objective, transparent, specific, measurable, meaningful, relevant, simple, easy to understand, easy to use, repeatable, quantitative, also carry qualitative information, capturing all cost and performance drivers, reflect all trade-offs, holistic, low time and cost effort in providing input for criteria determination, fast assessment and evaluation, existing or easy to develop assessment and measurement tools, low equipment requirements, low staff requirement, applicable at all development stages while consistent in criteria and statement and at different levels of content, detail and accuracy, and so on.
It is not possible to satisfy all of the above-mentioned properties for assessment criteria at the same time, as there are several contradictions and related trade-offs inherent in these characteristics. To be in a position to develop realistic techno-economic airborne wind energy performance assessment criteria that are applicable for effective use, supporting successful technology development, it is crucial to formulate all relevant

requirements for these assessment criteria. In the process of formulating these requirements it is helpful to consider and answer several fundamental and guiding questions not limited but including the following:
At what system level should criteria be applicable? Plant level as an investment product, farm with specific site conditions, generic farm, single system, balance of plant, device sub-systems, component level. Should criteria be agnostic? Across different airborne wind energy archetypes, and/or different archetype subsystems, components? Where is the connection between criteria, observables and measurables? Should the same criteria be determinable from the different measurables? Are criteria justified solely to ensure awareness? Known unknown versus Unknown unknown. Are criteria justified when they are difficult to quantify but important for the overall system performance? What level of accuracy of criteria is acceptable and realistic? Should systems of criteria be usable for sensitivity analysis? What level of consistency and similarity is desired across different applications/markets? Could the adaptation of the criteria be achieved with the same fundamental
criteria or combined with strongly differing weightings? Should there be required thresholds for individual criteria or combinations of these? What should the cost for the criteria determination and assessment be as a portion of the technology development cost? What should the time effort for the criteria determination and assessment be as a portion of the technology development time?
The above list contains only a selection of key questions to be addressed and answered for a development of airborne wind energy technology assessment criteria. This contribution will formulate and consider a set of relevant questions and give recommendations on the development of realistic and effective wave energy technology development criteria to further research and development success in analogy to (Weber et al. 2019).

References:
Weber, J., Costello, R., Nielsen, K., Roberts, J. (2019) Requirements for Realistic and Effective Wave Energy Technology Performance Assessment Criteria and Metrics. European Wave and Tidal Energy Conference, Naples, Italy
Hodges J., Henderson J., Ruedy L., Soede M., Weber J., Ruiz-Minguela P., Jeffrey H., Bannon E., Holland M., Maciver R., Hume D., Villate J-L, Ramsey T., (2021) An International Evaluation and Guidance Framework for Ocean Energy Technology, IEA-OES

From wind resource potential towards a public tool for predicting the power generation of airborne wind energy systems

Roland Schmehl[1], Mark Schelbergen[1], Lavinia Thimm[2], and Philip Bechtle[2,*]
[1]Delft University of Technology
[2]Universität Bonn
[*]Presenting author

Keywords: Resource Potential | Airborne Wind Energy | Power Harvesting Characteristics

The assessment of the power generation capacity of wind energy systems is important for all stakeholders: legislators, investors, wind park operators, and designers of wind turbines or future technology options. The optimal location of a wind park as well as the choice of future technology crucially depend on a realistic assessment of the amount and time profile of future energy generation in relation to the expected energy demands. Bechtle et al. [1] provided an open source tool to estimate the resource potential of airborne wind energy (AWE) in Europe, based on the comprehensive ERA5 re-analysis data [2] and accounting for the option to adapt the harvesting altitude of AWE systems to the vertical wind profile, while reaching significantly higher altitudes than conventional wind turbines.

In this presentation, an update of this resource analysis is presented. It is based on a finer spatial and temporal binning of the ERA5 data, and includes an update path towards a parametric representation of the power harvesting characteristics of different AWE technologies. To increase the computational speed, the processing of the ERA5 data is parallelized. Figure 1 shows the estimated wind power density for Central Europe for a variable harvesting height below a ceiling height of 500 m. The contour plots of the 5th, 32nd and 50th percentile characterize the statistics of the maximum instantaneous wind power density below a maximum altitude of 500 m. As expected, the highest wind power densities occur above the Atlantic Ocean, with a secondary peak offshore from Norway.

Wind power density generally decreases from North European coastal regions towards the interior of the continent. Figure 2 shows the relative increase of the wind power density distribution depicted in Figure 1 to the wind power density distribution at 100 m, which is considered the hub height of a typical wind turbine.

The new tool chain includes the option to compare generated power curves with publicly available power curves of reference wind turbines. The power harvesting characteristics are computed with an efficient quasi-steady model (QSM) that was originally developed and validated for pumping kite power systems [3,4,5]. A special emphasis is placed on the validation chain for the power characterization modeling, which covers the full path from the parametrization of the AWE system and its operation, over the QSM to reference simulations with a dynamic model. The dynamic model is validated with flight data of the tethered aircraft AP-2, that has been developed and tested by Ampyx Power B.V. [6,7]. A proposal for more detailed validations including comparisons with flight test data and the support of AWE system developers is presented for general discussion.

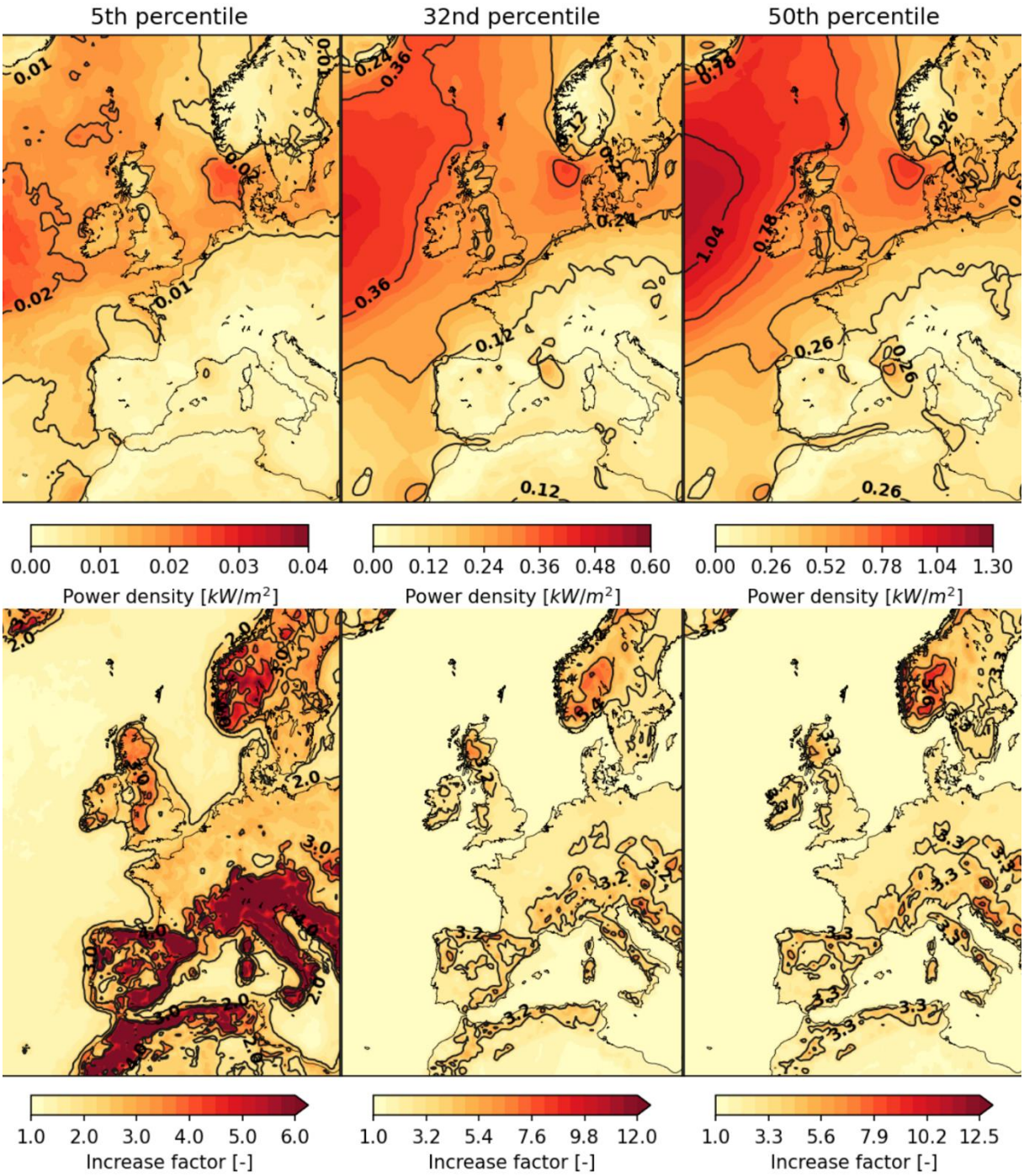

Figure 1: Top: Percentiles of the wind power density for an AWE System with a ceiling of 500m altitude above ground, with the ability to adapt the flight altitude to the wind profile. Bottom: Relative increase of the available power density over the wind condition at the wind turbine reference altitude of 100m. Especially for the 5% percentile - corresponding to the minimal wind speed available for at least 95% of the time - the increase exceeds a factor of 2 over the coastal waters and the land mass.

The developed toolchain, including wind resource model and performance model, is available in open source to easily assess the power generation potential of AWE systems at specific locations and regions in Central Europe.

References:
[1] P. Bechtle, M. Schelbergen, R. Schmehl, U. Zillmann, S.J. Watson: "Airborne wind energy resource analysis". Renewable Energy, Vol. 141, pp. 1103-1116, 2019. https://doi.org/10.1016/j.renene.2019.03.118
[2] Olauson, J.: ERA5: The new champion of wind power modelling? Renewable Energy, Vol. 126, pp. 322-331, 2018.
[3] Van der Vlugt, R., Bley, A., Noom, M., Schmehl, R.: Quasi-Steady Model of a Pumping Kite Power System. Renewable Energy, Vol. 131, pp. 83-99, 2019. https://doi.org/10.1016/j.renene.2018.07.023

[4] Schelbergen, M., Kalverla, P.C., Schmehl, R., Watson, S.J.: Clustering wind profile shapes to estimate airborne wind energy production. Wind Energy Science, Vol. 5, No. 3, pp. 1097-1120, 2020. https://doi.org/10.5194/wes-5-1097-2020
[5] Schelbergen, M., Schmehl, R.: Validation of the quasi-steady performance model for pumping airborne wind energy systems. Journal of Physics Conference Series, Vol. 1618, pp. 032003. 2020. https://doi.org/10.1088/17426596/1618/3/032003
[6] Ruiterkamp, R., Sieberling, S.: Description and Preliminary Test Results of a Six Degrees of Freedom Rigid Wing Pumping System. In: Ahrens U., Diehl M., Schmehl R. (eds) Airborne Wind Energy. Green Energy and Technology. Springer, Berlin, Heidelberg, 2013. https://doi.org/10.1007/978-3-642-39965-7_26
[7] Licitra, G.: Identification and Optimizationof an Airborne Wind EnergySystem. PhD Thesis, University of Freiburg, 2018. https://doi.org/10.6094/UNIFR/16226

awebox – Towards an extensible optimal control framework for airborne wind energy systems

Jochem De Schutter[1,*], Rachel Leuthold[1], Thilo Bronnenmeyer[2], Elena Malz[3], Sebastien Gros[4], and Moritz Diehl[1]
[1]University of Freiburg
[2]Kiteswarms GmbH
[3]Chalmers University of Technology
[4]Norwegian University of Science and Technology
[*]Presenting author

Keywords: airborne wind energy | optimal control | open-source software

Airborne wind energy (AWE) systems are typically characterized by highly dynamic flight behavior, nonlinear and unstable dynamics with multiple in- and outputs, as well as structural and flight envelope constraints. These properties make the offline computation of dynamically feasible, poweroptimal flight trajectories in combination with system design optimization an intricate endeavour.
Optimal control arises as an obvious candidate to tackle this task due to its inherent ability to handle precisely these types of systems. However, despite numerous successful applications in the past decade, as of today there does not exist a generic and open-source optimal control framework tailored to AWE, thereby hindering further dissemination of optimal control as a tool in AWE-related research and industry.
We present awebox (awebox, 2021), an open-source Python toolbox for modeling and optimal control of AWE systems. Among others, it provides an implementation of validated models tailored for optimal control (Malz, 2019), and it takes away from the user the burden of formulating and numerically solving common AWE optimal control problems (OCP). A distinctive feature of awebox is that it supports optimization of multi-drone systems next to the prevalent single-drone variant as well. The toolbox supports rigid-wing, lift- and drag-mode AWE systems and is capable of embedding user-provided 3D wind profiles. Building on the open-source optimization framework CasADi (Andersson, 2018), it can be a particularly useful component in AWE system toolchains for performance assessment, system design, controller synthesis, or in a wide area of academic research ranging from AWE modeling to optimization algorithms.

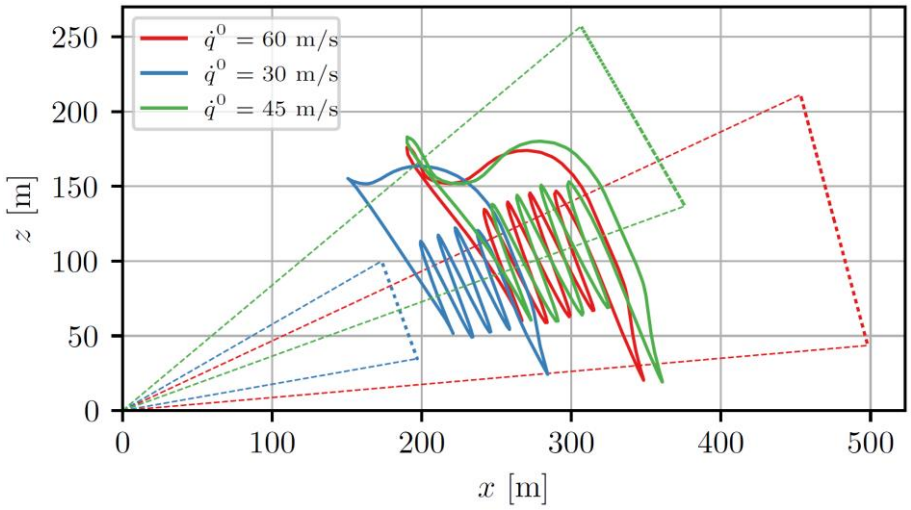

Figure 1: Side view of different OCP initial flight trajectory guesses (dashed) with differing tether lengths, elevation angles and flight speeds, and corresponding optimal power cycles (solid) for a single-drone lift-mode system.

In practice, it is often difficult to produce a dynamically feasible or close-to-optimal initial guess, which is generally required to find a numerical solution to the highly nonlinear and non-convex OCPs.
Also, the AWE models should be modularly extensible towards higher fidelity, without tightening the requirements on the user-provided initial guess. Therefore, the particular focus of the toolbox is robustness

with respect to initialization. To achieve this, awebox utilizes a modular homotopy-based initialization procedure. Here, the OCP initial guess is generated by a homotopy strategy which first solves a highly simplified version of the OCP based on the user-provided initial guess. Then, the OCP is repeatedly reformulated and solved, where the solution of each homotopy step provides the initial guess for the next. Each homotopy step gradually introduces model nonlinearities and couplings or changes the OCP objective. The final solution of the homotopy is then used as an initial guess for the fully dynamic power optimization problem. This strategy enables the tool to reliably compute optimal power cycles based on a wide range of (poor) initial guesses for the same OCP, as shown in Fig. 1.

In this presentation, we introduce the different AWE modeling modules and the available optimal control problem formulations. We explain the homotopy strategy and provide a high-level overview of the software package. We also discuss a tutorial example where we illustrate the efficacy of the homotopy strategy while optimizing a single-drone lift-mode system. In a second example, we showcase the tool's multi-drone capability by investigating the effect of adding drone-to-drone tethers on the power output fluctuation of a large-scale triple-drone system. This is relevant since power output variability increases drastically when upscaling AWE systems, due to the growing influence of gravity-induced asymmetry in lift power availability.

References:

awebox: Modeling and Optimal Control of Single- and Multi-kite Systems for Airborne Wind Energy (2021). https://github.com/awebox

Malz, E., Koenemann, J., Sieberling, S. and Gros, S. (2019). A Reference Model for Airborne Wind Energy Systems for Optimization and Control. Renewable Energy 140, pp. 1004-1011.

Andersson, J., Gillis, J., Horn, G., Rawlings J.B. and Diehl, M. (2018). CasADi: a Software Framework for Nonlinear Optimization and Optimal Control. Mathematical Programming Computation 11(1), pp. 1-36.

Performance model and design drivers for large-scale ground-generation airborne wind energy systems

Rishikesh Joshi[1], Michiel Kruijff[2], Vincent Bonnin[2], and Roland Schmehl[1]
[1]Delft University of Technology
[2]Ampyx Power B.V

Keywords: Airborne wind energy | Performance model | Analytical modeling | Day-ahead electricity market | Correlation analysis

Ampyx Power is developing large-scale airborne wind energy systems (AWES) for the future energy system [1]. This work aims to overcome the challenges like scalability and commercialization of airborne wind energy (AWE) as identified in [2]. In this study, we present an analytical performance model for ground-generation AWES and apply this to preliminarily size new designs. The model is based on the ideal power production [3,4] and is enhanced to account for parametric losses, physical limits, component limits, and control limitations. The goals are to have a basic framework for performance prediction based on a minimal set of design parameters, to understand the scalability of ground-gen AWES, and to identify the sensitivity to key design drivers. This is ultimately to accelerate the sizing of new designs.

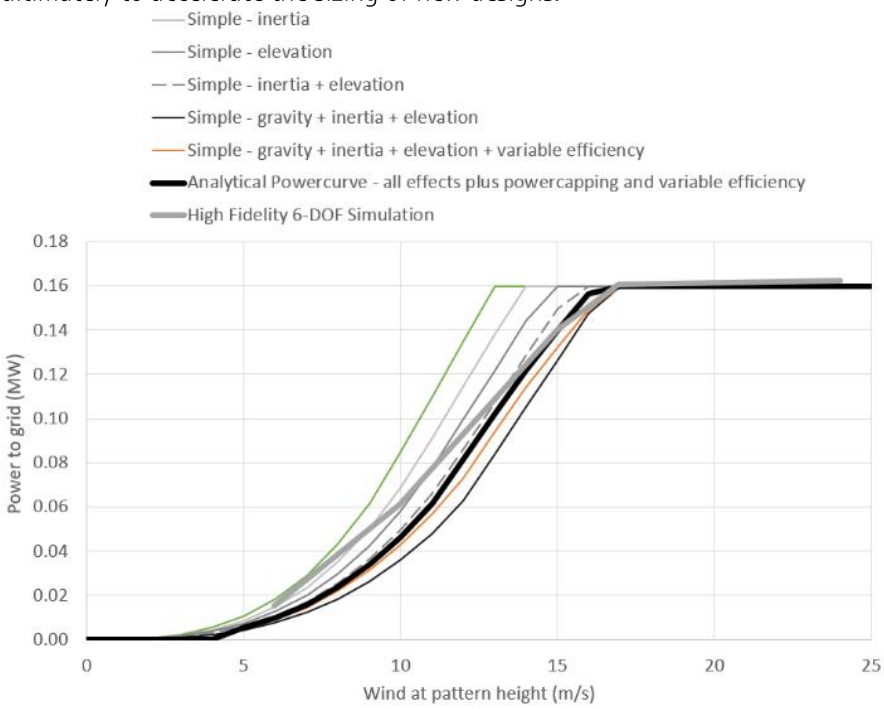

Figure 1: Power curve example using the simple sensitivity model (thick black), showing the contribution of various factors affecting performance (thin curves), versus high fidelity 6-DOF simulation (thick gray).

Typical scaling parameters are wing area and aspect ratio, peak tether tension and generator rated power. Typical constraints are due to aerodynamic performance of the wing, tether tensile strength, maximum allowable roll angle and minimum flight altitude. The allowable composite strain, on the other hand, implies a lower limit for the structural mass, which affects minimal tether length and size of the flight patterns. The structural mass also affects the variation of instantaneous power caused by the exchange of potential and kinetic energy during the downward and upward motions within a flight cycle. The actuation of aerodynamic control surfaces reduces the amount of total lift force that is available for power generation. Oversizing of the generator and its conversion efficiency for variable torque and rotational speed affects the generated electrical power. Wind gusts and a limited control authority require margins on the maximum tether tension. Eventually, a set of feasible flight paths can be determined from the above-mentioned limits and constraints, which can then be used to determine cosine losses[4] and evaluate the loss fraction of the lift vector that is

required to compensate for gravitational and inertial forces. Losses are derived using sink rate as a convenient concept for analysis.

The resulting performance estimations are validated against high fidelity 6-DOF simulations[5,6]. Figure 1 shows a computed power curve for an arbitrary sizing that highlights the contribution of various limitations and its comparison with a high-fidelity simulation.

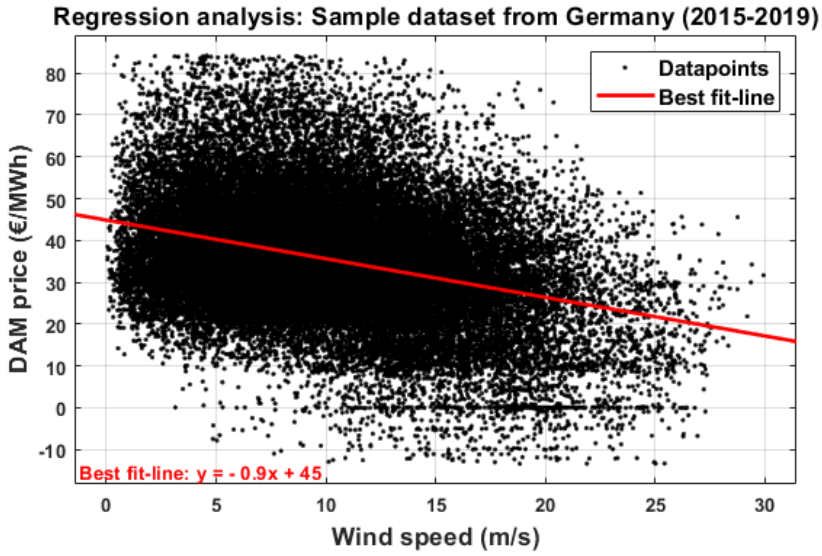

Figure 2: Regression analysis results for the DAM prices and wind speeds from the sample dataset from Germany (2015:2019)

We present an improved AWES design framework, combining the above-mentioned performance model, the component cost models and a revenue model based on the European electricity market[7]. Levelized cost of energy (LCoE) is commonly regarded as the key design driver for AWES design. However, a subsidy-free future electricity market will introduce new aspects and interdependencies that will affect the optimal system size. We use a data-driven statistical model to quantify the dynamics of a typical liberalized European electricity market. The computed results show that the day-ahead electricity market (DAM) prices and wind speeds have a negative correlation, which directly affect the revenue generated by wind energy technologies. Figure 2 shows the correlation between the DAM prices and wind speeds for an offshore location in Germany based on five years of data with an hourly resolution.

Using this framework, in addition to the levelized cost of energy (LCoE), a new design driver is identified and is defined as the levelized revenue of energy (LRoE). The results indicate a need to shift from cost-driven system design to value-driven system design for the future electricity markets with sufficient wind energy penetration.

References:

[1] M. Kruijff, R. Ruiterkamp: A Roadmap Towards Airborne Wind Energy in the Utility Sector. In: Schmehl R. (eds) Airborne Wind Energy. Green Energy and Technology. Springer, Singapore. https://doi.org/10.1007/978-981-10-1947-0_26

[2] K. Hussen et al.: Study on challenges in the commercialisation of airborne wind energy systems. Technical Report PP-05081-2016, prepared by Ecorys BV for the European Commission's DG Research and Innovation, Brussels, September 2018. https://doi.org/10.2777/87591

[3] M. L. Loyd, "Crosswind Kite Power.," J. energy, vol. 4, no. 3, pp. 106–111, 1980

[4] Diehl M.: Airborne Wind Energy: Basic Concepts and Physical Foundations. In: Ahrens U., Diehl M., Schmehl R. (eds) Airborne Wind Energy. Green Energy and Technology. Springer, Berlin, Heidelberg, 2013. https://doi.org/10.1007/978-3-642-39965-7_1

[5] Ruiterkamp R., Sieberling S. (2013) Description and Preliminary Test Results of a Six Degrees of Freedom Rigid Wing Pumping System. In: Ahrens U., Diehl M., Schmehl R. (eds) Airborne Wind Energy. Green Energy and Technology. Springer, Berlin, Heidelberg. https://doi.org/10.1007/978-3-642-39965-7_26

[6] P. Williams, S. Sieberling and R. Ruiterkamp, "Flight Test Verification of a Rigid Wing Airborne Wind Energy System," 2019 American Control Conference (ACC), Philadelphia, PA, USA, 2019, pp. 2183-2190, doi: 10.23919/ACC.2019.8814338

[7] R. Joshi: Influence of the European Electricity Market on the System Design of Airborne Wind Energy. MSc Thesis, Delft University of Technology, 2020. http://resolver.tudelft.nl/uuid:a19bf3fb-9f86-4fc2-985d-d9af6481e273

TU Delft kite power data 2010 – 2015

Roland Schmehl[1,*], and Uwe Fechner[2]
[1]Delft University of Technology
[2]Aenarete - Smart Wind
[*]Presenting author

Keywords: Airborne Wind Energy | Kite Power | Flight Tests | Experimental Data | TU Delft

With regular test flights since January 2010, the 20 kW kite power system of Delft University of Technology (TU Delft) was one of the worldwide first and probably also one of the most productive and best documented airborne wind energy (AWE) technology demonstrators and research platforms [1,2]. Early 2016, the system and its operation were transferred to the spin-off company, Kitepower [3], to continue as a commercial development platform within the European Union Horizon 2020 "Fast Track to Innovation" project REACH [4]. The high productivity during these six years of university-based research and development is also manifested by the 38 contributing graduation projects of TU Delft students and visiting students from other universities around the world. We decided to release the archived data and related documentation of this period in open access, as a reference for validation and comparison of computational simulation tools [5,6,7], and to support researchers without access to a well-instrumented and expensive platform.
The data set comprises the recordings of 52 instrumented test flights, each containing the time histories of up to 81 different sensor values and control signals at a sampling rate of 20 Hz. The data set is complemented by comprehensive audio-visual material documenting the test activities between 2010 and 2015. In this time period, the three leading edge inflatable (LEI) tube kites illustrated in Figure 1 were used for testing: a smaller, commercially available Genetrix Hydra kite, with 16 m^2 wing surface area, for strong wind and two larger, custom-developed kites, with 25 m^2 wing surface area, for low to moderate wind speeds. A highlight of the test campaign was the public demonstration of fully automatic pumping cycle operation during two days in June 2012 on the new Maasvlakte 2 area of Rotterdam Harbor, flying up to 800 m altitude (Figure 2). Other notable events were a test day in January 2013, with snowfall, fog and strongly impaired vision, and several test days in summer 2012 and later, of an experimental mast-based launch system. The data and audio-visual material also covers a number of anomalies that occurred during the early test flights, such as tether or weak link ruptures, as well as reversible and irreversible wing collapses. The availability of detailed information proved to be of crucial importance for building up knowledge and understanding how the operational reliability and safety of the system could be improved systematically [2].

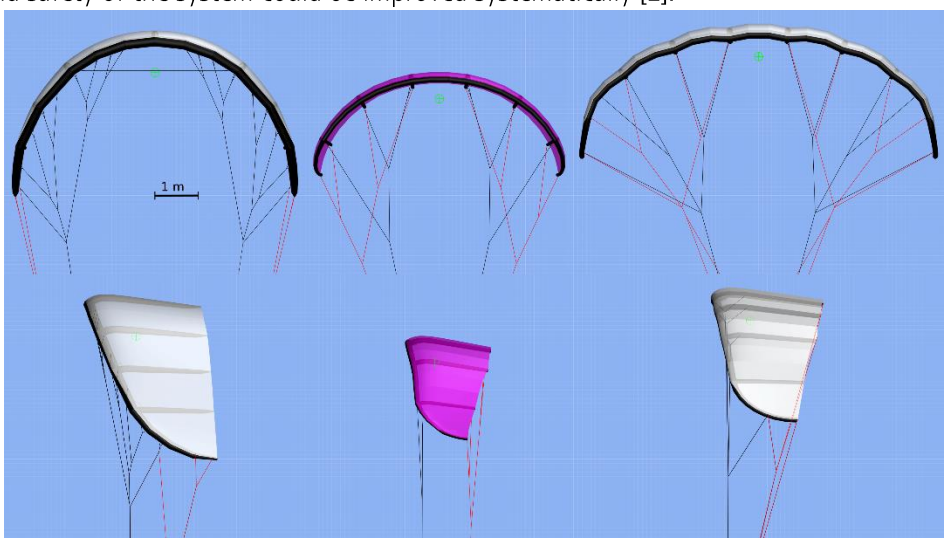

Figure 1: Front views (top) and side views (bottom) of the Mutiny V2 kite (left), Genetrix Hydra V4 kite (center) and TU Delft V3 kite (right), which were used during the 6-year experimental campaign.

The data set is provided as a single hdf5 file, from which the data recordings of individual flights can be exported in csv format, as comma-separated values, which is compatible with common programming environments. Alternatively, the csv files of the recorded flights can be downloaded directly. A set of Python scripts is provided for extracting meta data (Figure 2), filtering the data and plotting the data. The tool chain to construct the data set from individual ProtoLogger files (the native recording format based on Google Protocol Buffers) is also included. Basic examples of how to use the data are also provided in the programming languages Julia and Matlab [8].

```
Recording key, idx:   DF_2012_06_23_1, 26
Recording start:      2012-06-23 12:54:32
Launch after:         515 s     Land after:      7811 s Duration:  7296 s
Kite:                 Hydra
Max alt:             1083.27 m  Max height:          734.94 m
Max trimble_alt:      783.72 m
Max mech power:      22843.6 W  Av wind vel at 6m:     9.8 m/s
```

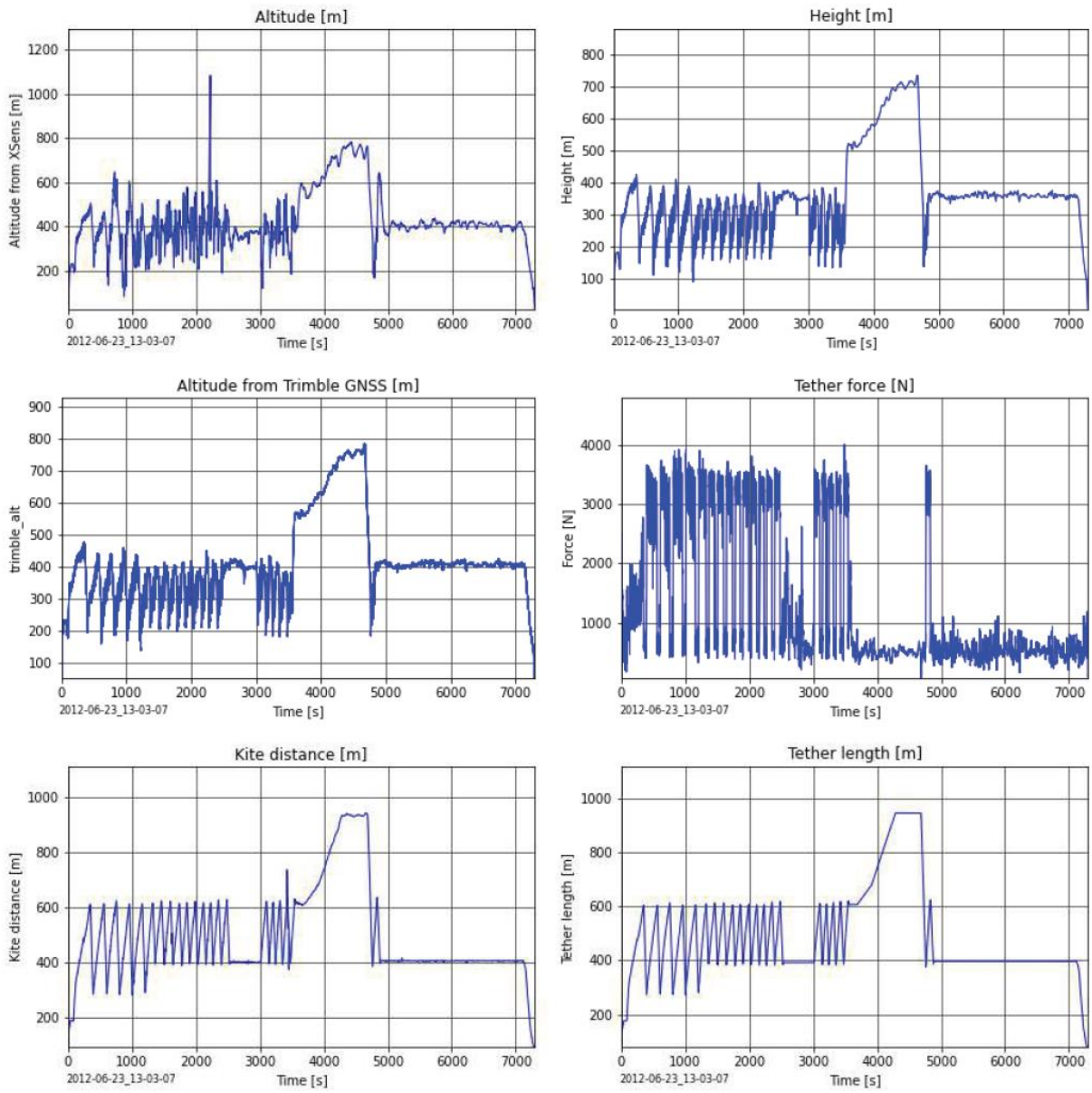

Figure 2: Summary page of a test flight on 23 June 2012, starting at 13:03:07 (hh:mm:ss) and lasting more than 2 hours, with automatic pumping cycle operation between 200 and 450 m altitude in the first half of the flight, then climbing to a maximum altitude of almost 800 m and after that parking at 400 m.

A deficiency of the data set is the insufficient and often inaccurate measurement of the apparent wind speed at the kite. This was improved in subsequent studies with the commercial development platform, allowing for an improved aerodynamic characterization of the kite [9,10].

References:
[1] R. van der Vlugt, J. Peschel, R. Schmehl: Design and Experimental Characterization of a Pumping Kite Power System. In: U. Ahrens, M. Diehl, R. Schmehl (eds.) Airborne Wind Energy. Springer, Berlin Heidelberg, 2013. doi:10.1007/978-3-642-39965-7_23
[2] V. Salma, F. Friedl, R. Schmehl: Improving Reliability and Safety of Airborne Wind Energy Systems. Wind Energy, Vol. 23, No. 2, pp. 340-356, 2019. doi:10.1002/we.2433
[3] Kitepower: https://kitepower.nl (Accessed 17 January 2021)
[4] European Commission: REACH - Resource Efficient Automatic Conversion of High-Altitude Wind. H2020-FTIPilot-691173. https://cordis.europa.eu/project/id/691173 (Accessed 31 January 2021)
[5] U. Fechner, R. van der Vlugt, E. Schreuder, R. Schmehl: Dynamic Model of a Pumping Kite Power System. Renewable Energy, Vol. 83, pp. 705-716, 2015. doi:10.1016/j.renene.2015.04.028
[6] R. van der Vlugt, A. Bley, M. Noom, R. Schmehl: Quasi-Steady Model of a Pumping Kite Power System. Renewable Energy, Vol. 131, pp. 83-99, 2019. doi:10.1016/j.renene.2018.07.023
[7] U. Fechner: A Methodology for the Design of Kite-Power Control Systems. PhD thesis, Delft University of Technology, 2016. doi:10.4233/uuid:85efaf4c-9dce-4111-bc91-7171b9da4b77
[8] R. Schmehl: Kite Power Data 2010-15. 4TU.ResearchData. doi:10.4121/uuid:5e1fda11-9ae1-4c0a-ab31-4a2c04f70740
[9] J. Oehler, R. Schmehl: Aerodynamic characterization of a soft kite by in situ flow measurement. Wind Energy Science, Vol. 4, pp. 1-21, 2019. doi:10.5194/wes-4-1-2019
[10] A. Roullier: Experimental analysis of a kite system's dynamics. MSc thesis, École polytechnique fédérale de Lausanne (EPFL), 2020.

Regular Session: Innovative Rotor Concepts and Small Wind Turbines

Research on utilizing wind energy in urban area

Donguk Yang[1,*], Seonghwan Kim[2], Haeseong Shin[3], Sanggyu Kang[3], Sukho Lee[1], and Seungyun Seol[4]
[1]Green Energy Institute
[2]Busan Campus of KOREA POLYTECHNIC
[3]Gwangju Institute of Sicence and Technology(GIST)
[4]Chonnam National University
[*]Presenting author

Keywords: VAWT | CFD | Residential Energy

Due to the environmental issues, Renewables are a great way to solve our problems. From the national policy in the republic of South Korea, the residential energy sector in an urban area is a much more allocation of investment via the Green New Deal strategy. The government drives zero energy into the public building area until 2025 and aims to build zero energy house until 2030.
Among several renewables, wind energy is utilized in this paper for the sake of feasible characteristics to the environment.
In this study, a design program for analysis, which was four types of Vertical Axis Wind Turbine(VAWT), was developed. Four types of blade straight type, convex type, helical type, and a new type are analyzed. The new shape of the designed blade consists of a blade shape with helical and convex at the same time, and the number of blades is three in total. They were investigated according to the discussed analysis method using a computer program. In the analysis process, the lift and drag coefficients according to the angle of attack of the airfoil, which used NACA0018, were developed to be automatically calculated by the extracted data. Using both coefficients, the lift and drag forces along the azimuth were gained, and the torque values for one blade were summed up with a simple formulation The output and the power coefficient of the wind turbine generator were considered through the sum of the total blade torques. The output performance and stability of the wind turbine generator finally were evaluated. Therefore, the power coefficients were discussed as design variables such as radius and helical shape.

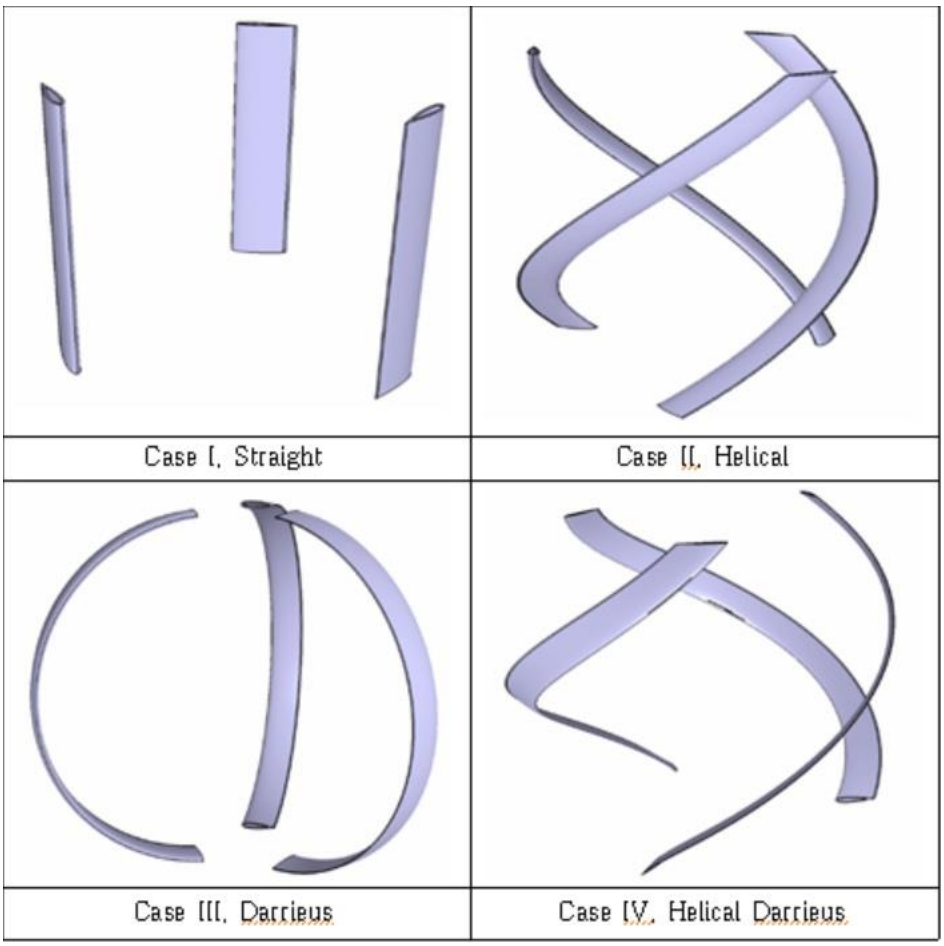

Figure 1: Four types of VAWT

Furthermore, a computational fluid analysis using a computer program was developed to decide a prominent option for utilizing the house and building energy sector in the urban area. Analysis of the comparative structures was performed according to the wind speed and capabilities. The process was as follows. Design conditions were assumed to analyze the model. The simulation range of the wind speed was from the cut-in speed of the wind turbine to cut out the speed of the wind turbine, respectively. In this study, nonlinear methods in each model were computed to take into consideration the complex wind environment in the urban area. Additionally, the performance of a reliable wind turbine system was evaluated.

As a result, the new type, which is called the helical Darrieus type, was the feasible way to adapt in modern houses compared to other structures based on the analysis with the computer program.

However, further experiments are needed to verify this research. For the manufacturing technology, the new design is highly complicated to mold, hence the cost of the total blades will be a challenge.

This study will be used as an application of the BEMS in our future research.

References:

Tjiu, W., Marnoto, T., Mat, S., Ruslan, M. H., & Sopian, K. (2015). Darrieus vertical axis wind turbine for power generation I: Assessment of Darrieus VAWT configurations. Renewable Energy, 75, 50-67.

Bhutta, M. M. A., Hayat, N., Farooq, A. U., Ali, Z., Jamil, S. R., & Hussain, Z. (2012). Vertical axis wind turbine–A review of various configurations and design techniques. Renewable and Sustainable Energy Reviews, 16(4), 1926-1939.

Gorlov, A. M. (1995). U.S. Patent No. 5,451,137. Washington, DC: U.S. Patent and Trademark Office.

Fatigue analysis concepts for a multi-rotor support structure

Sven Störtenbecker*, Rudolf Anselm, and Peter Dalhoff
Hamburg University of Applied Sciences (HAW Hamburg)
*Presenting author

Keywords: multi-rotor | wind turbine | support structure | space frame | fatigue analysis

Multi-rotor wind turbine systems (MRSs) are an innovative alternative to conventional single rotor (SR) wind turbines. Studies from the INNWIND project showed the potential to reduce the levelized cost of energy (LCoE) of an MRS, with 45 rotors and an overall capacity of 20 MW, compared to a power-equivalent single rotor (SR) (Jamieson et al., 2015). Results from Vestas' four-rotor MRS demonstrator revealed advantages in aerodynamic efficiency and in wake recovery when compared to an SR (van der Laan et al., 2019).
The support structure of a multi-rotor is composed of the tower and the space frame, connecting the rotor nacelle assemblies (RNAs) with the tower. An example of a simplified MRS design with the support structure, rotor and yaw bearings positions can be seen in Figure 1.

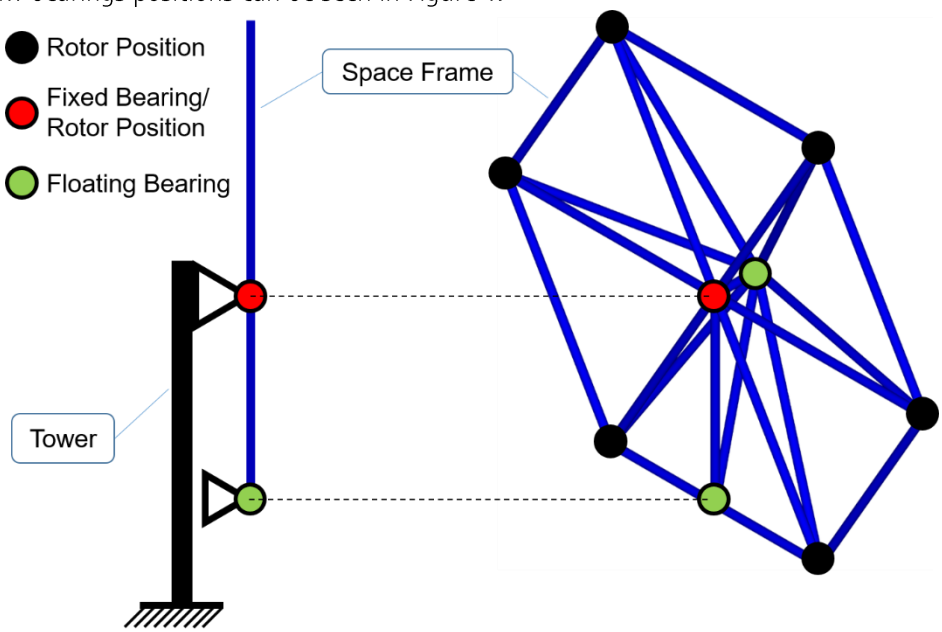

Figure 1: Support structure of a MRS (Störtenbecker et al., 2020b)

In [Störtenbecker et al., 2020a] several MRS designs with a number of rotors, ranging from three to nine, were designed and optimized regarding their simplified cost of energy (SCoE) in a preliminary concept analyses. This was based on a simplified approach and design load case: maximum thrust forces, resulting from steady rated wind speed, and gravitational forces of the RNAs acting on the MRS support structure. The space frame was considered as an ideal truss work. Basic geometric design parameters, like the depth of the space frame and the yaw bearings positions, were varied in the optimization.
In [Störtenbecker et al., 2020b] the same simplified approach was used to optimize MRS support structures for a higher numbers of rotors in a hexagonal design, ranging from 7 to 207, and a fixed overall capacity of 20 MW. A better understanding of the masses and therefore cost, defined by the optimized geometric design parameters, dependent on the different number of rotors was gained.
The importance of the thrust forces, compared to the gravitational forces resulting from the RNAs, and buckling behaviour in the designing and dimensioning process was shown depending on the number of rotors. In this study a more detailed designing process and analyses for selected MRS designs with an overall capacity of 20 MW is presented. The results of the preliminary concept analyses in [Störtenbecker et al., 2020a] and [Störtenbecker et al., 2020b] are used in the designing and dimensioning process. This dimensioning process is extended here to other design load cases (DLCs), especially turbulent wind. A binning of the dimensioned

space frame members is investigated, in contrast to the dimensioning of each individual space frame member in the preliminary concept analyses.

One focus will be the fatigue analysis of the support structure. A simplified approach is presented as a counteract to the relatively high number of degrees of freedom (DoFs) and therefore computational times in a fully aeroelastic MRS simulation, when compared to an equal SR simulation.

References:

Jamieson, P., Branney, M., Hart, K., Chaviaropoulos, P., Sieros, G., Voutsinas, S., Chasapogiannis, P., and Prospathopoulos, J. M., (2015). Innovative Turbine Concepts – Multi-Rotor System, INNWIND Deliverable 1.33.

Störtenbecker, S., Dalhoff, P., Tamang, M. and Anselm, R., (2020). Simplified support structure design for multi-rotor wind turbine systems. Wind Energy Science, [online] 5(3), pp.1121-1128. Available at: https://wes.copernicus.org/articles/5/1121/2020/ [Accessed 15 January 2021].

Störtenbecker, S., Anselm, R. and Dalhoff, P., (2020). Simplified approach for the optimal number of rotors and support structure design of a multi rotor wind turbine system. Journal of Physics: Conference Series, [online] 1618, p.032009. Available at: https://iopscience.iop.org/article/10.1088/1742-6596/1618/3/032009 [Accessed 15 January 2021].

van der Laan, M., Andersen, S., Ramos García, N., Angelou, N., Pirrung, G., Ott, S., Sjöholm, M., Sørensen, K., Vianna Neto, J., Kelly, M., Mikkelsen, T. and Larsen, G., (2019). Power curve and wake analyses of the Vestas multi-rotor demonstrator. Wind Energy Science, [online] 4(2), pp.251-271. Available at: https://wes.copernicus.org/articles/4/251/2019/ [Accessed 15 January 2021].

Comparison of yaw control strategies of 20 MW multi-rotor systems

Rudolf Anselm*, Sven Störtenbecker, and Peter Dalhoff
Hamburg University of Applied Sciences (HAW Hamburg)
*Presenting author

Keywords: multi-rotor | wind turbine | yaw system | control strategies

Scientists and engineers around the globe managed to optimise conventional wind turbines and defied the manufacture and logistic challenges of even bigger units, which brought the wind energy sector to a serious competitor in the power generation industry. To keep up the speed and expand the possibilities in using the wind as a power source, alternative concepts shall be analysed in parallel to optimise the predominant single rotor technology. A multi-rotor system (MRS) with many small rotors connected via a space frame to the tower could be an alternative concept to overcome these challenges.
Vestas already built with their 4R-V29 wind turbine a recent MRS demonstrator. Experimental Investigations of the four rotor MRS demonstrator revealed the advantage in aerodynamic efficiency and wake recovery compared to a single rotor (van der Laan et. al., 2019). The INNWIND.EU project showed in their studies with a 45 rotor MRS and an overall capacity of 20 MW the benefits considering the levelised costs of energy (LCoE) (Jamieson et. al., 2015). MRS also provide alternative opportunities for the yaw system, which could make conventional yaw drives obsolete (MacMahon et. al., 2018). There the INNWIND.EU MRS design with 45 rotors was also used and investigated.

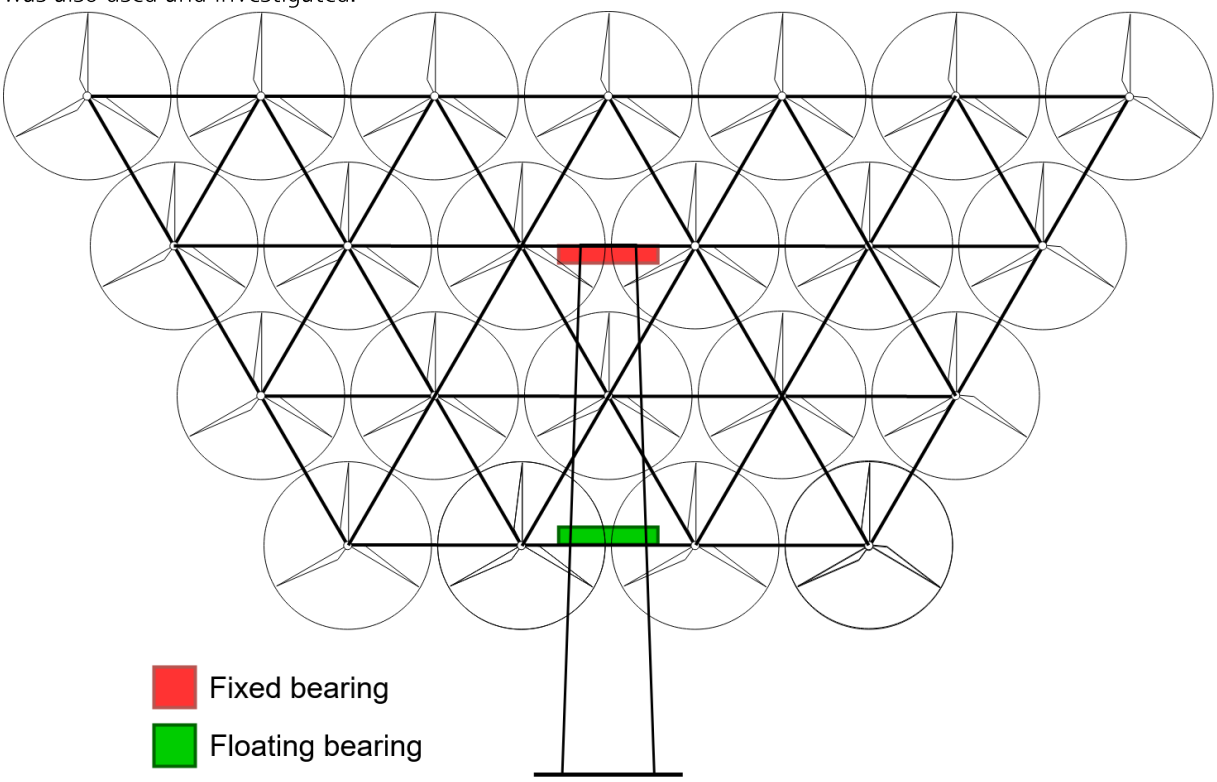

Figure 1: Position of the fixed and floating bearings of an MRS

In this study a Matlab/ Simulink model of a 20 MW MRS is built with different number of rotors, two yawing strategies and different designs will be shown and compared to a conventional yaw system.
The two strategies are named yaw by pitch and yaw by speed control. Both of the strategies are creating a difference in thrust between the right and the left side of the MRS, generating a yaw moment. The yaw misalignment is monitored via a controller, which manipulates, dependent of the yaw strategy, either the pitch angle of a required number of rotors (yaw by pitch) or changes the rotors speeds (yaw by speed control). The moment of inertia of the rotors are assumed as point masses while the space frame is considered a rigid

body. The space frame of the MRS connects all rotor nacelle assemblies (RNAs) and is built up as an ideal truss work. The tower and the space frame are connected via a floating and a fixed bearing (figure 1).The friction moments of the bearings are also considered. The aerodynamics of the rotor blades are computed with the blade element momentum theory. The yawing strategies are compared regarding the power losses and the reliability while yawing. To see the influence of the number of rotors, both strategies are simulated for a small (<10 rotors) and high (>10 rotors) number of rotors. At last, the power output of the chosen MRS designs is compared to an equivalent single rotor turbine with a conventional yaw system.

References:

van der Laan, M., Andersen, S., Ramos García, N., Angelou, N., Pirrung, G., Ott, S., Sjöholm, M., Sørensen, K., Vianna Neto, J., Kelly, M., Mikkelsen, T. and Larsen, G., (2019). Power curve and wake analyses of the Vestas multi-rotor demonstrator. Wind Energy Science, [online] 4(2), pp.251-271. Available at: https://wes.copernicus.org/articles/4/251/2019/ [Accessed 15 January 2021].

MacMahon, E. and Leithead, W., 2018. Performance Comparison of Optimised and Non-Optimised Yaw Control for a Multi Rotor System. (2018) IEEE Conference on Control Technology and Applications (CCTA), [online] Available at: https://ieeexplore.ieee.org/document/8511353 [Accessed 15 January 2021].

Jamieson, P., Branney, M., Hart, K., Chaviaropoulos, P., Sieros, G., Voutsinas, S., Chasapogiannis, P., and Prospathopoulos, J. M., (2015). Innovative Turbine Concepts – Multi-Rotor System, INNWIND Deliverable 1.33.

CFD analysis of a roof-top mounted H-rotor Darrieus vertical axis wind turbine under turbulent inflow conditions

Pradip Zamre*, Amgad Dessoky, Thorsten Lutz, and Ewald Krämer
University of Stuttgart
*Presenting author

Keywords: Small VAWT | Urban terrain | DDES | Inflow turbulence

Due to low turbulence sensitivity, small dimensions, absence of any yaw control, low noise vertical axis wind turbines (VAWTs) can be considered more suitable for harnessing the wind source in urban environment compared to horizontal axis wind turbines (HAWTs) (Riegler, 2003, p. 44). However, the behaviour of VAWT is complex due to the 3D unsteady aerodynamics, such as continuously changing angle of attack and dynamic stall. Moreover, the interaction of atmospheric boundary layer with the different structures, objects present in urban environment leads to the highly turbulent inflow conditions with continuously changing inclination, direction etc. Consequently, all these factors can influence the performance of VAWT significantly. So far, limited research is available in literature about the behaviour of VAWTs and its complex flow field in urban environment under realistic inflow conditions. For the current study, "Morgenstelle Campus" of University of Tübingen is considered, where 4-5 buildings with average height around 40m are present along with a forested hill in the upstream area as shown in Fig. 1. The objective of the present research is to investigate the aerodynamic performance, loads and wake propagation of straight bladed H-Darrieus VAWT in realistic urban environment under instationary and turbulent inflow conditions. A roof-top mounted H-VAWT has been investigated with help of highly resolved Delayed Detached Eddy Simulations (DDES) at different operating points and at different suitable positions.

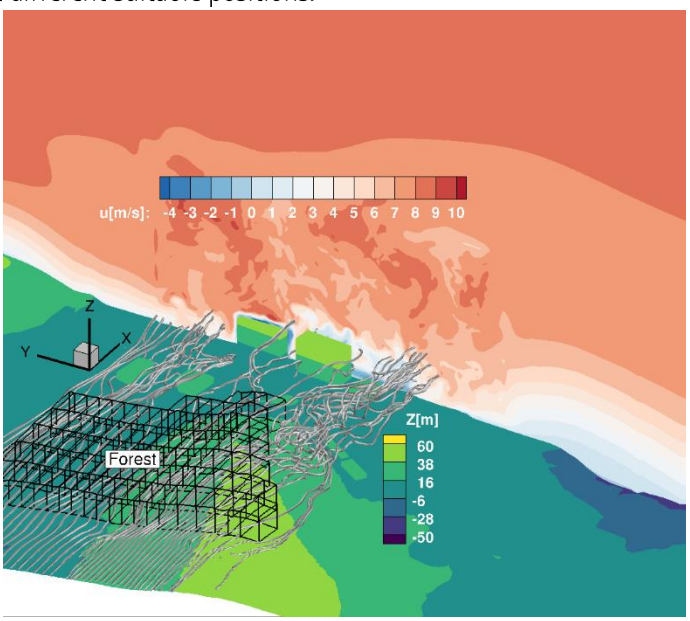

Figure 1: Flow field in urban environment

In order to simulate the impact atmospheric boundary layer using FLOWer compressible flow solver (Rossow, Kroll, Schwamborn, 2006, p. 3), a generic wind profile with superimposed turbulence generated by Mann model is prescribed at the inflow domain of urban terrain . The hill covered with vegetation is modelled using an approach based on (Shaw, Schumann, 1992, p. 47). For the current study, the H-VAWT is selected based on experimental data from (Li et al, 2014, p.51). It is also numerically investigated using high fidelity DDES approach with FLOWer solver in (Dessoky et al, 2019, p. 404) and good agreement is found with experimental data. However, for current application, the H-VAWT is geometrically scaled-up maintaining the same solidity.

It has diameter 7m, blade length 4.2m, symmetric NACA0021 profile with chord length 0.9275m. The H-VAWT is investigated at multiple locations under turbulent inflow conditions.

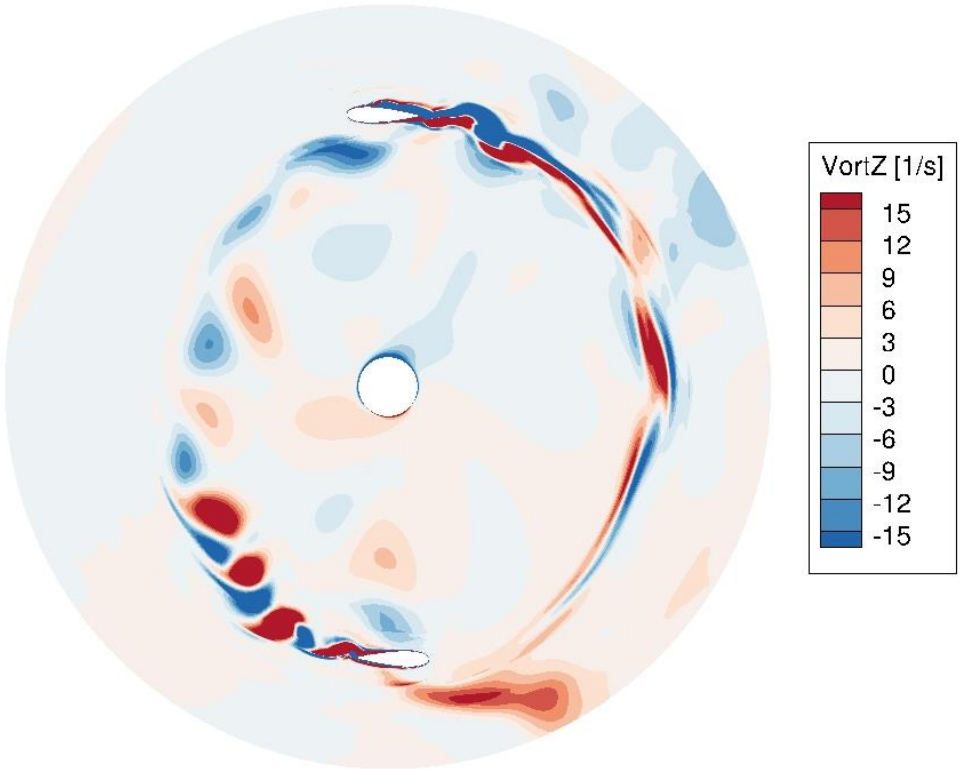

Figure 2: Z Vorticity contours

It is found that the orography and vegetation present in upstream region has profound influence on the inflow conditions for the roof-top mounted small wind turbines in the selected urban environment (Zamre et al, 2020, p. 042005). Near built environment, higher turbulence levels are observed. Primary investigation of roof-top mounted H-VAWT under such complex operating conditions shows significant variations in the its behaviour. At operating point tip speed ratio 3, the vorticity contours in horizontal plane passing through wind turbine are shown in Fig. 2. In general, the blade vortex interaction (BVI) takes place between azimuth 180° and 270°. However, in current case, strong BVI can be seen unexpectedly in the first quarter of the revolution around azimuth 10°.

The flow separation after azimuth 90° results into the dynamic stall. Overall, under these operating conditions, the performance of H-VAWT is negatively affected. The root causes for such behaviour are investigated through different ongoing test cases.

References:

Riegler H., (2003) HAWT versus VAWT, Small VAWTs find a clear niche. Refocus, vol. 4(4), pp 44-46.

Rossow, C., Kroll, N., and Schwamborn, D., (2006) The MEGAFLOW Project - Numerical Flow Simulation for Aircraft Springer Berlin Heidelberg pages 3-33.

Shaw, R., H., Schumann, U., (1992) Large-eddy simulation of turbulent flow above and within a forest, vol. 61 pp. 47-64

Li, Q., Maeda, T., Kamada, Y., Murata, J., Kawabata, T., Kogaki, T. (2014). Study on flow around straight-bladed vertical axis wind turbine under low tip speed ratio. Journal of Fluid Science and Technology. vol.9, pp. JFST0051-JFST0051.

Dessoky, A., Lutz, T., Bangga, G. and Krämer, E. (2019) Computational studies on Darrieus VAWT noise mechanisms employing a high order DDES model Renewable Energy, Elsevier, vol. 143(C), pages 404-425

Zamre, P., Dessoky, A., von der Grün, M., Lutz, T., Krämer E. (2020) Numerical Study of the Impact of Urban Terrain on the Loads and Performance of a Small Vertical Axis Wind Turbine Journal of Physics, vol. 1618 p.042005

Pilot-scale performance of AeroMINE at low wind speeds

Brent Houchens[1,*], David Marian[1], Suhas Pol[2], and Carsten Westergaard[3]
[1]Sandia National Laboratories
[2]Texas Tech University
[3]Westergaard Solutions Inc
[*]Presenting author

Keywords: distributed wind | AeroMINE | remote power

Introduction

Existing distributed wind solutions typically suffer from three major weaknesses: i) small swept areas resulting in proportionally small power, ii) many moving components at height, often exposed to harsh environments, leading to vibrations and mechanical failures, and iii) fast moving blades that require large standoff distances and can produce significant aero-acoustic noise. This has negatively impacted the penetration of distributed wind solutions in the market; for example, distributed wind made up less than 2% of the 2016 U.S. wind energy market (Orrell et al., 2017). AeroMINE (Motionless, INtegrated Extraction) wind energy harvesters have large swept-areas with no external moving parts, making them transformative for distributed wind energy in power production, reliability and safety.

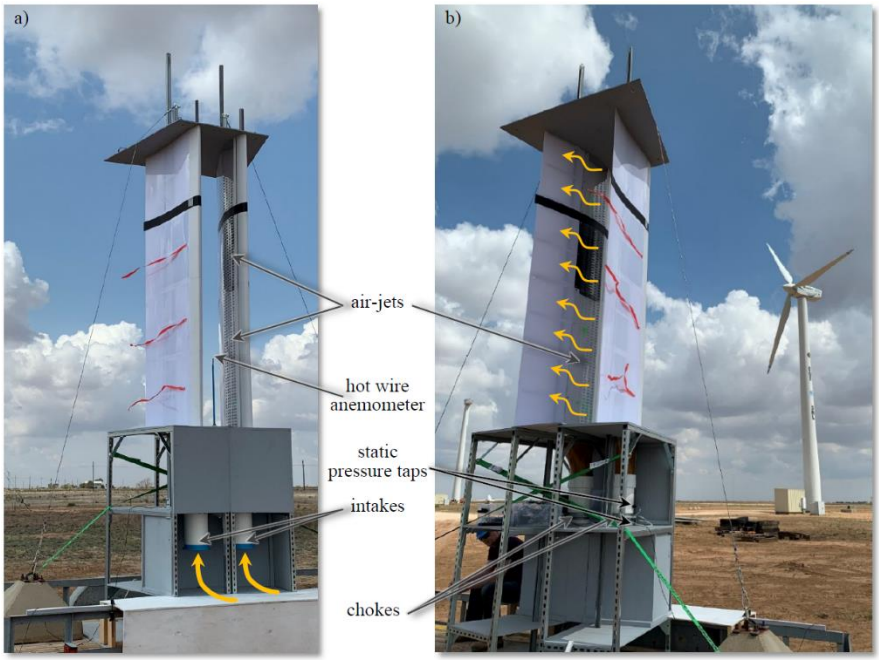

Figure 1: Pilot-scale (3-m tall, 1-m chord) AeroMINE test at SWiFT shown from a) in front and b) behind.

AeroMINE Operation

A pilot-scale AeroMINE prototype is shown in Figure 1 at the Sandia National Laboratories (SNL) Scaled Wind Farm Technology (SWiFT) site in Lubbock, Texas. Very low-pressure regions are created by wind flowing between the foil-pairs that make up the external body of AeroMINEs. Here the design uses an S1210 foil for its strong lift characteristics over a wide range of wind speeds (Selig, 1995). The low-pressure surfaces of the foils contain orifices (air-jets). The foils themselves are hollow. The low pressure between the foils pulls air out of the air-jets, which is supplied by the interior of the foils. Air to the interior of the foils is in turn supplied ducts and a manifold. In practice this manifold contains an internal, pneumatically-driven turbine-generator that produces electricity.

The turbine-generator section is protected to avoid harsh environments and is isolated from people and wildlife. The inlet to the system can be either inside or outside the building, as desired.

Low-speed Test Results

Here the manifold is removed and variable size chokes are place in the ducts to represent the load of the turbine-generator. The average velocity and pressure drop across the chokes is measured to estimate the power at the inlets. Figure 2 shows the impact of off-axis wind on performance for lowspeed (<5 m/s) flow. The foils are able to realign the off-axis flow, such that wind misaligned by as much as ±45° does not impact power production. Some misalignment is even shown to be beneficial, though this is likely within the error of the measurements.

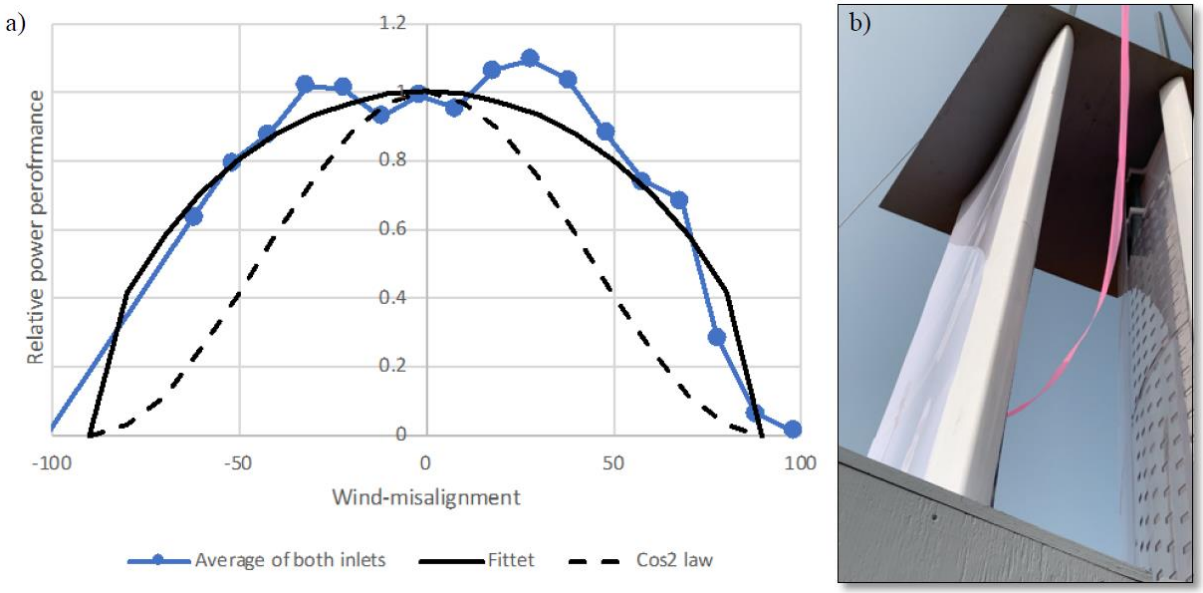

Figure 2: a) Off-axis performance normalized to performance with perfect alignment. b) Flow turning from offaxis as indicated by a marker ribbon.

Acknowledgments

This work was funded primarily by SNL Laboratory Directed Research and Development (LDRD) funds through the 2019 Innovation Challenge initiative of the Environment and Homeland Security Investment Area. Additional funding was supplied in part by awards from the 2017 Sandia Pitch Competition, the 2017 DOE-wide National Lab Accelerator Pitch Event, the GLEAMM Spark Fund, and in-kind by Westergaard Solutions Inc.

SNL is managed and operated by NTESS under DOE NNSA contract DE-NA0003525. This paper describes objective technical results and analysis. Any subjective views or opinions that might be expressed in the paper do not necessarily represent the views of the U.S. Department of Energy or the United States Government.

References:

Houchens, B. C., Marian, D. V., Pol, S. and Westergaard, C. H. (2019) A Novel Energy Conversion Device for Wind and Hydrokinetic Applications, Proceedings of the ASME-JSME-KSME 2019 Joint Fluids Engineering Conference, AJKFLUIDS2019-5542, ASME, San Francisco, CA, USA.

Orrell, A. C., Foster, N. F., Morris, S. L. and Homer, J. S. (2017) "2016 Distributed Wind Market Report," Prepared for the U.S. Department of Energy Office of Energy Efficiency and Renewable Energy by the Pacific Northwest National Laboratory.

Pol, S., Houchens, B. C., Marian, D. V. and Westergaard, C. H., (2020) Performance of AeroMINEs for Distributed Wind Energy, Proceedings of the 2020 AIAA SciTech Conference, Orlando, FL, USA.

Selig, M. S., Guglielmo, J. J., Broeren, A. P. and Giguere, P. (1995) "Summary of Low-Speed Airfoil Data," Vol. 1.